Oklahoma
Geological
Survey
1999

Special Publication 99-3

Geological Perspectives of Reservoir Engineering: A Waterflood Workshop

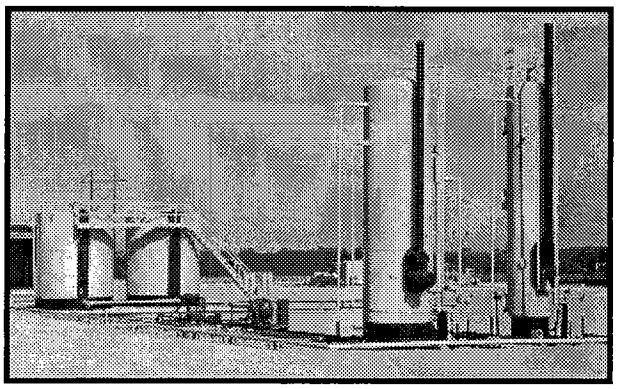

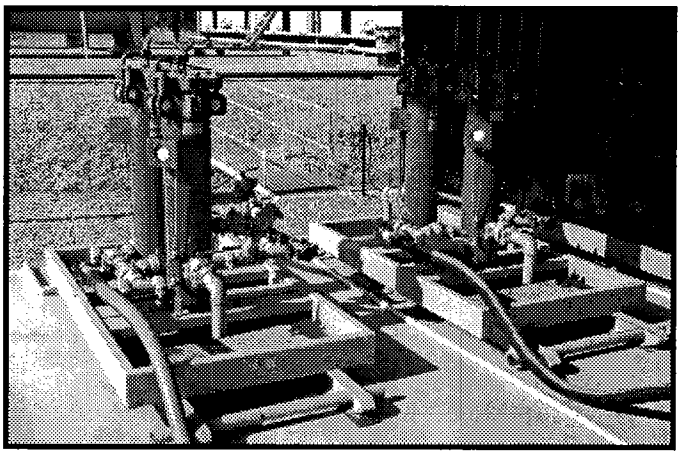

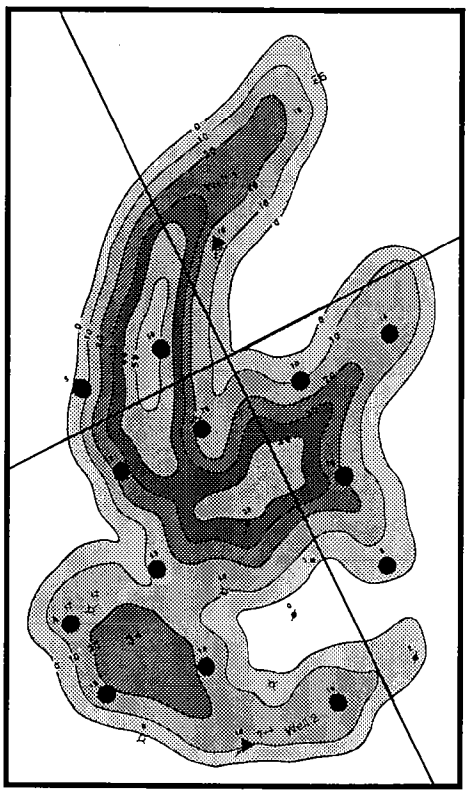

Workshop co-sponsored by:
Oklahoma Geological Survey
and
Petroleum Technology Transfer Council

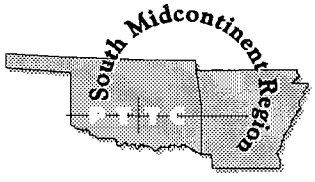

ERRATA

Oklahoma Geological Survey Special Publication 99-3
Geological Perspectives of Reservoir Engineering:
A Waterflood Workshop

Page 8, left column, line 35: "solution GORs" should read "produced GORs"

Page 17, Figure 28A: equation 3.12 should read $r = \frac{N_p}{N} = \frac{B_o - B_{oi} + B_g\,(R_{si} - R_s)}{B_o + B_g\,(R_p - R_s)}$

Page 21, Figure 33A: "V_B = Bulk Volume = A" should read "V_B = Bulk Volume = $A \times H$ (Height)"

Page 22, Figure 34B: equation 3.19 should read $C_o = -\frac{1}{V}\frac{dV}{dp} = \frac{V_o - V_{oi}}{V_{oi}\,(p_i - p)} = \frac{B_o - B_{oi}}{B_{oi}\,(p_i - p)}$

Page 75, right column, line 12: "BWPD" should read "BWPM"

Page 77, Figure 121B: equation 7.2 should read $M = \frac{k_w/\mu_w}{k_o/\mu_o} = \frac{k_w\,\mu_o}{k_o\,\mu_w} = \frac{k_{rw}\,\mu_w}{k_{ro}\,\mu_w}$

Page 78, Figure 122: equation 7.3 should read $M = \frac{\mu_o}{\mu_w}\ \frac{(k_{rw})\,\bar{S}_{w\,BT}}{(k_{ro})\,S_{wi}}$

Oklahoma Geological Survey
Charles J. Mankin, *Director*

Special Publication 99-3
ISSN 0275-0929

Geological Perspectives of Reservoir Engineering: A Waterflood Workshop

by

Kurt Rottmann
Consultant Geologist
Oklahoma City, Oklahoma

with contributions from

David R. Crutchfield
Consultant Petroleum Reservoir Engineer
Oklahoma City, Oklahoma

This volume is published as part of a continuing series of workshops to provide information and technical assistance to Oklahoma's oil and gas operators.

Co-sponsored by:
Oklahoma Geological Survey
and
Petroleum Technology Transfer Council

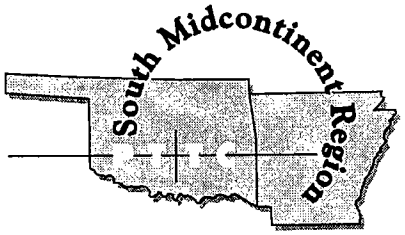

The University of Oklahoma
Norman, Oklahoma
1999

SPECIAL PUBLICATION SERIES

The Oklahoma Geological Survey's Special Publication series is designed to bring timely geologic information to the public quickly and economically. Review and editing of this material has been minimized in order to expedite publication.

On the cover – Examples of production equipment, injection equipment, and geologic mapping, which suggests the cooperation necessary among the various disciplines for a waterflood project to be successful, and for which the primary emphasis of this publication is based.

This publication, printed by the Oklahoma Geological Survey, is issued by the Oklahoma Geological Survey as authorized by Title 70, Oklahoma Statutes, 1981, Section 3310, and Title 74, Oklahoma Statutes, 1981, Sections 231–238. 750 copies have been prepared at a cost of $4,210 to the taxpayers of the State of Oklahoma. Copies have been deposited with the Publications Clearinghouse of the Oklahoma Department of Libraries.

CONTENTS

continued on next page →

LIST OF FIGURES

continued on next page →

continued on next page →

LIST OF TABLES

1

Purpose and Goals of the Workshop

CHAPTER 1

Purpose and Goals of the Workshop

INTRODUCTION

This second waterflood workshop is a continuation and extension of the first. The first workshop dealt with basic principles that a geologist would need when evaluating a waterflood candidate (Rottman and others, 1998). The following list outlines the subjects that were discussed:

- Determining reservoir data
- Deciphering production data
- Determining and isopaching net pay
- Defining sand geometry and boundaries
- Implications of structure
- Understanding analogies
- Coring and core results
- Distinguishing natural and induced fractures
- Water-supply evaluation
- Permitting

These topics form the essence of a geologist's review of reservoir parameters and characteristics that contribute to a waterflood evaluation.

But the preliminary evaluation by a geologist cannot be complete without an understanding, at least on a cursory basis, of the following two fundamental questions: First, is there enough oil to validate a profitable waterflood project? Second, how much oil probably will be produced from secondary recovery for preliminary reserve purposes? These two questions require knowledge of basic reservoir-engineering fundamentals. It is not the purpose of this workshop to define in detail (from a reservoir engineer's perspective) these principles. However, it is the purpose of this workshop to examine these principles so that a geologist, operator, or field personnel will be able to assist, use, and communicate these principles to the engineers during the cursory-review process.

GOALS OF THE WORKSHOP

As was just mentioned, the first waterflood workshop was devoted to understanding the importance for the geological department and the engineering department to work together (Rottman and others, 1998). One of the most important concepts a company can learn—a pitfall to avoid—is the importance of eliminating knowledge segregation that tends to exist or that can develop between such internal departments. The first workshop illustrated two prime examples (Rottman and others, 1998, figs. 7–10) of how the lack of cooperation and communication between internal departments can have a negative effect on a company. The examples clearly illustrate that a company's financial welfare depends on this cooperation. But the question remains, what is the basis of this cooperation? It depends on geologists and engineers understanding rudimentary principles and fundamentals of the others' discipline. Understanding fundamental reservoir-engineering principles from a geological perspective, therefore, is the goal of this workshop.

To understand these fundamentals better, let's look closely at the geological example of lack of communication between the geological and engineering departments from the first workshop, mentioned previously. A certain oil company's geological department became interested in a field they thought might be a waterflood candidate (Fig. 1). They apparently proceeded on the assumption that since only 20 million barrels of oil (MMBO), of a total of 100 MMBO in place, had been produced, the remaining 80 MMBO should be sufficient to supply some secondary reserves for the waterflood prospect. The department spent close to 1 man-year of time and energy evaluating the project. Notice the keyword *some* as used in the phrase: "sufficient to supply *some* secondary reserves." This is the crux of the problem for many geologists, operators, or field personnel when they evaluate waterflood projects. This lack of knowledge or understanding of how to calculate

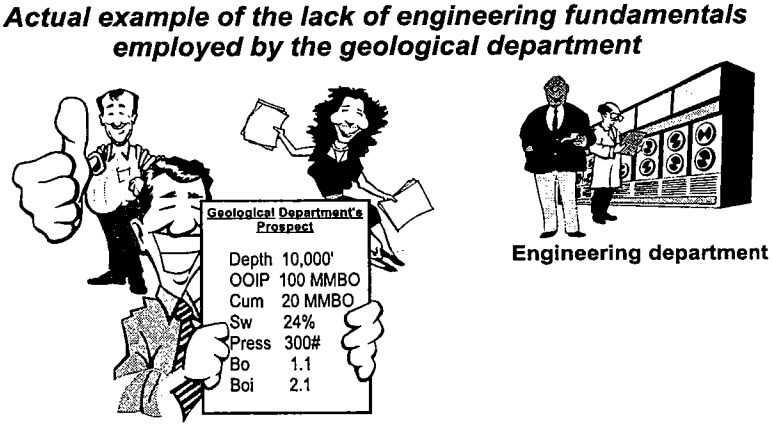

Figure 1. Geological department's 1-man-year evaluation of a potential waterflood prospect.

those remaining reserves, the effects of production on those reserves, and some of the rudimentary principles involved in displacing the reserves can put the prospect or company at risk. As the example continues, the geological department submitted their preliminary geological review to the engineering department. By using the parameters of depth, original oil in place (OOIP), cumulative production, salt-water saturation, current pressure, and current and initial formation volume factor supplied by the geological department for this prospect, and plugging the data into the formula for current oil saturation, the engineering department determined within an hour of work (Fig. 2) that there was not enough remaining oil to waterflood because of the high shrinkage of the oil. Had the geological personnel understood the meaning and implications behind the principles of current oil and gas saturations and shrinkage, wasted company resources could have been avoided.

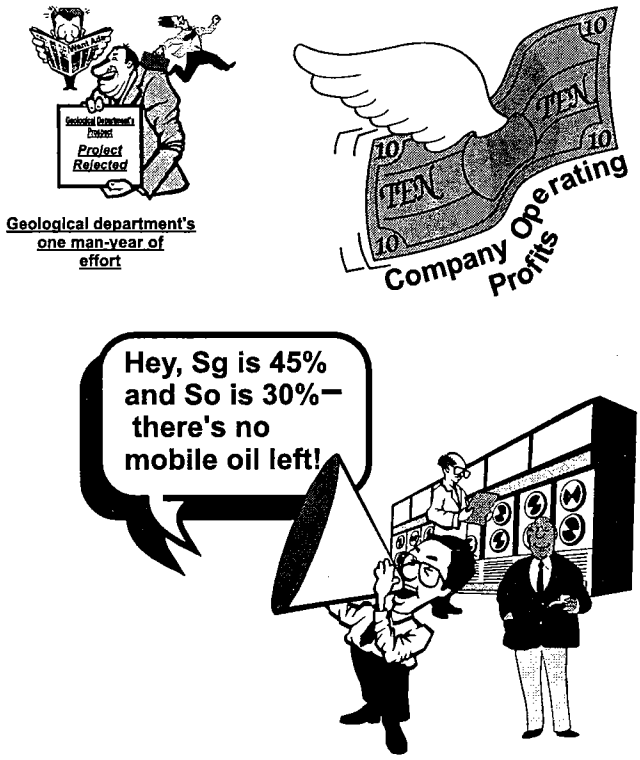

Figure 2. Engineering department's 1-man-hour evaluation killed the prospect from the geological department.

The first workshop stressed sharing and communication between departments (Rottman and others, 1998). This workshop will build on that concept by stressing basic engineering fundamentals so that a geologist or operator can communicate effectively with the engineering department. The goal of this workshop is to look at two basic waterflood concepts: (1) Is there enough oil? and (2) predicting how much oil will be recovered. Basic geologic principles, such as electric-log interpretation and normal geological routines and practices normally conducted during the course of business, will not be discussed. Also, the engineering principles addressed in this workshop will be examined only to the extent that the author feels would constitute adequate principles for geologists, operators, or field personnel to responsibly communicate with engineers. It is not the purpose of this workshop, therefore, to teach detailed reservoir or waterflood engineering principles but only those that share commonality with both geological and engineering fundamentals of a waterflood project. The hoped-for outcome of this workshop is to take the preliminary evaluation of a project one step higher, which includes estimating reserves in place and recoverable reserves.

The Oklahoma Geological Survey hopes to persuade the petroleum industry that familiarity with engineering principles by geologists, and geological principles by engineers, is to the industry's benefit. Thus, the mindset that the geological department or the engineering department is solely responsible for the success of a waterflood project can be a costly one. The success of a waterflood candidate is not based on personal evaluation but on the evaluation of the project's economic analysis (Fig. 3). The economic analysis, with all the incorporated data from the geologists

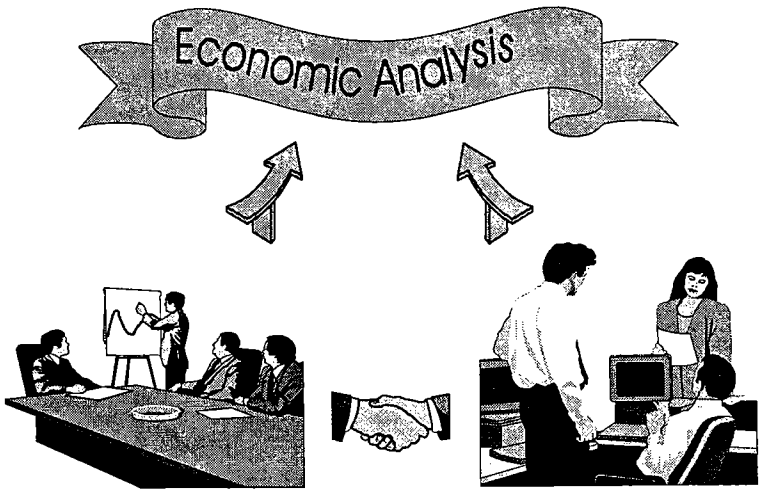

Geological department
- Reservoir data
- Production history
- Net pay
- Structure
- Analogies
- Cores
- Environmental
- Simulation
- Waterflood design
- Installation
- Monitering
- Injection rates and production
- Operations
- Water supply

Engineering department
- Simulation
- Waterflood design
- Installation
- Monitoring
- Injection rates and production
- Operations
- Water supply
- Reservoir data
- Production history
- Net pay
- Structure
- Analogies
- Cores
- Environmental

Figure 3. The geological and engineering departments are responsible for their respective contributions to the economic analysis of the waterflood project.

and engineers, predicts the success of the project. Figure 4 is the tabular and graphical representation of various geological and engineering variables from a reservoir model used to evaluate a waterflood prospect. Those variables circled were defined or discussed in the first workshop (Rottman and others, 1998), and those bracketed will be discussed in this workshop. As can be seen from this figure, almost all the pertinent

Miscellaneous

(Pi)	2,156 psi
(P)	265 psi
Depth	4,950 ft
(P-grad)	0.436 psi/ft
(T)	117 °F
(k)	30 md
[Oil Grav]	40.0 °API
[Gas Grav]	0.75
[NaCl %]	0.0%

Material Balance

(N)	1,263,225 stbo	
(G)	2,706 mcf	
m	0.00	
Gas Cap %	0.2%	
[SGDI]	99.14%	217,703 stbo
[GCDI]	0.48%	1,046 stbo
[WDI]	0.00%	0 stbo
[PVCI]	0.39%	851 stbo

PVT Data

Condition	Initial	Current	BP
(P)(psi)	2,156	265	1,687
[Rs (scf/stb)]	475	53	475
[Bt (cf/stb)]	7.02	30.75	7.06
Bo (rb/stb)	1.2502	1.0583	1.2572
μo (cp)	0.9306	2.5215	0.8873
Co (1/psi)	1.194E-05	2.232E-03	1.525E-05
Bg (cf/scf)	0.0056	0.0588	0.0073
μg (cp)	0.0189	0.0116	0.0162
Cg (1/psi)	4.407E-04	3.597E-03	4.967E-04
Bw (rb/stb)	1.0071	1.0098	1.0078
μw (cp)	0.5724	0.5724	0.5724
Cw (1/psi)	3.326E-06	3.242E-06	3.318E-06

Volumetrics

(N)	1,263,313 stbo	(A)	252.90 ac
(G)	2,706 mcf	(φ)	12.5%
		(Sw)	25.0%

	Total	Oil	Gas
(h)(ht)	8.6	8.6	0.0
[Vb (ac-ft)]	2,175.20	2,171.52	3.68
[Vp (ac-ft)]	271.90	271.44	0.46
[Vphc (ac-ft)]	203.93	203.58	0.35

Reserves

	stbo	bpaf	Rf
[Np]	219,600	101.13	17.4%
[Nwf]	157,066	72.33	12.4%
[Nult]	376,666	173.46	29.8%
[N]	1,263,313	581.76	100.0%
[Gp]	504,036 mcf		
[G]	2,706 mcf		
[Wp]	0 bw		
[We]	0 bw		
(Rp)	2,295 scf/stb		
Nwf/Np	0.72 to 1		

Waterflood

(Vb flood)	1,492.10 ac-ft	(Vb flood)	68.7%
Inj Rate	1,000 bwpd	[Ea]	72.0%
(V fillup)	478,967 bw	[Ev]	72.0%
t fillup	1.31 yrs	[Ed]	42.5%
(Sor)	30.0%	[Et]	22.0%

Oil Column Conditions

	Initial	Current
[Sw]	25.0%	25.0%
[So]	75.0%	52.2%
[Sg]	0.0%	22.8%

Comments:

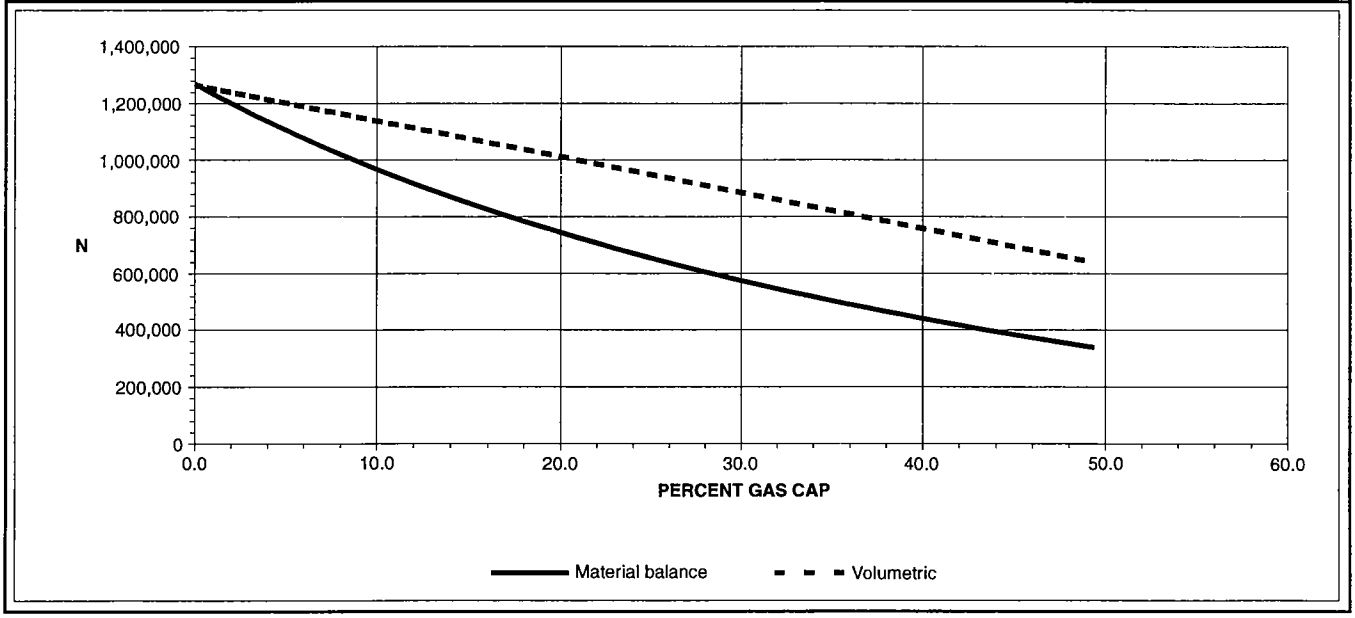

Figure 4. Example of a reservoir model used to evaluate a potential waterflood prospect. Circled variables were defined or discussed in the first workshop; bracketed variables will be discussed in this workshop. See Appendix 1 for explanation of abbreviations.

parameters necessary for a waterflood review will be highlighted in this series.

METHOD FOR ADDRESSING PRINCIPLES

The examples used in this workshop are those familiar to the author and those that have been contributed by operators for use in this publication. The practice of confidentiality will be observed for all examples. If readers wish to pursue additional information for any of the examples, they may contact the author, who will seek permission from the contributing operator to release data. A list of the abbreviations and definitions for these variables is included in Appendix 1.

ACKNOWLEDGMENTS

Sincere appreciation is extended to those individuals and companies who have contributed to the success of this workshop and publication:

I would like to thank the Petroleum Technology Transfer Council for their support in making this series of workshops possible; and to the Oklahoma Geological Survey, whose tireless dedication and encouragement as a group, was responsible for the quality and professionalism of these workshops. In particular, I would like to thank Rick Andrews and Jock Campbell, OGS geologists, whose encouragement lead to the origination of this workshop. I thank Wayne Furr, OGS manager of cartography, and Jim Anderson and Charlotte LLoyd, OGS cartographic drafting technicians, for their work on the figures and tables. To Christie Cooper, OGS editor, and William D. Rose, geologist/contract editor for their input and effort to the publication. Sincere appreciation is extended to Bill Jackson, geologist (Oklahoma City), William Cobb, William Cobb & Associates, Inc. (Dallas, Texas), and Lewis Boyce, Statco Engineering (Edmond, Oklahoma), for their review of the manuscript. I am especially grateful to Michelle Summers, OGS technical project coordinator, for her organization and support of the workshops. I am deeply grateful to Charles J. Mankin, director of the OGS, whose support and dedication to this project was responsible for its success.

I wish to thank the many companies and individuals who have contributed information, data, and advice to this publication. Due to the confidential nature of the case histories used, I cannot publicly acknowledge the names of those companies contributing reservoir information, but this thank you is directly expressed to them. I thank George Sutherland, operations engineer, retired (Mineral Wells, Texas), for his contribution to this workshop. Sincere appreciation is extended to Dan Wilson, geologist, Surtek, Inc. (Golden, Colorado), George Tew, Tew Testers (Perry, Oklahoma), Mark Sutherland, National Petrochem (Ada, Oklahoma), and Saleem Nizami, APEC, Inc. (Oklahoma City), for their technnical and professional contributions to this publication. I am especially grateful to David Crutchfield, reservoir engineer (Oklahoma City), for his dedication, support and contribution that made this publication possible.

And, I would like to thank my wife, whose contribution and support for this effort was appreciated more than she will ever know.

2

Definition of Terms

CHAPTER 2

Definition of Terms

INTRODUCTION

In the course of waterflood exploitation, geologists are usually responsible for the initial review and evaluation of the potential waterflood candidate. Various geological concepts and techniques, such as mapping and production evaluation including rock-property analysis, are employed to analyze the reservoir with the goal of providing the reservoir engineer an in-depth geological description of the waterflood candidate. In the case of the consultant geologist, the goal is to present a viable waterflood candidate to an interested company. The first workshop in this series (Rottman and others, 1998) attempted to highlight some of the basic facets of a review that a geologist would ordinarily undertake, plus a few of those problems that may be encountered concerning those facets.

The next important topic concerns the calculation of original oil in place (OOIP) and the estimation of expected secondary reserves to be recovered for the prospect. Geologists understand most of the basic criteria necessary for these calculations. However, the importance of estimating secondary production sometimes takes a back seat to the often misleading information based on the amount of primary production from the potential waterflood candidate. Thus, all too often, the amount of primary production simply is used as an indicator for the secondary-production potential of the waterflood. This general rule of thumb can lead to disastrous consequences for the company, because many factors that would otherwise be scrutinized to make an educated estimate of secondary reserves often go unheeded or ignored. Therefore, this workshop will be dedicated to the fundamental understanding of how much oil is in place, how much oil is available after primary production, and how much oil could be expected to be recovered from a cursory review. A majority of the fundamental concepts and principles of these topics will be reviewed for two reasons. First, geologists and engineers must be able to communicate with each other, which requires a knowledge and understanding of these common concepts and principles. This was the core of the problem with the geological department's evaluation and recommendations of the prospect to the engineering department in the case history presented in chapter 1. Not only did the geologists not understand some of these concepts and their potential effect on the waterflood candidate, but also the lack of communication between the two departments resulted in considerable wasted time and effort. The second reason that a geologist should be familiar with these concepts and principles is because they are constantly in effect during the origin, migration, and entrapment of hydrocarbons in sediments. Figure 5 is a graphical representation of this concept. The geologic time line of hydrocarbons can be summarized by three major events: origination, equilibrium, and depletion. Origination includes the creation of hydrocarbons and their subsequent migration and entrapment. All the concepts that will be discussed, such as permeability, formation volume factor, viscosity, and material balance, pertain to the reservoir and reservoir fluids during this development period. Therefore, it is critical that a geologist know and understand these rock and fluid properties. The second event illustrated in Figure 5 (point *B*) is termed *equilibrium* because the fluids within a reservoir are at equilibrium at the time of discovery. It is at discovery that we become involved with producing the hydrocarbons, and those same principles of permeability, formation volume factor, etc., take on an important role in maximizing production of those hydrocarbons. However, all the principles that an engineer needs to know for producing hydrocarbons are also important for a geologist to understand when interpreting how the fluids migrated and became trapped. A geologist's responsibility to the reservoir generally changes from a leadership role to a supporting role shortly after development of the field, whereas an engineer's role usually starts at discovery and continues to its depletion (point *C*). Thus, the geologist and engineer have an overlap of responsibility in the reservoir's development, requiring understanding and communication. The following terms described in this

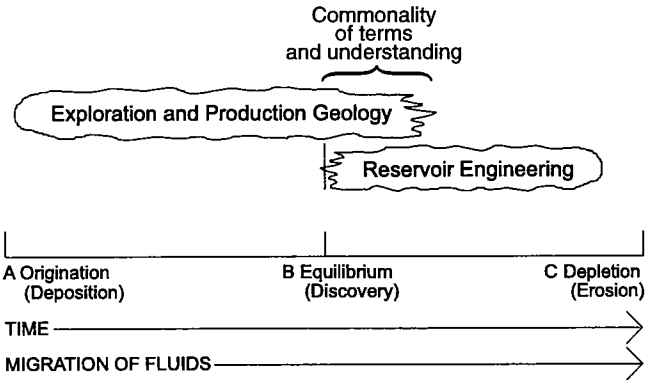

Figure 5. Time line of a reservoir: origination, equilibrium, and depletion. The geological and engineering departments' relative areas of primary influence are highlighted.

chapter are those necessary to understand OOIP and current oil saturation. Let us first describe the physical state between gas and oil in a reservoir.

SATURATED AND UNDERSATURATED RESERVOIRS

The solubility of natural gas in an oil column depends on pressure, temperature, and the composition of the oil and gas. As the composition of the gas approaches that of the oil, the solubility of the two increases. Likewise, if the pressure remains constant and the temperature increases, the amount of gas that can dissolve in oil decreases; and if the temperature remains constant and the pressure increases, the solubility between the oil and gas increases. Figure 6 illustrates two basic types of reservoirs found today that pertain to the relationship between oil and gas. Given a common temperature and pressure between these two reservoirs, both reservoirs contain oil with dissolved gas. When a slight pressure drop is equally applied to both reservoirs, a free-gas state develops in reservoir A by gas breaking out of solution. With this pressure drop, reservoir B remains completely liquid with no free-gas state. Reservoir A is said to be saturated with gas at this pressure. Because of the slight pressure drop with no associated release of free gas in reservoir B, reservoir B is said to be undersaturated at this pressure. What this implies is that the amount of gas dissolved in reservoirs A and B were not equal, with reservoir A containing more dissolved gas than reservoir B. Because of the constant pressure and temperatures, and assuming a similar composition of the gas and oil, it can be assumed that if additional gas were available to reservoir B it would become dissolved until the amount of dissolved gas is equal to that of reservoir A. It is also important to understand that reservoirs in an undersaturated state have no associated gas cap, and those reservoirs with a gas cap are saturated with respect to the current pressure and temperature conditions. As was discussed in the first workshop (Rottman and others, 1998), the amount of gas dissolved in oil is usually stated in terms of standard cubic feet of gas per stock-tank barrel of oil (SCF/STB). In this workshop, the initial solution gas/oil ratio (GOR, which can be similar in value to the produced GOR at discovery or at initial reservoir conditions) will be termed R_{si}. Figure 7 illustrates the changes of a reservoir's GOR from discovery to depletion.

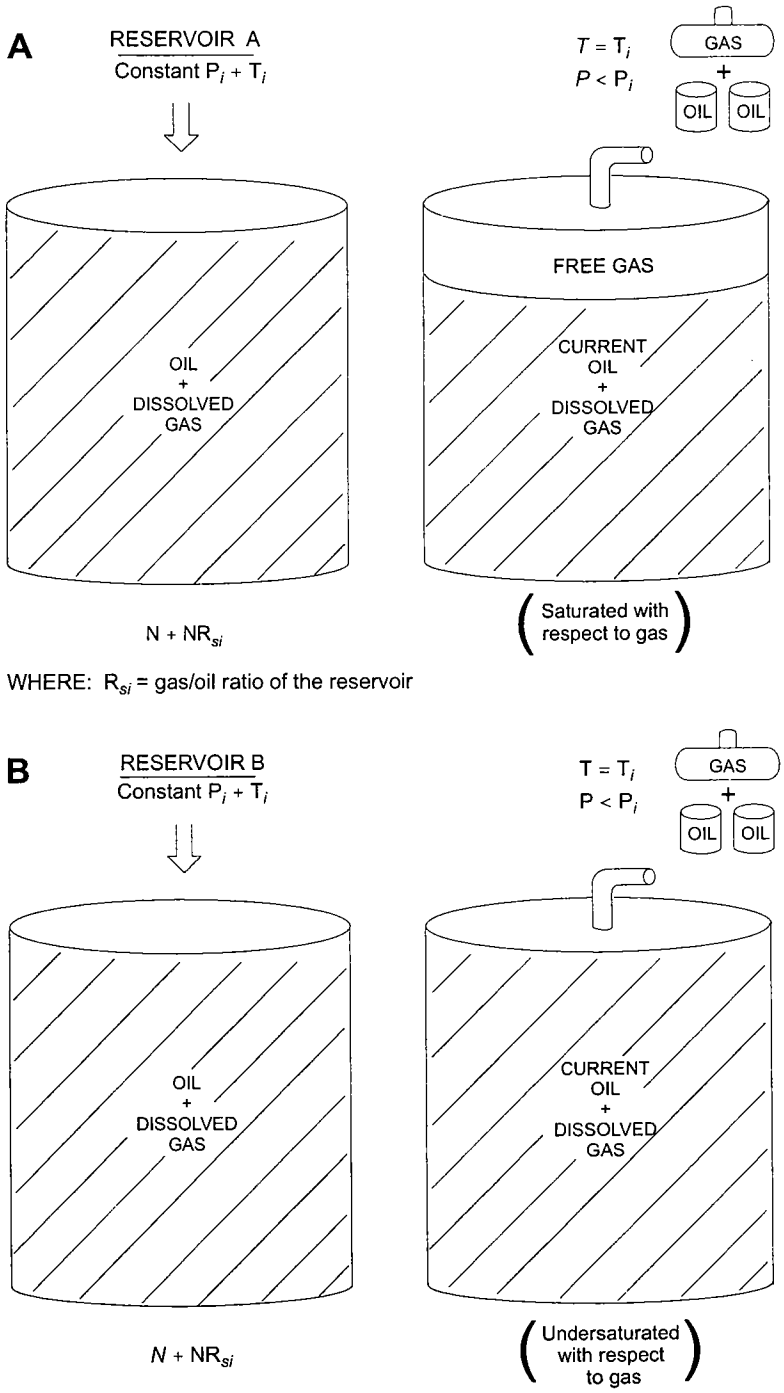

Figure 6. Two basic types of reservoirs that pertain to the relationship between oil and gas. (A) Saturated reservoir. (B) Undersaturated reservoir.

Figure 7A illustrates a reservoir composed of oil and dissolved gas. Because the reservoir is at initial conditions, the oil and gas are in equilibrium with each other, and the initial GOR, or R_{si}, is a constant. As production occurs and reservoir pressure starts to decline, gas breaks out of solution, lowering the solution GOR for the oil. The solution GOR at any time after production and prior to depletion is termed R_s, or the GOR at current conditions. At depletion, the reservoir's dissolved gas has almost completely dissolved from the oil, leaving primarily oil and free gas. A more exact way to describe the change in a reservoir's GOR for an un-

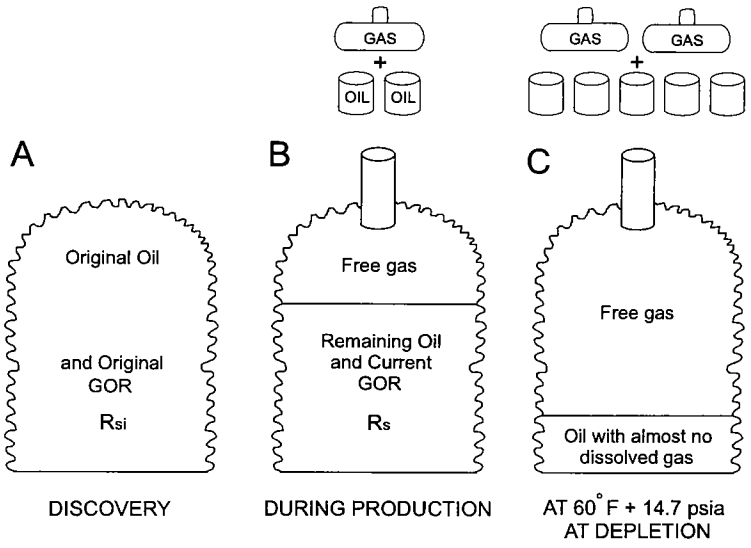

Figure 7. Changes that occur to a reservoir's gas/oil ratio (GOR) from discovery to depletion.

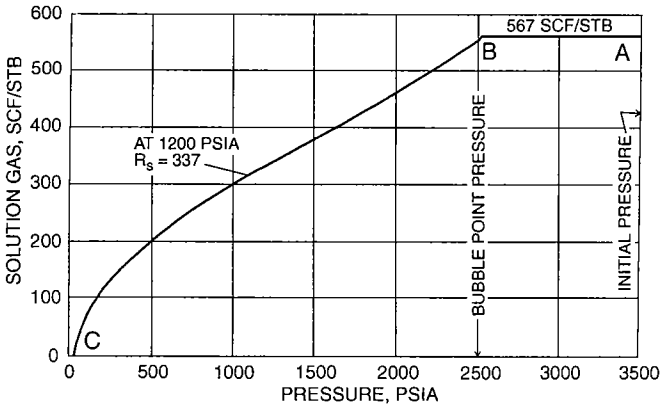

Figure 8. Solution gas to oil curve for Big Sandy field in eastern Kentucky. (Craft and Hawkins, ©1959, fig. 3.1; reproduced by permission of Prentice-Hall, Inc.)

dersaturated reservoir is seen in Figure 8. This figure is a graphical representation of the solution GOR versus pressure from the time of discovery (point *A*) to the time of depletion (point *C*). At discovery, the reservoir is at equilibrium, and the initial solution GOR, or R_{si}, is equal to approximately 567 SCF/STB. With production and a subsequent pressure drop, the solution GOR remains the same while production occurs, until the GOR starts to drop at a pressure of 2,500 psia (point *B*). Because the solution GOR did not change between points *A* and *B*, the reservoir is said to be undersaturated, and there is no free-gas phase within the reservoir as illustrated by the GOR and reservoir-oil relationship of reservoir B in Figure 6. When the pressure drops to approximately 2,500 psia, the solution GOR, now in a saturated condition, starts to drop because the gas is being liberated from the oil as a result of the gas having become saturated with respect to the relative amounts of oil and gas and the pressure, volume, and temperature (PVT) conditions within the reservoir. This oil and gas relationship is represented by reservoir B in Figure 6.

The pressure at which gas first starts to break out of solution is termed the bubble-point pressure for the reservoir. Thus, the bubble-point pressure for the reservoir in Figure 8 is 2,500 psia and is represented by point *B*. The solution GOR at the bubble-point pressure is also equal to the solution GOR at discovery, whose pressure was 3,500 psia, so the solution GOR in an undersaturated reservoir at any pressure above the bubble point will always be the same. In this particular example, the initial reservoir pressure is said to be above the bubble-point pressure of the reservoir. Most oil fields in Oklahoma have solution GOR versus pressure plots similar to that in Figure 9. This curve suggests that the discovery (initial) pressure (P_i) is close to the bubble-point pressure for the reservoir. With the slightest pressure drop within the reservoir, gas would break out of solution, thus incrementally lower-

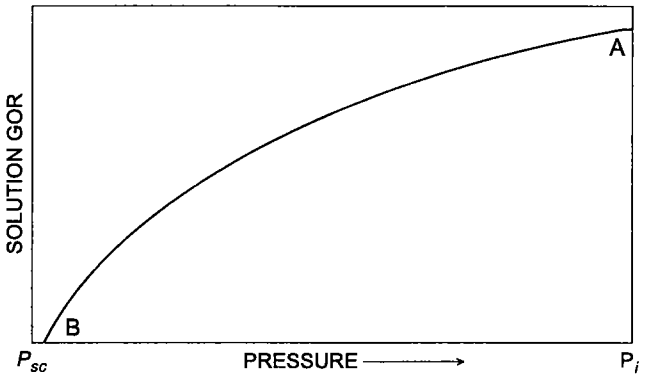

WHERE: P_{sc} = Pressure at standard conditions
P_i = Initial pressure

Figure 9. Typical GOR curve for reservoirs in Oklahoma.

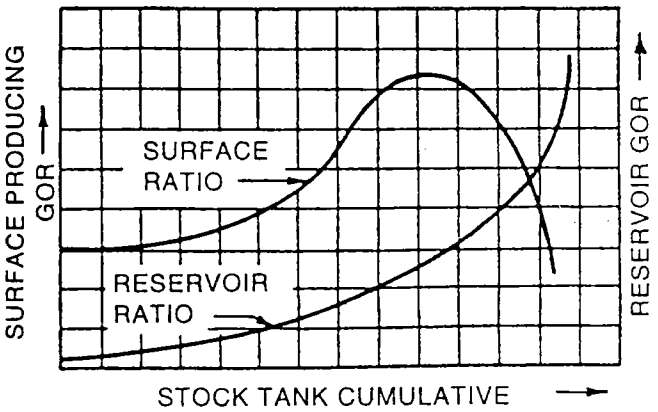

Figure 10. Typical solution surface and reservoir GOR curves for a solution-gas-drive reservoir. (Frick and Taylor, ©1962, fig. 29-16; reprinted by permission of Society of Petroleum Engineers.)

ing the solution GOR for the reservoir. These reservoirs are saturated at discovery pressure and temperatures. It should be noted that a reservoir's solution GOR should not be confused with the produced GOR as described in chapter 2 of the first workshop (Rottman and others, 1998). Figure 10 is from that publication and illustrates both the surface GOR (produced GOR) and the reservoir GOR plotted against stock-tank production.

Craft and Hawkins (1959) mention that variations in a reservoir's fluid properties are generally not large but do exist. These variations are often associated with large closures. Variations in the solution GOR values on the order of 25 SCF/BO per 100 ft of elevation were cited for the Tensleep reservoir of Elk Basin field in Wyoming and Montana (Fig. 11) and 25 to 46 SCF/BO per 100 ft of elevation for the Weber Sandstone of Rangely field, Colorado, and for the Scurry Reef field, Texas. These variations were suggested as occurring from (1) temperature gradients within the reservoir, (2) gravitational segregation, and (3) a lack of oil and gas equilibrium. The variations are significant and have an impact on the evaluation of the reservoir, as discussed in greater detail in subsequent sections. In Oklahoma, these variations exist, but probably not on as large a scale for reservoirs with low structural relief. An example of what may be considered segregation of the oil column can be interpreted from the data in Figure 12. This particular curve was generated by plotting the produced GORs for the first 23 wells of a reservoir in central Oklahoma. The produced GOR at point *A* is from the discovery well and was considered to represent the initial solution GOR for the saturated reservoir, which was also independently verified by laboratory evaluation. Notice the solution GORs for wells B–F, which were drilled between 9 and 20 months after completion of the discovery well. The reservoir in these wells was structurally lower by as much as 100 ft in comparison to the discovery well. These wells all have a slightly lower producing GOR, which may be a result of some of the factors listed above, especially gravity segregation. The solid line represents the best-fit solution GOR curve expected versus time of development for the reservoir.

FORMATION VOLUME FACTOR

Owing to the similarity of gas and oil compositions, gas can become readily soluble in oil. In fact, given an unlimited amount of pressure and available gas, the solubility of gas in oil is infinite (Craft and Hawkins, 1959). Figure 13 illustrates this concept. Frame A is composed of two phases, gas and oil at standard conditions at a temperature of 60°F and an atmospheric pressure of 14.7 psia. With an increase in pressure (Fig. 12B), part of the gas changes phase and becomes soluble in the oil. Thus, the physical volumetrics of the oil increase from addition of the soluble gas. In Figure 13C, all the available gas has dissolved in the oil with the increased pressure, and the oil has expanded to its largest volume. This pressure represents the

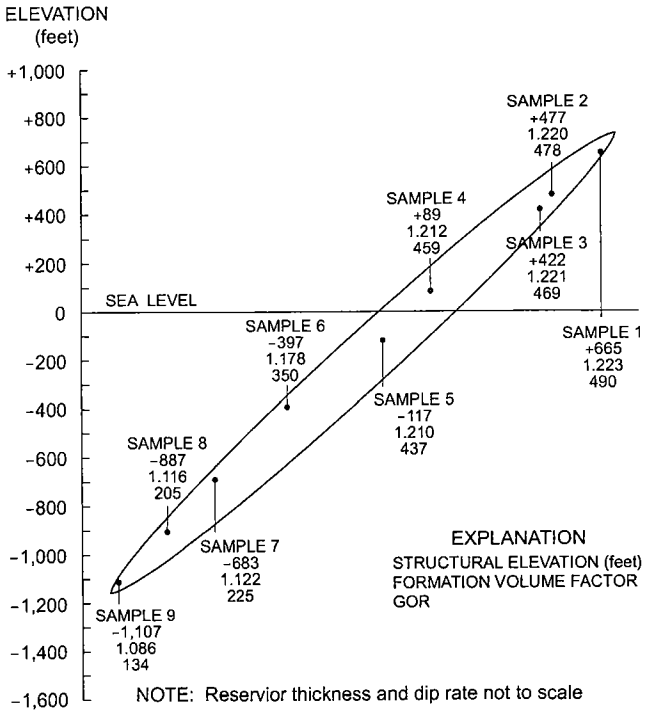

Figure 11. Variations of the formation volume factor and solution GOR for the Tensleep reservoir, Elk Basin field, Wyoming and Montana.

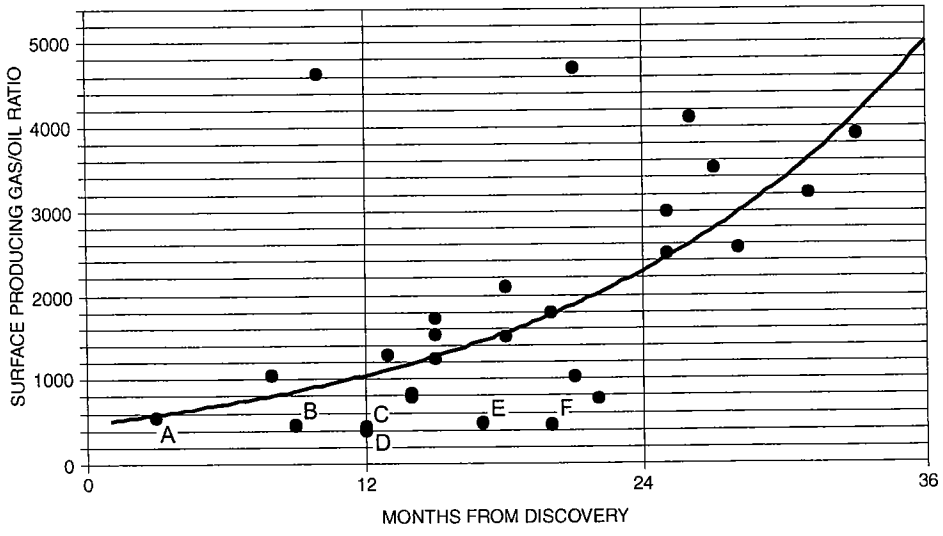

Figure 12. Plot of initial-potential (IP) GOR versus time for wells drilled in first 3 years of development for a reservoir in central Oklahoma. Wells B–F exhibit producing GORs lower than the discovery IP GOR (well A), possibly because of gravity segregation.

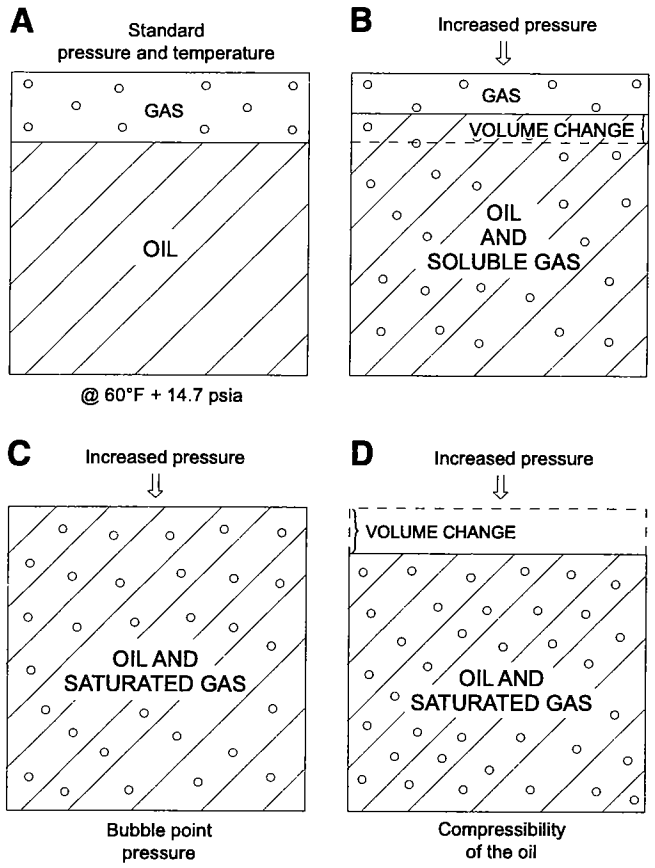

Figure 13. Changes between the phase relationship of free gas and oil in a reservoir with increasing pressure. (A) Free gas and oil at standard pressures and temperatures. (B) Increasing pressure forces some gas into solution. (C) All gas is dissolved at the bubble-point pressure. (D) Continued increase in pressure compresses the oil.

bubble-point pressure for the reservoir. This ratio of reservoir-barrel volume to stock-tank volume is termed the *formation volume factor* (FVF) for the oil and is represented by the symbol B_o. According to Craft and Hawkins (1959), the formation volume factor "at any pressure may be defined as the volume in barrels that one stock tank barrel occupies in the formation (reservoir), i.e., at reservoir temperature and with the solution gas which can be held in the oil at that pressure. Because both the temperature and the solution gas increase the volume of the stock tank oil, the factor will always be greater than one." Once the reservoir reaches the bubble-point pressure—that is, the point at which all the available gas has dissolved in the oil—a continued increase in pressure will actually start to decrease the volume of the oil owing to the compressibility of the oil (Fig. 12D). We will discuss implications of the compressibility of oil in subsequent chapters.

Figure 14 is a graphical representation of the FVF-versus-pressure plot and represents the same reservoir illustrated in Figure 8. At standard conditions, the FVF (B_o) is 1.0 BBL/STB. This implies that the volume of oil is the same at the surface as in the reservoir. With increasing pressure and the solution of free gas, the volume of the oil increases, as does the value of the FVF, until all the gas is dissolved. The FVF has increased to a value of 1.333 BBL/STB at 2,500 psia. This is the bubble-point pressure for the reservoir and is represented by the symbol B_{oB}. With increased pressure, the oil compresses to a factor of 1.310 BBL/STB owing to the compressibility of the oil. If this had been the condition at discovery, the formation volume factor of 1.310 would be termed the initial formation volume factor, or B_{oi}.

Gas reservoirs also have a formation volume factor; however, this is not covered in the present workshop. Gas FVFs (B_g), like oil FVFs, relate the volume of gas in a reservoir to the volume at the surface under standard conditions. Their units are measured in cubic feet of gas or barrels of reservoir volume per standard cubic foot of gas. Equation 2.1 of Figure 15 describes B_g. To understand the gas deviation factor (Z), one would have to first look at the Ideal Gas Law.

As a result of experiments with ideal gases, it was found that the relationship expressed by Figure 16A holds true where P_1, V_1, and T_1 are the pressure, vol-

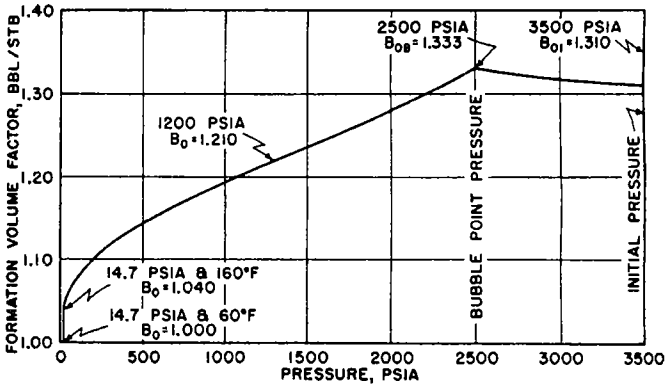

Figure 14. Graphical representation of the formation volume factor (FVF, B_o) versus pressure for the Big Sandy field, eastern Kentucky. (Craft and Hawkins, ©1959, fig. 3.2; reproduced by permission of Prentice-Hall, Inc.)

$$B_g = \frac{P_{sc}\, Z\, T}{T_{sc}\, P} \qquad \text{(eq 2.1)}$$

WHERE:

P_{sc} = Standard pressure of 14.7 psia

T_{sc} = Standard temperature measured in absolute temperature (which is 459.7°Rankine + 60°F

Z = Gas deviation factor

T = Absolute temperature of the reservoir

P = Absolute pressure of the reservoir

Figure 15. Equation used to calculate the gas FVF (B_g).

ume, and temperature of state 1, and P_2, V_2, and T_2 are the pressure, volume, and temperature of state 2. V_1 and V_2 may be measured in any comparable units, P_1 and P_2 may be measured in comparable units provided they are absolute pressures, and T_1 and T_2 may be measured in any comparable units provided they are absolute temperatures. An example of this relationship, illustrated in Figure 16B, demonstrates that if the temperature is constant—that is, T_1 and T_2 are equal—and if the volume of V_2 is half that of V_1, then P_2 would have to be twice P_1 for equilibrium to exist. However, in the realm of petroleum gases, this relationship does not hold true. For example, if the gas involved were natural

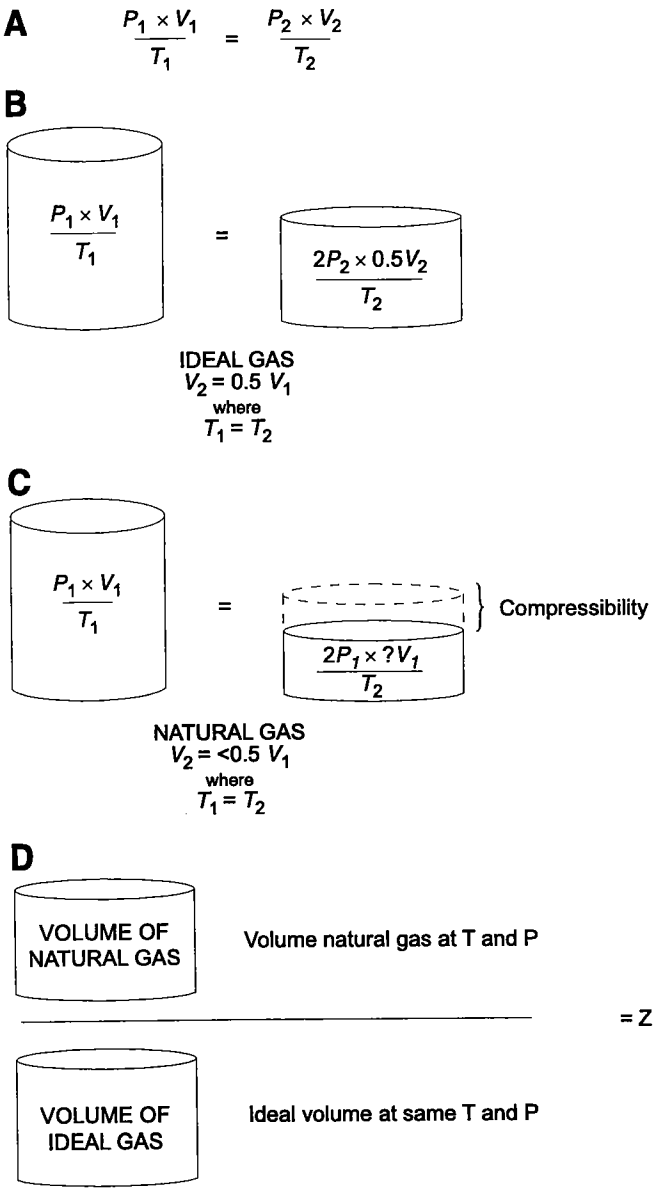

Figure 16. (A) Pressure, volume, and temperature relationship given in Craft and Hawkins (1959). (B) Graphical representation of Ideal Gas Law for ideal gases. (C) Graphical representation of Ideal Gas Law for natural gas. (D) Graphical definition of gas deviation factor.

A

$$B_g = \frac{14.7\ \text{psia} \times \left(\frac{V_A\ \text{CF}}{V_i\ \text{SCF}}\right) \times T\ ^\circ\text{F}}{(459.7 + 60)\ ^\circ\text{F} \times P\ \text{psia}} =$$

B

$$B_g = 0.02829\ \frac{ZT}{P}\ \text{CF / SCF}$$

$$1\ \text{BBL} = 5.614\ \text{CF}$$

C

$$B_g = \frac{0.02829\ \frac{ZT}{P}\ \text{CF / SCF}}{\frac{5.614\ \text{CF}}{\text{BBL}}} =$$

$$B_g = 0.00504\ \frac{ZT}{P}\ \text{BBL / SCF}$$

Figure 17. (A) Substitution of standard pressure (14.7 psia) and standard temperature (459.7°F) in equation 2.1 for B_g. (B) Hatch marks indicate simplification of the expression to illustrate the unit relationship. (C) Conversion of B_g from CF/SCF to BBL/SCF.

gas, decreasing the volume of V_2 by one-half will not double the pressure of P_2. In fact, the pressure will generally be less than twice as great, owing to the compressibility characteristics of natural gas (Fig. 16C). Craft and Hawkins (1959) state that the amount or number that gases deviate from the PVT relationships of ideal gases can be measured and is called the *super compressibility factor,* or *compressibility factor,* and is commonly called the *gas deviation factor,* whose symbol is *Z.* By definition, then, the gas deviation factor is the ratio of the volume actually occupied by a gas at a given pressure and temperature to the volume it would occupy if it behaved ideally as illustrated in Figure 16D. This dimensionless quantity usually varies between 0.70 and 1.20, with a value of 1.00 representing the behavior of ideal gases (Craft and Hawkins, 1959). There are many ramifications and uses for the *Z* factor, which are not dealt with in this workshop; however, the author recommends additional reading from either Craft and Hawkins (1959) or Slider (1983) for more information.

As mentioned previously, the units for volume in the Ideal Gas Law may vary, and thus the units for the *Z* factor may also change. In a two-phase system—that is, where free gas and oil are present—the units should be similar. Thus, the oil volume should be expressed in cubic feet, or the gas volume should be expressed in barrels. Figure 17A substitutes the values for standard pressure and temperature in equation 2.1. Reducing the equation results in the expression for B_g in Figure 17B. Figure 17C illustrates how the units of B_g can be modified from cubic feet per stock-tank barrel to barrels per standard cubic feet.

3

Material-Balance Determination of Original Oil in Place

CHAPTER 3

Material-Balance Determination of Original Oil in Place

INTRODUCTION

Material balance is essentially a method for calculating the oil in place in a reservoir using the conservation of mass or equating mass balance. Standing (1977) states that the term, "when applied to petroleum reservoir engineering, has come to mean a particular type of calculation. In fact, to many petroleum engineers, it connotes a particular equation proposed by Schilthuis in 1936. As the two words 'material' and 'balance' suggest, the calculations attempt to evaluate the quantity of 'material' present in the reservoir by maintaining a running 'volumetric balance' on the material remaining in the reservoir at any particular time during the depletion of the reservoir." Another way of stating this definition is that these equations are a method of equating masses of reservoir fluids, both in and out of the reservoir, at different times. However, it is generally easier to derive the equations by equating volumes of reservoir fluids at different times.

The object of describing material balance in this workshop is not to provide an in-depth, detailed study of the equations that are required for reservoir-engineering evaluations but to provide a cursory and fundamental background to the principles and ramifications that these equations have on rock and fluid properties from a geological viewpoint. Some basic assumptions must be clarified prior to developing material-balance formulas. One of the assumptions that will be used when working with the equation is that the pressure at any time during the depletion of the reservoir is distributed equally within the reservoir. This assumption does not really occur during production; however, treating the reservoir as tank type for analysis purposes accurately predicts the behavior of the reservoir, given accurate pressure and production data for the reservoir (Standing, 1977). Also, fluid-flow characteristics are not dealt with in this workshop. The material-balance equation derived simply will provide information on performance or cumulative production as a function of the average pressure in the reservoir. And finally, a general material-balance equation will be derived that may be applicable to any hydrocarbon reservoir. However, all the variables involved in the equation may not be necessary or relevant at the same time.

Many aspects are involved with the material-balance equation. This workshop is intended to highlight the geological significance involved with each aspect of the equation. There are also many derivatives of the equation that will not be touched on here, it being the intent of the author to cover enough of the equation to allow geologists, operators, and field personnel to gain a basic understanding of the underlying principles. The equation will be derived in the simplest manner possible, and its basic terms have been predefined in this writing and in the previous workshop (Rottmann and others, 1998). The various reservoir types described are used simply as a means to derive various portions of the formula and not to imply that there is a different formula for each type of reservoir. Thus, all the changes and interactions that occur to the variables of the equation during production within a reservoir can be handled by one equation.

GAS-RESERVOIR MATERIAL-BALANCE EQUATION

Perhaps the simplest material-balance equation is that for a dry-gas reservoir. It simply states that the mass of gas in place initially is equal to the mass of gas remaining plus the mass of gas produced. Another way of stating the equation in terms of balance of volume is that the volume of the original gas in place at reservoir conditions is equal to the volume of the gas remaining in the reservoir at the new pressure–temperature conditions after the gas has been produced. This equation assumes no oil-influx drive, and a pore-volume change with pressure loss at zero.

Figure 18A is the material-balance equation for a dry-gas reservoir. In the equation, G represents the original gas in the reservoir, and B_{gi} is the gas formation volume factor (FVF) at the original pressure and temperature of the reservoir. The amount of gas (G) multiplied by the FVF for the gas, as determined by the reservoir parameters, results in a specific volume of gas at reservoir pressure and temperature. G_p, on the right side of the equation (Fig. 18B) represents the amount of gas produced, which implies that a pressure drop from production must have occurred. Since the pressure has dropped and the amount of gas has decreased by the amount G_p, the remaining gas in the reservoir would have to expand in order to occupy the same volume as GB_{gi}. Thus, B_g would have to be a larger number than B_{gi} for this relationship to hold true. The relationship between the gas FVFs and pressure can be seen in Figure 19. The curves referenced by point A are

A $G B_{gi} = (G - G_p) B_g$ (eq. 3.1)

B

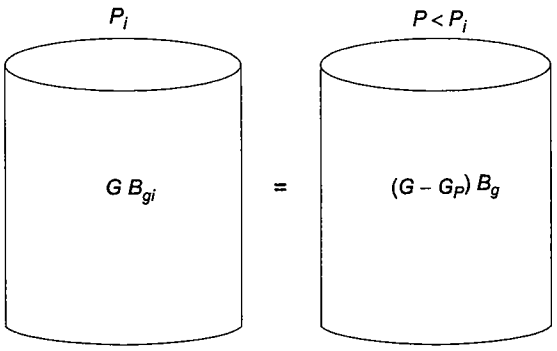

WHERE:
G = Total gas
B_{gi} = Initial gas FVF
G_g = Gas produced
B_g = Current gas FVF
P_i = Initial pressure
P = Current pressure

C (Total gas)(Initial gas FVF) = [(Total gas - Produced gas) × (Current gas FVF)]

D SCF × RESERVOIR BBL / SCF = (SCF – SCF) × RESERVOIR BBL / SCF

~~SCF~~ × RESERVOIR BBL / ~~SCF~~ = ~~SCF~~ × RESERVOIR BBL / ~~SCF~~

RESERVOIR BBL = RESERVOIR BBL

Figure 18. (A) Material-balance equation for dry gas and no fluid entry. (B) Graphical representation of A. (C) Descriptive account of equation 3.1. (D) Unit relationship of equation 3.1.

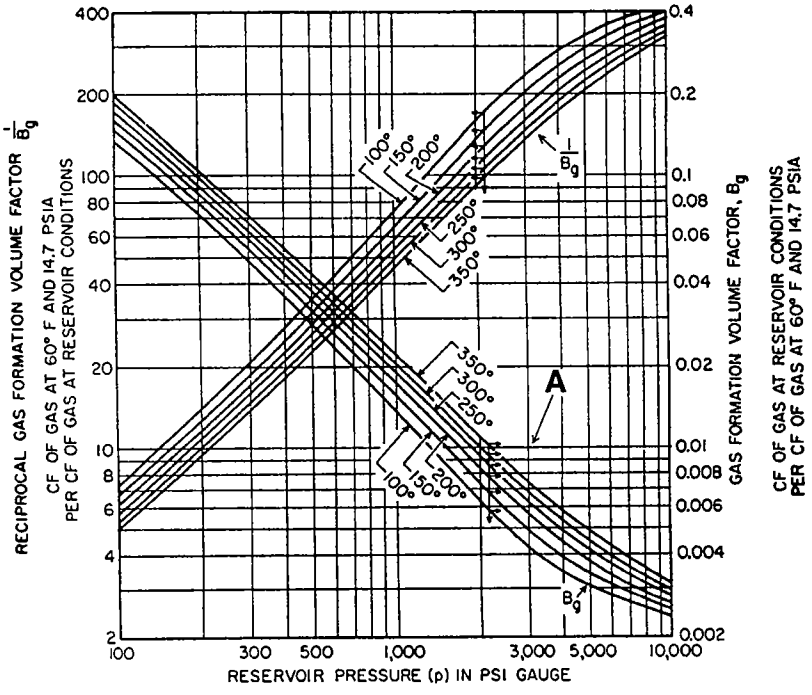

Figure 19. Plot of gas FVF at various temperatures for a gas whose specific gravity is 0.60 versus pressure. (Modified from Frick and Tayler, ©1962; reprinted by permission of Society of Petroleum Engineers.) See text for further explanation.

the gas FVF curves for a gas at various reservoir temperatures and whose gas gravity is equal to 0.6, with air being 1.0. Notice that as pressure declines, the gas FVF increases for any B_g value on any of the curves. Therefore, in the equation of Figure 18A, if production has occurred and pressure declined, B_g would have to be a larger number than B_{gi} for the equation to be equal. Figure 18C is a descriptive account of the equation. Figure 18D illustrates the units of the equation and the volumetric equality implied. Original gas and produced gas are in standard cubic feet, and B_{gi} and B_g are in reservoir barrels per standard cubic feet. When the variables are multiplied together, the standard-cubic-feet units are nullified, leaving the result of the equation as reservoir barrels (of the original gas) equaling reservoir barrels (of the current gas). Thus volume equates to volume.

Equation 3.1 can easily be modified to account for volume changes of the gas cap if the gas cap is in contact with an active water column or oil column. Figure 20A represents a formula modification to equation 3.1 (Fig. 19), owing to water encroachment from a water drive, by adding the term $(W_e - W_p)$, which is the net encroached water in the gas cap and is described as water entry (W_e) minus water produced (W_p). In this scenario, the net water enters the gas cap and occupies the pore space originally occupied by the produced gas of the gas cap. Thus, as Figure 20B implies, the original volume, GB_{gi}, is now being occupied by the volume $(G - G_p)B_g$ at the current pressure and current gas FVF plus the volume of the encroached water. If the pressure in the reservoir remains constant even with production, B_{gi} would be equal to B_g. Figure 20C illustrates the descriptive account for this formula, with part D illustrating the units involved. Factoring the equation results in reservoir barrels equaling reservoir barrels.

When gas-cap expansion is considered for a gas reservoir, the change in gas-cap volume can be a result of either production from the oil column with no gas breakthrough (where G_{pc} would be equal to zero and G_{pc} is defined as gas production from the gas cap) or production from the oil column and the gas cap. Figure 21A represents the equation for the change in gas-cap volume from gas-cap expansion. The equation simply states that the ex-

A $$G B_{gi} = (G - G_p) B_g + (W_e - W_p) \quad \text{(eq. 3.2)}$$

B

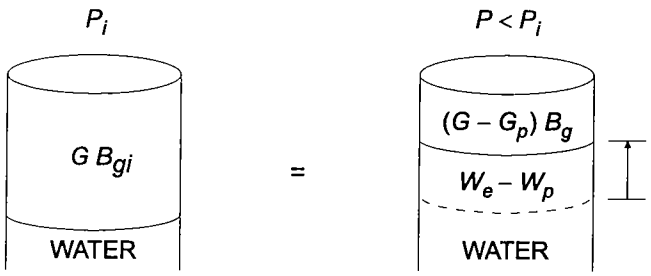

WHERE:
W_e = Water entry
W_p = Water produced

C (Total gas)(Initial gas FVF) = [(Total gas – Produced gas) × (Current gas FVF)] + (Water entry – Water produced)

D SCF × RESERVOIR BBL / SCF = (SCF - SCF) × RESERVOIR BBL / SCF + RESERVOIR BBL – RESERVOIR BBL)

~~SCF~~ × RESERVOIR BBL / ~~SCF~~ = ~~SCF~~ × RESERVOIR BBL / ~~SCF~~ + RESERVOIR BBL

RESERVOIR BBL = RESERVOIR BBL

Figure 20. (A) Material-balance equation for a gas reservoir, including volumetric changes from water entry. (B) Graphical representation of equation 3.2. (C) Descriptive account of equation 3.2. (D) Unit relationship of equation 3.2. See text for further explanation.

pression $(G - G_{pc})B_g$ represents the current volume of the gas cap, which is larger than the original volume (GB_{gi}) of the gas cap. Thus, the change in gas-cap volume is equal to the smaller initial gas-cap volume minus the larger current gas-cap volume. This results in a negative number. Equation 3.3 of Figure 21C is the material balance for a gas reservoir influenced by gas-cap expansion and simply states that the initial gas-cap volume is equal to the current gas-cap volume plus the change in gas-cap volume. Since the current gas-cap volume is larger than the initial gas-cap volume, adding the change in the gas-cap volume (a negative number) brings the left and right sides of the equation to equality. Figure 21D represents the terms for the equation, and Figure 21E illustrates the mathematical relationship of the units involved.

MATERIAL BALANCE FOR OIL RESERVOIRS ABOVE THE BUBBLE POINT (UNDERSATURATED)

The next type of reservoir we will look at with respect to the general material-balance equation is an undersaturated reservoir whose initial pressure is above the bubble point. For the purpose of developing a general material-balance equation, let us make the following assumptions. First, the production associated with pore-volume changes, or compressibility of the matrix as internal fluid pressures decrease, will be ignored. This concept can actually be a significant drive mechanism and is explained in more detail in following chapters. Second, this formula assumes no water encroachment. Reservoirs with no water encroachment and minimal compressibility changes are termed constant-volume or volumetric reservoirs. Third, this formula assumes that the average reservoir pressure is uniform and above the bubble point for the oil. The fourth assumption is that the solubility of gas is low in the formation water and is considered negligible. The fifth assumption is that the reservoir is initially undersaturated, which means there is no gas cap and the reservoir fluid basically consists of formation water and oil plus the oils associated with solution gas. The sixth and last assumption is that water production is minimal and will be considered zero.

Points *A* to *B* of Figure 22 illustrate where on the formation GOR curve this formula applies. As mentioned previously, the formation GOR is constant for any pressure above the bubble-point pressure in an undersaturated reservoir. Also, the value of the FVF is largest at the bubble-point pressure (P_{BP}). With increased pressure and subsequent compressibility of the oil, the value decreases until the initial pressure at discovery (virgin reservoir pressure) is obtained, resulting in the value B_{oi} (point *A* on the FVF curve). With the assumptions previously mentioned, a material-balance equation for an oil reservoir above the bubble point, which is similar to that of a dry-gas reservoir, can be written as illustrated in Figure 23A. The term NB_{oi} refers to the volume of initial oil in place measured in stock-tank barrels times the value of the FVF at the initial pressure. Multiplying the stock-tank barrels by the FVF gives the volume of the oil measured in reservoir barrels. This type of reservoir will produce by liquid expansion owing to the drop in reservoir pressure and the decompression of the oil. The expansion of the oil can be seen mathematically by examining the value of the FVF from point *D* to point *E* in Figure 22 as pressure in the reservoir drops. The reservoir oil pore volume would remain a constant, assuming negligible rock and compressibility effects, as seen on the right side of the equation of Figure 23B. The expansion of the oil occupies the entire volume by multiplying the remaining oil $(N - N_p)$ by the larger FVF. The pictorial representation of equation 3.4 (Fig. 23B) shows that the volume of the original oil times the original FVF is equal to the current volume of the oil, which by definition is the original oil minus the produced oil $(N - N_p)$ times the FVF at current pressure conditions of the reservoir. Figure 23C is a descriptive

A Change in gas-cap volume = $G\,B_{gi} - (G - G_{pc})\,B_g$ (eq. 3.3)

B

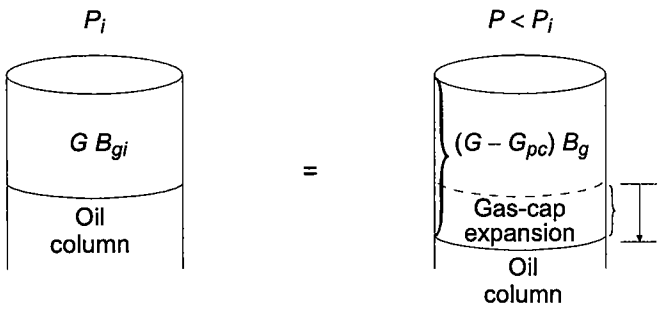

WHERE:

C $G\,B_{gi} = (G - G_{pc})\,B_g + (G\,B_{gi} - (G - G_{pc})\,B_g)$ (eq. 3.3)

Initial gas-gap volume = Current gas-cap volume + Change in gas-cap volume

D Change in gas cap = (Total Gas × Initial gas FVF) – [(Total gas – Gas produced) (Current gas FVF)

E Reservoir BBL = (SCF × Reservoir BBL / SCF) – (SCF – SCF) (Reservoir BBL / SCF)

Reservoir BBL = (~~SCF~~ × Reservoir BBL / ~~SCF~~) – ~~SCF~~ × Reservoir BBL / ~~SCF~~

Reservoir BBL = Reservoir BBL

Figure 21. (A) Equation for defining the change in gas-cap volume. (B) Graphical representation of change in gas-cap volume. (C) Material-balance equation for a gas reservoir influenced by gas-cap expansion. (D) Descriptive account of equation 3.3. (E) Unit relationship of equation 3.3.

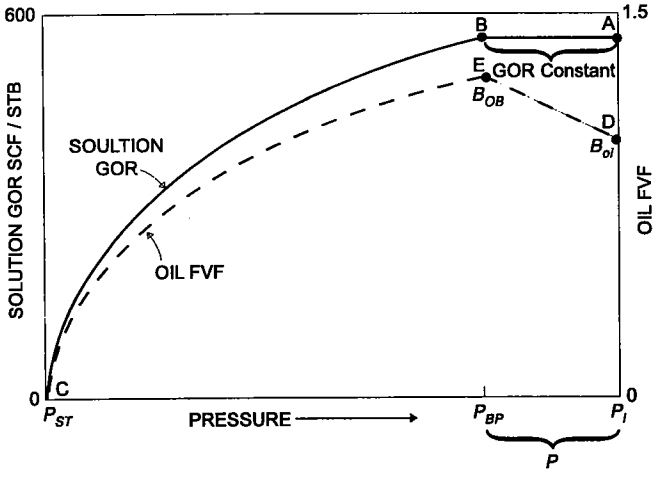

WHERE: $P_{BP} < P < P_I$
$B_{OB} < B_{BC} < B_{oi}$

B_{BC} = Current FVF
B_{OB} = Bubble-point FVF
B_{oi} = Initial FVF
P_{BP} = Bubble-point pressure
P = Current pressure (above the Bubble Point)
P_I = Initial pressure
P_{ST} = Pressure at stock tank conditions

account of equation 3.4. Figure 23D demonstrates the mathematical relationship of the units involved and shows that the formula is essentially equating volumes of reservoir barrels of fluids. Gas is produced along with the oil at the surface, although within the reservoir a free-gas state does not exist because the pressure of the reservoir is above the bubble point, and the gas remains in solution. Gas does not break out of solution, at least theoretically, until the pressure drops below the bubble point in the production string as the oil approaches the surface. The amount of gas produced is equal to the GOR (R_s) of the reservoir times the amount of oil produced, assuming that all the gas breaks out of solution (Fig. 23E). The phrase *gas in solution* is used to define the occurrence of a phase change when, owing to a pressure drop, liquid hydrocarbons change phases and form gaseous hydrocarbons with similar compositions.

One of the primary uses of the material-balance equation is in calculating the original oil in place (OOIP) for a reservoir. Equation 3.5 from Figure 24 solves equation 3.4 for the value N, which is the original oil in place. Thus if the produced oil is known, and If B_o and B_{oi} are known, it is possible to calculate the OOIP by using equation 3.5. Also, the fractional recovery (r), which is defined as the produced oil divided by the OOIP, can be calculated, given these variables, by mathematically rearranging equation 3.5 to the form of equation 3.6. The fractional recovery can now be expressed as a fraction of the produced oil in stock-tank barrels to the initial stock-tank oil in place that has been produced, or as the difference of the current FVF minus the original FVF divided by the current FVF. This relationship holds true for those conditions where the pressure remains above the bubble point.

MATERIAL BALANCE FOR OIL RESERVOIRS AT OR BELOW THE BUBBLE POINT (SATURATED)

Most reservoirs in the Midcontinent, when discovered, are at or very near the bubble point, which is point *B* in Figure 22. This implies that a slight reduction of reservoir pressure, from production, will allow free gas to break out of solution, and the reservoir GOR will start to decrease along with the oil FVF. Thus the reservoir, with respect to the dissolved gas, is termed *saturated.* Assuming the lack of free gas from a gas cap, and with water entry and water production minimal and no pore-volume changes with pressure drop, the

Figure 22 *(left).* Plot of FVF and solution GOR curve for a hypothetical undersaturated oil reservoir above the bubble point.

A $N B_{oi} = (N - N_p) B_o$ (eq. 3.4)

B

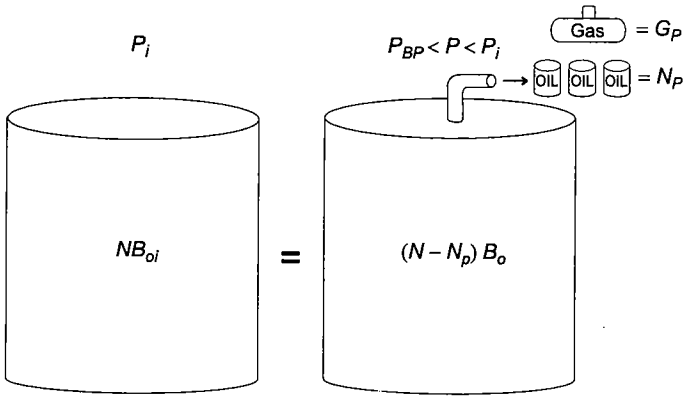

WHERE:
P_{BP} = Bubble-point pressure
N = Original oil in place
B_{oi} = Initial oil FVF
N_p = Produced oil
B_o = Current oil FVF

C (Original oil)(Initial oil FVF) = [(Original oil – Produced oil)(Current oil FVF)]

D STB × Reservoir BBL / STB = (STB – STB) × (Reservoir BBL / STB)

~~STB~~ × Reservoir BBL / ~~STB~~ = ~~STB~~ × (Reservoir BBL / ~~STB~~)

Reservoir BBL = Reservoir BBL

E Gas produced = $G_p = N_p R_s$ Total oil produced × Solution GOR for the oil produced

Figure 23. (A) Material-balance equation for an undersaturated reservoir above the bubble point. (B) Graphical representation of equation 3.4. (C) Descriptive account of equation 3.4. (D) Unit relationship of equation 3.4. (E) Descriptive account of gas produced.

volume of the reservoir at initial condition is represented by the variable V_{oi} in equation 3.7 of Figure 25A. V_{oi} is equal to the volume of oil (V_o) plus the volume of gas (V_g). This is illustrated pictorially by the left side of Figure 25B. The original oil is saturated with gas and represented by NR_{si}, which states that the amount of saturated gas is equal to the original oil (N) times the initial GOR (R_{si}). With a pressure drop from production, gas starts to break out of solution from the single-phase saturated oil volume such that the reservoir now contains two phases and two volumes of fluids, oil and gas, as defined on the right side of equation 3.7 from Figure 25A. The volume of the oil phase (V_o) plus the volume of the free-gas phase (V_g) is equal to the volume of the initial saturated oil (V_{oi}). How does one determine the volume of the free gas in the reservoir? Figure 25C is a descriptive expression for determining the free gas and states that the free gas in a reservoir, in standard cubic feet, is equal to the original gas in solution (represented by NR_{si}) minus the current gas in solution (represented by N_pR_p) and the amount of the produced gas (represented by N_pR_p). Equation 3.8 of Figure 25D represents this relationship. A knowledge of the gas in solution, or GOR at various pressures, is needed to calculate this equation. Figure 25E represents the units involved for equation 3.8.

Equation 3.7, which is an equation for the volume of the reservoir and is represented by the summation of the volumes of oil and gas (of Fig. 25) can now be modified as shown in equation 3.9 of Figure 26 by substituting the previously derived expressions for current oil (right side of equation 3.4) and free gas (equation 3.7). Equation 3.9 states that the volume of the initial oil (NB_{oi}) is equal to the volume of the remaining or current oil after production, $(N - N_p)B_o$, plus the volume of the free gas (G_F). We can now substitute equation 3.8 for the value of the free-gas phase represented by G_FB_g in equation 3.9 to form equation 3.10, which is the material-balance equation for a reservoir at or below the initial bubble-point pressure, assuming that the parameters at the beginning of this section are in effect. Because geologists and engineers are concerned with the volume of OOIP, equation 3.10 can be solved for N as seen in equation 3.11 of Figure 26C. Once equation 3.11 has been solved for N, it is possible to determine the fractional recovery, r, for the reservoir (Fig. 26D). The fractional recovery, r, is equal to the produced oil divided by the OOIP, or equation 3.12 of Figure 26, and can be expressed in terms of produced oil and OOIP or as current and original gas and oil FVFs and solution GORs. Figure 27 is a plot of fractional recovery, or the percentage of oil produced versus pressure. The average recovery factors are shown for the three primary drive mechanisms. Gas-cap-drive and water-drive mechanisms make highly inefficient waterflood candidates because their recovery factors

Original oil in the reservoir	$= N B_{oi} = (N - N_p)B_o$	(eq 3.4)
Original oil STB	$= N = \frac{B_o N_p}{B_o - B_{oi}}$	(eq 3.5)
Fractional recovery	$= r = \frac{N_p}{N} = \frac{B_o - B_{oi}}{B_o}$	(eq 3.6)

Note: For conditions above bubble point pressure

Figure 24. Solving equation 3.4 of Figure 23 for the value N (original oil in place). Equation 3.6 defines the recovery factor for production above the bubble point in terms of the formation volume factors B_{oi} and B_o.

A $V_{oi} = V_o + V_g$ (eq. 3.7)

WHERE: $V_g = G_F B_g$

G_F = Free gas in the reservoir

B

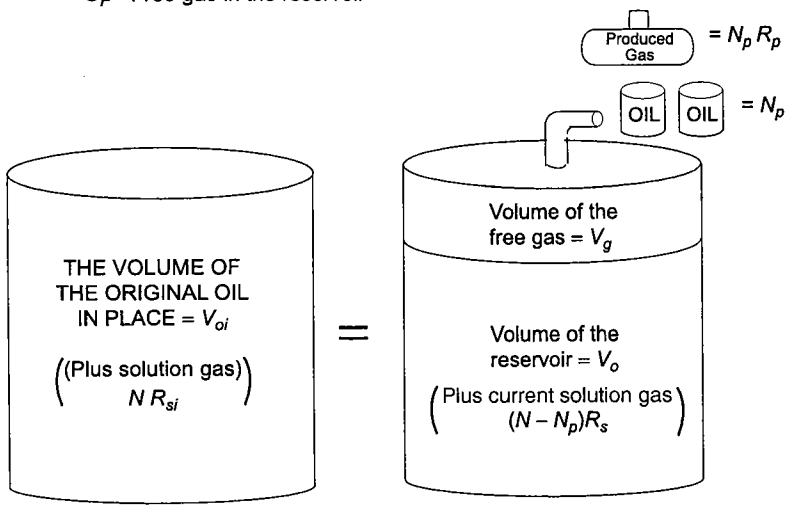

WHERE:

V_{oi} = Volume of the original saturated oil

V_o = Volume of the oil phase

V_s = Volume of the gas phase

$N R_{si}$ = Amount of gas in solution

$(N - N_p)$ = Gas remaining in solution after production of N_p

C Free gas = V_g = Initial gas – Solution gas – Produced gas

D $G_F = N R_{si} - (N - N_p)R_s - N_p R_p$ (eq. 3.8)

WHERE:

R_{si} = Original gas to oil ratio

R_s = Current gas to oil ratio in reservoir

R_p = Produced gas to oil ratio

E G_F = (STB × SCF / STB) – (STB – STB) SCF / STB – (STB × SCF / STB)

G_F = (~~STB~~ × SCF / ~~STB~~) – (~~STB~~ × SCF / ~~STB~~) – (~~STB~~ × SCF / ~~STB~~)

G_F = SCF

Figure 25. (A) Equation for the total hydrocarbon pore volume of a saturated reservoir. (B) Graphical representation of equation 3.7. (C) Descriptive account of free gas in the reservoir. (D) Equation for defining free gas in a reservoir. (E) Unit relationship of equation 3.8.

are so high and they have little mobile oil remaining. Solution-gas-drive ratios in the range of 12–20% represent viable targets for waterflood candidates because the amount of mobile oil remaining and available for secondary-recovery operations is a significant percentage compared to that of other drive types.

One important observation should be made at this point. The variable R_p in equation 3.12 of Figure 26 is the net cumulative produced GOR for the reservoir. Because this variable is in the denominator, it stands to reason that the larger the cumulative GOR is, the smaller the fractional recovery will be. As an example, case 1 and case 2 of Figure 28 represent fluid properties for a hypothetical reservoir to illustrate the effects that either a high or a low produced GOR has on the recovery factor of a reservoir.

Case 1 represents an example in which the gas has been produced with no effort either to shut in the gas wells or to re-inject the gas. Therefore, the cumulative GOR for the example is 3,200 SCF/STB of oil produced. The variable R_p, which represents the cumulative produced GOR, is in the denominator, and the cumulative produced GOR minus the current GOR represents a value of 2,450. By completing the formula, the recovery factor turns out to be 4.3%.

Case 2 represents an example in which two-thirds of the original solution gas remains in the reservoir ei-

A $N B_{oi} = (N - N_p) B_o + G_f B_g$ (eq 3.9)

WHERE: $G_F = N R_{si} - (N - N_p)R_s - N_p R_p$ (eq 3.8)

$N B_{oi} = (N - N_p)B_o + [N R_{si} - (N - N_p)R_s - N_p R_p]B$ (eq 3.10)

B Volume of reservoir initial oil = Volume of current oil + [Volume of initial gas – Volume current solution gas – Volume produced gas]

C $N = \dfrac{N_p [B_o + B_g (R_p - R_s)]}{B_o - B_{oi} + B_g (R_{si} - R_s)}$ (eq 3.11)

D Fractional recovery $= r = \dfrac{N_p}{N} = \dfrac{B_o - B_{oi} + B_g (R_{si} - R_s)}{B_o + B_g (R_p - R_s)}$ (eq 3.12)

Figure 26. (A) Equation 3.9 represents the total volume of the reservoir as the sum of the current oil plus the free gas. Material-balance equation for a reservoir at or below the bubble point. (B) Descriptive account of the material-balance equation for a reservoir below the bubble point. (C) Equation 3.10 solved for the value N. (D) Equation for the fractional recovery represented by production and OOIP or in terms of oil and gas FVFs and current OIP and OOIP.

ther by re-injecting the produced gas or by shutting in the high gas producers at the same pressure at which the B_o was determined. The cumulative produced GOR from this method results in a value of only 1,066 SCF/STB. Subtracting the initial GOR value of 750 from 1,066 results in a value of only 316, which is considerably less than 2,450 for case 1. By solving the equation of case 2, the recovery factor is 10.7%, which is almost 2.5 times as great as the production from case 1. This case should illustrate how much more effective a gas-drive reservoir is than a solution-gas-drive reservoir. Case 1 is strictly a solution-gas-drive reservoir. By re-injecting the gas, or by shutting the high-GOR wells in, case 2 represents a gas-drive mechanism. The increased recovery factor for primary production represents a portion of the oil that cannot be recovered from a waterflood standpoint.

Case history 30 of the first workshop (Rottmann and others, 1998, p. 100–101) presents an excellent example of this principle. Figure 29 illustrates the decline curve for a reservoir under consideration as a waterflood prospect in north-central Texas. Several miles to the north, a reservoir in the same formation with almost identical rock and fluid properties had been successfully waterflooded; its production curve is illustrated in Figure 30. The assumption was that because the reservoir to the north had successfully responded to water injection, the prospect represented by the decline curve of Figure 29 should also be a viable candidate. The recovery factor for the analogy to the north was 13.7%, which is typical for a solution-gas-drive reservoir. However, when the evaluators of the prospect determined the recovery factor for the candidate, it turned out to be over 22%. This is a considerable discrepancy when comparing recovery factors from two identical reservoirs producing under assumed similar circumstances. Further investigation of the waterflood candidate represented by the production curve of Figure 29 revealed that all the wells with high gas saturation had been shut in and that the operator had employed the practice of perforating and completing the oil wells only from the very bottom of the porous reservoir. In fact, it was learned later that the field had a gas cap, which effectively expanded, driving oil to the

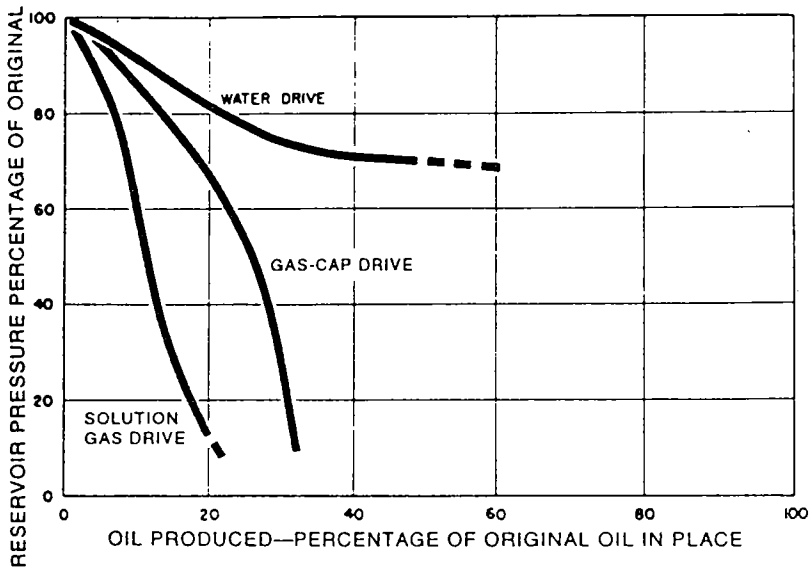

Figure 27. Plot of percentage of oil produced versus pressure for water-, gas-cap-, and solution-gas-drive reservoirs. (Clark, 1969, fig. 69; reprinted by permission of American Petroleum Institute.)

A

$$r = \frac{N_p}{N} = \frac{B_o - B_{oi} + B_g (R_{si} - R_s)}{B_o + B_p (R_p - R_s)} \qquad \text{(eq 3.12)}$$

WHERE:

N_p = Cumulative production
N = Original oil in place
B_o = Current oil formation volume factor = 1.450 SCF / STB
B_{oi} = Initial oil formation volume factor = 1.510 SCF / STB
B_g = Current gas formation volume factor = 0.00103 BBL /SCF
R_{si} = Initial reservoir GOR = 950 SCF / STB
R_s = Current reservoir GOR = 750 SCF / STB
R_p = Net cumulative produced GOR = 3,200 SCF / STB

B

CASE 1. $r = \dfrac{1.450 - 1.510 + 0.0013\,(950 - 750)}{1.450 + 0.0013\,(3{,}200 - 750)}$

$r = \dfrac{0.2}{1.450 + 3.185}$

$r = 0.043$

$r = 4.3\%$

C

CASE 2. (Where two-thirds of gas is reinjected) and R_p = 1,066 SCF / STB

$r = \dfrac{1.450 - 1.510 + 0.0013\,(950 - 750)}{1.450 + 0.0013\,(1{,}066 - 750)}$

$r = \dfrac{0.2}{1.450 + 0.4108}$

$r = 0.107$

$r = 10.7\%$

Figure 28. (A) Equation 3.12, defining recovery factor. (B) Case 1. Example of a recovery factor for a reservoir with a high produced GOR. (C) Case 2. Example of a recovery factor for a reservoir with a low produced GOR.

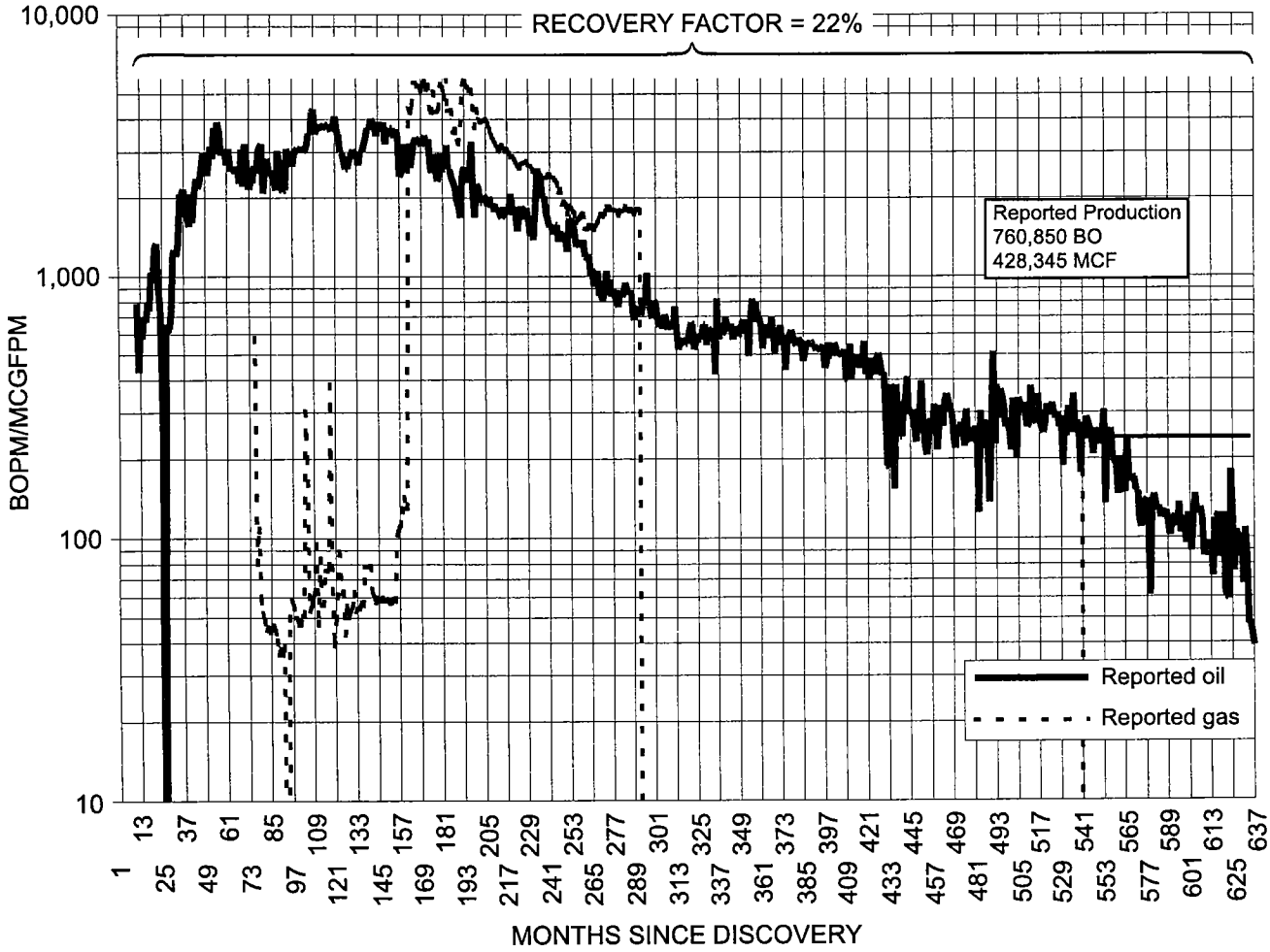

Figure 29. Production curve for a reservoir in north-central Texas under consideration as a potential waterflood candidate.

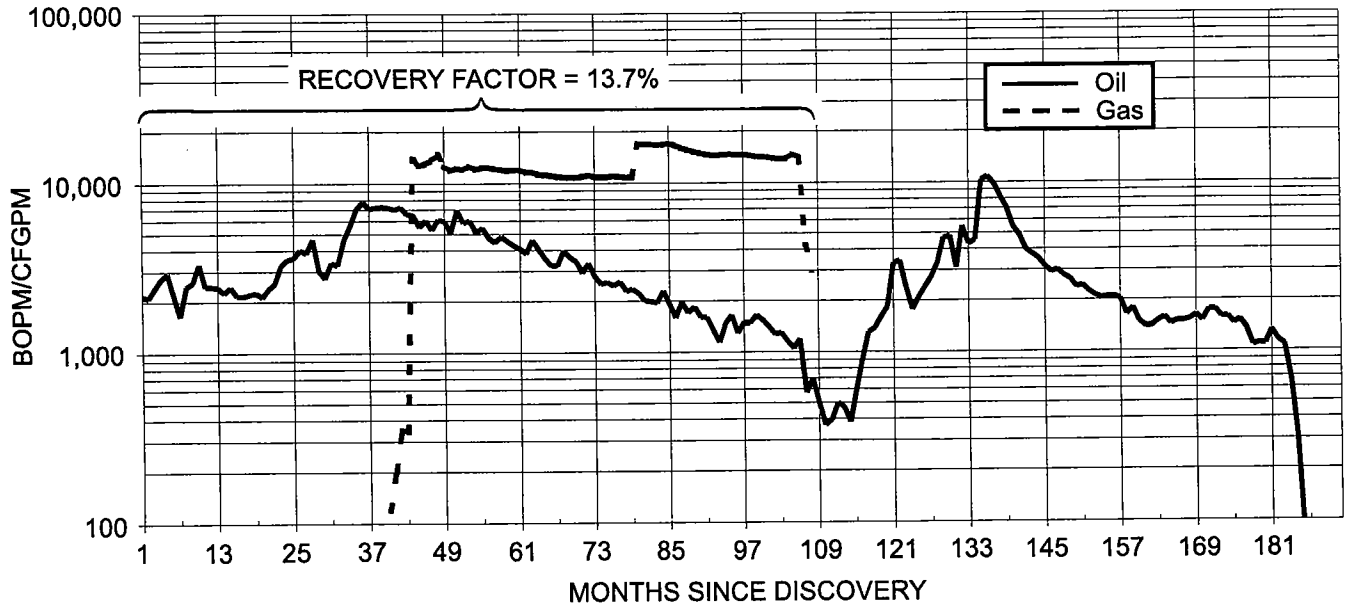

Figure 30. Production curve for a successful waterflood field used as an analogy for the reservoir represented by Figure 29. Response to injection occurred at month 115.

producers in the oil column. The great difference in recovery factors for these two reservoirs implies that the oil saturations at depletion were controlled by two totally different types of drive mechanisms; the analogous reservoir had a higher oil saturation at depletion, which allowed the waterflood response to be successful. To date, the field represented by the production curve of Figure 29 has not been waterflooded.

EFFECTS OF CHANGE IN GAS-CAP AND WATER ENTRY

The left side of equation 3.10 (Fig. 26) represents the reservoir volume of the OOIP and is equal to the right side of the equation, which represents the volume of the current oil plus the volume of the free gas in the reservoir. The underlined expression N_pR_p in equation 3.10 of Figure 31A represents the amount of solution gas produced where N_p is the amount of oil produced and R_p is the produced GOR. Equation 3.13 is a modification of equation 3.10 by substituting G_p (produced gas) for N_pR_p. Figure 31B illustrates graphically that the volumetric balance of a reservoir remains the same when the modifications derived earlier for the addition of water entry and/or expansion of a gas cap are factored in. If fluid encroaches either from an expanding gas cap or from water entry, the right side of equation 3.13 (which up to this point only accounts for the volume of the current oil and free gas within the reservoirs) would be smaller than the left unless the volume of the encroaching fluid from the gas cap or water entry is added in. Thus, Figure 31C describes how these variables of water entry and gas-cap expansion would be added to the material-balance expression derived thus far. Substituting the mathematical expression for the various parts of Figure 31C results in the material-balance equation for a reservoir with gas-cap and water-drive components (Fig. 31D). As mentioned previously, one of the goals of this chapter is to develop a means for calculating the OOIP. Therefore, by solving equa-

A

$$N B_{oi} = (N - N_p) B_o + [N R_{si} - (N - N_p) R_s - N_p R_p] B_g \qquad \text{(eq. 3.10)}$$

IS EQUAL TO:

$$N B_{oi} = (N - N_p) B_o + [N R_{si} - (N - N_p) R_s - G_p] B_g \qquad \text{(eq. 3.13)}$$

WHERE: $G_p = N_p R_p$ = GAS PRODUCED

B

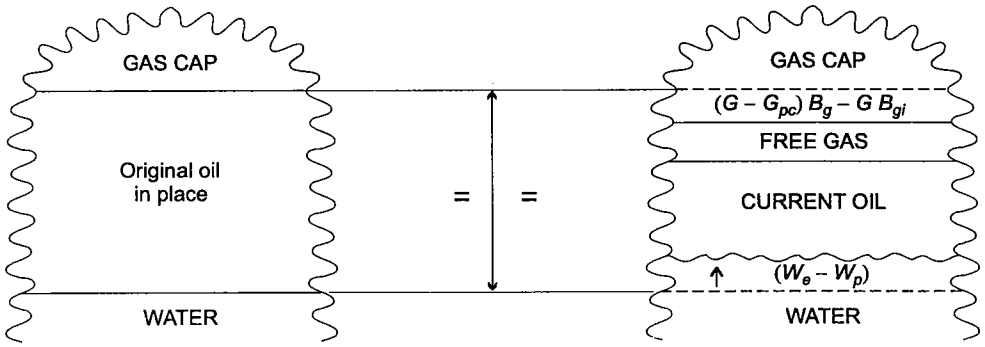

C

Original Reservoir Barrels of Oil = Current Reservoir Barrels of Oil + Volume of Free Gas + Change in Gas-Cap Volume + Volume of Water Entry in Barrels

D

$$N B_{oi} = (N - N_p) B_o + [N R_{si} - (N - N_p) R_s - G_p] B_g + (G - G_{pc}) B_g - G B_{gi} + (W_e - W_p) \qquad \text{(eq. 3.14)}$$

E

$$N = \frac{N_p B_o + B_g (G_{pc} - N_p R_s) - [(G - G_{pc}) B_g - G B_{gi}] - (W_e - W_p)}{B_o - B_{oi} + (R_{si} - R_s) B_g} \qquad \text{(eq 3.15)}$$

Figure 31. (A) Material-balance equation for reservoir at the bubble point. Equation 3.13 represents substitution of the variable N_pR_p in equation 3.10 with G_p. (B) Graphical representation of the changes in reservoir original oil volume by expansion of gas cap and water entry. (C) Descriptive account of B. (D) Material-balance equation for a saturated reservoir with a gas cap and an active water drive. (E) Equation 3.14 solved for N (OOIP).

tion 3.14 for N, which represents the OOIP, we obtain equation 3.15 (Fig. 31E). Figure 32A illustrates the terms used for equation 3.15. Notice the terms G_{ps} and G_{pc}, which represent the amount of solution-gas production and the amount of gas-cap production, respectively. Although it is difficult to distinguish gas-cap and solution-gas production, the production of either has the same effect on the material-balance equation. Equation 3.16 (Fig. 32B) replaces G_{ps} and G_{pc} with the term G_p, where G_p is simply the gas produced. Equation 3.16 represents a material-balance expression for all the natural reservoir energies except pore-volume changes, gas released from solution from formation water, and volumetric changes of current water saturation (assumed minimal).

PORE-VOLUME CHANGES

The last major principle of the material-balance equation that we will consider is the effect of rock and fluid compressibility. These factors can play a large role in production for those undersaturated reservoirs above the bubble point. First, a few basic terms need to be defined.

Figure 33A illustrates a mass of material whose dimensions are length times width times height. This volume of 100% mass is called the *bulk volume*, or V_B. With the introduction of porosity or pore space, as illustrated in Figure 33B, the bulk volume is reduced, and the volume of the pore space is now termed the *pore volume*, or V_p. Subtracting the amount of the pore volume from the bulk volume yields a net volume, which is termed the *solids volume*. With the introduction of gas, oil, and water into the pore volume, as illustrated in Figure 33C, and by treating the pore volume as unity, the pore volume is divided into volumes of gas, oil, and water, with the terms *gas saturation* (S_g), *oil saturation* (S_o), and *water saturation* (S_w). The addition of all saturations equals 1, as seen in equation 3.17. That part of the pore volume represented by the addition of the oil and gas saturations is referred to as the *hydrocarbon pore volume*, or V_{HC}, of the original mass.

We will consider three basic types of compressibility: oil, water, and rock compressibility. The first type to be discussed is oil compressibility above the bubble point. Reservoirs above the bubble point have all their available gas in solution, and thus with an increase in pressure, there is a decrease in volume, which depends on the temperature and composition of the fluid. Craft and Hawkins (1959) suggest values of compressibility for undersaturated oils ranging from 5 to 100×10^{-6} psi^{-1}. An oil compressibility of 5×10^{-6} psi^{-1} means that the volume of 1 million barrels of reservoir oil would increase by 5 barrels for every drop of 1 psi in pressure. This number could be larger for higher temperature reservoirs, API gravities, or greater quantities of solution gas (Craft and Hawkins, 1959). Although the relationship of oil compressibilities is already addressed when the material-balance equation uses FVFs, Figure 34A illustrates an expression for oil compressibility, C_o. The expression on the right is the same equation that has been solved for ΔV, which is the change in pore volume. Figure 34B illustrates the direct relationship between reservoir volume and FVF, which states that the current FVF minus the initial FVF divided by the initial FVF times the pressure differential is equivalent to the oil compressibility. It must be noted that this relationship holds true for a volumetric reservoir, which by definition means that the reservoir is bounded on all sides by impermeable strata (Craft and Hawkins, 1959).

The second type of compressibility is that of water. It is even smaller than that of oil by almost a factor of 10. It is in the range of 10^{-6} fractional volume change per psi reduction. Water compressibilities can be generated from two sources, which are illustrated in Figure 35. First, water expansion can occur from a downdip water column, which contributes water influx from a water-drive reservoir. This entry of water has already been examined and incorporated into the material-balance equation by the term $(W_e - W_p)$. A second compressibility factor that influences volumetric changes is formation water in the pore space above the oil–water contact (OWC). As pressure drops, these minute volumes of water expand, contributing to the

A

$$N = \frac{N_p B_o + B_g (G_{ps} - N_p R_s) - [(G - G_{pc}) B_g - G B_{gi}] - (W_e - W_p)}{B_o - B_{oi} + (R_{si} - R_s) B_g} \qquad \text{(eq 3.15)}$$

WHERE:

N = Original oil in place
N_p = Produced oil
B_o = Current oil FVF
B_{oi} = Initial oil FVF
B_g = Current gas FVF
B_{gi} = Initial gas FVF
G_{ps} = Solution gas production
G_{pc} = Gas-cap production
} Cannot differentiate = G_p
G = Initial gas in place
W_e = Water entry
W_p = Water produced
R_{si} = Initial reservoir GOR
R_s = Current reservoir GOR

B

$$N = \frac{N_p B_o + B_g (G_p - N_p R_s) - G (B_g - B_{gi}) - (W_e - W_p)}{B_o - B_{oi} + (R_{si} - R_s) B_g} \qquad \text{(eq 3.16)}$$

WHERE: G_p = Gas produced from either solution gas or gas cap

Figure 32. (A) Material-balance equation for a saturated reservoir with gas-cap and water entry, with definition of variables. G_{ps} and G_{pc} cannot be differentiated. (B) Substitution of G_p for variables G_{ps} and G_{pc} in equation 3.15.

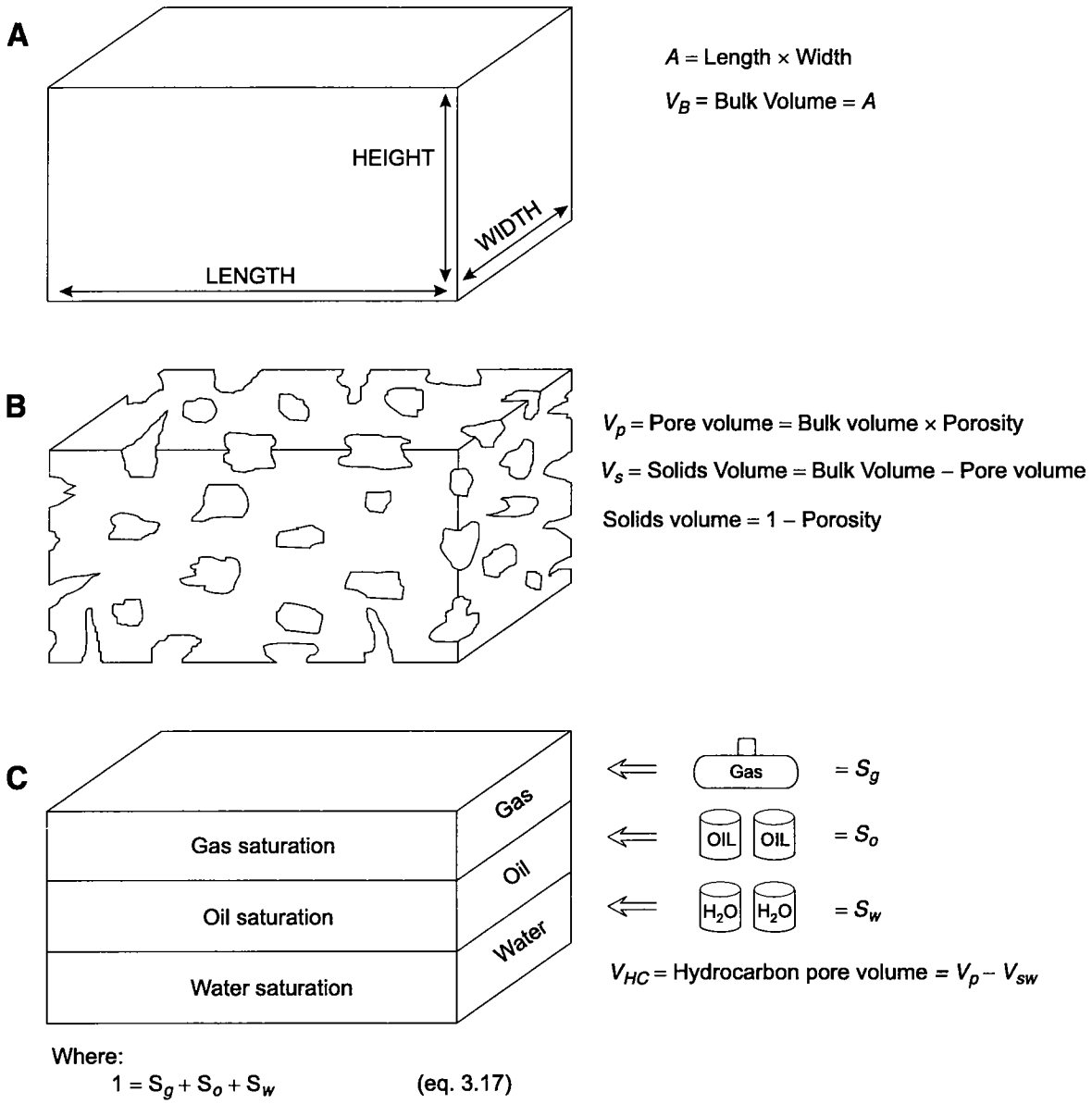

Figure 33. (A) Graphical illustration for definition of bulk volume. (B) Graphical definition of pore volume. (C) Graphical definition of gas, oil, and water saturations within pore volume.

hydrocarbon-pore-volume reduction in reservoirs above the bubble point.

Figure 36 shows graphs used to calculate the compressibility of water, the solubility of natural gas in fresh water, and corrections for the salinity. Notice that the solubility of natural gas in water is low compared to that of oil. Just as oil compressibility has been described in equation 3.18 of Figure 34, water compressibility is similar and is described in equation 3.20 of Figure 35A. This equation shows that the change in pore volume is equal to the water-compressibility factor in volumes of change per psia reduction times the pressure differential times the reservoir pore volume.

The last form of compressibility that will be addressed is rock compressibility. With burial, overburden pressure is exerted on a reservoir, which is simply a compressive force on the rock. The average pressure gradient—that is, the amount of pressure with depth—is approximately 1 psi/foot of depth (Slider, 1983), although this overburden pressure can vary widely and depends on many variables such as structure and consolidation of the sediments. In normal situations, such as consolidated sediments, the overburden pressure is not transmitted directly to the pore space because of the support from the matrix material. In areas such as the Gulf Coast of Texas and Louisiana, the pore pressures of the reservoir may approach those of the overburden owing to the unconsolidated nature of the sandstones, and the transfer of the overburden pressure is directed to the fluids in the pore volume owing to the

Figure 34 *(right)*. (A) Equation for oil compressibility. (B) Oil compressibility expressed as a change in initial and current oil volumes and pressures, and with respect to current and initial oil formation volume factors and pressures.

A

$$C_o = -\frac{1}{V}\frac{dV}{dp} \qquad \Delta V = C_o \Delta p\, V \qquad \text{(eq 3.18)}$$

WHERE: V = Volume
dV = Change in volume
dp = Change in pressure

B

$$C_o = -\frac{1}{dp}\frac{dV}{} = \frac{V_o - V_{oi}}{V_{oi}(p_i - p)} = \frac{B_o - B_{oi}}{B_{oi}(p_i - p)} \qquad \text{(eq 3.19)}$$

WHERE: V = Original reservoir volume
V_{oi} = Initial reservoir volume
p_i = Initial pressure
p = Pressure

Note: For reservoirs above the bubble point

A $\Delta V_p = C_w\ \Delta_p\ V_p$ (eq. 3.20)

B

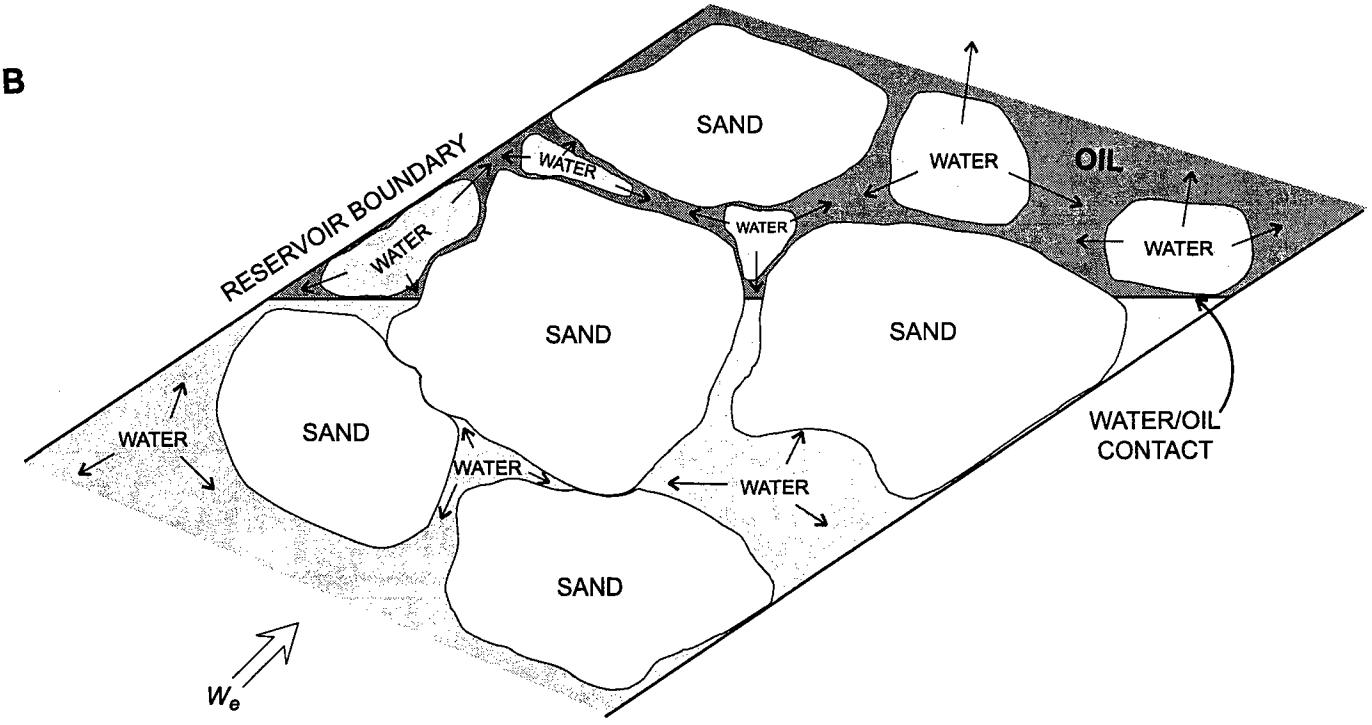

Where:
ΔV_p = Change in Pore Volume
C_w = Water Compressibilty
Δ_p = Change Pressure
V_p = Pore Volume

C Change in Pore Volume = Water Compressibility × Change in Pressure × Pore Volume

Figure 35. (A) Equation for the change in pore volume from water compressibility. (B) Graphical illustration of sources of water compressibility. (C) Descriptive account of equation 3.20.

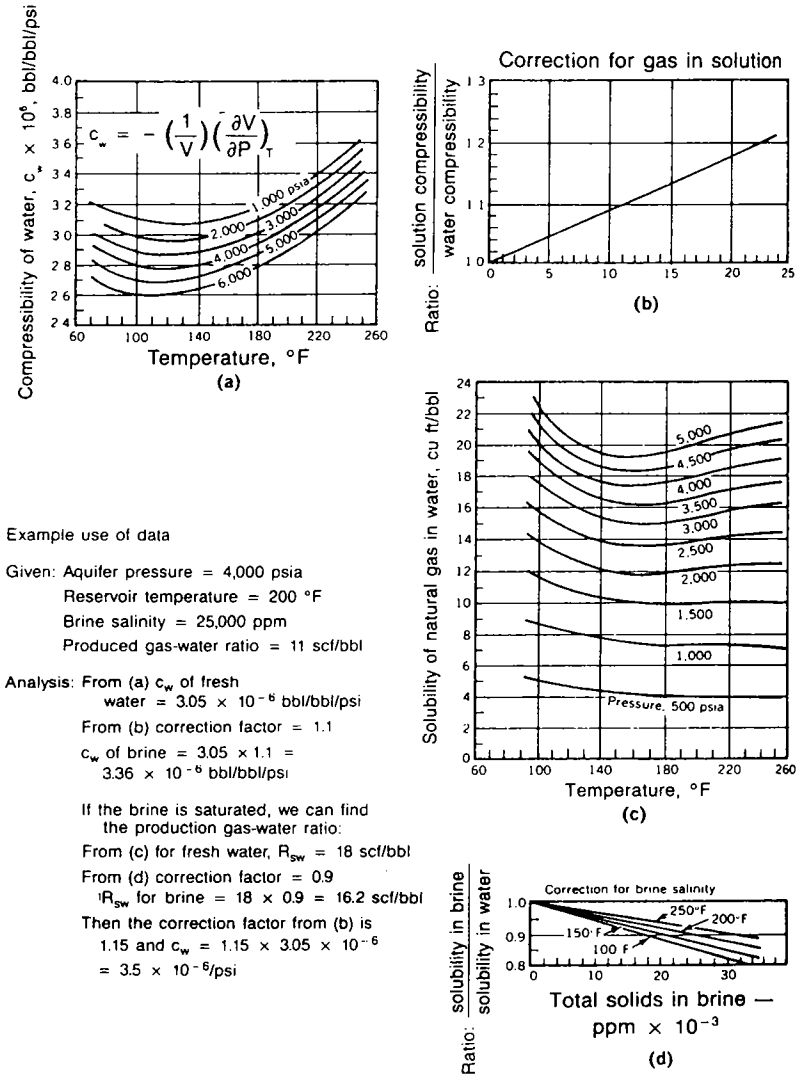

Example use of data

Given: Aquifer pressure = 4,000 psia
Reservoir temperature = 200 °F
Brine salinity = 25,000 ppm
Produced gas-water ratio = 11 scf/bbl

Analysis: From (a) c_w of fresh water = 3.05×10^{-6} bbl/bbl/psi
From (b) correction factor = 1.1
c_w of brine = $3.05 \times 1.1 = 3.36 \times 10^{-6}$ bbl/bbl/psi

If the brine is saturated, we can find the production gas-water ratio:
From (c) for fresh water, R_{sw} = 18 scf/bbl
From (d) correction factor = 0.9
R_{sw} for brine = $18 \times 0.9 = 16.2$ scf/bbl
Then the correction factor from (b) is 1.15 and $c_w = 1.15 \times 3.05 \times 10^{-6} = 3.5 \times 10^{-6}$/psi

Figure 36. Charts used for determining water compressibility and gas and salinity corrections. (From Dobson and Standing, ©1944; reprinted courtesy of the American Petroleum Institute.)

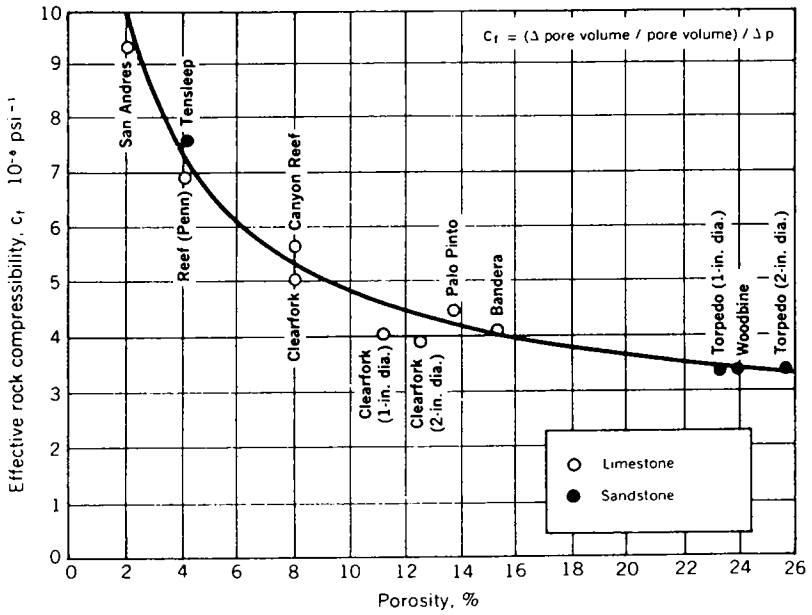

decrease in pore volume from compaction. However, in most cases, the matrix partially supports the overburden pressure, and only a part of the pressure is transmitted to the pore space. This pore pressure is generally in the range of 0.5 psi/foot of depth (Slider, 1983).

In response to external pressure, the matrix can become compressible; that is, the pore volume of the reservoir solids becomes slightly smaller. Craft and Hawkins (1959) suggest that the degree of compressibility for sandstone and limestone reservoirs lies in the range of 2×10^{-6} to 25×10^{-6} psi^{-1}. The compressibility can be on a bulk-volume basis. Dividing the compressibility of the bulk volume by the porosity gives the compressibility on a pore-volume basis. Figure 37 shows the compressibilities for a number of limestone and sandstone reservoirs. These samples were subjected to 3,000 psia of external pressure (overburden pressure), and the internal pore pressure varied from 0 to 1,500 psia. The compressibilities are plotted against porosities because lower porosities seemed to have higher compressibilities.

Thus, the reduction in pore volume that can occur with reduction in pressure can come from two sources. First, a pore-volume loss results from a reduction in the gross volume of the reservoir from compaction, which results from a pressure loss owing to production. Second, pore-volume loss can occur from an increase in the volume of reservoir solids with a decrease in pressure. Figure 38 illustrates these two components of rock compressibility. Note that the decrease in reservoir pore volume by default decreases the average porosity of the reservoir. This porosity change is usually on the order of 0.5% for every 1,000-psi change in the internal fluid pressure (Craft and Hawkins, 1959). In unconsolidated sediments, the porosity changes might be considerably higher. van der Knaap (1958) pointed out that the change in porosity for a sediment does not depend on the absolute pressure (the overburden pressure) but on the difference between the internal and external pressures of the rock.

Figure 37 *(left)*. Formation-rock compressibility from various reservoirs and pressure differentials of 0 to 1,500 psia plotted against porosity values. (Hall, ©1953; reprinted by permission of Society of Petroleum Engineers.)

A $\Delta V_p = C_f \Delta_p V_p$ (eq. 3.21)

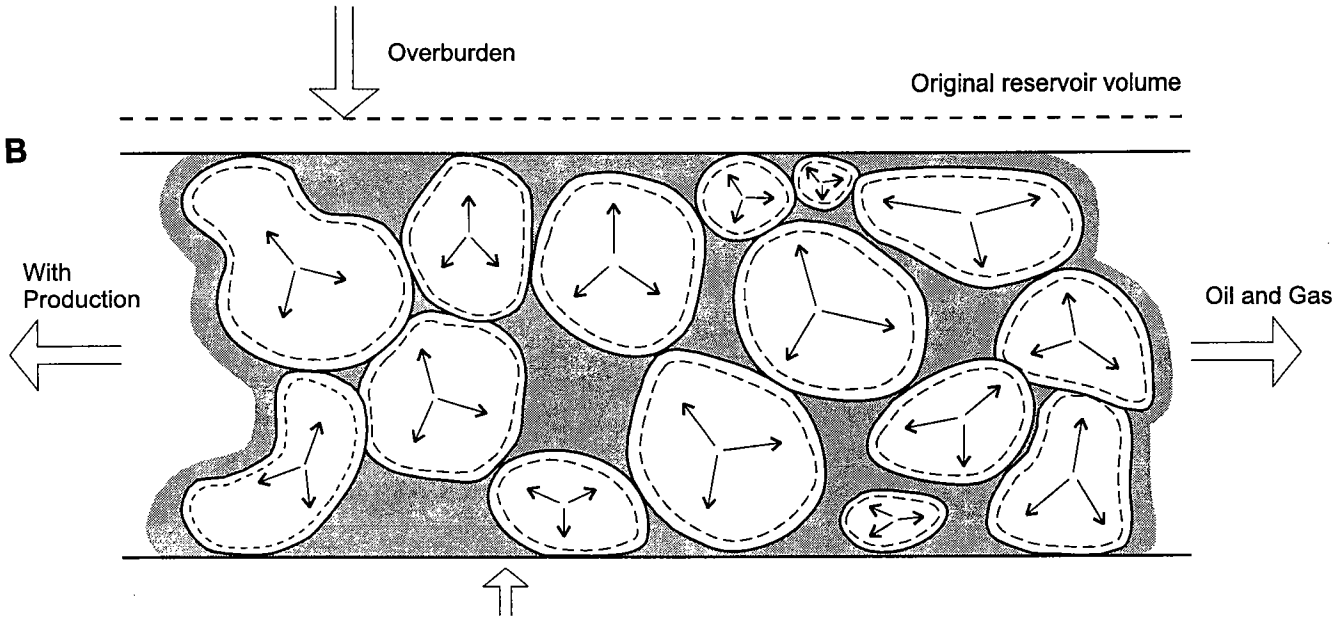

1. Decrease pore volume with pressure drop
2. Increases solids size (decreases porosity) due to compressibility

= OIL AND GAS

Where:

ΔV_p = Change in Pore Volume
C_f = Rock Compressibility
Δ_p = Change in Pressure
V_p = Pore Volume

C Change in Pore Volume = Rock Compressibility × Change in Pressure × Pore Volume

Figure 38. (A) Equation for change in pore volume from rock compressibility. (B) Graphical illustration of source of rock compressibility. (C) Descriptive account of pore-volume loss from rock compressibility.

Figure 39A shows the formulas for water compressibility (equation 3.20) and rock compressibility (equation 3.21) previously derived. The pore-volume changes from these two sources can be added together as demonstrated in equation 3.22. Rearranging equation 3.22 and factoring out (p and V_p results in equation 3.23, which is a more convenient form. Because the general material-balance equation is a balance of volumes, equation 3.23 could be added to equation 3.14 (Fig. 31), which now accounts for all the volumetric changes including those from water and rock compressibilities. However, V_p in equation 3.23 would be introducing the new variable V_p. Because V_p represents the original pore volume of the reservoir, another way of stating it in terms already expressed would be by equation 3.24, where V_p is equal to the volume of the OOIP divided by the percentage of oil volume or oil saturation represented by the value of 1 (or unity) minus the formation-water saturation. Substituting this expression for V_p into equation 3.23 gives equation 3.25, which is an expression for the volumetric change in the reservoirs from the changes of rock and water compressibilities.

For all the expressions derived to this point there are many variations, ramifications, and intricacies that we have bypassed in the name of simplicity. The purpose thus far has been to derive a fundamental knowledge of the concepts behind the material-balance formula. Because the pore-volume changes from water and rock compressibilities have been defined in equation 3.25 of Figure 39, this expression can now be added to the general material-balance equation derived thus far for the other volumetric changes of free gas in the reservoir, gas-cap volumetric changes, and water-entry volumetric changes (equation 3.14, Fig. 31).

Equation 3.26 of Figure 40C is the revised general material-balance equation with all the variables described to this point. The formula states that the original reservoir barrels of oil is equal to the current reser-

A

$$\Delta V_p = C_w \ \Delta p \ S_{wc} \ V_p \qquad \text{(eq 3.20)}$$

WHERE: S_{wc} = Formation water saturation

$$\Delta V_p = C_f \ \Delta p \ V_p \qquad \text{(eq 3.21)}$$

$$\Delta V_p = C_{wc} \ \Delta p \ S_{wc} \ V_p + C_f \ \Delta p \ V_p \qquad \text{(eq 3.22)}$$

$$\Delta V_p = (C_f + C_w \ S_{wc}) \ \Delta p \ V_p \qquad \text{(eq 3.23)}$$

$$\text{Change in reservoir pore volume} = \left(\text{Rock compressibility} + \text{Water compressibility}\right) \times \text{Change of pressure} \times \text{Pore volume}$$

B

$$V_p = \frac{N B_{oi}}{(1 - S_{wc})} \qquad \text{(eq 3.24)}$$

$$\text{Pore volume} = \frac{\text{Original reservoir barrels of oil}}{\text{Original oil saturation}}$$

Substituting eq 3.22 into eq 3.21

C

$$\Delta V_p = (C_f + C_w \ S_{wc}) \ \Delta p \times \frac{N B_{oi}}{1 - S_{sw}} \qquad \text{(eq 3.25)}$$

Figure 39. (A) Pore-volume changes (equation 3.23) in a reservoir derived by the addition of the effects of water compressibility (equation 3.20) and rock compressibility (equation 3.21). (B) Equation for total pore volume of a reservoir expressed by the terms *original oil in place* and *original oil saturation*. (C) Substitution of V_p of equation 3.22 with equation 3.24.

voir barrels of oil, plus the volume of free gas in the reservoir, plus the change in any gas-cap volume, plus the change in volume from the barrels of net water entry, plus the volumetric changes in hydrocarbon pore volume and the pore volume, in barrels, from the water and rock compressibility. Because we are interested in obtaining the OOIP for the reservoir in stock-tank barrels, we can solve equation 3.26 for N, resulting in equation 3.27, which is a general equation for material balance that accounts for the major sources of reservoir energies.

DATA SOURCES FOR MATERIAL-BALANCE CALCULATIONS

If the variables of equation 3.27 are known and accurate, this general formula is all that is necessary to derive OOIP. It is unnecessary to have special equations for each scenario of a producing reservoir such as an equation for production above the bubble point or a separate equation for solution-gas drive or water drive. Also, it should be noted that many of the variables are not appropriate at all stages of a reservoir's life. For instance, for reservoirs above the

A

$$N B_{oi} = (N - N_p) B_o + [N R_{si} - (N - N_p) R_s - G_p] B_g + (G - G_{pc}) B_g - G B_{gi} + (W_e - W_p) \qquad \text{(eq 3.14 of Figure 31)}$$

$$\text{Original reservoir barrels of oil} = \text{Current reservoir barrels of oil} + \text{Volume of free gas} + \text{Change in gas-cap volume} + \text{Volume of water entry}$$

B

$$\text{Change pore volume} = (C_f + C_w S_{wc}) \ \Delta p \times \frac{N B_{oi}}{1 - S_{wc}} \qquad \text{(eq 3.25 of Figure 39)}$$

C

$$N B_{oi} = (N - N_p) + [N R_{si} - (N - N_p) R_s - G_p] B_g + (G - G_{pc}) B_{gi} - G B_{gi} + (W_e - W_p) + (C_f + C_w S_{wc}) \ \Delta p \times \frac{N B_{oi}}{1 - S_{wc}} \qquad \text{(eq 3.26)}$$

$$\text{Original reservoir barrels of oil} = \text{Current reservoir barrels of oil} + \text{Volume of the free gas} + \text{Change in gas-cap volume} + \text{Volume of water entry} + \text{Change in pore volume from rock and water compressibility}$$

D

$$N = \frac{N_p B_g + B_g (G_p - N_p R_s) - G(B_g - B_{gi}) - W_e - W_p}{B_o - B_{oi} + (R_{si} - R_s) B_g + (C_f + C_w S_{wc}) \ \Delta p \ B_{oi} / (1 - S_{wc})} \qquad \text{(eq 3.27)}$$

Figure 40. (A) Material-balance equation 3.14 from Figure 31. (B) Pore-volume change from rock and water compressibility. (C) Addition of pore-volume changes from rock and water compressibility to the material-balance equation, 3.14. (D) Rearranging equation 3.26 to solve for the original oil in place.

bubble point, the gas-expansion term would be equal to zero, because free gas would be absent in a reservoir under these circumstances. Also, the liberated-gas term in the denominator would be zero, because R_s, or the current GOR, would be equal to R_{si}, or the original GOR. Furthermore, W_e would become zero if a reservoir is not under a water-drive energy. However, the water-production variable, W_p, should be included because most reservoirs produce some water.

The general material-balance formula is only as accurate as the data input. Reservoir engineers have a responsibility for decisions made that are based on the results of material-balance equations. These decisions include economic expenditures based on reserves expected, which in turn are based on the amount of OOIP and the amount of remaining mobile oil. However, all too often the geologist or the operator is responsible for obtaining data for these calculations. Thus, it is the geologist's responsibility to provide accurate rock-property data. These data can be determined from open-hole electric logs, but information from cores, sample studies, and/or drillstem tests is invaluable to the analysis of the reservoir. Accurate correlations of the pay zones is also of utmost importance for the purpose of allocating production, reserves, or OOIP to those zones. Because of the importance of accurate data, every opportunity should be made at the outset to acquire PVT data.

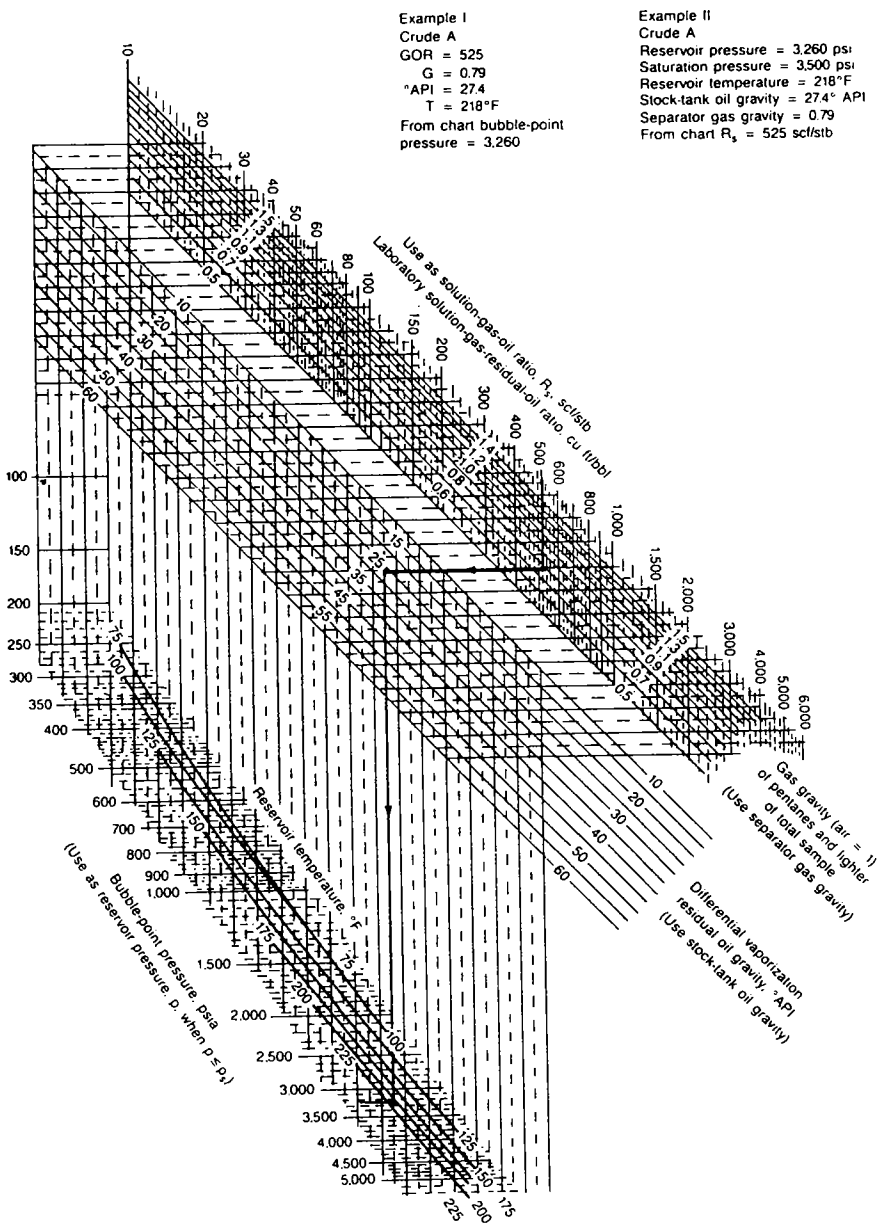

Figure 41. Correlation chart used for estimating GORs or bubble-point pressures. (Modified from Borden and Rzasa, ©1950; reprinted by permission of Society of Petrolem Engineers.)

For older reservoirs from which these types of data were not obtained, various methods and empirical data are available to estimate this information. Figures 41 and 42 are examples of empirical data that allow the calculation of FVFs and gas in solution if the reservoir temperatures, pressures, and oil and gas gravities are known. Empirical PVT data can be obtained from Standing's correlations, which are found in Amyx and others (1960). However, when a discovery well is completed, obtaining bottom-hole-fluid samples and determining PVT data are critical for the proper evaluation of the reservoir for future opportunities.

A second major concern for the geologist, operator, or engineer is the accuracy of the production data. Because oil is sold and its amount is not generally questioned except for old reservoirs, or where several zones are commingled, a question arises about the accuracy of the stated water and gas production. The reason for this is that gas is not always sold, because it may be used for lease purposes, as demonstrated by case history 11A from the first waterflood workshop (Rottmann and others, 1998, p. 35). In that example, 13% of the gas produced was not sold because it was being used to fuel the gas engines in the lease pumping units. Since the cumulative GOR (R_p) (equation 3.10), or the total gas produced (G_p) (equation 3.27), are predominant variables in the general material-balance equation, any deviation from this accuracy will significantly affect the equation's outcome. The same holds true for water production and water entry. Because water is a commodity that is not sold, its production data often are

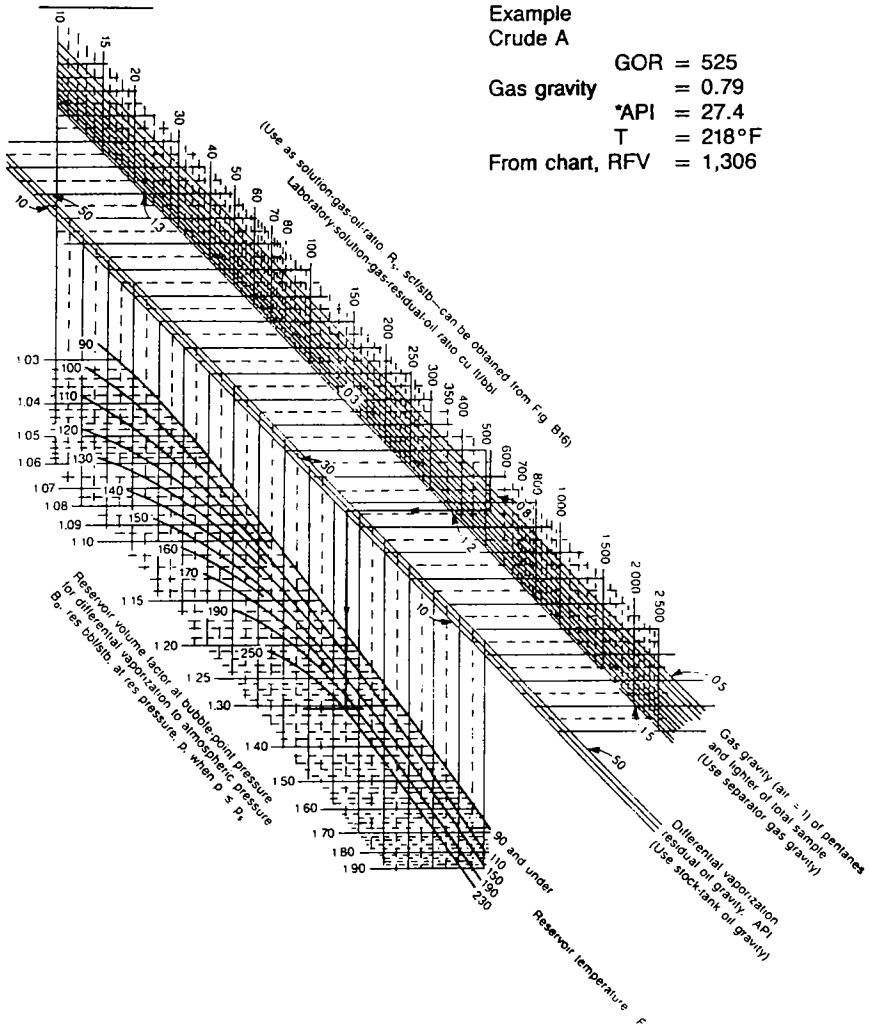

Figure 42. Correlation chart used to estimate GORs or FVFs for oil. (Modified from Borden and Rzasa, ©1950; reprinted by permission of Society of Petrolem Engineers.)

not accurate. Thus, a dedicated effort should be made to determine accurate data for water production, including examination of surface equipment and discussions with knowledgeable personnel.

A good example of the importance of accurate knowledge of water production, and assumptions made concerning water-saturation calculation, is given in case history 5 of the first waterflood workshop (Rottmann and others, 1998, p. 18–20). In that example, it was assumed that because water production was not reported for a majority of the wells, it was not a significant factor. As it turned out, water production and its associated water saturation proved to be the downfall of the project.

Another factor critical to material balance is the amount of water entry. This factor is difficult at best to estimate, although some formulas do so that are based on the pressure differential of the reservoir, water viscosity, relative permeabilities, and the geometry of the aquifer. A water drive usually results from one or a combination of the following causes: (1) artesian flow, water entering at the surface whose source is structurally higher than the reservoir, creating a hydrostatic-pressure gradient; (2) expansion of the water or other sources of oil or gas within the reservoir; and (3) compaction of the aquifer portion of the reservoir rock. Fluid-flow fundamentals, which are beyond the scope of this workshop, are necessary to evaluate water influx.

A third type of data critical to the general material-balance evaluation of a reservoir is accurate pressure data. These data include initial-pressure data at discovery plus current pressure data at some point in the life of the reservoir. One note of caution concerning pressure analysis is to make certain that any pressure-buildup tests remain in the reservoir long enough to allow the bottom-hole pressure to stabilize. If the recorded pressure is still changing even slightly when examined, the actual bottom-hole pressure could be considerably higher than the buildup test indicates, especially in low-permeability strata.

As stated previously, one goal of presenting the material-balance equation is to illustrate the effects of pressure changes within a reservoir on its fluids and on the reservoir itself. Reservoir engineering is usually concerned with a reservoir from discovery to abandonment, as described in Figure 5. Geologists are concerned with the origin, or the deposition and entrapment, of hy-

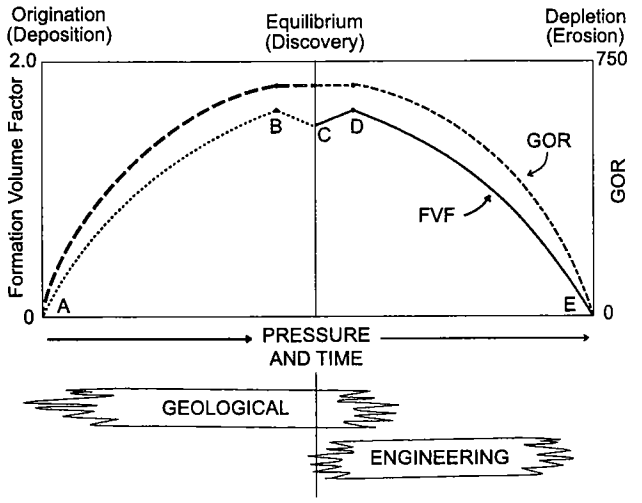

Figure 43. Time line of a reservoir from origination to depletion. FVF and gas to oil curves are shown representing conditions that may exist for the fluids in a reservoir from origination (deposition) through depletion (erosion).

drocarbons; diagenesis of the reservoir; and structural effects. Figure 5 can now be modified, as illustrated by Figure 43, which adds the GOR curve and the formation volume curve for a typical reservoir to Figure 5. At point *C*, which represents discovery of the reservoir, reservoir engineering becomes involved and follows through to point *E*, which represents abandonment. The geologist, on the other hand, should be concerned with those rock and fluid properties that occur from origination (point *A*) to discovery (point *C*). As described in this chapter, a reservoir becomes undersaturated with increased pressure and an absence of additional gas. This condition causes the fluids to compress, as shown by the FVF curve from point *B* to point *C*. Compression of the fluids implies compression of the reservoir as well. Thus, the principles governing the reservoir-fluid properties must be understood by the geologist. Likewise, geologists attempting to explain migration of fluids need to understand phase and saturation changes with respect to pressure that can occur or need to occur in order to deal with such saturations found in reservoirs today.

4 Volumetric Determination of OOIP

CHAPTER 4

Volumetric Determination of OOIP

INTRODUCTION

A second method for calculating original oil in place (OOIP) is the volumetric method. This method is the one most commonly used by geologists for estimating OOIP when evaluating cursory parameters for a new waterflood project. The variables for the formula, except for the formation volume factor (FVF) and the barrels per acre-foot constant, were discussed in detail in the first waterflood workshop (Rottmann and others, 1998, p. 34–85), although the formula for oil in place was not. The volumetric method is based on the values, bulk volume, porosity, salt-water saturation, barrels per acre-foot constant, and reservoir FVF. Figure 44A illustrates the equation for volumetric oil in place. Figure 44B is a pictorial representation of the equation. One point should be mentioned: this equation is an estimation of OOIP and is independent of free gas in the reservoir or a gas cap. This point will be expanded later in this chapter. The following sections give a brief description and review for each of the variables in the formula.

VARIABLES OF THE VOLUMETRIC OOIP EQUATION

Constant 7,758

The constant 7,758 refers to the amount of barrels of material that can be contained in a volume whose dimensions are 1 acre of area and 1 ft thick. Thus, 1 acre-foot is defined as 1 acre in area times 1 ft in thickness.

Area

The term *area* refers to the amount of acres contained in a net-isopach depiction of the reservoir. The term can apply to the summation of acres for multiple layers. Chapters 4 and 5 of the first waterflood workshop (Rottmann and others, 1998) were devoted to determining net pay and mapping net pay. This task is perhaps the geologist's single most important responsibility, because mapping the pay zone will ultimately reflect reserves and expenditures to recover those reserves. The following topics are a review of considerations that need to be made when isopaching and ultimately determining area for the oil-in-place (OIP) formula:

1. The appropriate porosity cutoff should be considered. A porosity cutoff that is too low will yield exaggerated OIP estimates. This can have tremendous ramifications for a waterflood candidate, because the smaller recovery factor from primary production will yield overly optimistic remaining oil reserves. Table 10 of the first workshop illustrates this concept (Rottmann and others, 1998, p. 44).
2. Every effort should be made to interpret pay thickness correctly from the various electric and porosity logs. Minor thickness variations dramatically affect OIP numbers, as demonstrated by table 11 of the first workshop (Rottmann and others, 1998, p. 45).
3. Non-pay reservoir should be understood. It is not uncommon for non-water-bearing strata to have porosity-log values above the porosity cutoff value, which would indicate an acceptable net-pay thickness for a reservoir, whereas, in fact, that part of the reservoir never contributed to production, as in case history 15 of the first workshop (Rottmann and others, 1998, p. 48–50).
4. The proper interpretation and mapping of an oil–water contact and a gas–water contact are critical to the correct geometry and volumetrics of the oil column, as in case histories 16 and 17 of the first workshop (Rottmann and others, 1998, p. 51–58).
5. Incorporation of the environment of deposition into the mapping of a reservoir is needed to approximate the proper geometry of the reservoir. This is especially important where individual layers are present, because the cumulative-isopach depiction does not represent the geometry of the individual layers (illustrated in case history 19 of the first workshop; Rottmann and others, 1998, p. 63–70).

Height

Calculating the correct average height for a reservoir can also affect the final OIP figure dramatically. Table 6 from case history 12 and table 10A from the first workshop (Rottmann and others, 1998, p. 39, 44) illustrate the magnitude of error that can occur by misjudging average height for a reservoir. Great care must be taken when picking net pay from electric logs, as was pointed out in the preceding section on *area*.

Porosity

The porosity value in the OIP formula refers to the average porosity that is representative of the reservoir. Just as in the discussion of *area* and *height*, any deviation from the actual value for average porosity can have dramatic effects on the OIP figure. Case history 13 and

A

$$OOIP = \frac{7758 \times A \times H \times \emptyset \times (1 - S_w)}{B_{oi}} \qquad \text{(eq. 4.1)}$$

B

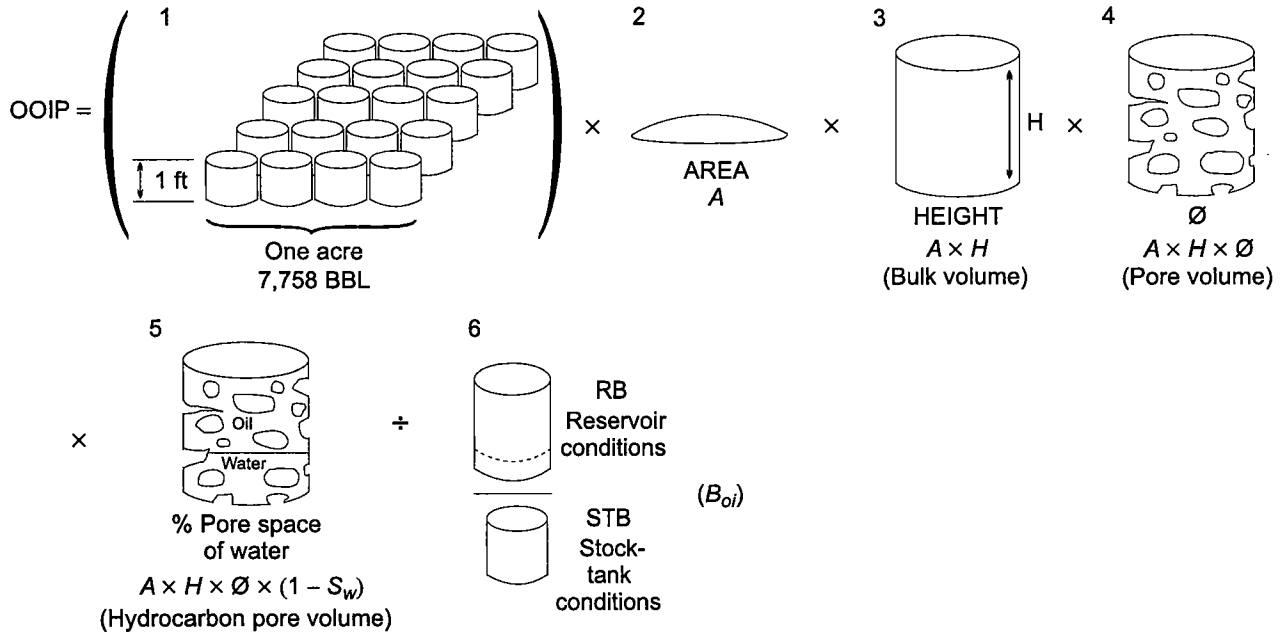

C

$$BBL = \frac{STB / AC\text{-}FT \times AC \times FT}{\frac{RES\ BBL}{STB}}$$

Figure 44. (A) Volumetric equation for determining OOIP. (B) Graphical representation of equation 4.1. (C) Unit relationship of equation 4.1.

table 6 of the first waterflood workshop (Rottmann and others, 1998, p. 39) illustrate these effects. It is important to point out that porosity, in this formula, is influenced by the minumum porosity value used to determine net pay. Smaller minimum-porosity values allow the amount of net pay used in the height variables to become larger, which can make OIP calculations overly optimistic.

Expression $(1 - S_w)$

In the expression $(1 - S_w)$, the numeral 1 refers to the pore volume of the reservoir. Subtracting the decimal percentage of the water saturation yields the percentage of the pore volume that is oil saturated. This oil-saturated pore volume was illustrated in Figure 33 of this report. The water-saturation percentage should be treated similarly to those of porosity and height. In other words, an average value would need to be determined for use in the OIP formula.

Variable B_{oi}

The variable B_{oi} is the initial formation volume factor (FVF) for the reservoir as determined from fluid analysis or correlation charts. The expression $7{,}758 \times A \times H \times (1 - S_w)$ represents the amount of oil, in reservoir barrels, in the defined reservoir. Dividing this amount by the FVF converts the amount of reservoir barrels to the amount of OIP measured in stock-tank barrels.

COMPARISON OF MATERIAL-BALANCE AND VOLUMETRIC OOIP CALCULATIONS

If all field variables are equal, the calculations for OIP from the material-balance method and the volumetric method should be equal. However, there are at least two situations in which these calculations may not be equal.

The first situation arises where the material-balance equation is less than the volumetric calculation. Data

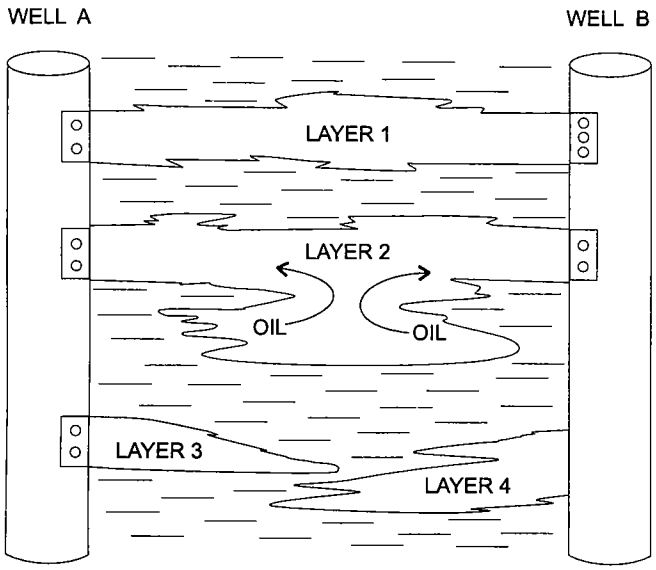

Figure 45. Hypothetical reservoir, illustrating perforated layers contributing to production.

for volumetric calculations come from open-hole electric logs and core data. If the field is developed, or if the limits and geometry of the reservoir are known, values for volumetric OIP should represent the actual OIP regardless of production trends. The reason material-balance OIP calculations are less than volumetric OIP calculations is because all the potential pay zones in the reservoir may not be contributing to production—that is, the production is discontinuous or not in communication. Figure 45 illustrates this scenario. Well A has three productive layers, each of which is perforated and contributing to production. Well B has three layers also, but only two are perforated and contributing to production; layer 4 in this well is not perforated and is not contributing to production. Material-balance calculations rely on production pressure differentials that are directly related to FVFs. Because layer 4 is not contributing to the production, its production potential is unaccounted for. Thus, the material-balance calculations will be less than the volumetric calculations because layer 4 would be included in the latter. Therefore, only those layers connected to a wellbore and that have effective porosity or permeability and proper well spacing will affect material-balance calculations.

As was mentioned in the first waterflood workshop (Rottmann and others, 1998, p. 80–84), volumetric calculations for OIP are considered representative of the actual OIP value because of the limitations just mentioned for the material-balance method. George and Stiles (1978) consider the ratio of material-balance to volumetric OIP calculations as a measure of continuity for a reservoir, which indicates a measure of well spacing and effective-interval completions. As a hypothetical example of this, consider the reservoir of Figure 46. The material-balance calculation of OIP, based on production, pressure, and fluid properties, indicates a value of 3.75 MMBO. However, the volumetric OIP calculation suggests a value of 4.5 MMBO. The ratio of material-balance OIP to volumetric OIP is 83.3%. This percentage suggests that only 83.3% of the reservoir is effectively completed either by proper well spacing, all productive zones perforated, or permeability adequately enhanced.

A ratio of material-balance to volumetric OIP greater than 1 may suggest that the reservoir's volumetric information is not adequately defined (i.e., more reservoir is participating in production than is mapped). Figure 45 illustrates how this might occur. Layer 2 is perforated in both wells A and B, and the zones at the wellbore are similar in thickness. However, between the two wells lies an additional part of the reservoir, which is contributing to production. This effect, on a larger scale, would cause the material-balance calculation to be larger than the volumetric calculation of OIP.

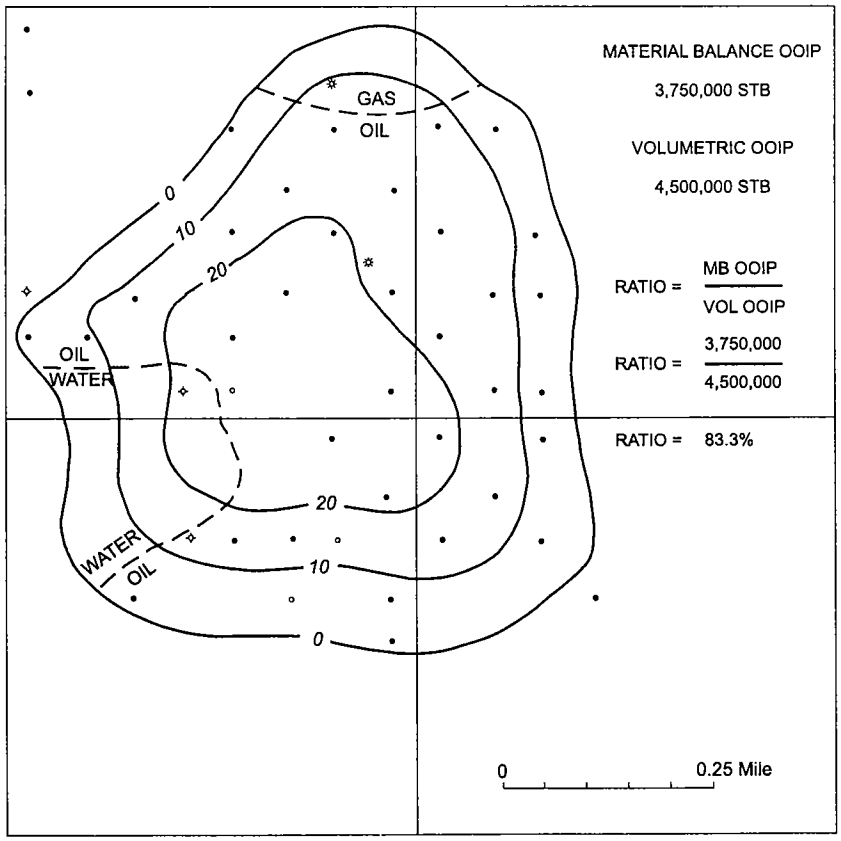

Figure 46. Hypothetical reservoir, comparing material-balance OIP calculations to volumetric OIP calculations.

Case history 23 of the first workshop illustrates another example of this concept (Rottmann and others, 1998, p. 82–85).

CALCULATING CURRENT OIL AND GAS SATURATIONS

The most important step, next to determining OOIP, is determining the oil saturation at the beginning of the waterflood. In the oil column of a reservoir at discovery, the oil saturation is simply the percentage of pore volume minus the percentage of water volume, as described previously. Or, as stated in equation 4.2 of Figure 47A, the oil saturation is equal to 1 minus the formation-water saturation. The oil saturation can also be stated as a percentage of the total pore volume, as expressed in equation 4.3 of Figure 47B. In this expression, the oil saturation is equal to the oil volume divided by the total pore volume. This is perhaps the most commonly used equation and one that we will develop later in this chapter.

Determining the oil saturation really occurs from two perspectives, the oil saturation at or above the bubble point and the oil saturation below the bubble point. These two situations represent different behaviors with respect to oil saturation. Figure 48A is a formation-volume curve for a reservoir producing above the bubble point. As was described in the last chapter, solution gas remains dissolved in the reservoir oil as production occurs, and as pressure depletes in the reservoir from point *A* to point *B*, the oil expands from the pressure drop and decompression of the oil. A free-gas state does not exist in the reservoir, because the pressure is sufficient for all the gas to remain in solution. Thus, the volume of oil in the reservoir is still the same, no matter how much production has occurred, until the pressure in the reservoir reaches the bubble point. Therefore, the oil saturation at or above the bubble point will not change. The amount of oil in barrels in the reservoir changes, but the saturation percentage with respect to volume will always remain the same. This assumes, of course, that variations in water entry and rock compressibility are ignored or insignificant.

The second situation for oil-saturation variation occurs when the reservoir pressure is at or below the initial bubble-point pressure, as indicated in Figure 49A. The decrease in value for the FVF now indicates that the volume of oil will decrease as gas breaks out of solution from the oil. The reservoir oil continues to shrink in volume until the pressure is at stock-tank conditions if they could be achieved. In this stage, the oil volume is constantly changing; Figure 49B illustrates this relationship. Some of the gas that breaks out of solution remains in the reservoir, and some flows to the wellbore and is produced. Assuming no water entry, the pore volume is now equal to

A

Oil saturation = 1 – water saturation

$$S_{oi} = 1 - S_{wi} \qquad \text{(eq 4.2)}$$

WHERE: S_{oi} = Oil saturation at discovery
S_{wi} = Water saturation at discovery
1 = Pore volume of the reservoir

B

Oil saturation = reservoir oil volume / reservoir pore volume

$$S_{oi} = \frac{\text{Initial reservoir oil volume}}{\text{Reservoir pore volume}} \qquad \text{(eq 4.3)}$$

Figure 47. (A) Equation defining oil saturation in a reservoir. (B) Second method of defining oil saturation in a reservoir, using the parameters of reservoir pore volume and oil volume.

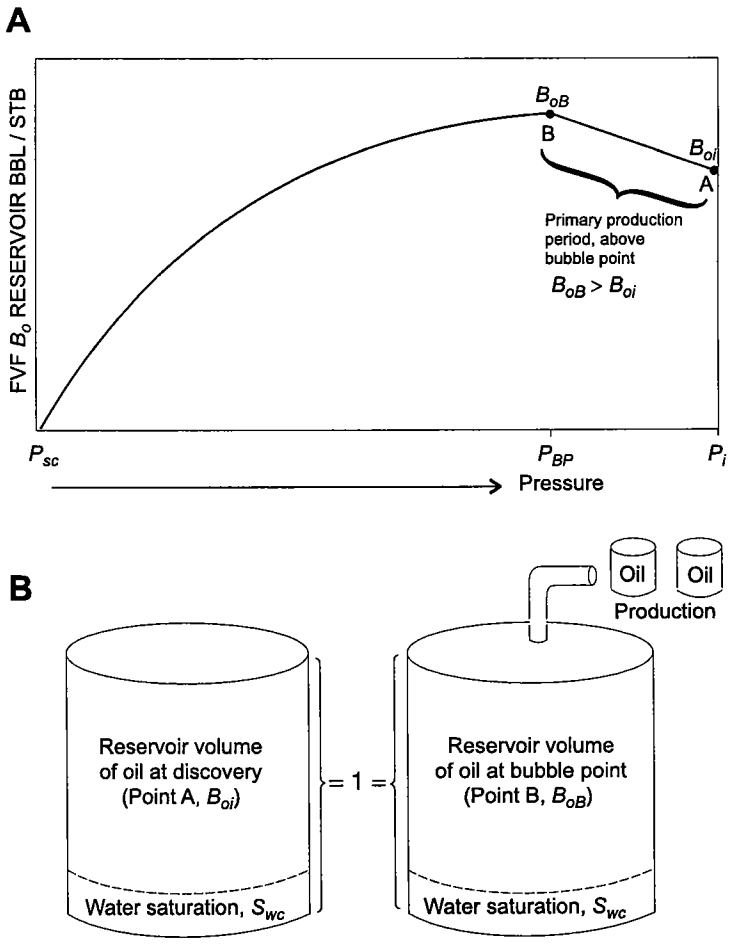

C

Cumulative production = $N - N_p$ (above BP)

D

$S_o = 1 - S_{wc}$

Figure 48. (A) Typical FVF curve for a reservoir producing above the bubble point. (B) Graphical representation of production occurring above the bubble point. (C) Equation defining cumulative production above the bubble point. (D) Equation for calculating current oil saturation above the bubble point.

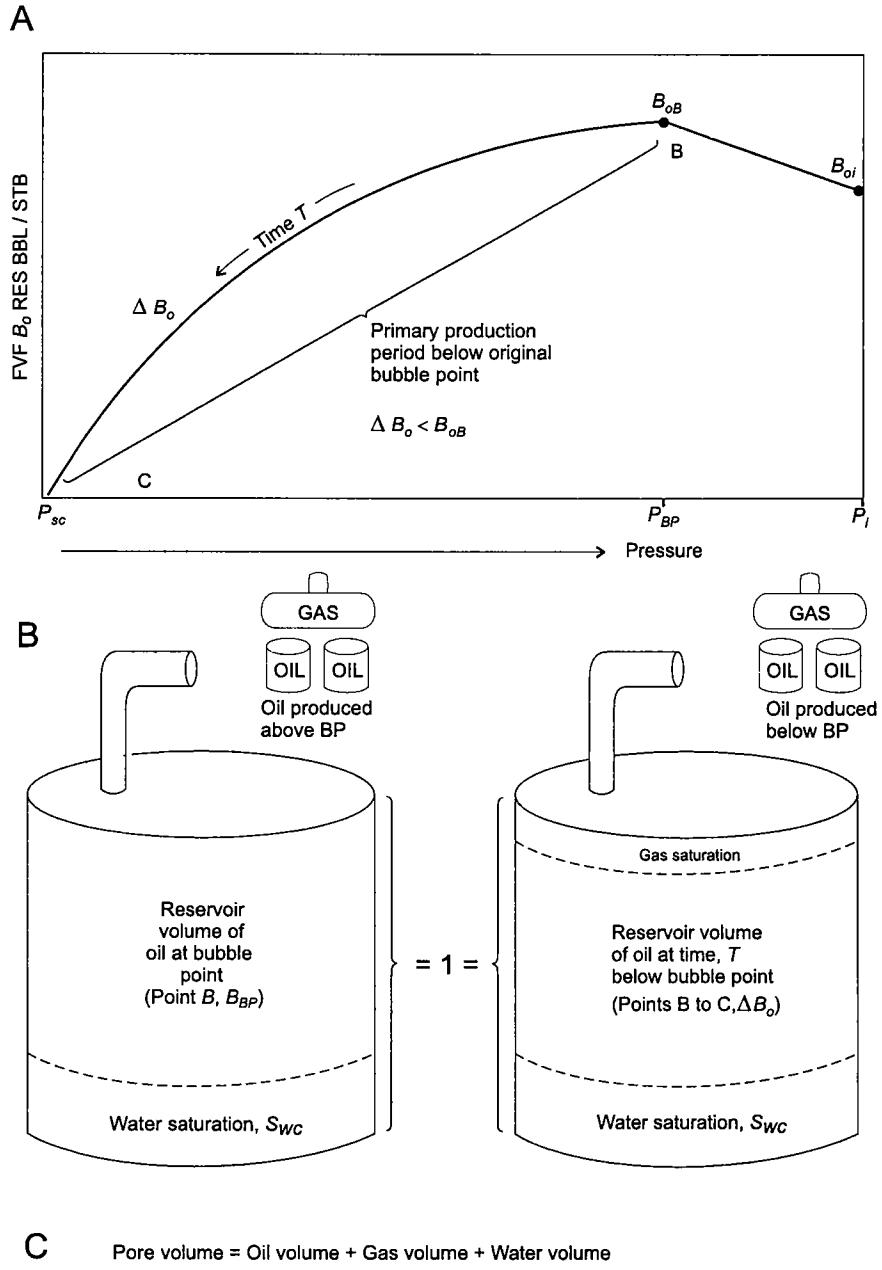

Figure 49. (A) Typical FVF curve for a reservoir producing at or below the initial bubble-point pressure. (B) Graphical representation of phase changes that occur in a reservoir producing at or below the initial bubble-point pressure. (C) Equation for pore volume in a reservoir.

the addition of the reservoir oil volume plus the gas volume plus the water volume, as shown in Figure 49C.

In order to calculate the current oil saturation below the bubble point, it is necessary to determine the OOIP at the bubble point for those reservoirs whose initial pressures were above the bubble point and the amount of production that occurred above the bubble point. The reason that the OIP at the bubble point is used is because it is at the bubble point that oil saturation starts to decrease, as illustrated in Figure 49B. The calculations would be misleading by using production and OIP values representative of the reservoir when the reservoir pressure is above the bubble point.

There are two methods for calculating the amount of oil produced above the bubble point. Figure 50A illustrates that by using the OOIP value, the initial FVF value, and the bubble-point FVF value, equation 3.4 may be solved for N_p, which is the amount of oil produced above the bubble point. Figure 50B illustrates a second approach. Equation 3.6 solves for the recovery factor by inserting the initial FVF and the bubble-point FVF. The recovery factor then is multiplied by the OOIP to determine the amount of production that will occur above the bubble point. For reservoirs in which water influx is negligible and whose initial state is at the bubble point, these steps are not necessary.

Figure 51 illustrates an example of how to determine the amount of production above the bubble point and how to determine the OIP at the bubble point for a reservoir that is partially depleted and whose initial pressure was above the bubble point. Water-entry and rock-compressibility factors are considered negligible for this example. Figure 51A gives the known parameters for the reservoir, which has a cumulative production of 7.5 MMSTBO and a current FVF of 1.15. The bubble-point FVF is 1.350, and the initial FVF is 1.310. The first step is to determine the amount of production above the bubble point. By inserting the initial and the bubble-point FVFs into equation 3.6, the recovery factor is above the bubble point at 2.9%. This means that 2.9% of the 38 MMSTBO, or 1,125,925 STBO, was produced above the bubble point, as illustrated in Figure 51C. Figure 51D calculates the amount of oil that was produced below the bubble-point pressure by subtracting the 1,125,925 STBO from the cumulative production. The OIP at the bubble point is determined by subtracting the oil produced above the bubble point from the OOIP, as illustrated in Figure 51E. The 36.8 MMSTBO value is the OIP at the bubble point for the reservoir.

Equation 4.3 calculates the current oil saturation for a reservoir below the bubble point (Fig. 52A). The oil saturation is equal to the reservoir oil volume divided by the reservoir pore volume. The reservoir oil volume can be expressed as the OIP at the bubble-point pres-

A

$$N B_{oi} = (N - N_{p\ (above\ BP)})\ B_{BP} \qquad \text{(eq 3.4)}$$

$$\text{OOIP} = (\text{Original oil}_{STB} - \text{Produced oil}_{(above\ BP\ STB)})\ \text{Current FVF}_{(at\ or\ above\ BP)}$$

$$N_p = \frac{N_{BP} - NB_{oi}}{B_{BP}}$$

B

$$r = \frac{N_{p\ (above\ BP)}}{N} = \frac{B_{oB} - B_{oi}}{B_{oB}} \qquad \text{(eq 3.6)}$$

$$r \times N = N_{p\ (above\ BP)}$$

$$\text{Recovery factor}_{(above\ BP)} \times \text{OOIP} = \text{Produced oil above } BP$$

Figure 50. Two methods for calculating the amount of production above the bubble point. (A) Oil produced above the bubble point with respect to bubble-point FVF and OIP and OOIP values. (B) Equation for oil produced above the bubble point with respect to FVFs initially and at the bubble point.

sure (measured in reservoir barrels) minus the produced oil below the bubble point (measured in reservoir barrels) (Fig. 52B). The reservoir oil volume can also be expressed by equation 3.6, with the stipulation that N_{BP} is the OIP at the bubble point and N_p is the amount of production below the bubble point.

The reservoir pore volume, the denominator in equation 4.3, can be expressed as the OIP at the bubble point, measured in stock tank barrels, multiplied by the FVF at the bubble point divided by the oil saturation at the bubble point (expressed as salt-water saturation, S_{wc}) as shown in Figure 52C. To determine the current oil saturation for a reservoir, we can substitute the expression that we derived for reservoir oil volume (Fig. 52B) and the expression for reservoir pore volume (Fig. 52C) into equation 4.3, resulting in equation 4.5. Rearranging equation 4.5 results in equation 4.6, which is the commonly used oil-saturation formula.

Figure 53A illustrates the saturations that occur in a solution-gas-drive reservoir at some depleted state. The pore volume is composed of the oil volume plus the water volume plus the gas volume (equation 4.7). The oil-saturation formula derived in the preceding section calculates the oil saturation at any point below bubble point in the productive life of the reservoir if the current FVF is known. By knowing the initial water saturation (assuming no water input) and the current oil saturation, equation 4.8 calculates the gas saturation at that point in the life of the reservoir.

Figure 54 is an example for calculating the current oil and gas saturations for the example reservoir of Figure 51. The current oil saturation may be calculated by inserting the current FVF, the bubble-point FVF, and the initial water saturations along with the previously determined OIP at the bubble point and the amount of production below the bubble point. Solving the equation results in a current oil saturation of 49.1%, and an associated-gas saturation of 20.9%.

A

Reservoir parameters:

Cum prod = 7,540,000 STBO
OOIP = 38 MM STBO
B_o = 1.15
B_{oi} = 1.310
B_{oB} = 1.350
S_w = 30%

B

$$\text{Recovery factor} = \frac{1.350 - 1.310}{1.350} = 2.9\%$$

C

$$\text{Production above bubble point} = 38{,}000{,}000 \times 0.029 = 1{,}125{,}925 \text{ BO}$$

D

$$\text{Production below bubble point} = 7{,}540{,}000 - 1{,}125{,}925 = 6{,}412{,}882 \text{ BO}$$

E

Calculating OOIP at bubble point

$OOIP_{BP}$ = OOIP – oil produced above bubble point

$OOIP_{BP}$ = 38,000,000 – 1,125,925 BO

$OOIP_{BP}$ = 36,874,075 STBO

Figure 51. Example of determining production above the bubble point. (A) Parameters used for example. (B) Equation 3.6 for recovery factor. (C) Estimating oil produced above the bubble point (from B). (D) Determining oil produced below the bubble point. (E) Calculating OIP at the bubble point.

A

$$S_o = \frac{\text{Reservoir oil volume}}{\text{Reservoir pore volume}} \qquad \text{(eq 4.3)}$$

B

$$\text{Reservoir oil volume} = \underset{\text{(res bbl)}}{\text{OOIP}_{(at\ BP)}} - \underset{\text{(res bbl)}}{\text{Produced oil}_{(below\ BP)}}$$

$$\text{Reservoir oil volume} = \left(\underset{(STB)}{N_{BP}} - \underset{(STB)}{N_{p\ (below\ BP)}}\right) B_o \qquad \text{(eq 3.6)}$$

C

$$\text{Reservoir pore volume} = \frac{N_{BP} \times B_{oB}}{1 - S_{wc}} \qquad \text{(eq 4.4)}$$

D

$$S_o = \frac{(N_{BP} - N_p)\, B_o}{\left(\frac{N_{BP} \times B_{oB}}{1 - S_{wc}}\right)} \qquad \text{(eq 4.5)}$$

$$S_o = \left(1 - \frac{N_p}{N_{BP}}\right) \times \left(\frac{B_o}{B_{BP}}\right)(1 - S_{sw}) \qquad \text{(eq 4.6)}$$

WHERE: N_p = Oil produced below bubble point

Figure 52. (A) Equation for calculating current oil saturation at or below the initial bubble point. (B) Calculation for determining reservoir oil volume. (C) Equation for determining reservoir pore volume. (D) Equation for determining current oil saturation, substituting equations 3.6 and 4.4 into equation 4.3.

A

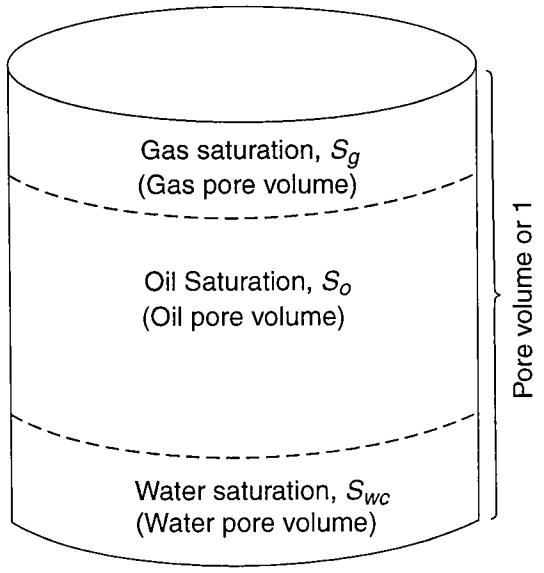

B

1 (Pore volume) = Pore volumes of oil + water + gas

$$1 = S_o + S_{wc} + S_g \qquad \text{(eq 4.7)}$$

$$S_g = 1 - S_o - S_{wc} \qquad \text{(eq 4.8)}$$

Figure 53. (A) Saturations that occur in a solution-gas-drive(?) reservoir at some point during depletion. (B) Definition of pore volume with respect to oil, gas, and water saturations.

A

$$S_o = \left(1 - \frac{N_p}{N_{BP}}\right) \times \frac{B_o}{B_{BP}} \times (1 - S_w) \qquad \text{(eq 4.6)}$$

B

Calculating current oil saturation

$$S_o = \left(1 - \frac{6{,}412{,}882\ BO}{(38{,}000{,}000 - 1{,}125{,}925)}\right) \times \frac{1.15}{1.350} \times (1 - 0.30)$$

$$S_o = (1 - 0.174) \times 0.85 \times 0.7$$

$$S_o = 49.1\%$$

$$S_g = 1 - 0.491 - 0.3$$

$$S_g = 20.9\%$$

Figure 54. (A) Equation used for calculating current oil saturation. (B) Example of calculating current oil saturation.

Equation $N_p = N \times E_d \times E_a \times E_v$ **5**

CHAPTER 5

Equation $N_p = N \times E_d \times E_a \times E_v$

INTRODUCTION

Previous chapters in this report were dedicated to defining rock and fluid properties of producing oil fields and presenting two separate methods for establishing original oil in place (OOIP) and current oil in place (OIP). OOIP, coupled with cumulative production, gives the evaluator an idea of the recovery factor for the reservoir. The recovery factor can be a helpful indicator to the viability of a potential waterflood candidate, because the lower the recovery factor, the higher the probability for a successful waterflood. But the recovery factor by itself does not suggest or imply the amount of secondary production to be expected from the waterflood candidate. As noted previously, it is a mistake to believe that the recovery factor from primary production is an indication of potential secondary reserves by waterflooding, although many prospects are evaluated under the assumption that primary recovery is an indication of secondary reserves.

The following chapters illuminate factors used for estimating how many barrels of oil may be expected from secondary operations. As mentioned previously, this workshop is designed to familiarize geologists, operators, and field personnel with the basic or fundamental principles involved with a cursory review, and also for the purpose of improving communication with the engineering department. Although the following chapters do not treat all the fundamentals, principles, or derivatives of waterflood engineering in detail, they do look at the basic rock and fluid properties that affect these fundamentals and principles and offer a brief introductory description of those fundamentals and principles that would allow a geologist or operator to make a quick estimate of secondary reserves.

OIL IN PLACE AT THE START OF THE WATERFLOOD

Predicting waterflood recovery is perhaps the most critical aspect of project evaluation. This prediction should be done on two levels: first, a preliminary, cursory evaluation for the purpose of deciding the viability of the project and continuation of the evaluation, and second, a thorough, detail-oriented review of all aspects of reserve evaluation. This and the following chapters will highlight the principles and fundamentals of the first method.

Equation 5.1 of Figure 55 represents the basic formula for waterflood-recovery prediction. N_p is the variable that represents the amount of oil to be displaced, taking into consideration the variables E_d (displacement efficiency), E_a (areal sweep efficiency), and E_v (vertical sweep efficiency). N_p in this equation represents the maximum amount of oil recovery to be expected. Certain effects, such as gas re-saturation, are not deducted from this total.

The variable N represents the amount of oil present within the floodable area as represented by equation 5.2 of Figure 56. This number is different from the N in equation 4.1 and is controlled by the area itself. In equation 4.1, A refers to the area of the oil column of the reservoir. In equation 5.2, A refers to the floodable area. The material-balance and volumetric OIP value

$$N_p = N \times E_d \times E_a \times E_v \qquad \text{(eq 5.1)}$$

WHERE:

N_p = Oil displacd by waterflood injection
N = Oil in place at the start of the waterflood within the floodable area
E_d = Displacement efficiency
E_a = Areal-sweep efficiency
E_v = Vertical-sweep efficiency

Figure 55. General equation for estimating oil displaced by waterflooding.

$$N = \frac{7{,}758\, A\, H\, \phi\, S_o}{B_o} \qquad \text{(eq 5.2)}$$

WHERE:

N = Oil in place at the start of the waterflood within the floodable area
7,758 = Total barrels per acre-foot constant
A = Floodable area
H = Average height of floodable area
ϕ = Average porosity of floodable area
S_o = Current reservoir oil saturation
B_o = Current formation volume factor

Figure 56. Equation for determining OIP within the floodable area.

represents the amount of oil at discovery. This value of N represents the amount of oil at the start of the waterflood within the floodable area and is modified by the variable S_o, which represents the amount of oil saturation currently within the reservoir (assuming equilibrium and uniform saturation) and will always be less than the original oil saturation if production has occurred. The variable S_o was defined by equation 4.6 of the previous chapter (Fig. 52) and is also an almost immediate indicator of a potential waterflood's chance of economic success. This topic will be discussed after *wettability* and *residual oil saturation* are defined in subsequent chapters.

The variables H (for average height) and ϕ (for average porosity) are treated in the same manner, except they represent those parameters in the floodable area only.

FLOODABLE AREA

Defining the floodable area is much like mapping the original reservoir. However, in this case, instead of defining the reservoir by its productive limits, it is defined by the economic influence of water injection between all injectors and producing wells. Consider Figure 57A, which represents a reservoir under a solution-gas drive. This is a reservoir composed of five producers bounded by a zero reservoir line. All five wells are producing, and the direction of the pressure sinks are shown heading toward all five producers, which will probably completely drain the reservoir of primary oil. In this case, the entire reservoir is affected by drainage. However, as illustrated in Figure 57B, when the four outside wells are converted into injectors, water is injected in all directions. As water is injected into well A, an oil bank forms. The oil bank is moved radially from the well (assuming a homogeneous reservoir). Most of the injected fluid moves along stream lines to the pressure sink, or producing well, as illustrated by well B. These stream lines would cover the entire reservoir of this example if ample time were allowed. As the injection pattern increases, the oil bank ultimately will meet adjacent banks, as shown between wells C and D. Some of the squeezed oil goes to the pressure sink, or producing well, and some goes in the opposite direction as unrecoverable oil. The water injected within the approximate area of the dashed line will hopefully drive oil to the pressure sink, or center producing well. Water injected outside the dashed line will drive oil toward the reservoir boundary, and eventually some of the oil will be driven back into the pattern. However, the water cut from water being injected into the pattern may cause that portion of the production to be uneconomical by that time. Therefore, the dashed line represents the potential drainage area for the producer in the pattern. This example illustrates the need for defining the swept area of a pattern or reservoir, because only the swept area will contribute to production. With injection, oil will be moved around outside the pattern, but for all practical purposes it does not contribute significantly toward secondary-oil recovery. Therefore, the variable A in equation 5.2 (Fig. 56) refers to the area potentially swept.

In more complex reservoirs, the manner of determining the swept area is similar. Figure 58 is a reservoir under consideration for waterflood. Wells 2, 5, 8, 11, 13,

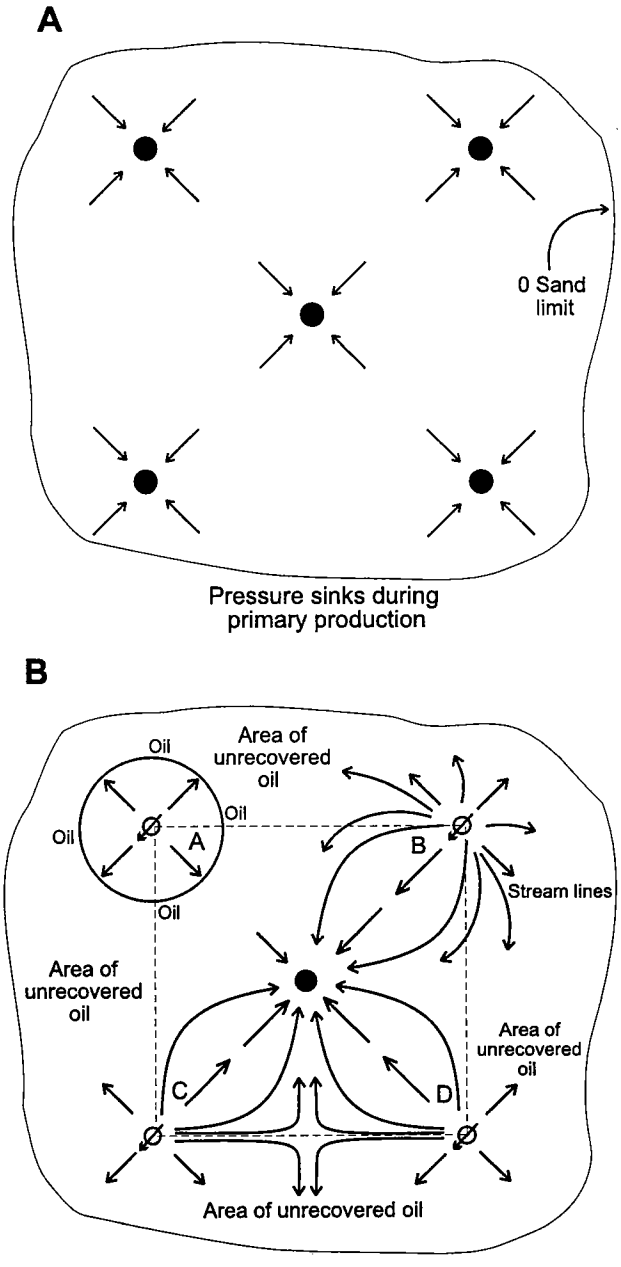

Figure 57. (A) Direction of drainage and pressure directions for producing wells. (B) Four outside wells converted to injection. Dashed line indicates possible area of production for center producing well.

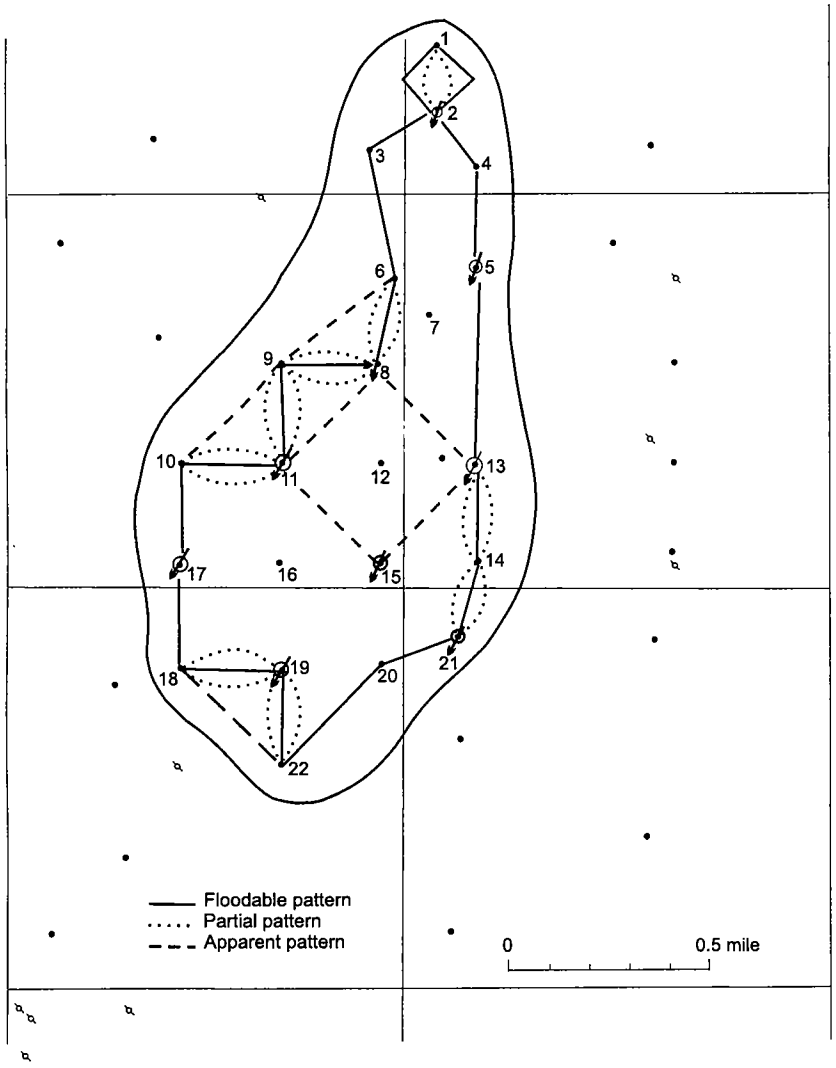

Figure 58. Hypothetical reservoir, showing floodable boundary. Solid line represents potential swept area used as the variable *A* in equation 5.2. Dashed line represents area that may not be swept because of producer–injector geometry. Dotted line represents partial patterns.

15, 17, 19, and 21 have been determined to be the injectors. The method of determining the swept area is to determine the pattern resulting from the injector–producer pattern proposed. Some patterns are fairly easy to determine, such as the pattern of wells 8, 11, 13, and 15, with well 12 as the producer. However, some patterns are more difficult to determine, such as the pattern of wells 18, 19, and 22; these wells represent only a part of a pattern. The dashed line between wells 18 and 22 would represent the normal swept area; however, if gas saturations are very high, the pattern should go from wells 18 to 19 to 22. This is particularly true where the edge wells are producers, but this would not be the case if wells 18 and 22 were injectors. However, from the author's experience, it would be best to create flow streams from injector to producer as illustrated between wells 18 and 19 and between wells 19 and 22. Flow-stream patterns would be particularly useful for determining the swept area for partial patterns such as that of wells 1 and 2. The solid line would represent one quarter of a five-spot pattern as illustrated in Figure 57, but the flow-stream pattern would probably be better suited for this situation. The floodable area for this example would be the acre-feet of the reservoir within the pattern outline.

Determining the swept area from net-sand isopach maps depends on all wells in the reservoir being in direct communication. However, a net-sand isopach map that has been derived from the addition of multiple layers can have disastrous consequences for a potential waterflood candidate. Several case histories were reviewed in the first waterflood workshop that dealt with this subject (Rottmann and others, 1998). Those cases illustrated the need to break multilayered reservoirs into genetically related components for the purpose of establishing the geometry of each sand body, for it is the geometry of the sand body that is critical in establishing an effective injector–producer pattern for a waterflood candidate.

Consider the case of the reservoir in Figure 59, which is the same reservoir used in case history 19 of the first workshop (Rottmann and others, 1998, p. 63–70). This map represents the net-sand isopach for the reservoir as interpreted by the original operators. It implies that all the wells in the reservoir are in communication. An engineering firm, using this map and its interpretation, recommended that four injection wells, with a possible fifth, would be adequate for flooding the entire reservoir. These wells would inject into the gas cap, filling it and subsequently sweeping oil to the producers. The pattern was considered viable, assuming that injection capacity was adequate and directional channeling did not occur. However, in the first workshop it was demonstrated that this reservoir (case history 19) was composed of four distinct and genetically related sand bodies, which are not everywhere in direct communication (Rottmann and others, 1998, p. 63–70).

Figures 60–62 represent three of the four sand bodies and the associated injector–producer plan suggested for each. The idea was to create an effective injector–producer pattern for each sand body that also includes common injectors and producers from the other sand bodies. The patterns were established for each sand, and the floodable area was determined by connecting the injectors and producers with a straight line.

When these maps are overlaid, common injectors and producers amongst the three layers can be deter-

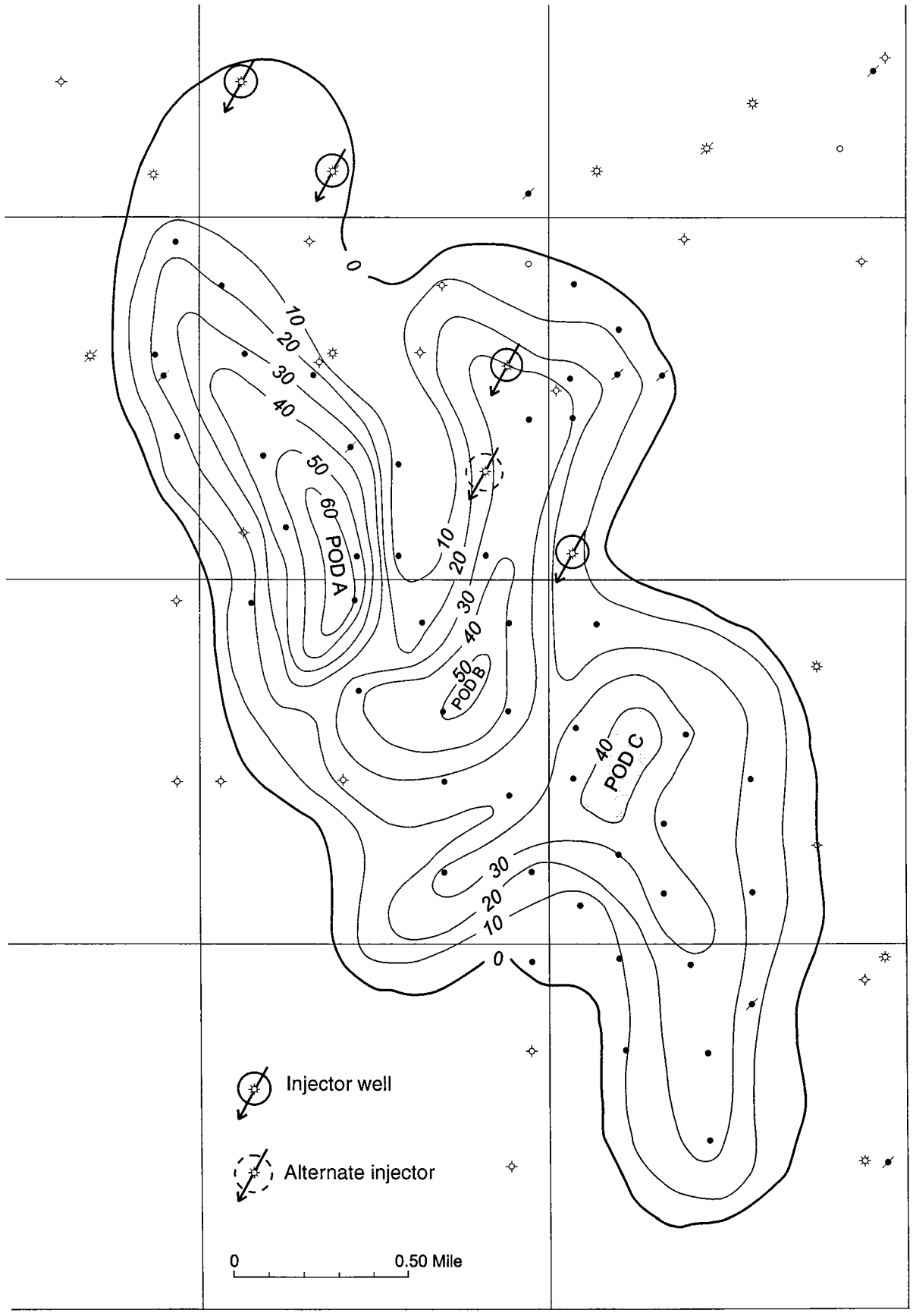

Figure 59. Isopach map of potential waterflood reservoir. Contours (in feet) represent thicknesses of >10 ohms resistivity, as interpreted from open-hole electric logs. Four proposed injection wells are shown with one alternate injector. Reservoir is in east-central Oklahoma.

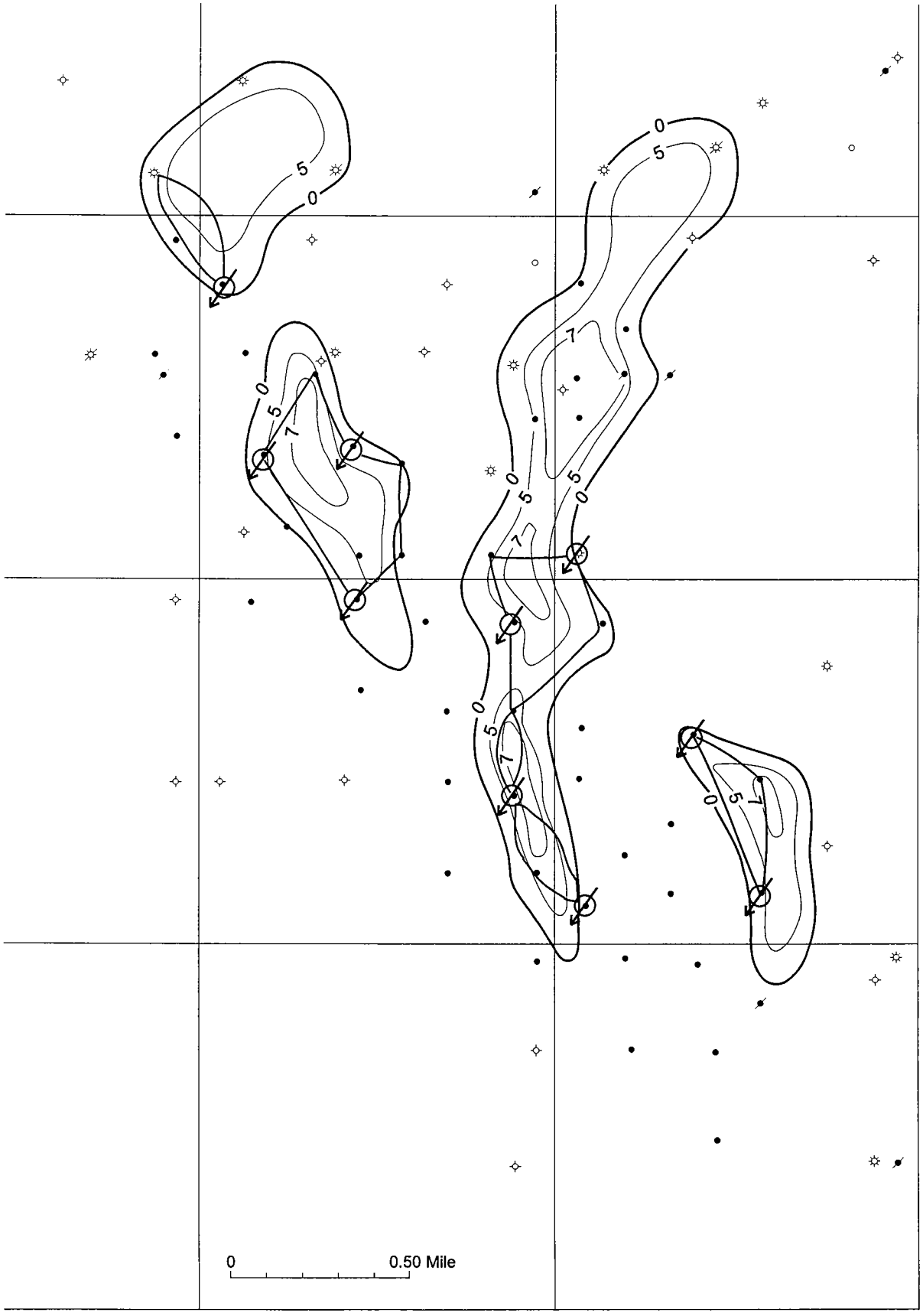

Figure 60. Map outline of sand layer A, the topmost of four layers constituting the reservoir of case history 19 (from first waterflood workshop, Rottmann and others, 1998, fig. 76). Proposed injector–producer pattern and potential swept area are shown. Contours in feet.

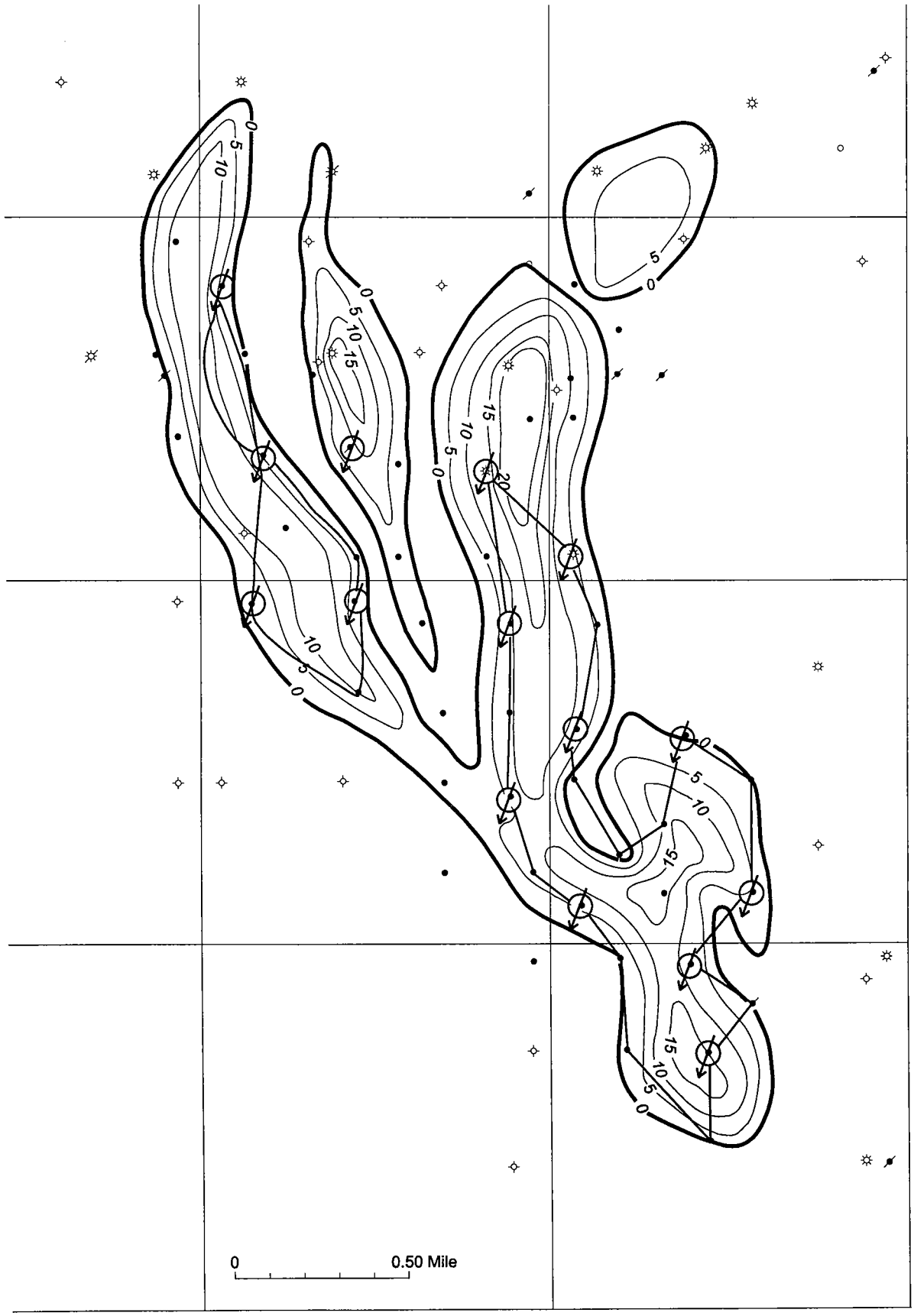

Figure 61. Map outline of sand layer B, the second of four layers constituting the reservoir of case history 19 (first waterflood workshop, Rottmann and others, 1998, fig. 77). Proposed injector–producer pattern and potential swept area are shown. Contours in feet.

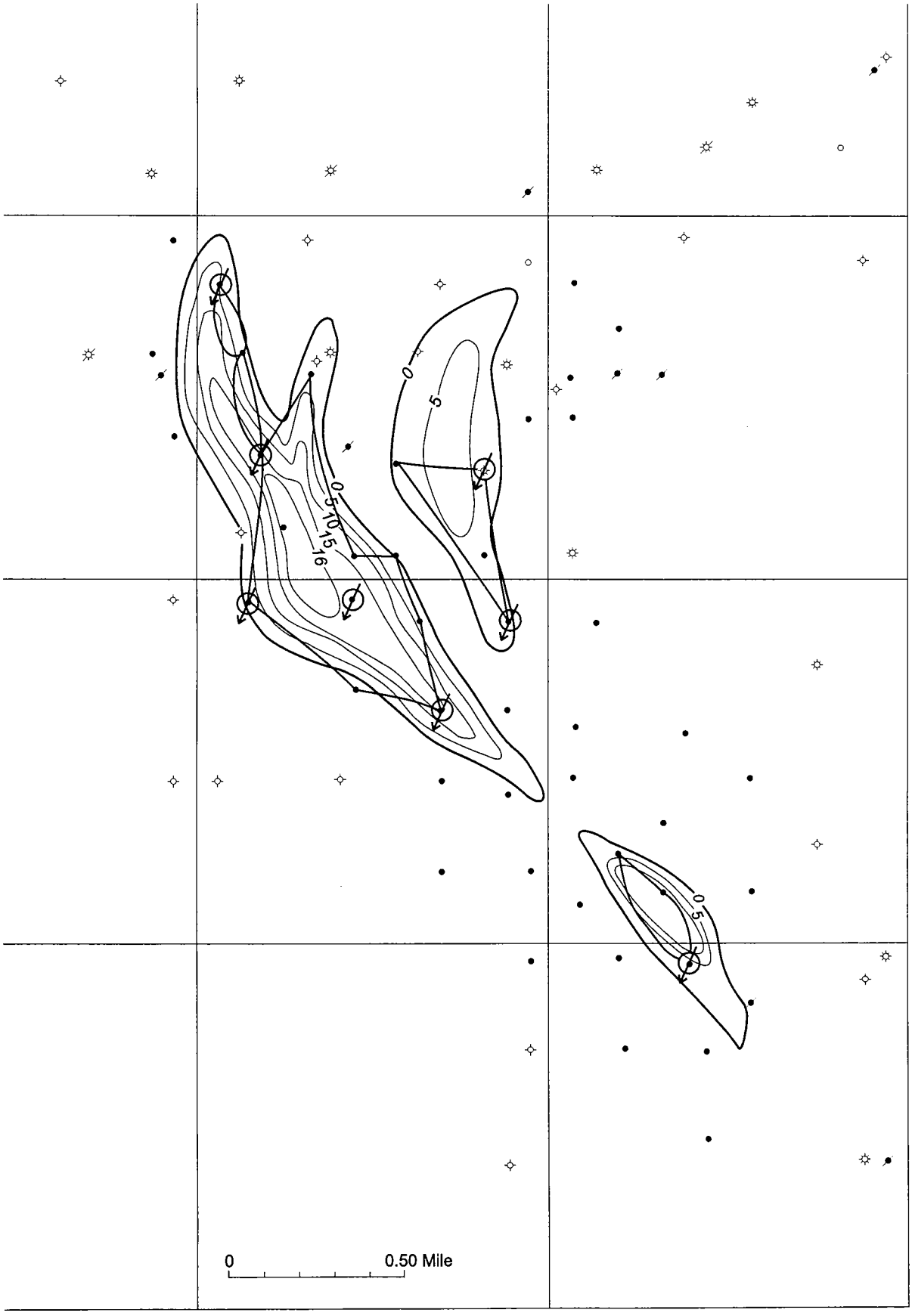

Figure 62. Map outline of sand layer C, the third of four layers constituting the reservoir of case history 19 (first waterflood workshop, Rottmann and others, 1998, fig. 78). Proposed injector–producer pattern and potential swept area are shown. Contours in feet.

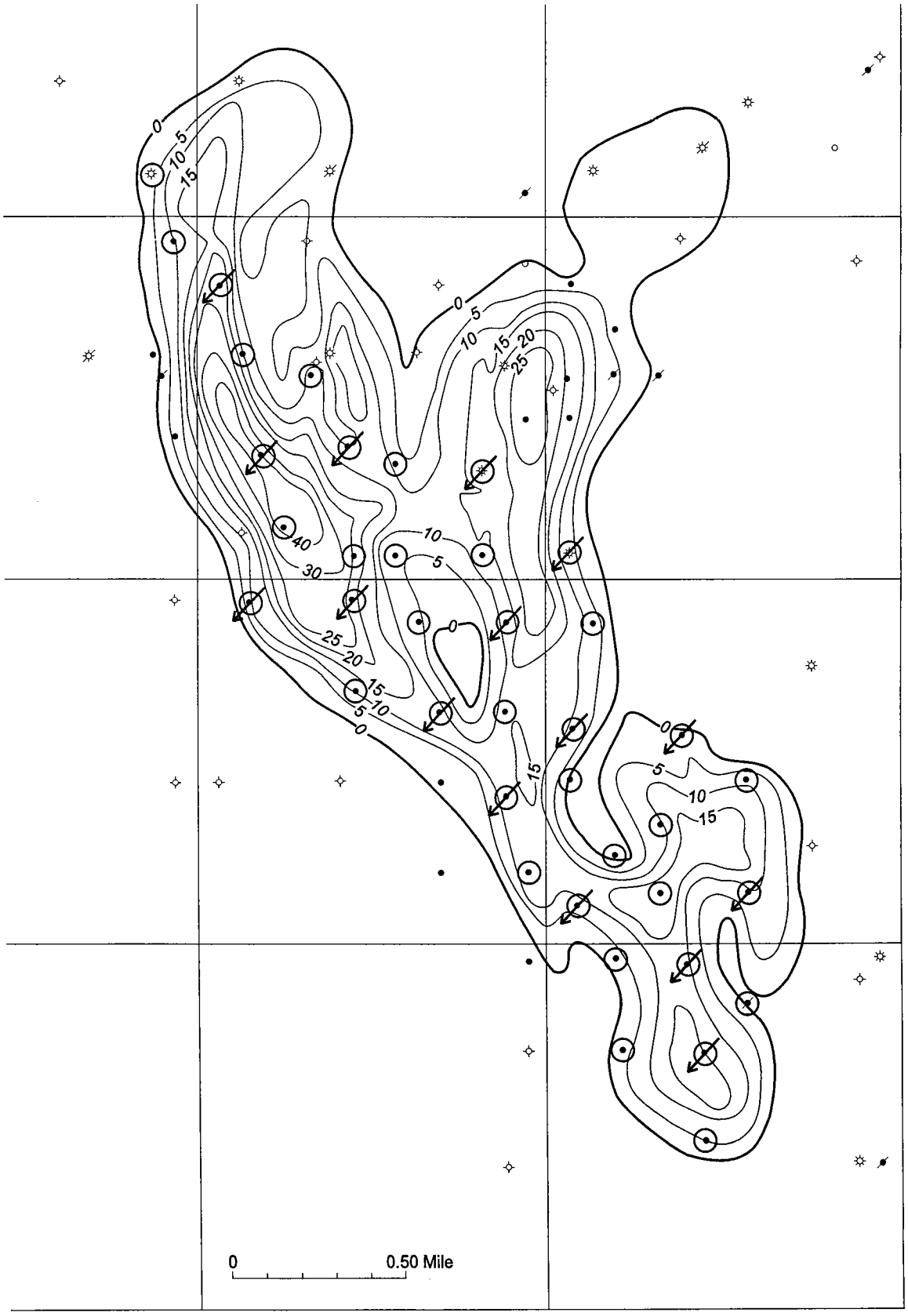

Figure 63. Composite map of the three layers that compose the net-sand reservoir of case history 19 (first waterflood workshop, Rottmann and others, 1998, fig. 81). Injector–producer pattern takes into account wells that are common to all three layers. Contours in feet.

mined. Figure 63 illustrates these combined patterns, using common injectors and producers. This pattern considers the geometry of the sand bodies of the three primary layers of the reservoir, so that this pattern in comparison to the original operator's pattern is obviously different. The economic evaluation of the operator's original feasibility study did not include money for conversion of additional wells to injectors, a fact that was soon to become obvious because of the geometry of the individual sands.

Displacement Efficiency

6

CHAPTER 6

Displacement Efficiency

INTRODUCTION

The displacement of oil by water or another immiscible injected fluid is the essence of secondary recovery. In the previous chapter, we talked about the waterflood pattern that would be affected economically by water injection. However, the displacement of oil by water within that pattern was not mentioned. The displacement efficiency, E_d, is the variable in equation 5.1 that accounts for the economic mobile oil available for production within the floodable area. Equation 6.1 of Figure 64 is the formula for displacement efficiency, represented as a fraction, and is simply the amount of mobile oil in the floodable area divided by the current oil saturation. The current oil saturation was defined by equation 4.6. This chapter is dedicated to understanding how to determine displacement efficiency for a reservoir. However, a few terms must be defined first.

Mobile oil is only a component of the current oil saturation. The oil column of any reservoir actually could be considered to be composed of four components (Fig. 65). The water portion of the oil column is divided into mobile-water saturation and irreducible (residual) water saturation. The same is true for the oil portion, which is divided into mobile-oil saturation and irreducible (residual) oil saturation. The *irreducible saturation* for both oil and water is defined as that saturation percentage that is nonmobile in the reservoir, regardless of the amount of displacing phase passing through it. The residual saturations for both oil and water vary with the wettability of the rock. The *wettability* can be defined as "the tendency of one fluid to spread on or adhere to a solid surface in the presence of other immiscible fluids" (Craft and Hawkins, 1959). In this workshop we will consider only water and oil as a possible wetting phase. Residual saturations for nonwetting-phase fluids depend on capillary-pressure and pore-size considerations. These subjects are explained in more detail in the references listed for this chapter. The properties of residual oil saturation and wettability will be discussed in following sections, but in order to define them adequately, we must first define permeability, viscosity, and capillary pressure.

A

$$\text{Displacement efficiency} = \frac{\Delta S_o}{S_o} \qquad \text{(eq 6.1)}$$

$$\text{Displacement efficiency} = \frac{\text{Amount of mobile oil remaining}}{\text{Current oil saturation}}$$

B

$$\text{Displacement efficiency} = \frac{S_o - S_{or}}{S_o} \qquad \text{(eq 6.2)}$$

Figure 64. (A) Equation for displacement efficiency in terms of mobile oil and current oil saturation. (B) Equation for displacement efficiency in terms of current and residual oil saturations.

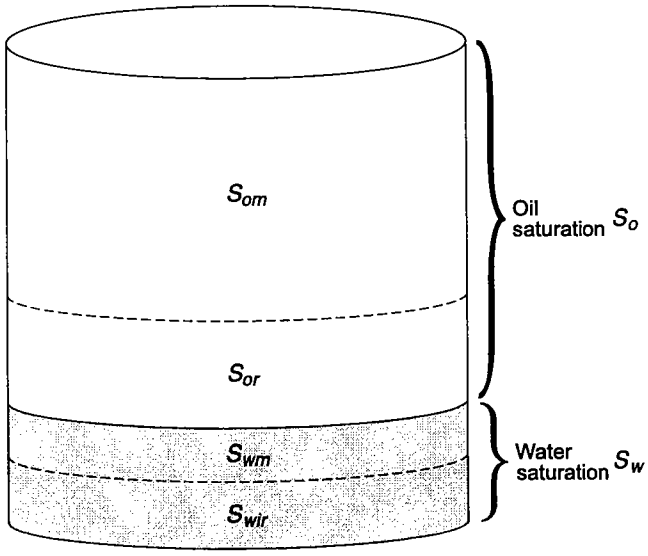

Where:
- S_o = Total Oil Saturation
- S_{om} = Mobile Oil Saturation
- S_{or} = Irreducible Oil Saturation (residual oil saturation)
- S_w = Total Water Saturation
- S_{wm} = Mobile Water Saturation
- S_{wir} = Irreducible Water Saturation (residual water saturation)

Figure 65. Four components that occupy the oil column of a reservoir (diagram).

PERMEABILITY

Permeability is the characteristic of a porous material to have the capability for a fluid to flow through it. The units of permeability were chosen to honor Henry Darcy, who developed the concepts of basic quantitative fluid flow. The unit for permeability is the darcy and is described as the flow of 1 cubic centimeter of fluid with a viscosity of 1 centipoise (water) flowing through 1 square centimeter of rock in 1 second under a pressure gradient of 1 atmosphere per centimeter of length in the direction of flow.

The permeability of a rock is called the absolute permeability if the fluid fills 100% of the pore volume of the rock. It must be stressed again that the permeability of a rock is not a function of the fluid but is a property of the rock itself. Figure 66 illustrates the relationships of porosity and permeability for various packed-sphere geometries. The cubic relationship between spheres has the highest porosity and permeability values of the four patterns, whereas the rhombohedral-sphere pattern has the lowest porosity and permeability. This demonstrates that tighter packing can affect permeability. Figure 52 of the first waterflood workshop (Rottmann and others, 1998, p. 41) illustrates the relationship of compaction and sorting to porosity and permeability and describes the need for understanding the relationship between depositional properties and permeabilities.

Equation 6.3 of Figure 67 is the equation for absolute permeability. Figure 68A gives an example of determining the absolute permeabilities for a sample of oil and water. In the first example, a 1.0-cp fluid (water) is injected into a porous medium whose cross-sectional area is 2.0 cm^2 at a pressure differential of 2.0 atmospheres over a length of 3.0 cm. The resulting flow rate, given these criteria, is 0.5 cm^3/sec. Inserting these data into equation 6.3 gives a permeability of 0.375 darcy (Fig. 68B). To demonstrate how the permeability is a function of the rock, consider the second example using the parameters from Figure 68C. Now we inject a 3.0-cp oil into the porous sample, which results in a flow rate of 0.167 cm^3/sec. Placing these data into equation 6.3 also yields a result of 0.375 darcy (Craft and Hawkins, 1959). This

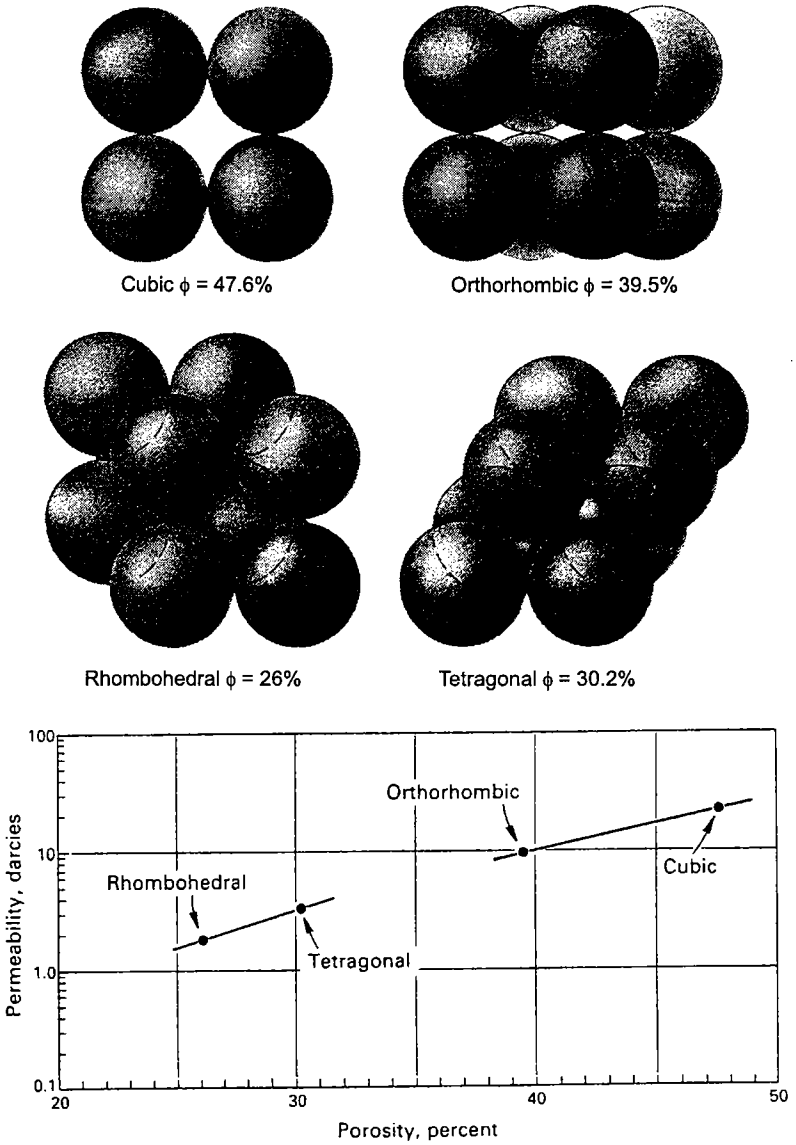

Figure 66. Some ideal geometric packing patterns of 500-μm-diameter spheres and a plot of their permeability-versus-porosity values. (Courtesy of Schlumberger.)

A

$$\text{Absolute permeability} = k = \frac{q\,\mu\,L}{A\,\Delta p} \qquad \text{(eq 6.3)}$$

WHERE:

q = Flow rate
μ = Viscosity of fluid
L = Length of flow
A = Cross-section area of flow
Δp = Pressure differential

B

$$\text{Absolute permeability} = \frac{\text{(Flow rate)(Viscosity)(Length of flow)}}{\text{(Cross-section area of flow)(Pressure differential)}}$$

Figure 67. (A) Expression for absolute permeability. (B) Definition of the expression for absolute permeability.

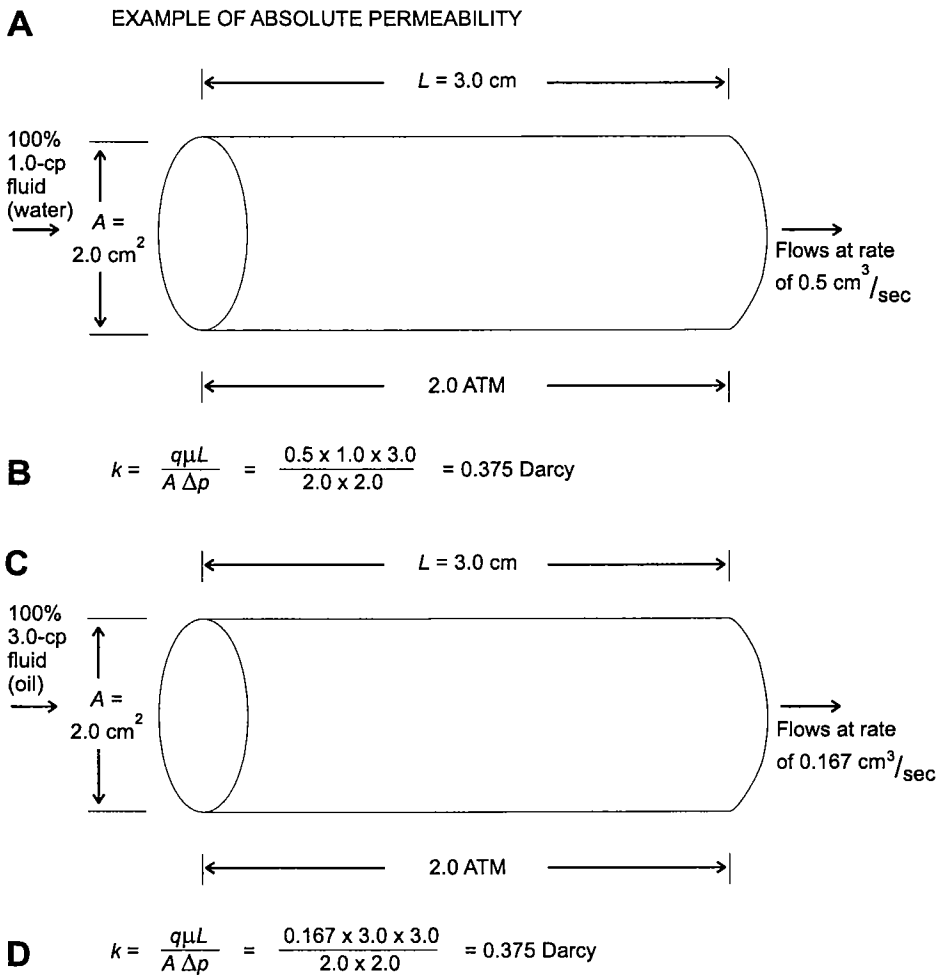

Figure 68. (A) Example of determining absolute permeability of a 1.0-cp fluid (water). (B) Equation 6.3 and its solution for the variables listed in A. (C) Second example of determining the absolute permeability of a 3.0-cp fluid (oil). (D) Equation 6.3 and its solution for the variables listed in C. (Example from Craft and Hawkins, 1959.)

example demonstrates that the absolute permeability remains the same, no matter what fluid passes through the medium, as long as the fluid occupies 100% of the pore space.

The fluid within an oil reservoir is not always homogeneous. Generally, two or more phases are involved. Figure 69A illustrates how the permeabilities are calculated when two or more phases are present. The fluid injected into the same core described previously (Fig. 68) is now composed of 70% S_w at 1.0 cp and 30% oil at 3.0 cp. The two fluids flow through the core at different rates. The salt water flows at 0.3 cm^3/sec, and the oil flows at 0.02 cm^3/sec. Substituting the flow rate for the water into equation 6.3 yields a permeability of 0.225 darcy. Also, substituting the flow rate of the oil into equation 6.3 yields a permeability of 0.045 darcy. Notice that the sum of the two permeabilities does not (and will not) equal the absolute permeability. The permeability of one fluid, in the presence of another immiscible fluid, is termed the *effective permeability* for oil or for water.

Relative permeability is defined as the ratio of the effective permeability to the absolute permeability, as shown by equations 6.4 and 6.5 (Fig. 70). These are the equations for relative permeabilities to water and oil, respectively. When various fractions of oil and water are injected into a core, a plot of the relative permeabilities can be plotted, as illustrated in Figures 71 and 72. These curves, when derived from core-fluid analysis, yield considerable information about the reservoir they represent. This information includes the wettability of the reservoir (or at least that portion of the reservoir from which the core was taken) and the residual oil and water saturations. Figure 71 represents the water–oil relative-permeability curves for a typical strongly oil-wet rock, or, as previously described, where the rock preferentially adheres to oil. Figure 72 is a typical water–oil relative-permeability curve for a strongly water-wet rock, or where water is the wetting agent of the rock. As an example, point *A* in Figures 71 and 72 represents the relative permeability of oil to water when water is at irreducible saturation (point *B*, Figs. 71, 72). The relative permeability of oil is equal to 1.0, which means that when water is nonmobile or irreducible, only oil will flow in the reservoir.

Point *D* in Figures 71 and 72 is the point at which the relative permeability of the oil is zero: in other words, oil will not flow. The *x*-axis represents the salt-water saturation at this point. Point *D* in Figure 71 implies that oil becomes immobile in a strongly oil-wet reservoir when the water saturation is approximately 70%, or the oil saturation is 30%. Likewise, point *D* in Figure 72 corresponds to approximately 75% salt-water saturation, or 25% oil saturation.

It is also characteristic for the relative permeabilities of oil and water to be equal in approximately the same positions (point *C*, Figs. 71, 72) for strongly oil-wet and water-wet reservoirs. For strongly oil-wet reservoirs, the equality of relative permeability occurs at about 40% salt-water saturation. For water-wet reservoirs, this point occurs at about 65% salt-water saturation.

The end points of the water relativity curve are also indicative of strongly water-wet and oil-wet reservoirs. The relative permeability of water at residual-oil satu-

A EFFECTIVE PERMEABILITY

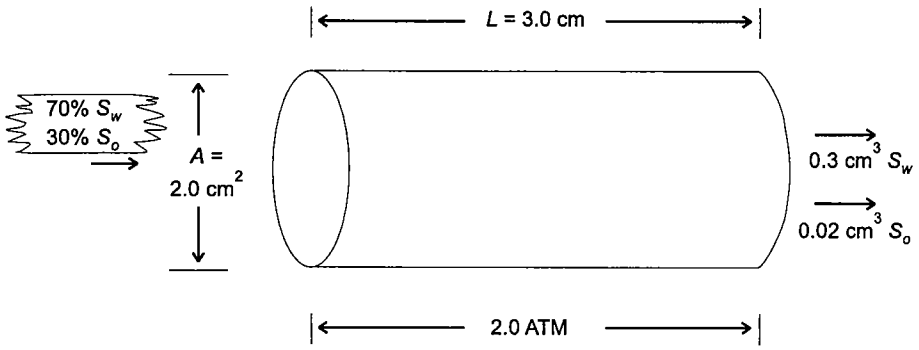

B

$$k_w = \frac{q_w \mu_w L}{A \Delta p} = \frac{0.3 \times 1.0 \times 3.0}{2.0 \times 2.0} = 0.225 \text{ Darcy}$$

$$k_o = \frac{q_o \mu_o L}{A \Delta p} = \frac{0.02 \times 3.0 \times 3.0}{2.0 \times 2.0} = 0.045 \text{ Darcy}$$

0.270 Sum of Effective Permeabilities

C Effective Permeabilities < Absolute Permeability

Figure 69. (A) Graphical illustration for determining effective permeabilities where two immiscible fluids are present. (B) Equation for determining effective permeability of the oil and water mixture. (C) Sum of effective permeabilities is always less than absolute permeability. (Example from Craft and Hawkins, 1959.)

ration is considerably higher in an oil-wet rock than in a water-wet rock. Table 1, from Craig (1971), shows some rules of thumb for interpreting the wettability of a reservoir based on information derived from the results of the relative-permeability curves for the reservoir.

A term often used is *relative permeability ratio.* This is discussed in more detail in subsequent sections. The ratio is simply the relative permeability of water to the (or divided by) the relative permeability of oil. Figure 73A illustrates the equal relationship of the relative-permeability ratio to the effective-permeability ratio.

VISCOSITY

Viscosity, by definition, is the property of a substance to offer internal resistance to flow; its internal friction. Viscosity is an important fluid characteristic and will be studied in greater detail in the next chapter, but the relationship of viscosity and wettability to waterflood recovery should be considered here. Figure 74 presents two sintered aluminum oxide cores, one oil wet and one water wet. The oil used was a 1.8-cp oil and a 2,500-cp oil. The dashed line represents the fraction of oil recovery prior to water breakthrough. The high oil/water viscosity ratio test had breakthrough with fewer pore volumes of water injected than did the lower oil/water ratio tests for both the oil-wet and water-wet cores. The experiment demonstrates that the higher the viscosity ratios, the easier it is for water to break through in both water-wet and oil-wet reservoirs.

CAPILLARY PRESSURE

Capillary pressure is, conceptually, the suction capacity of a rock for a fluid that wets the rock, or the repulsive capacity of a fluid that does not wet the rock. By definition, capillary pressure is the difference in pressure across the interface between two immiscible fluid phases jointly occupying the interstices of a rock. It is due to the tension of the interfacial surface, and its value depends on the curvature of that surface (Jackson, 1997).

Capillary pressure is an important variable for complex prediction models of waterflood behavior. It controls the vertical distribution of fluids in a reservoir and can predict the vertical water-wet distribution in a water-wet system. Capillary-pressure data can provide information on the pore-size distribution of a reservoir. As described in the first waterflood workshop, capillary-pressure data can also determine the irreducible water saturation (Rottmann and others, 1998). And probably most importantly, capillary pressure can influence the displacement efficiency by its influence on the movement of a waterflood front (Smith and Cobb, 1987).

Relative permeability

$$K_{rw} = \frac{K_w}{K} \qquad \text{(eq 6.4)}$$

$$K_{ro} = \frac{K_o}{K} \qquad \text{(eq 6.5)}$$

WHERE:

K_{rw} = Relative permeability to water
K_{ro} = Relative permeability to oil
K_w = Effective permeability to water
K_o = Effective permeability to oil
K = Absolute permeability

Figure 70. Equations for determining relative permeability.

Capillary-pressure data are not always available, as they require expensive core tests to obtain. Because this workshop centers on a cursory evaluation of oil in place and potential secondary recovery, we will not go into more detail on this subject.

WETTABILITY

Two terms must be defined when dealing with wettability. These are *imbibition* and *drainage* processes.

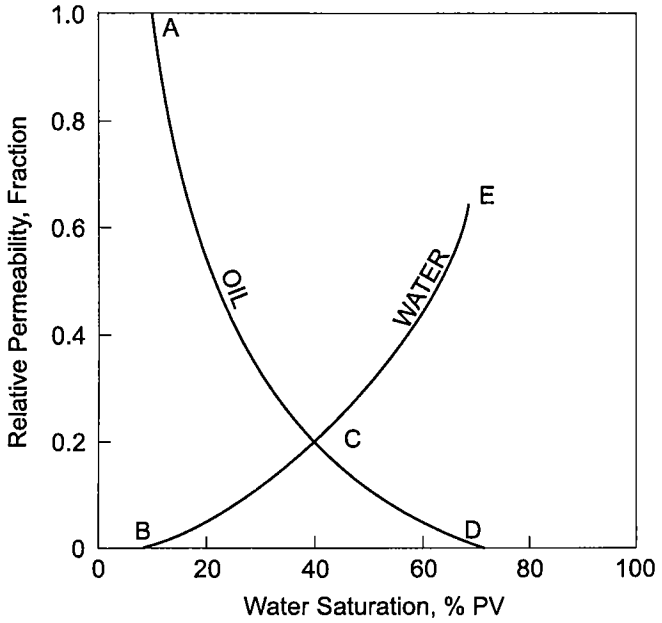

Figure 71. Water–oil relative-permeability curves for strongly oil-wet rock. (Craig, ©1971; reprinted by permission of Society of Petroleum Engineers.) See text for further explanation.

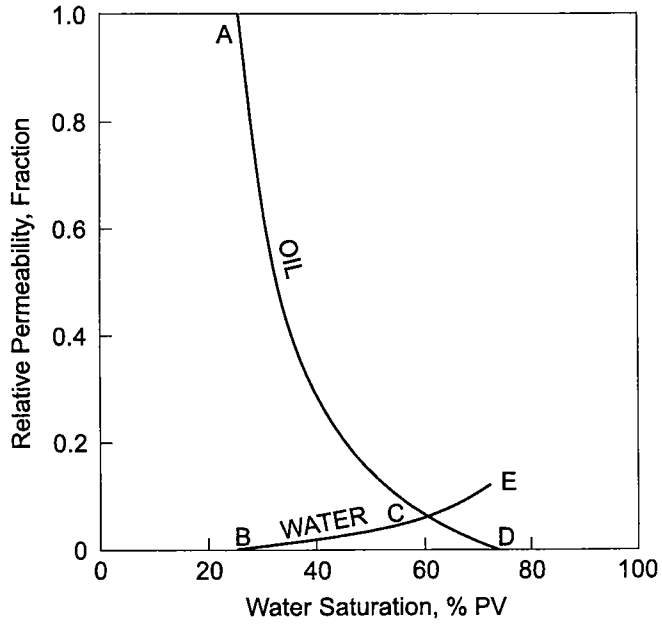

Figure 72. Water–oil relative-permeability curves for strongly water-wet rock. (Craig, ©1971; reprinted by permission of Society of Petroleum Engineers.) See text for further explanation.

TABLE 1. – Comparison of Water-Wet and Oil-Wet Properties[a]

	Water-Wet	Oil-Wet
Connate-water saturation	Usually greater than 20–25% PV	Generally <15% PV, frequently <10%
Saturation at which oil and water relative permeabillities are equal	>50% water saturation	<50% water saturation
Relative permeability to water at maximum water saturation; i.e., floodout	Generally <30%	>50% and approaching 100%

[a]Modified from Craig (©1971); reprinted by permission of Society of Petroluem Engineers.

Figure 75A illustrates imbibition, which is defined as increasing the wetting phase. Figure 75A1 illustrates the water-wet relationship with the sediment. Figure 75A2,3 shows the increase of the wetting phase—that is, the injection of water. The increase in the wetting phase is termed imbibition. Figure 75B illustrates an oil-wet environment. By injecting water, the wetting phase is decreased, and the term is called drainage. Wettability in reservoir rock was described previously in this chapter as being a fluid's tendency to adhere to a solid surface in the presence of other immiscible fluids. This phenomenon is probably due to the presence or absence of polar compounds existing in crude oils. These compounds probably exist in minute quantities and are apparently asphaltic in nature. They are absorbed in the rock surface, rendering them oil-wet. Several methods are used for determining the wettability of a reservoir. One is to use an uncontaminated sample of the reservoir crude oil and a polished crystal representing the predominant mineral within the reservoir in a contact-angle test described by Wagner and Leach (1959). The test can take hundreds of hours to accomplish because of the time necessary for equilibrium to occur. The advantage of the tests is in the reliability and the ease of obtaining uncontaminated fluid samples versus uncontaminated rock samples from cores used in other tests. Contact angles near 0° (Fig. 76) indicate strongly water-wet reservoirs, whereas those approaching 180° indicate strongly oil-wet reservoirs. Tests resulting in a 90° angle apply to reservoirs of intermediate wettability (Craig, 1971).

Water movement within a core has been described by Rasa and others (1968) and is illustrated in Figures 77 and 78 for water-wet and oil-wet reservoirs. Figure 77A represents a water-wet reservoir at initial water saturation. Because of capillary pressures, oil is confined to the center of the larger pores and as droplets within the smaller pores. Water forms a thin film over all the solid surfaces and is the wetting phase. Craig (1971) describes the movement of water through the reservoir as a uniform front. Figure 77B illustrates the

A

Relative-permeability ratio

$$\frac{K_{rw}}{K_{ro}} = \frac{K_w/K}{K_o/K} = \frac{K_w}{K} \times \frac{K}{K_o} = \frac{K_w}{K_o}$$

B

Effective-permeability ratio

$$\frac{K_w}{K_o}$$

Figure 73. (A) Equation for determining relative-permeability ratio. (B) Definition of effective-permeability ratio.

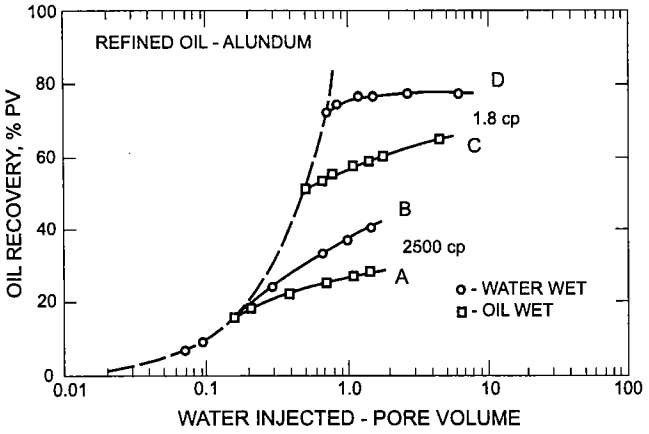

Figure 74. Effect of low viscosity and a high-viscosity oil on an oil-wet and water-wet sintered aluminum oxide core. (Jennings, ©1966; reprinted by permission of Society of Petroleum Engineers.)

introduction of injected water, which tends to move into the smaller pores, displacing oil in the process (Fig. 77C). Oil that has moved into the larger pores or is contained in the larger pores is moved out by the injected water. Ahead of the water front only oil is moving, and behind the front some of the oil is trapped in impermeable channels or forms globules that remain behind. This constitutes the bulk of the residual-oil saturation. Figure 77D demonstrates that after the water front has passed, almost all the oil is immobile, and because of this, at breakthrough little or no oil is produced from this stream line (Anderson, 1987).

Figure 78 describes oil displacement in an oil-wet environment. A waterflood in an oil-wet rock is much less efficient than one in a water-wet rock. Figure 78A illustrates rock surfaces coated with a thin film of oil. The water saturation forms as globules in the center of the pores. Water, at the beginning of the waterflood, is usually confined to the larger channels, displacing oil in the process (Fig. 78B). As water injection continues, the water works into the smaller pores and channels, displacing oil also (Fig. 78C). As production continues, the water/oil ratio (WOR) gradually increases as the oil from the smaller channels reaches the wellbore. When water is basically unrestricted to the producing well, oil production becomes negligible (Anderson, 1987).

The effect of wettability on waterflood performance can be generally summarized here by Figure 79, which is from a paper by Owens and Archer (1971) using a sample of oil-wet and water-wet Torpedo Sandstone (Pennsylvanian) cores from Oklahoma. The wettability was laboratory controlled, and relative permeability curves were measured, to calculate field performance for a 20-acre five-spot pattern with homogeneous properties. Water breakthrough is the point at which each curve becomes nonlinear. Notice that the strongly oil-wet test had water breakthrough first, and the strongly water-wet test had breakthrough after the greatest percentage of oil was recovered. The results of this test represent results of waterflood recoveries in general for uniformly wetted reservoirs that have a reasonable oil/water viscosity ratio. Oil-wet reservoirs generally have water breakthrough from a smaller amount of injected pore volume than water-wet reservoirs.

Figure 80 illustrates typical water-breakthrough relationships, oil-recovery percentages, WORs, and cumulative WORs for water-wet and oil-wet cores. Curve *A* represents the amount of oil recovery versus pore volumes of water injected for the water-wet core. Notice that most of the oil is recovered prior to water breakthrough, with very little recovered after breakthrough. Curve *C* represents the WOR for the water-wet core and illustrates that once breakthrough occurs, the amount of water can increase rapidly. This suggests that the amount of oil produced can be independent of the amount of water injected.

Breakthrough for an oil-wet reservoir occurs much earlier in the life of the injection process, as illustrated by curve *B* (Fig. 80). However, as opposed to a water-wet environment, water production increases gradually, and a significant amount of oil is produced after the onset of water production. The oil-wet system is less efficient than the water-wet system, because considerably more pore volumes of water are necessary to recover similar amounts of oil. Also, the oil recovery for an oil-wet system depends on the amount of water injected.

MIXED WETTABILITY

Mixed wettability refers to a reservoir that is not homogeneous in its wettability. This can be due to the various minerals contained in the sediment and the ionic exchange associated with them. Salathiel introduced the term to describe an occurrence in which the larger, well-connected pore spaces are oil-wet and the smaller, discontinuous ones are water-wet and contain no oil.

Mixed wettability can have a dramatic impact on a potential waterflood project. Consider the reservoir represented by the log suite of Figure 81, which was considered a potential waterflood candidate by a major oil company. The feasibility study did not mention or

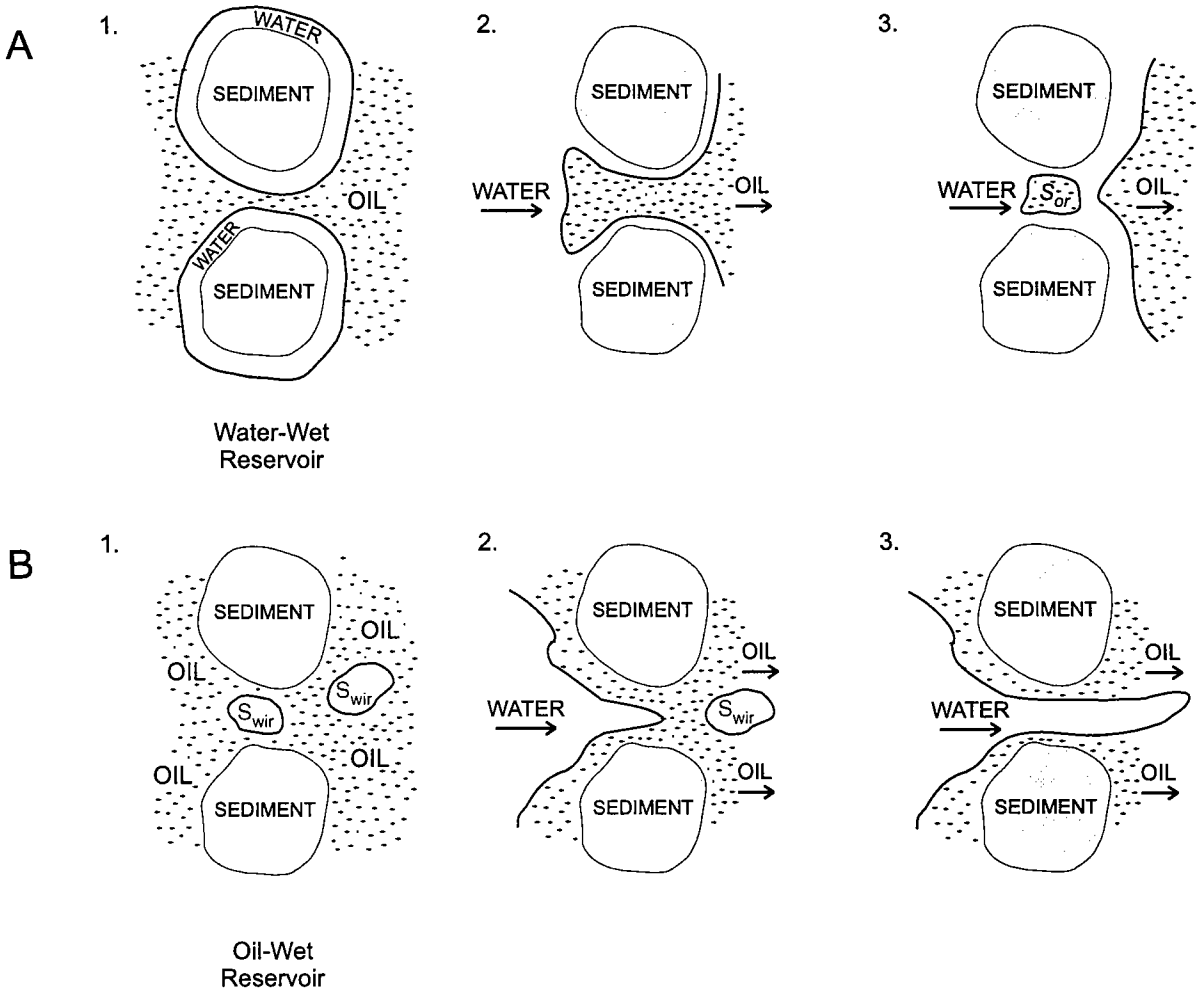

Figure 75. (A) Parts 1, 2, and 3 illustrate an increase in the wetting phase (water), a process termed *imbibition*. (B) Parts 1, 2, and 3 illustrate a decrease in the wetting phase (oil), a process termed *drainage*.

explain the significant resistivity contact at point *A*. Figure 82 is a series of core photographs from the same well. Notice at point *A* a dramatic facies change from a fine- to medium-grained sandstone to a limestone conglomerate. Relative-permeability curves and other criteria revealed the sandstone facies to be strongly oil-wet and the conglomerate facies to be strongly water-wet. This field was only several miles from a very successful waterflood in the same formation. However, that waterflood had only a small amount of the conglomerate facies. The original operator of the field assumed that the successful result of the offset waterflood was sufficient to predict a successful outcome for this field. When the reservoir started responding to injection, it became obvious that the flood would have a large water cut with the oil production, which was generally less than 5% of the produced fluid. Two wells were making all oil with no water cut. Figure 83 is a structural representation of the field, illustrating the sandstone and conglomerate facies. Wells A and an offset to Well B were the two wells that produced only oil. The difference between the 100%-oil producers and

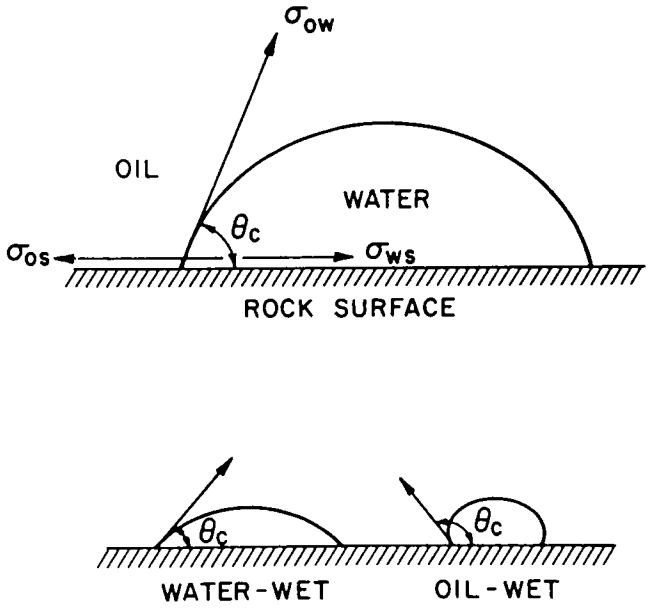

Figure 76. Illustration of contact angles used to determine wettability. (From Raza and others, 1968.)

wells with large water cuts depended on the absence or presence of the conglomerate facies. The permeabilities of the conglomerate were higher than those of the sandstone, and apparently the injected water was confined to this zone, bypassing oil in the sandstone above.

RESIDUAL-OIL SATURATION

Determining the residual-oil saturation is perhaps the key to displacement efficiency, because it describes the amount of oil within a reservoir that will not be produced. If relative-permeability data are available, the residual-oil saturation can be determined readily by determining where the relative permeability to oil is equal to zero. However, this information is not always available, especially for older reservoirs.

Often, a well within a reservoir has been cored, and only a basic core analysis has been made. Although such an analysis will generally supply the current sur-

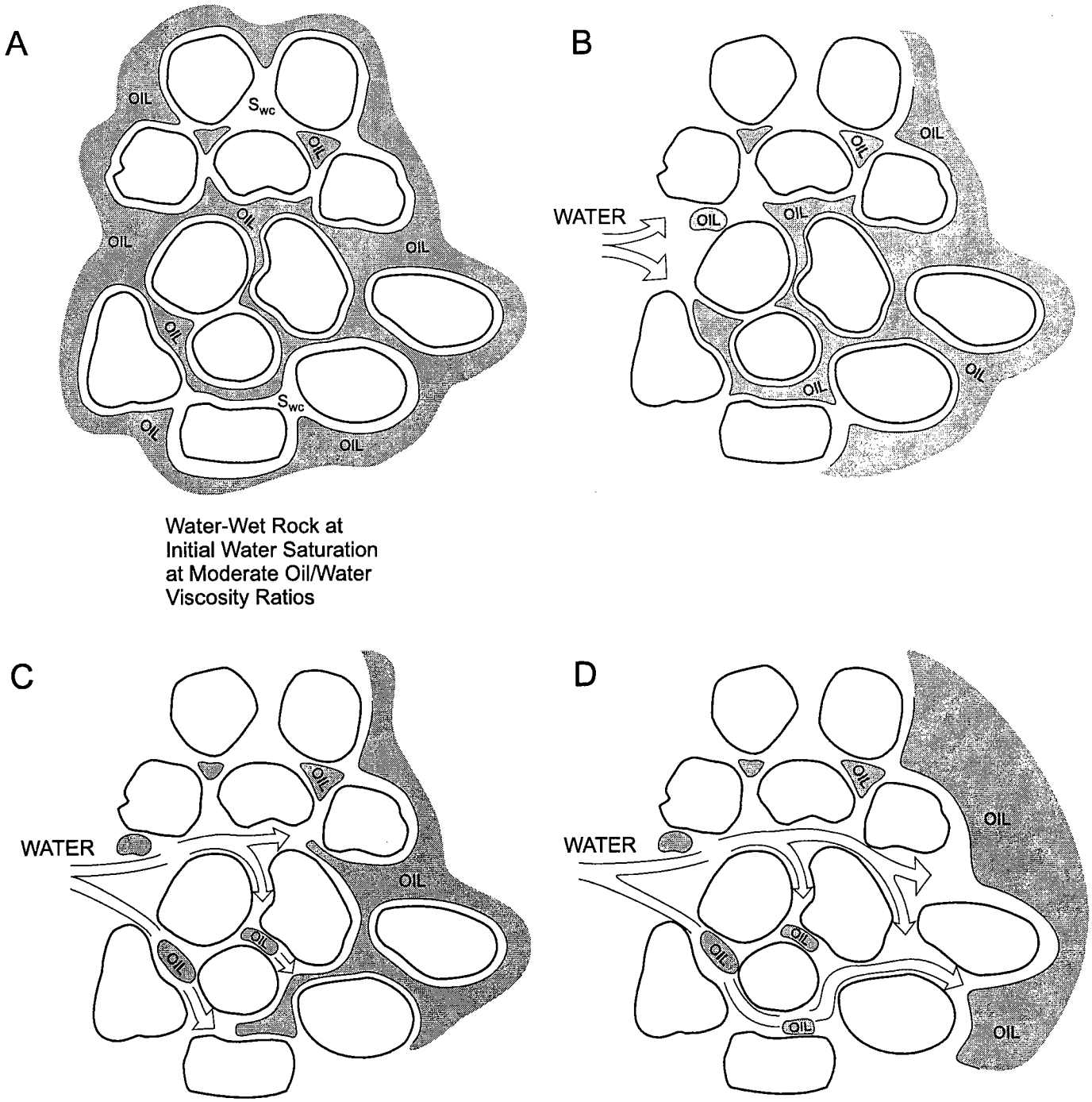

Figure 77. Oil displacement within a water-wet environment. (A) Initial conditions. (B) Entry of injected water. (C) Injected water moves into smaller pores, displacing oil. (D) Residual oil remains after water front has passed.

face saturation for oil and water in the core, this saturation does not represent the saturations present in the reservoir. Figures 133–136 of the first waterflood workshop (Rottmann and others, 1998) illustrate the saturation changes that occur to fluids in a core as it approaches the surface. Figure 84 is the same as figure 133 from the first workshop. Part of Figure 84 illustrates those saturation changes that occur when an oil column is cored by a water-based mud. In the water-based-mud system, the filtrates act as an injected fluid sweeping oil from the core and increasing the water saturation within the core. This behavior is similar to a waterflood process, and the saturations for the core probably would represent final saturations for the reservoir if the core could be preserved at those pressures. However, when the core approaches the surface and the dissolved gas breaks out of solution, it also expels oil and water, further reducing the volume of oil. A common

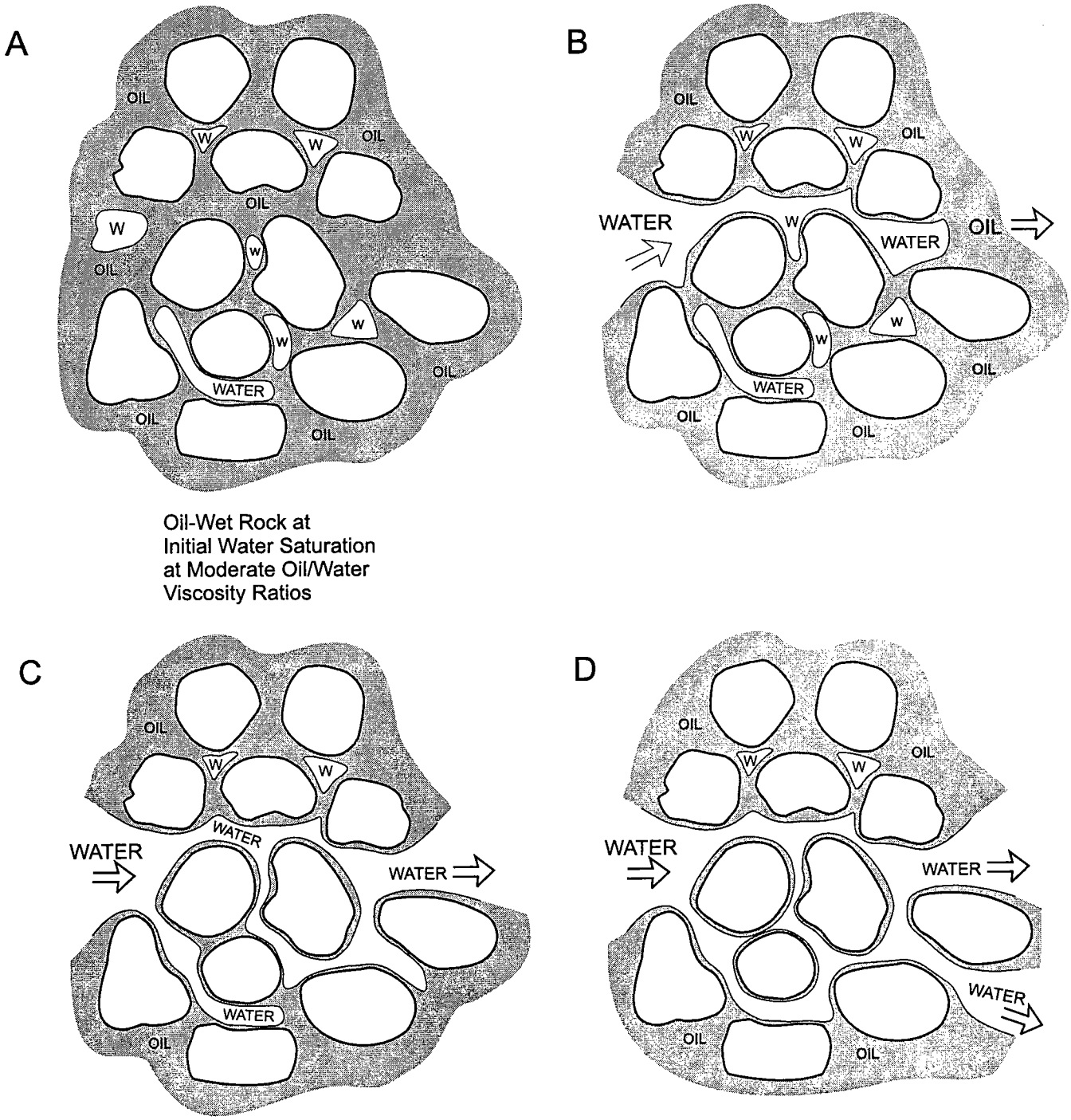

Figure 78. Oil displacement within an oil-wet environment. (A) Initial conditions. (B) Entry of displacing water through higher permeability channels. (C) Water starts permeating smaller permeability channels. (D) All permeability channels have been invaded by water, displacing the mobile oil.

result is oil saturations reported for the core that are below the residual saturations in the reservoir.

Jennings (1966) experimented with residual-oil saturations in sintered aluminum oxide plugs in which the wettability was controlled. The plugs were initially treated with 10% kerosene and then waterflooded. The water saturation at breakthrough was 75% for the water-wet plug and 53% for the oil-wet plug. When 40 pore volumes of water had been injected, the oil saturations were 85% for the water-wet plug and 81% for the oil-wet plug. If enough pore volumes of water is injected, the ultimate residual-oil saturations may approach the same percentage for oil-wet and water-wet environments. However, this is not practical for a waterflood project. The residual-oil saturation for a water-wet reservoir is lower than that of an oil-wet reservoir. It is the author's experience that water-wet and intermediate-wet reservoirs have residual saturations ranging from 25 to 35%, and for oil-wet reservoirs the saturations generally range from 30 to 45% or higher.

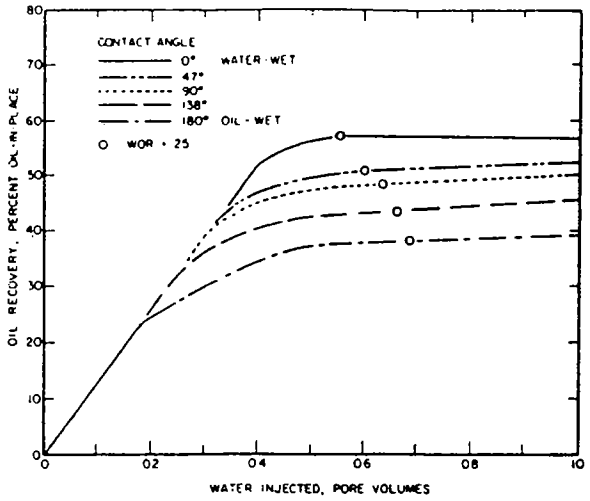

Figure 79. Effect of wettability on waterflood performance, using a controlled water-wet and oil-wet core for a simulated 20-acre five-spot pattern. (Owens and Archer, ©1971; reprinted by permission of Society of Petroleum Engineers.)

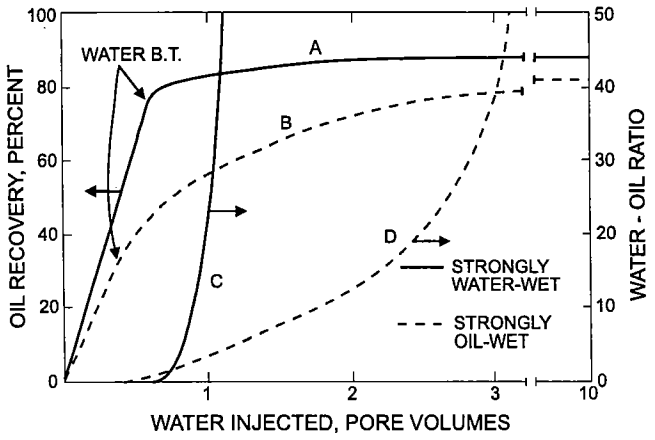

Figure 80. Typical waterflood performance in water-wet and oil-wet sandstone cores at moderate oil/water viscosity ratios. (Modified from Raza and others, 1968.)

The problem with residual-oil saturations and their influence on displacement efficiency is in estimating the residual-oil saturation from basic core-analysis data. Generally, determination of oil saturation from core analysis has been influenced from the flooding effects of the filtrate during coring and the expansion and expulsion of the oil from gas breaking out of solution. The following two examples illustrate typical core analyses for water-wet and oil-wet reservoirs with moderate GORs.

Figure 85 is an electric log from a field in east-central Oklahoma. The cored interval is represented by the crossed area. Table 2 is the core analysis for this well. Notice that the interval from 2,214 to 2,222 ft has an average oil saturation of approximate 16%. Owing to the effects of coring, this saturation is lower than expected for residual-oil saturation. A general rule used by the author is to essentially double the average oil saturation for the core and use this number to represent the residual-oil saturation for the reservoir. In this case, the saturation doubled would be approximately 32%. The wettability of the reservoir can be inferred from the calculated water saturation if the saturation also is assumed to be at or near residual. In this case, the initial production for the well and for the field did not report any water production; therefore, the water in the reservoir can be assumed to be immobile. In this case, the salt-water saturation for the reservoir also averages 32%. Comparing this to Craig's rule of thumb from Table 1 would imply that the reservoir is water-wet.

Figure 86 is an electric log from a reservoir in south-central Oklahoma. Table 3 lists the core analysis. The average oil saturation from the core analysis is 35%. Because of the processes involved with coring, this amount is below the actual residual-oil saturation for the reservoir. The author's rule of thumb of doubling the average core oil saturation does not apply for oil-wet reservoirs, but a factor of 1.5 may be in order until more thorough and exact data are obtained. In this case, 1.5 multiplied by the oil saturation from the core results in an approximate residual-oil saturation of 52%. The core analysis for this well yielded a 49.6% residual-oil saturation. The calculated water saturation was 8%. Because the wells in the field had no history of water production, this could represent the residual-water saturation. A comparison of these parameters to Craig's rule of thumb from Table 1 suggests that this reservoir is oil-wet.

RESTORED CORE AND CONTAMINATION

Figure 87 represents calculated waterflood data using a core that was contaminated with wettability-altering chemicals in the mud that rendered the core

oil-wet. The same core was cleaned and rendered water-wet. This test indicates significant differences in results that can occur from core that has not been preserved properly. According to Figure 87, the core would have a much better waterflood response after it was rendered water-wet in comparison to the contaminated oil-wet core. This demonstrates the care that must be given the core when special waterflood tests are planned. Native-state core refers to core whose wettability characteristics, and often fluid saturations, are preserved. Restored-state core refers to core that has been cleaned and dried and artificially returned to the same wettability and fluid saturations representative of the reservoir. Thus, restoring the core depends on an independent knowledge of those reservoir conditions.

Sometimes an attempt to restore the core can lead to properties that are not representative of the reservoir at all. Consider the case shown in Table 4. The operator of this reservoir submitted a section of core for analysis. The core had been preserved by wrapping the core in saran wrap and aluminum foil after the cores had been dipped in seal-peal wax. The core was assumed to be fresh. The results of the core analysis determined the core to be oil-wet and the residual oil saturation to be 52%. The analysis was flawed because of the aging effect on the core. The wettability determination and the residual-oil-saturation data were totally useless because of the alteration to the core. The reservoir was likely to be water-wet, because the salt-water saturation of 32% was at or near irreducible levels. Of interest for this reservoir was the fact that the current oil saturation at depletion was calculated to be near the 52% figure calculated for the residual saturation from the contaminated core. The field is now unitized and is producing about 600 BOPD at peak production.

FRACTIONAL-FLOW EQUATION

Displacement efficiency means essentially displacing one fluid by another. In the case of a waterflood, the mobile oil remaining is displaced by injected water (or other fluids). This concept implies that the movement of fluid within the reservoir at any particular point may

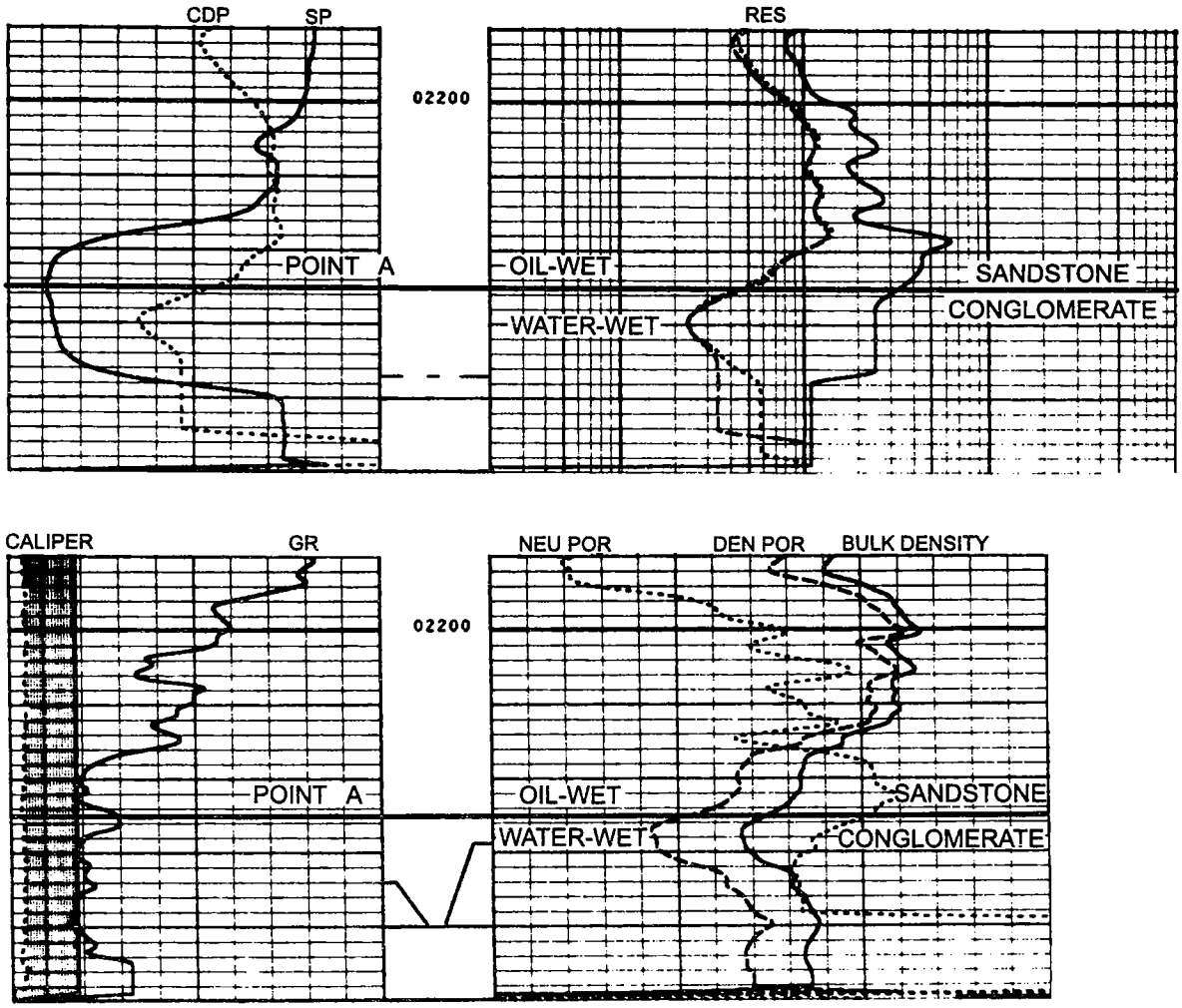

Figure 81. Log suite from a well within a reservoir under consideration as a waterflood candidate. Point *A* refers to a significant resistivity change. *CDP* = conductivity-derived porosity; *SP* = spontaneous potential; *RES* = resistivity; *GR* = gamma ray; *NEU POR* = neutron porosity; *DEN POR* = density porosity.

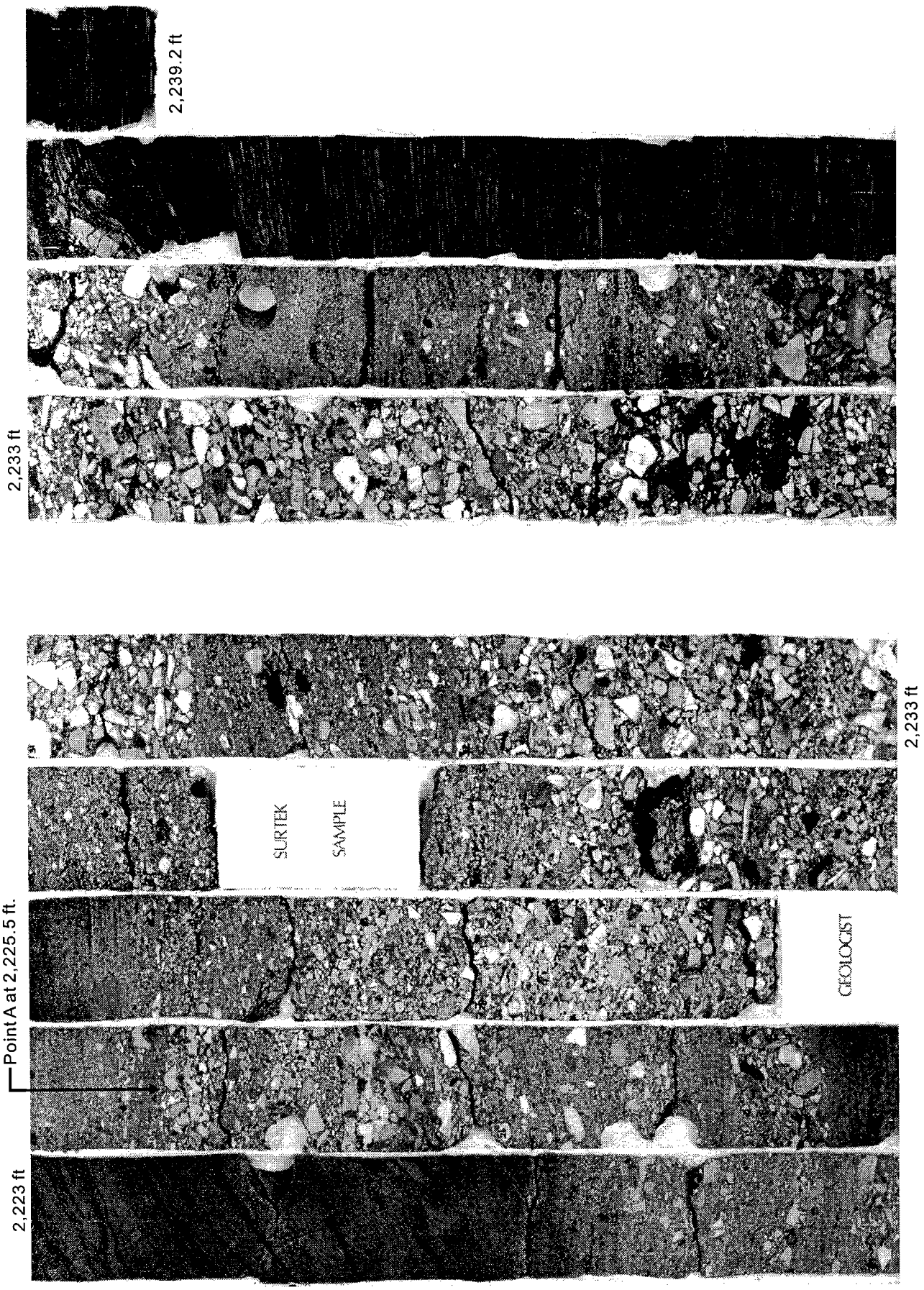

Figure 82 *(above and facing page)*. Core photographs of the cored interval from the well of Figure 81. Photographed under natural light.

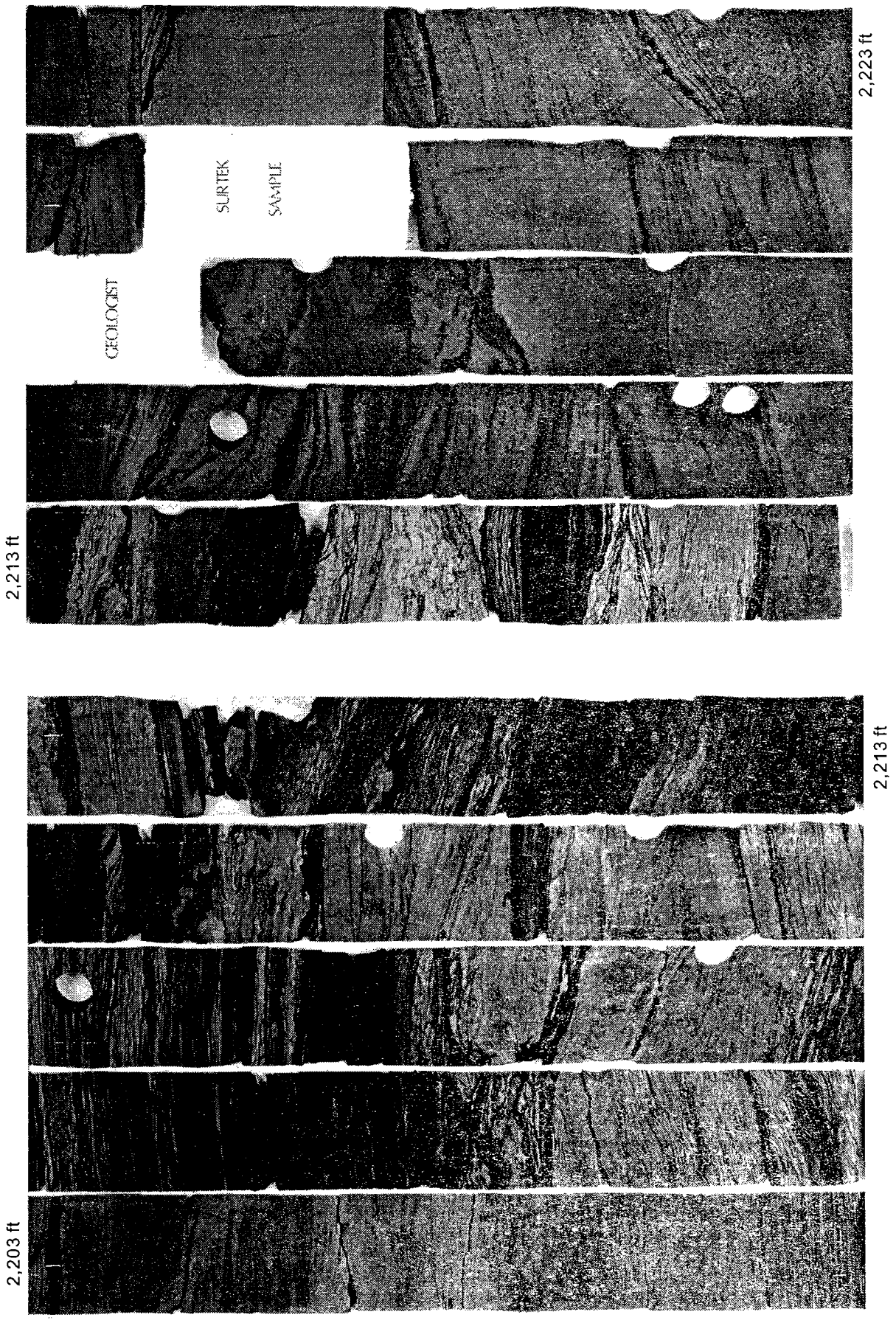

Figure 82 *(continued).*

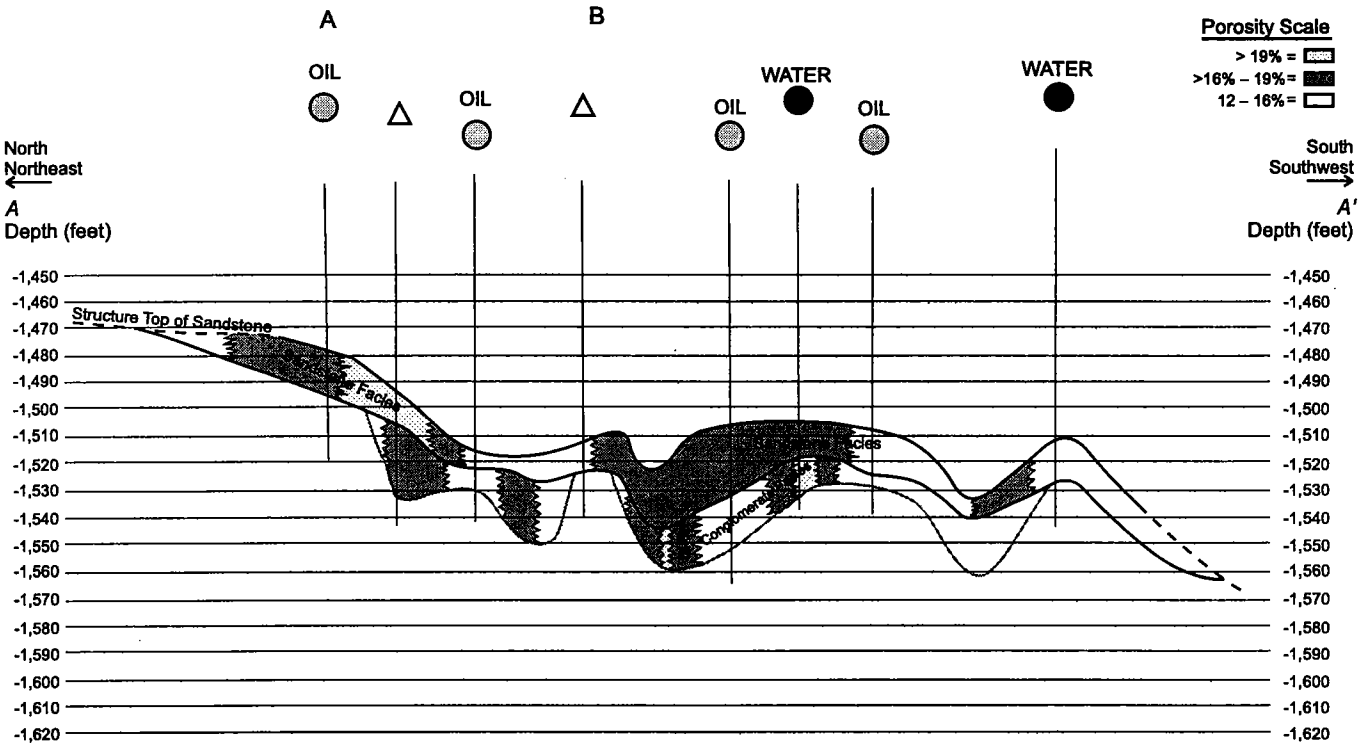

Figure 83. Structural facies representation of the reservoir under consideration as a waterflood candidate. The log suite and core described in Figures 81 and 82 are from this reservoir.

be composed of two or more immiscible fluids. *Fractional flow* is defined as the fraction of the total fluid flow that is caused by the flow of the displacing phase

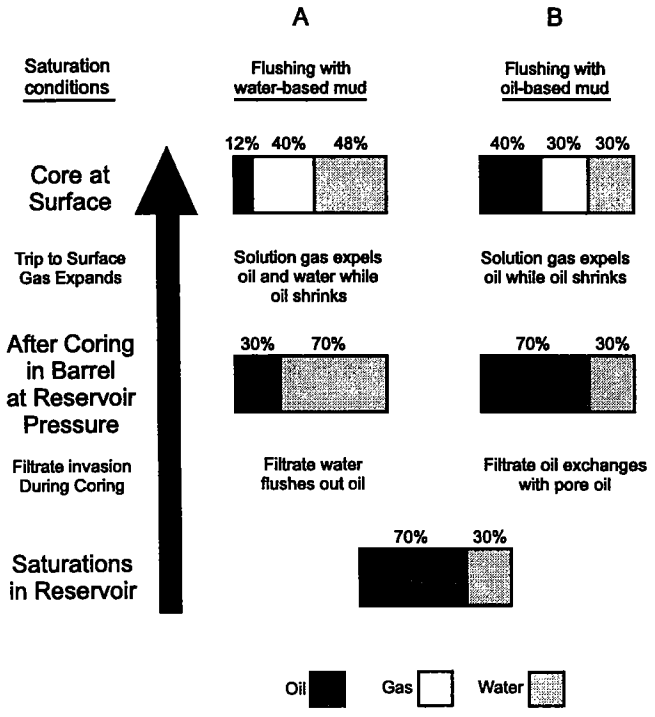

Figure 84. Typical fluid contents for a core as it goes from reservoir conditions to surface conditions. (Core Laboratories, ©1980; reprinted by permission.)

(Slider, 1983). In the case of a waterflood, the displacing fluid is water, and the displaced fluid is oil.

In 1942, Buckley and Leverett modified Darcy's law for water and oil (Fig. 88, eq. 6.6). This equation determines the fractional flow of water for any point in a reservoir if the salt-water saturation and other rock and fluid characteristics of the reservoir are known. If all the variables required for the fractional-flow equation are known for a particular reservoir, then it is possible to estimate the fraction of salt-water flow rate versus the salt-water saturation.

Plotting the fractional flow of water versus the various water saturations results in a curve similar to the solid curve of Figure 89. This curve is referred to as a *fractional-flow curve.* As an example of interpreting the curve, point *A* would imply that a salt-water saturation in the reservoir of 40% would indicate a fractional flow of water at that point to be less than 25%. A salt-water saturation of 60% (point *B*) would imply a fractional flow of water of almost 80% An example of a very efficient displacement is represented by the dashed curve. For example, if the water saturation were 50% (point *C*), the fraction of water flowing in the fluid would be 10%. An example of a very poor displacement efficiency would be represented by the dotted line. Point *D* would represent almost a 95% water cut for the same 50% water saturation. The fractional-flow curve also illustrates the irreducible saturations for oil and water. Point *E* represents the water saturation in the reservoir that is nonmobile. Point *F* represents the point at which, in reservoir salt-water saturation, oil becomes non-

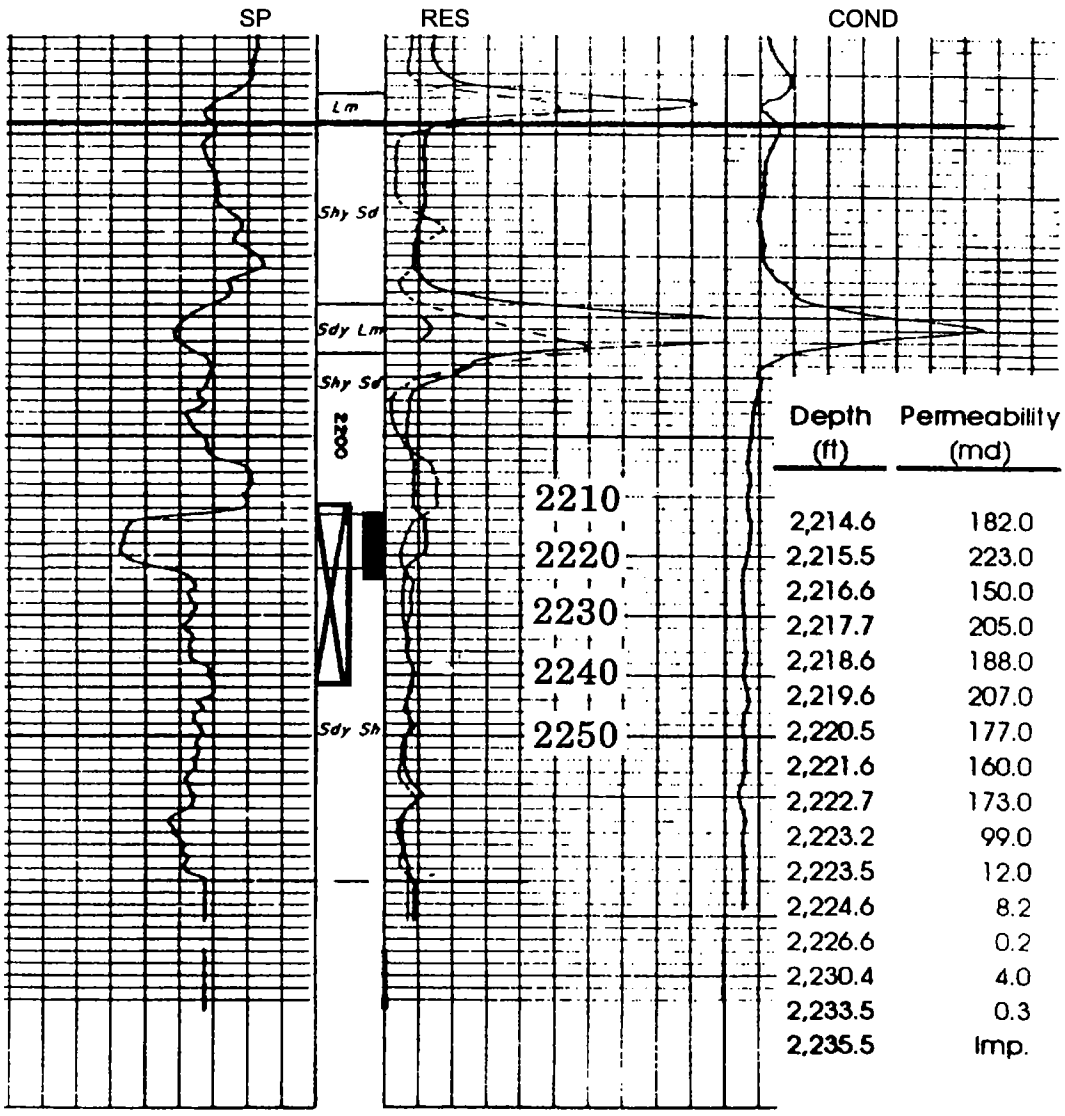

Depth (ft)	Permeability (md)	Porosity (%)	Residual Oil Saturation (%)
2,214.6	182.0	23.5	15.0
2,215.5	223.0	23.2	14.0
2,216.6	150.0	23.2	14.0
2,217.7	205.0	23.8	14.0
2,218.6	188.0	23.4	16.0
2,219.6	207.0	24.0	16.0
2,220.5	177.0	23.7	18.0
2,221.6	160.0	23.2	19.0
2,222.7	173.0	24.0	16.0
2,223.2	99.0	23.2	nd
2,223.5	12.0	19.7	6.6
2,224.6	8.2	20.6	4.8
2,226.6	0.2	18.8	4.6
2,230.4	4.0	20.0	2.9
2,233.5	0.3	19.7	3.0
2,235.5	Imp.	12.1	4.3

Figure 85. Electric log from a well in east-central Oklahoma. Cored interval is defined by the crossed area. Core analysis is given in Table 2. *SP* = spontaneous potential; *Res* = resistivity; *Cond* = conductivity.

mobile. Therefore, the residual-oil saturation is represented by $1 - S_w$ for this example.

The fractional-flow curve is also influenced by the wettability of the reservoir. Figure 90 represents a typical curve for a strongly water-wet reservoir, assuming that the viscosity of oil is similar to that of water. Figure 91 illustrates a typical fractional flow curve for a strongly oil-wet reservoir. The fractional-flow curve of Figure 90 will start to look like that of Figure 91 as the viscosity ratio of oil to water becomes greater.

Analyzing all the variables of equation 6.6 (Fig. 88) reveals that some of them are difficult or impossible to determine. The expression of the gradient of capillary pressure over length (Fig. 92, eq. 6.7) is just such a variable. The gradient of capillary pressure to salt-water saturation can be determined from a capillary-pressure curve. However, the expression for the gradient of salt-water saturation to length is not readily available. Fortunately, the value for equation 6.7 is small, and because of this the expression can be neglected and treated as zero, and the fractional-flow equation (6.6, Fig. 88) reduces to equation 6.8 (Fig. 92).

Another variable that should be considered is illustrated by Figure 93B. Equation 6.8 takes into consideration the structure or the angle of displacement. If the displacement is horizontal, the sine of 0° is zero, and equation 6.8 reduces to equation 6.9. Figures 94 and 95 illustrate the effect of formation dip on the fractional-flow curve. Both curves demonstrate that oil displacement is more favorable when water is injected in an

TABLE 2. – Core Analysis from the Well of Figure 85

Sample no.	Depth (ft)	Permeability (md)	Porosity (%)	Residual saturation percent pore space			Average oil content (BO/acre-foot)
				Oil (%)	Water (%)	Total (%)	
1	2,214.6	182.0	23.5	15.0	45.0	60.0	270.0
2	2,215.5	223.0	23.2	14.0	44.0	58.0	250.0
3	2,216.6	150.0	23.2	14.0	45.0	59.0	240.0
4	2,217.7	205.0	23.8	14.0	45.0	59.0	270.0
5	2,218.6	188.0	23.4	16.0	46.0	62.0	290.0
6	2,219.6	207.0	24.0	16.0	44.0	60.0	300.0
7	2,220.5	177.0	23.7	18.0	46.0	64.0	330.0
8	2,221.6	160.0	23.2	19.0	44.0	63.0	350.0
9	2,222.7	173.0	24.0	16.0	45.0	61.0	300.0
P10	2,223.2	99.0	23.2	nd	nd	nd	nd
10	2,223.5	12.0	19.7	6.6	58.0	65.0	100.0
11	2,224.6	8.2	20.6	4.8	54.0	59.0	77.0
12	2,226.6	0.2	18.8	4.6	66.0	71.0	68.0
13	2,230.4	4.0	20.0	2.9	63.0	66.0	44.0
14	2,233.5	0.3	19.7	3.0	66.0	69.0	47.0
15	2,235.5	imp.	12.1	4.3	61.0	65.0	40.0

Note: nd = no data; imp. = impermeable.

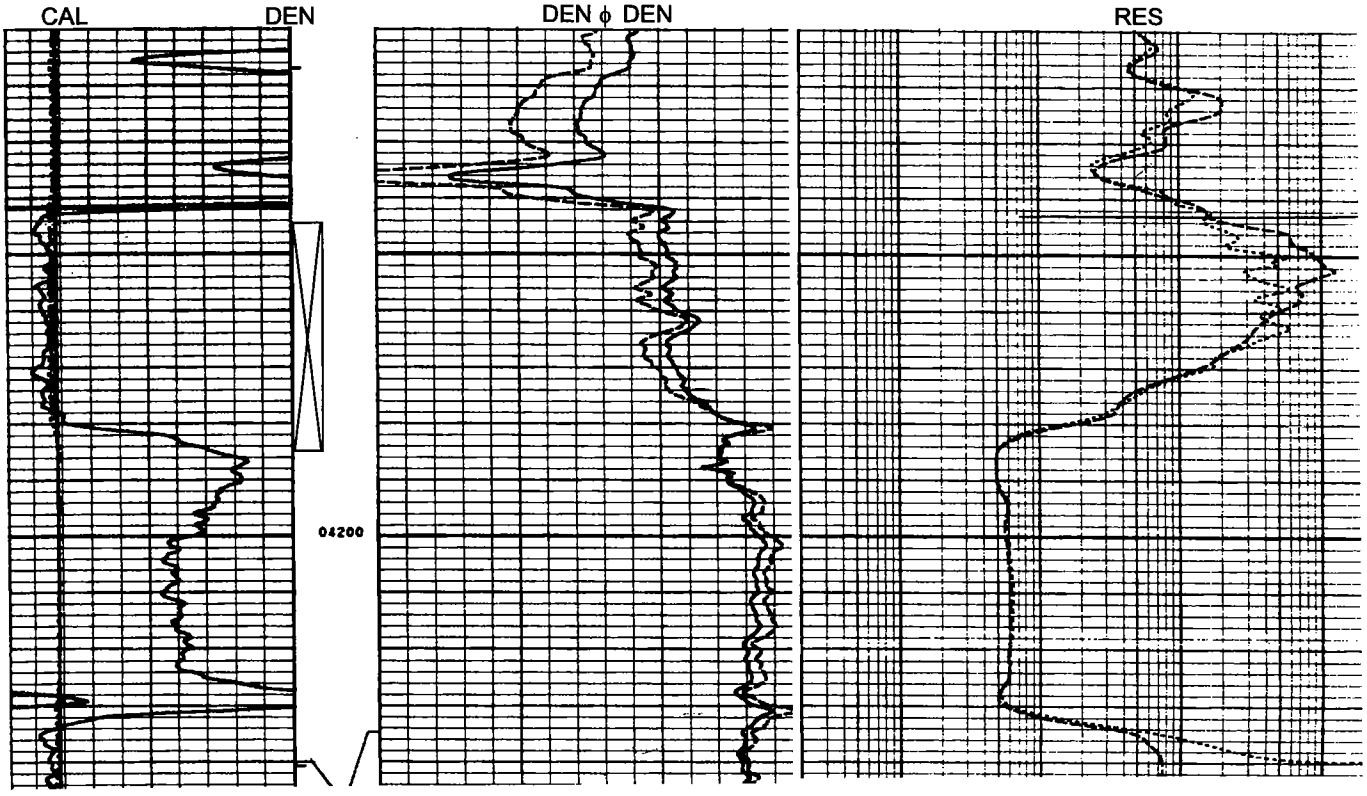

Figure 86. Electric log from a well in south-central Oklahoma. Cored interval is defined by the crossed area. Core analysis is described in Table 3. *CAL* = caliper; *DEN* = density; *DEN* ϕ = density porosity; *RES* = resistivity.

TABLE 3. – Core Analysis from the Well of Figure 86

Sample no.	Depth (ft)	Permeability (md)	Porosity (%)	Percent saturation in pore space	
				Oil (%)	Water (%)
1	4,145.0–46.0	0.54	4.20	27.50	17.70
2	4,146.0–47.0	3.10	9.40	36.40	15.60
3	4,147.0–48.0	7.60	11.50	41.60	17.40
4	4,148.0–49.0	2.00	8.70	39.70	15.80
5	4,149.0–50.0	9.00	10.50	35.20	15.50
6	4,150.0–51.0	na[a]	na	na	na
7	4,151.0–52.0	8.20	9.50	35.00	18.10
8	4,152.0–53.0	4.00	11.70	37.10	23.60
9	4,153.0–54.0	5.10	11.50	36.80	22.80
10	4,154.0–55.0	0.98	7.80	42.00	12.30
11	4,155.0–56.0	1.10	6.40	40.50	14.90
12	4,156.0–57.0	2.00	9.10	41.30	14.90
13	4,157.0–58.0	3.00	8.50	38.60	15.10
14	4,158.0–59.0	3.70	10.00	31.40	18.60
15	4,159.0–60.0	3.80	9.80	40.30	18.40
16	4,160.0–61.0	21.00	10.50	34.20	18.60
17	4,161.0–62.0	17.00	12.00	33.40	19.30
18	4,162.0–63.0	3.00	8.60	33.00	14.60
19	4,163.0–64.0	8.90	10.90	31.80	20.20
20	4,164.0–65.0	4.70	8.30	39.70	16.80
21	4,165.0–66.0	0.05	3.10	50.80	22.60
22	4,166.0–67.0	8.40	8.80	38.50	15.60
23	4,167.0–68.0	1.10	8.80	37.40	17.00
24	4,168.0–69.0	3.80	10.60	38.60	19.50
25	4,169.0–70.0	2.00	8.70	35.10	16.30
26	4,170.0–71.0	13.00	8.80	36.30	17.50
27	4,171.0–72.0	7.50	10.70	31.80	17.00
28	4,172.0–73.0	2.90	10.60	30.80	18.60
29	4,173.0–74.0	11.00	9.10	27.50	11.40
30	4,174.0–75.0	6.30	8.70	26.30	13.40
31	4,175.0–76.0	1.80	7.30	25.60	11.60
32	4,176.0–77.0	5.30	10.40	28.90	19.90
33	4,177.0–78.0	11.00	11.50	28.80	18.90
34	4,178.0–79.0	4.80	10.90	30.70	23.20
35	4,179.0–80.0	8.40	11.60	42.40	10.80
36	4,180.0–81.0	7.00	9.90	32.10	19.50
37	4,181.0–82.0	8.50	9.70	42.50	17.70
38	4,182.0–83.0	7.00	9.80	36.20	19.80
39	4,183.0–84.0	1.90	5.50	37.30	15.30
40	4,184.0–85.0	1.00	2.10	31.40	22.20

[a]na = not available.

updip direction and efficiency increases with the higher injection angle.

Figure 96B represents the mathematical relationship of the effective-permeability ratios of water and oil to the relative-permeability ratios of water and oil. Because these ratios are similar, as described previously, they can be substituted into equation 6.9 to obtain equation 6.10, which is the commonly used fractional-flow equation.

Figures 97 and 98 illustrate the effect of viscosity on the fractional-flow curve. Figure 97 illustrates the effects of viscosity on the fractional-flow curve for a strongly water-wet reservoir. As the viscosity of the oil increases, the displacement efficiency decreases. Figure 98 illustrates the effects of viscosity on the fractional-flow curve for a strongly oil-wet reservoir. It also shows that higher oil viscosities decrease the efficiency of the displacement.

FRONTAL-ADVANCE THEORY

There are many uses of the fractional-flow equation that pertain to waterflood-efficiency prediction. Most of these uses are beyond the scope of this workshop, whose objective is to offer insight on the fundamentals of a cursory evaluation of a potential waterflood candidate. However, it is important to understand how an injected fluid moves through a reservoir, displacing an immiscible fluid. Figure 99 is a modified version of figure 4 from the first waterflood workshop (Rottmann and others, 1998, p. 3). Figure 99B represents a cross section from an injection well to a producing well. As was explained in the first workshop, two fluid banks form and travel toward the pressure sink (producer) in response to injection (Rottmann and others, 1998). Point 1 refers to the discontinuity between the oil saturation and water saturation and is referred to as the *water bank*. Point 2 represents the discontinuity between oil saturations on the left and oil and gas saturations on the right and is termed the *oil bank*. We are going to look at the characteristics of fluid movement as a result of injection.

Slider (1983) described various situations and their characteristics of fluid movement. The first example illustrates fluid movement in a water-drive reservoir, with the stipulation that the water influx is equal and constant to the oil production. Figure 100 is a three-dimensional representation of the reservoir. Note that the reservoir has a cross-sectional area (A), which is the height (H) times the width (W) of the reservoir. The reservoir is tilted, with an oil–water contact (OWC) at the position of S_w =

TABLE 4. – Comparison of Electric-Log Data and Contaminated Core Data

	Electric log	Core
Salt-water saturations	32%	26%
Residual oil saturations	30%	52%
Wettability	Water-wet	Oil-wet
Porosity	12%	11.80%

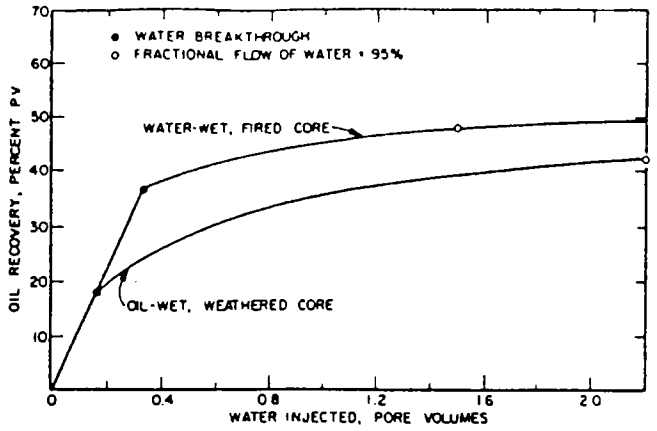

Figure 87. Calculated waterflood recovery data from a core that was contaminated with wettability-altering chemicals that rendered the core oil-wet. The core was cleaned and rendered water-wet. (Keelan, ©1972; reprinted by permission of *Journal of Canadian Petroleum Technology*.)

$$f_w = \frac{1 + \frac{k\,k_{ro}}{u_T\,\mu_o}\left(\frac{\delta P_c}{\delta L} - g\,\Delta p\,\mathrm{SIN}\,\alpha_d\right)}{1 + \frac{\mu_w}{\mu_o}\frac{k_o}{k_w}} \qquad \text{(eq 6.6)}$$

WHERE:

- f_w = Fraction of water in the flowing stream passing any point in the rock (i.e., the water cut)
- k = Formation permeability
- k_{ro} = Relative permeability to oil
- k_o = Effective permeability to oil
- k_w = Effective permeability to water
- μ_o = Oil viscosity
- μ_w = Water viscosity
- u_T = Total fluid velocity (i.e., q_T/A)
- P_c = Capillary pressure = $P_o - P_w$ = pressure in oil phase minus pressure in water phase
- L = Distance along direction of movement
- g = Acceleration due to gravity
- Δ_p = Water–oil density differences = $P_w - P_o$
- α_d = Angle of the formation dip to the horizontan
- δ = Gradient

Figure 88. Equation for determining the fractional flow of water from a predetermined salt-water saturation (Craft and Hawkins, 1959).

100%; this contact is defined by the pore volume containing 100% salt water. Successive layers show lesser amounts of salt-water saturation in an updip direction. Some geologists and engineers might use a different definition for the OWC, which could be the layer defined as S_w = 75% because any production structurally below this point would be only water owing to the immobility of the oil. In this example, the OWC (S_w = 100%) is termed the *influx face*, and the top of the structure with the producing wells is termed the *production face*.

Figure 101 is a modified figure illustrating the reservoir setup in Figure 100. Figure 101A is now a two-dimensional cross section of the reservoir looking in the X direction. Figure 101B is a schematic representation of the water saturations on the y-axis versus the distance from the influx face or original OWC (S_w = 100%). The curve generated defines the water saturations, which is ΔX from the OWC. Capillary pressures are the primary reason for the change in water saturations from $X_{1.0}$ to $X_{0.20}$. This is the transition zone, as was described in the first workshop (Rottmann and others, 1998, p. 16–17), and the water saturation above $X_{0.20}$ is termed the *irreducible water saturation*.

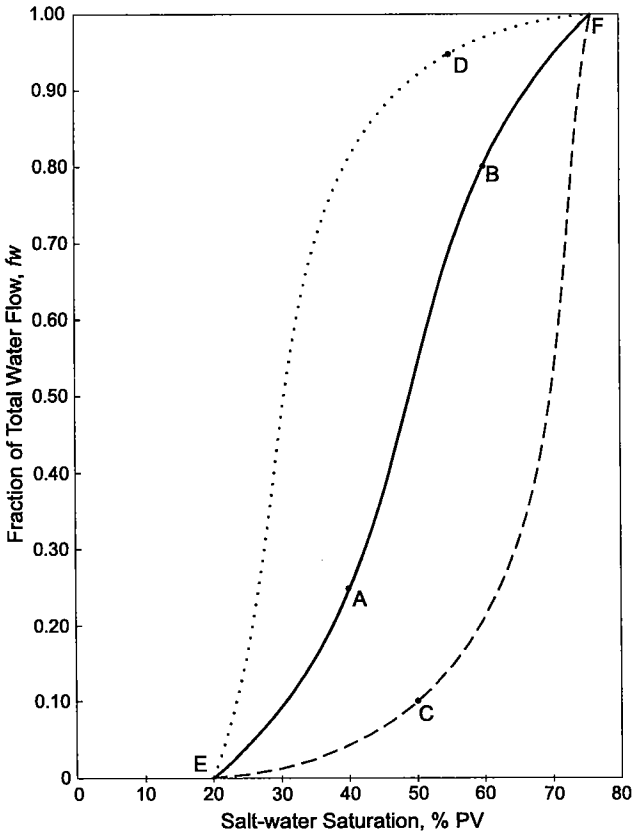

Figure 89. Typical fractional-flow curve (solid curve). Dotted curve represents very poor displacement efficiency; dashed line represents very effective displacement efficiency. See text for further explanation.

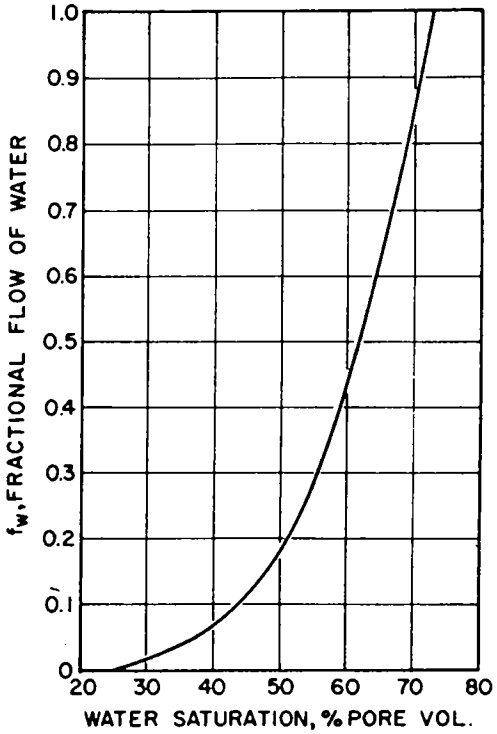

Figure 90. Typical fractional-flow curve for a strongly water-wet reservoir, with viscosity of oil 1 cp and viscosity of water 0.5 cp. (Craig, ©1971; reprinted by permission of Society of Petroleum Engineers.)

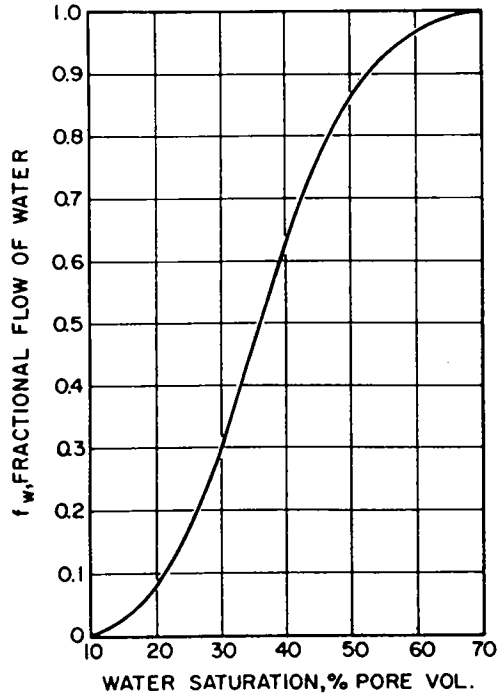

Figure 91. Typical fractional-flow curve for a strongly oil-wet reservoir, with viscosity of oil 1 cp and viscosity of water 0.5 cp. (Craig, ©1971; reprinted by permission of Society of Petroleum Engineers.)

Figure 102 illustrates the movement of the water saturations over 3 years. Notice that the saturations are referred to as S_{di}. This represents the initial saturation of the displacing fluid, in this case water, over the distance from the influx face (original OWC) to the nearest producer (producing face). Assuming constant production and water influx, the saturations are represented by the positions of curve *A* after 1 year. Likewise, after years 2 and 3, the curves are represented by curves *B* and *C*, respectively. Three important characteristics of the water movement can be drawn from this illustration:

1. First, a maximum water saturation is constant and is defined as $1 - S_{or}$. This represents the mobile-oil saturation for the reservoir.
2. There is an abrupt discontinuity of saturations at the fluid front. This point is labeled S_{df} for years 1, 2, and 3. Note how the saturation of the front slightly increases through the years.
3. The third characteristic of this fluid-movement example is that the rates of velocity for similar saturations are equal, assuming that water influx and production are constant. Notice the positions of the point labeled (X_j for the initial position, year 1 position, year 2 position, and year 3 position. The yearly change in position is equal with regard to the horizontal distance from the previous position. (X_j saturation moves faster than the maximum water saturation (labeled $1 - S_{or}$) and moves considerably slower than the front labeled S_{df}.

Figure 103 represents the second example described by Slider (1983). The conditions are similar to those of

A

$$f_w = \frac{1 + \frac{k\,k_{ro}}{\mu + \mu_o}\left(\frac{\delta P_c}{\delta L} - g\,\Delta p\,\text{SIN}\,\alpha_d\right)}{1 + \frac{\mu_w}{\mu_o}\frac{k_o}{k_w}} \qquad \text{(eq 6.6)}$$

B

$$\frac{\delta P_c}{\delta L} = \frac{\delta P_c}{\delta S_w}\frac{\delta S_w}{\delta L} \qquad \text{(eq 6.7)}$$

$\frac{\delta P_c}{\delta S_w}$ Determined from water–oil capillary pressure curve

$\frac{\delta S_w}{\delta L}$ Saturation gradient (information is not readily available)

C

$$f_w = \frac{1 + \frac{k}{u}\frac{k_{ro}}{\mu_o}(-g\,\Delta p\,\text{SIN}\,\alpha_d)}{1 + \frac{\mu_w}{\mu_o}\frac{k_o}{k_w}} \qquad \text{(eq 6.8)}$$

Figure 92. (A) Fractional-flow equation 6.6 from Figure 88. (B) Description of capillary-pressure gradient versus change in length. (C) Simplification of equation 6.6 by assuming that equation 6.7 is negligible.

A

$$f_w = \frac{1 + \frac{k}{\mu}\frac{k_{ro}}{\mu_o}(-g\Delta p \,\text{SIN}\propto_d)}{1 - \frac{\mu_w}{\mu_o}\frac{k_o}{k_w}} \qquad \text{(eq. 6.8)}$$

B

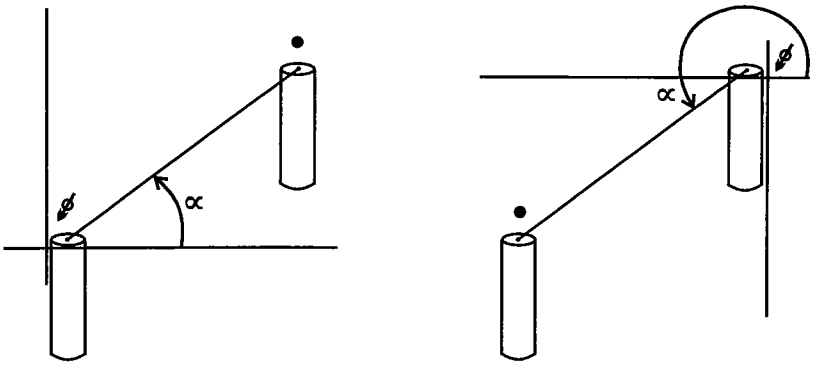

C $\propto = 0°$ SIN $0° = 0$

D

$$f_w = \frac{1}{1 + \frac{\mu_w}{\mu_o}\frac{k_o}{k_w}} \qquad \text{(eq. 6.9)}$$

Figure 93. (A) Reduced fractional-flow equation 6.8 from Figure 92. (B) Graphical illustration of angle of displacement used in equation 6.8. (C) Value of sin 0° = 0; (D) Simplification of fractional-flow equation for horizontal injection.

Figure 102 except that this scenario represents advancement of a fluid in a reservoir of uniform saturations. Notice that the initial water saturation at the front, S_{di}, is uniform throughout the interval represented by *X*. Some of the conclusions from the previous example need to be modified as follows:

4. The leading edge of the front retains the same saturation until it reaches the producing face.

5. The velocities of equal saturation are the same, assuming that the input and output rates are similar. The leading edge of the water bank represented by S_{df} will travel the fastest.

6. The reservoir water saturation will not increase above the value $1 - S_{or}$, as described previously.

In 1942, Buckley and Leverett proposed a formula that would explain the movement of fluids through a porous medium with respect to time—or to put it differently, the saturation distribution of various phases with respect to time. Equation 6.11 (Fig. 104) is the frontal-advance equation proposed by Buckley and Leverett. We will not derive the equation in this workshop, but its concepts and development can be found in the references for this chapter. The equation can be used to explain theoretically and mathematically the characteristics of fluid movement described by Slider (1983).

Figure 105 is the model we will use to demonstrate the frontal-advance formula. It is similar to the one used by Slider (1983) for a reservoir having a uniform fluid saturation. *A* (area) for the equation is shown as *W* (width) times *H* (height), which is the cross-sectional area of the influx face. The assumptions for the equation are given in Figure 105. Because 5.615, ϕ, W_i, and *A* are constants, the length, *L*, that a given water saturation travels in the example of Figure 105 is proportional to the derivative of df_w/dS_w, which is the slope of the tangent line to the fractional-flow curve for any salt-water saturation.

As an example, Figure 106 illustrates how to calculate the slope of the tangent at a salt-water saturation of 43%. The slope is simply the rise over the run, or the change in f_w, which is 0.32, divided by the change in S_w, which is 0.15. Therefore, the value for df_w/dS_w used in the fractional-flow equation is 2.13.

Figure 107 illustrates how the slopes for various salt-water saturations can be calculated at certain times and plotted versus salt-water saturation (curve *D*). If *A*, ϕ, and W_i are known, the various slopes for these water saturations can be inserted into the frontal-advance equation to determine the

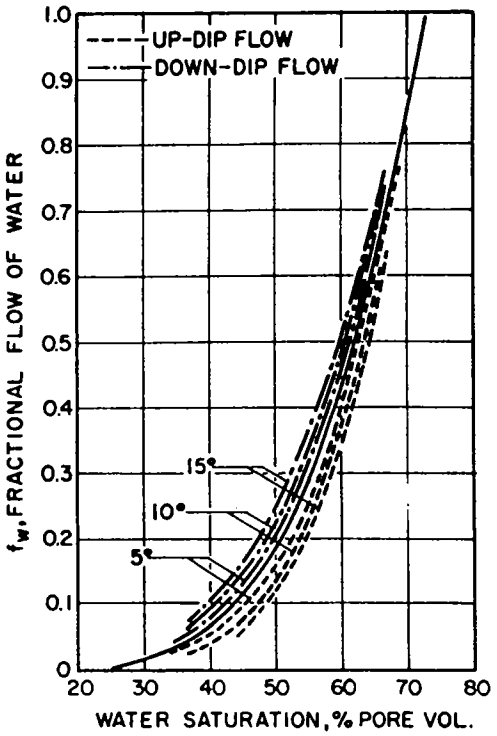

Figure 94. Effect of formation dip on the fractional-flow curve for a strongly water-wet rock. (Craig, ©1971; reprinted by permission of Society of Petroleum Engineers.)

distance, L, the saturations traveled at the time W_i was injected.

Figure 108 illustrates how the length, L, is plotted for salt-water saturations of $S_{w0.70}$, $S_{w0.60}$, and $S_{w0.50}$. This represents the distance these water saturations have traveled from the influx face at the time W_i was injected.

Figure 109 illustrates the results of plotting $S_{w0.40}$ and $S_{w0.30}$. These saturations require the curve to turn and be

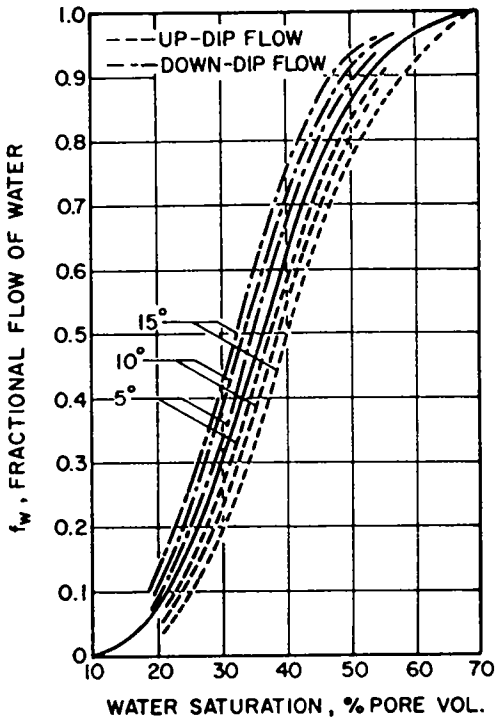

Figure 95. Effect of formation dip on the fractional-flow curve for a strongly oil-wet rock. (Craig, ©1971; reprinted by permission of Society of Petroleum Engineers.)

A

$$f_w = \frac{1}{1 + \frac{\mu_w}{\mu_o}\frac{k_o}{k_w}} \qquad \text{(eq 6.9)}$$

B

$$\frac{k_{rw}}{k_{ro}} = \frac{k_w/k}{k_o/k} = \frac{k_w}{k} \times \frac{k}{k_o} = \frac{k_w}{k_o}$$

C

$$f_w = \frac{1}{1 + \frac{\mu_w}{\mu_o}\frac{k_{ro}}{k_{rw}}} \qquad \text{(eq 6.10)}$$

Figure 96. (A) Fractional-flow curve in its common form. (B) Relationship of relative permeabilities for water and oil and effective permeabilities for water and oil. (C) Substitution of relative-permeability values into equation 6.9.

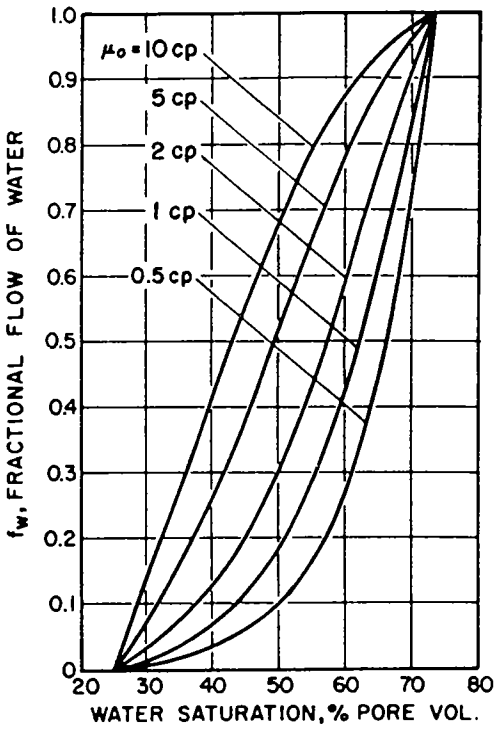

Figure 97. Effect of various oil viscosities on a fractional-flow curve for a strongly water-wet rock. (Craig, ©1971; reprinted by permission of Society of Petroleum Engineers.)

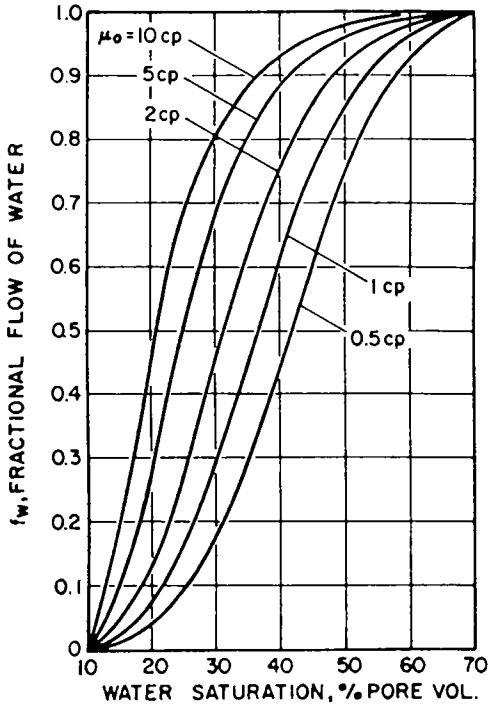

Figure 98. Effect of various oil viscosities on a fractional-flow curve for a strongly oil-wet rock. (Craig, ©1971; reprinted by permission of Society of Petroleum Engineers.)

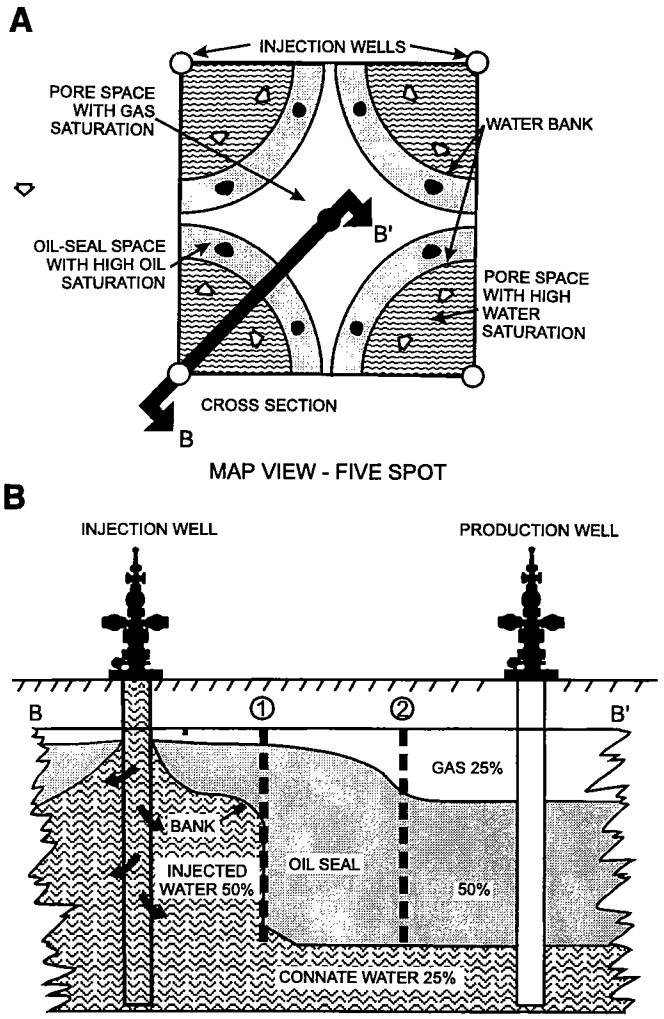

Figure 99. Areal (A) and cross-section (B) views of a five-spot pattern under injection for a solution-gas-drive reservoir. Point 1 is the water bank, and point 2 is the oil bank, as the result of water injection. (Clark, ©1969; reprinted by permission of Society of Petroleum Engineers.)

directed back toward the influx face. The anomaly for the curve now is that at the same distance, L, from the injector, two separate salt-water saturations ($S_{w0.65}$ and $S_{w0.40}$) appear to exist at the same point and time in the reservoir. Buckley and Leverett (1942) recognized this impossible situation. They pointed out that the correct interpretation should be that part of the computed saturation is imaginary and that the leading edge of the water front is actually a discontinuity.

The shaded parts of the curve (Fig. 110) illustrate those parts thought to be imaginary, according to Buckley and Leverett (1942). The point L_1 can be determined by the material-balance method and occurs at a point where areas A and B are equal. The vertical plane at L_1 represents a discontinuity from a water and oil saturation to the left of the plane, which is constantly changing with changing values for W_i, and a constant saturation distribution to the right of the plane. The plane at L_1 is the flood front referred to by Slider (1983) and by point 1 in Figure 99B.

Figure 111 illustrates what the flood front would look like by taking gravity and capillary forces into account. The area to the right of the front, or discontinuity, is termed the *oil bank*, and the area to the left, the *drag zone*. The area above the curve and below the irreducible oil saturation is the amount of oil that potentially can still be produced. The producer should be making 100% oil, with the stipulation that the assumptions of Figure 105 are still in effect.

Figure 112 illustrates the advance of the waterflood front and the water saturations at times W_{i+1}, W_{i+2}, and W_{i+3}, and at the time the flood front (W_i) reaches the producing face. The characteristics described by Slider (1983) now can be shown to be mathematically correct,

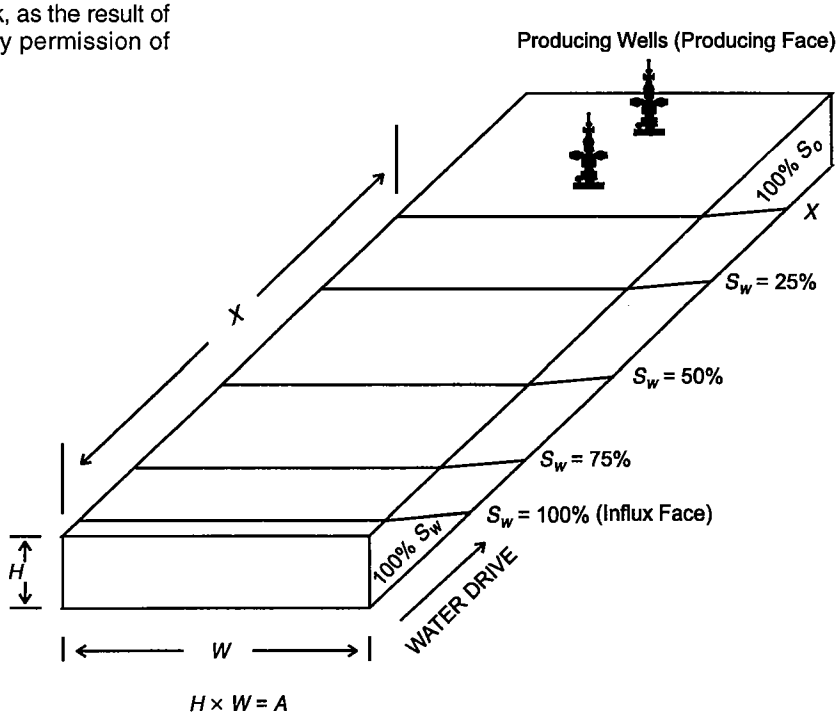

Figure 100. Tilted water-drive reservoir, illustrating oil–water contact (OWC) and transition zone. X represents that portion of reservoir where water saturation becomes irreducible. See text for further explanation.

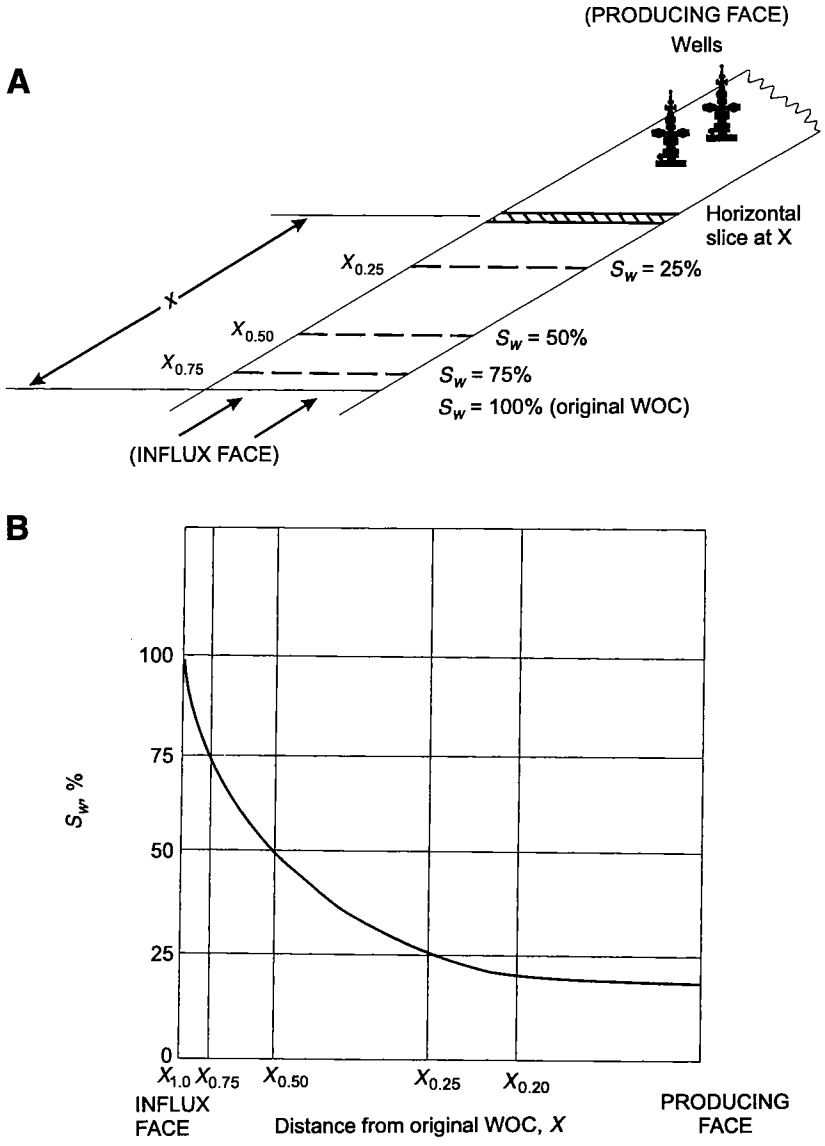

Figure 101. (A) Cross-section view of the reservoir from Figure 100, looking in the X direction. (B) Water-saturation profile for the reservoir in the X direction. (Modified from Slider, ©1983; reprinted by permission of PennWell Books.)

using the frontal-advance equation. The following is a summary of those characteristics:

7. The frontal discontinuity is a uniform saturation moving at a constant velocity, assuming constant input.
8. The irreducible oil saturation will not be reduced.
9. The velocities of the saturations are constant for each saturation and different from others, assuming constant input. A comparison of the two velocities (e.g., at salt-water saturations of 60% and 67%) would indicate, by the lengths, that the saturations prove the velocity of the 60% saturation to be faster than that of the 67% saturation, which is faster than the saturation directly below $1 - S_{or}$.

Once the water bank reaches the producing face, the oil cut goes almost immediately from 100% oil to 85% salt water and 15% oil. We will now discuss how this result can be derived.

The frontal-advance equation was a theory proposed by Buckley and Leverett in 1942. It was not until 1951 that a paper presented by Terwilliger verified by application the theory of frontal advance. In a model using gas–oil gravity drainage, and incorporating gravity and capillary pressures into the frontal-advance equation, he demonstrated that the observed advance of the displacing gas front and its saturation were in agreement with the calculated curve over time. Terwilliger also suggested an important concept illustrated by Figure 113. Simply stated, a tangent to the fractional-flow equation with the end point at S_{wi}, and $f_w = 0$, will yield the salt-water saturation within the front. This point and saturation are indicated by the dashed line, whose value would be 62%. Terwilliger also found that the saturation in the waterflood front moved at the same velocity and termed this saturation the *stabilized zone.*

In 1952, a paper was published by Welge that complemented the work of Buckley and Leverett (1942). Welge also showed that the tangent to the fractional-flow curve resulted in the same conclusion as the balancing of areas described by Buckley and Leverett (illustrated in Fig. 110) for finding the saturation at the leading edge of the advancing front.

Figure 114 illustrates another graphical interpretation of the fractional-flow curve. Extrapolating the tangent of the curve as S_{wi} and $f_w = 0$ to $f_w = 1.0$ yields the average water saturation behind the front at breakthrough for this linear system. In this particular example, the average water saturation at breakthrough is approximately 70% and is represented by the dotted line in Figure 114 (Craig, 1971). The dashed horizontal line to the y-axis will determine the frac-

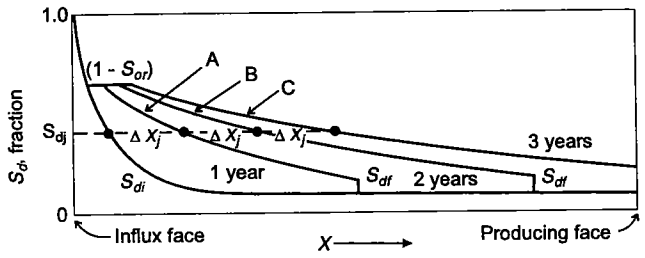

Figure 102. Movement of a fluid front over a 3-year period in a medium of variable water saturations. (Modified from Slider, ©1983; reprinted by permission of PennWell Books.)

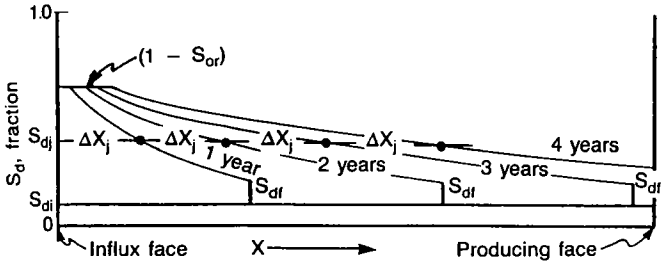

Figure 103. Movement of a fluid front over a 4-year period in a medium of uniform initial saturations. (Modified from Slider, ©1983; reprinted by permission of PennWell Books.)

Figure 104 *(right)*. Frontal-advance equation proposed by Buckley and Leverett (1942).

$$L = \frac{5.615\, W_i}{\phi A} \frac{d f_w}{d S_w} \qquad \text{(eq 6.11)}$$

WHERE:

L = Total distance that the plane of given water saturation moves

W_i = Cumulative water injected, reservoir bbl

$\frac{d f_w}{d S_w}$ = Slope of the fractional flow curve at the water saturation of interest

ϕ = Porosity

A = Cross-sectional area

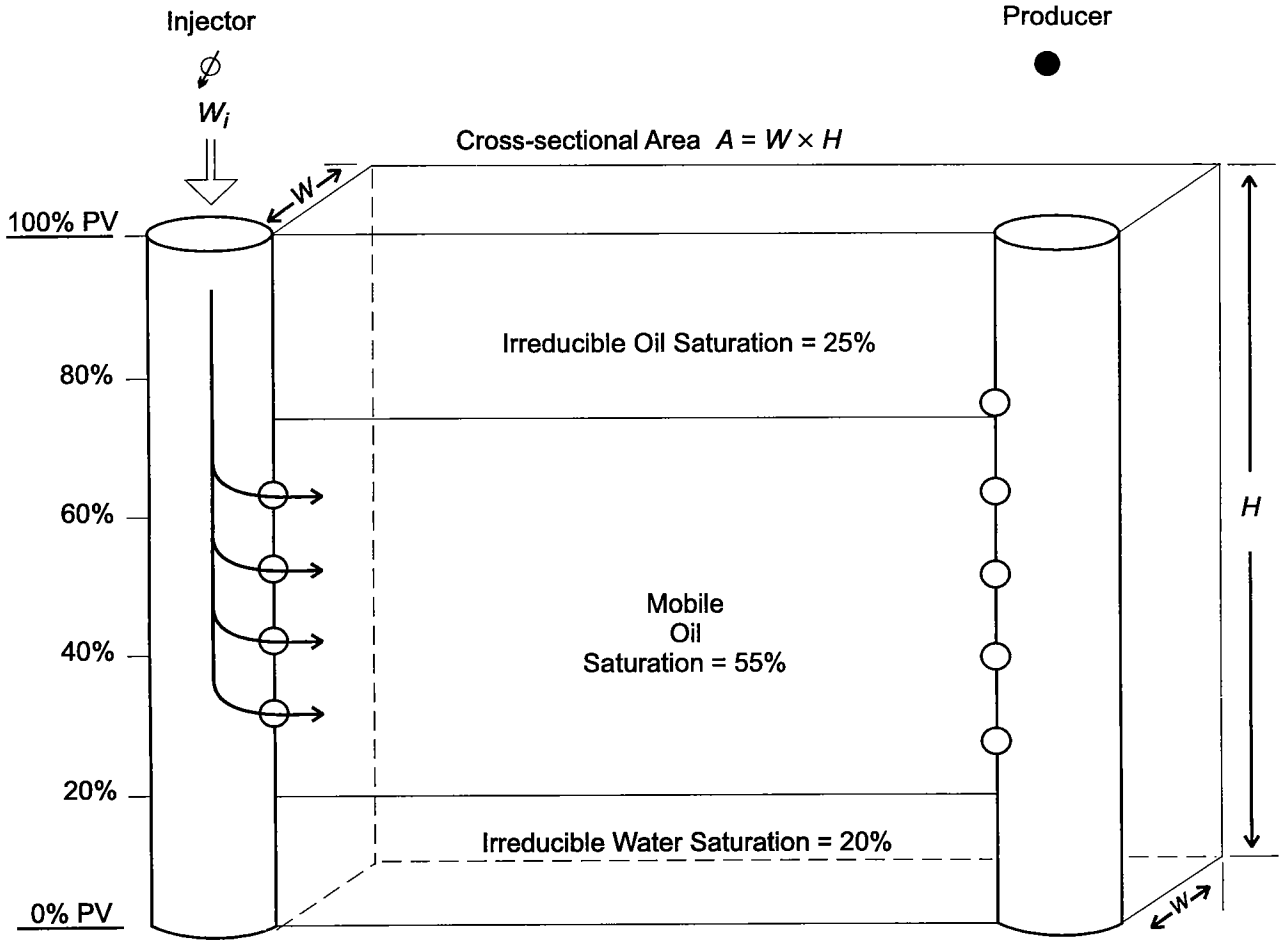

Assumptions:

1. No mass transfer between phases
2. The phases are incompressible
3. No significant gas saturation
4. E_a and $E_v = 1.0$
5. Homogeneous reservoir
6. Linear flow
7. Saturations distributed uniformly within reservoir
8. Gravity and capillary forces neglected

Figure 105. Model used for illustrating the frontal-advance equation. Model represents a cross-sectional area from injector to producer in a homogeneous reservoir with uniform saturations. PV = pore volume; E_a = areal sweep efficiency; E_v = vertical sweep efficiency. See text for further explanation.

tional flow of water and oil when the flood front, with a saturation of 62%, reaches the producing face.

The concept of the flood front moving as a smooth plane through the reservoir was expanded on by Craig (1971). Figure 115 illustrates displacement of one fluid by another immiscible fluid (van Meurs, 1957). The presence of viscous fingering probably increases as the oil/water viscosity ratio increases (van Meurs, 1957). Craig suggests that viscous fingering probably does occur in a reservoir, perhaps owing to variations in porosity and permeability, which undoubtedly do occur.

The development of the frontal-advance theory, which is the physical movement of injected water and the displacement of an immiscible fluid, has been touched on in this chapter to demonstrate some of the major principles involved with the theory. But this, by no means, is a comprehensive evaluation of the frontal-advance formula. Subjects such as displacement efficiency after breakthrough, water saturation above irreducible saturation, and presence of gas saturation are but a few of the influences not touched on. These are subjects that the reservoir engineer would evaluate for an in-depth analysis of the prospect. This chapter is devoted mainly to an overall cursory review of a potential waterflood project, as described by equations 6.1 and 6.2 of Figure 64, which, it is hoped, will give the reader a basic understanding of how water displaces oil.

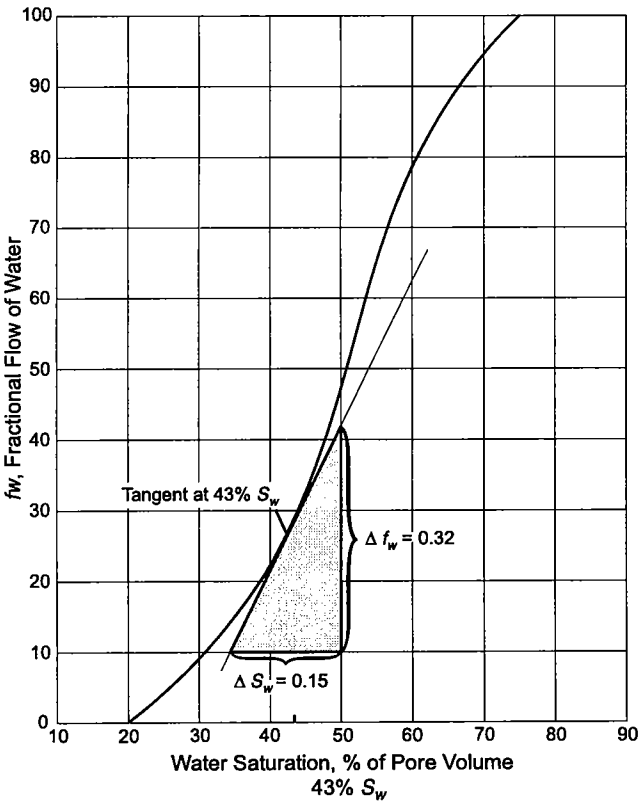

$$\frac{df_w}{dS_w} = \frac{0.32}{0.15} = 2.13$$

Figure 106. Example of calculating the slope of the tangent to the fractional-flow curve at a salt-water saturation of 43%. The slope of the tangent is the derivative of the variable df_w/ds_w in equation 6.11.

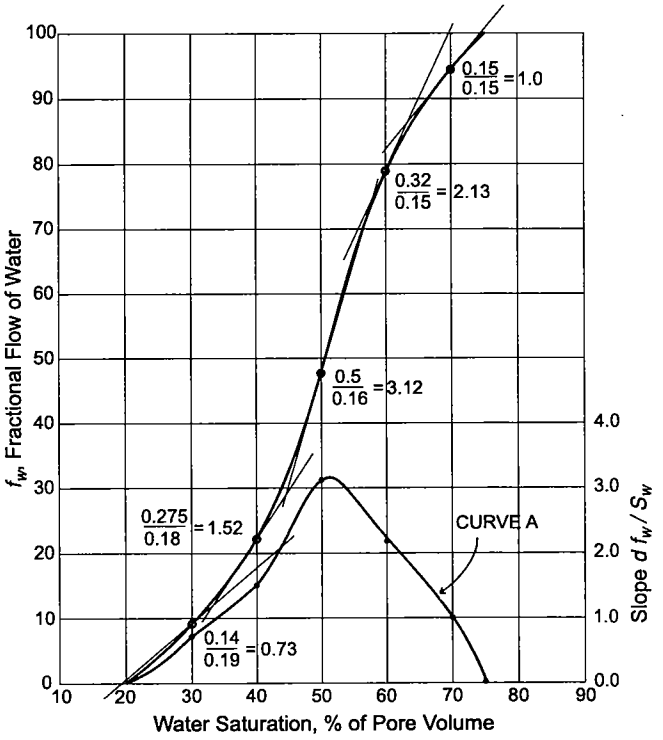

Figure 107. Calculation of the slopes to the fractional-flow curve at various salt-water saturations. Curve *A* is a plot of the slopes versus salt-water saturations.

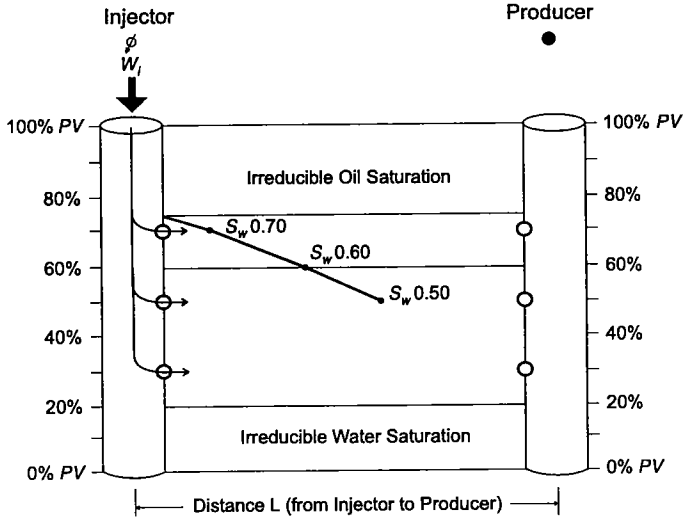

Figure 108. Plot of the distance, *L*, from the injector, as derived from equation 6.11 for salt-water saturations of 50%, 60%, and 70%.

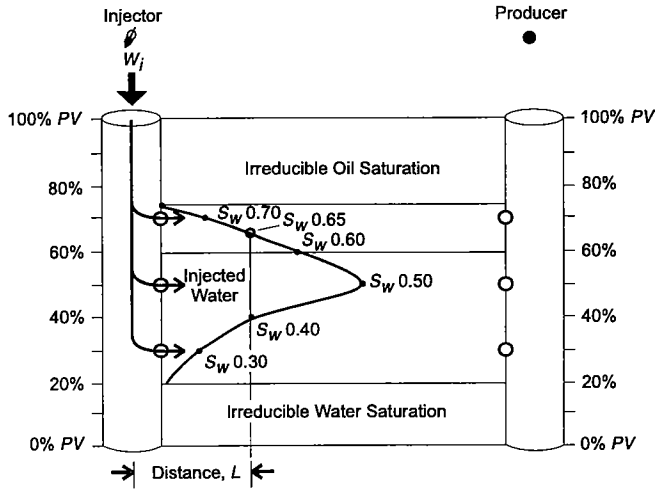

Figure 109. Plot of distance, L, from the injector, as derived from equation 6.11 for salt-water saturations of 30% and 40%. See text for further explanation.

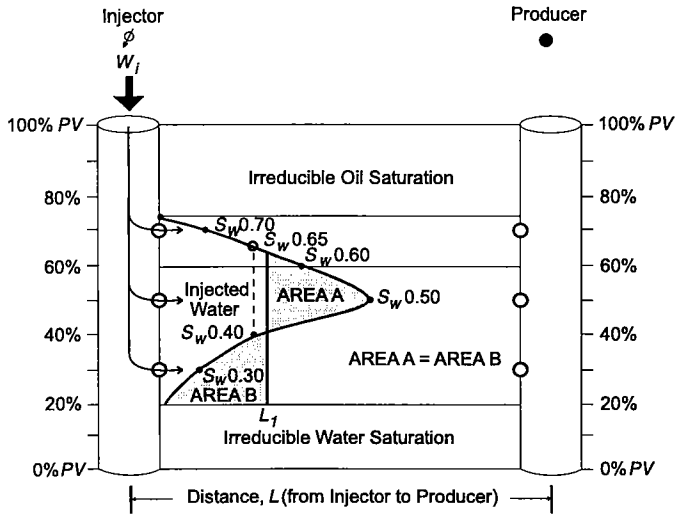

Figure 110. Shaded area represents the imaginary part of the frontal-advance formula for various salt-water saturations (Buckley and Leverett, 1942). L_1 represents the leading edge of the waterflood front at a point where areas A and B are equal.

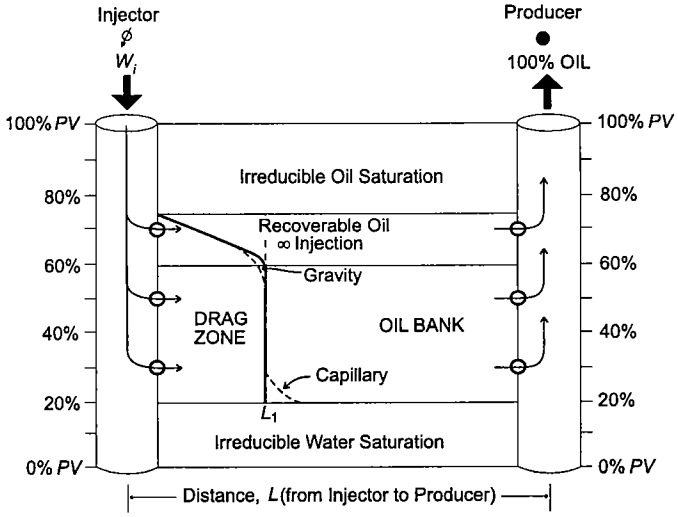

Figure 111. Geometry of the flood front, with gravity and capillary effects taken into consideration.

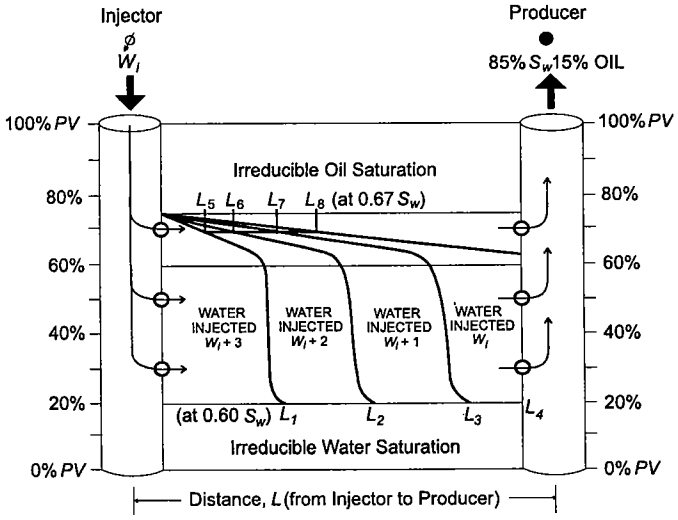

Figure 112. Advance of the flood front at times W_i, W_{i+1}, W_{i+2}, and W_{i+3}. W_i has intersected the producing face, and the oil cut has gone from 100% to 15%. See text for further explanation.

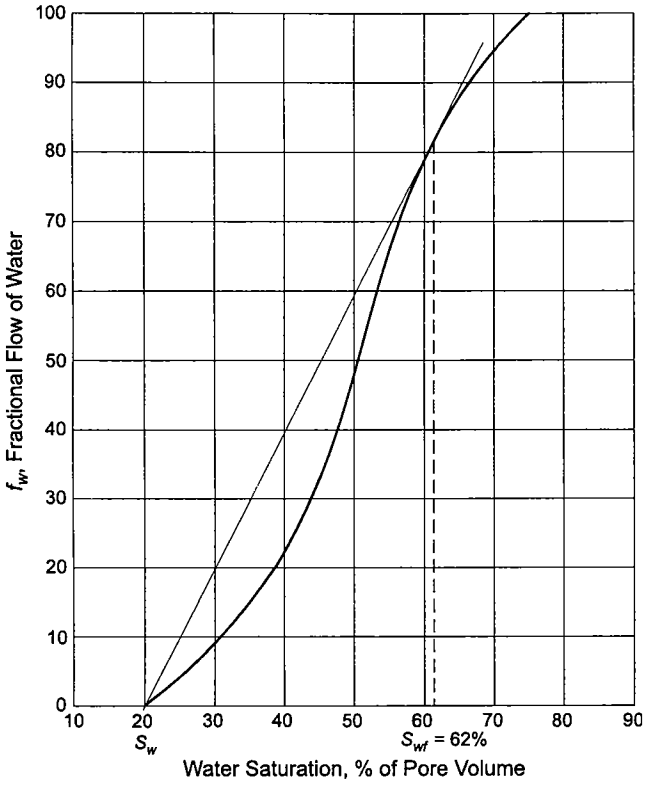

Figure 113. The average salt-water saturation at the flood front can be determined by the intersection of the tangent, whose end point is at $f_w = 0$, and the fractional-flow curve. Average salt-water saturation at the flood front is 62% in this example.

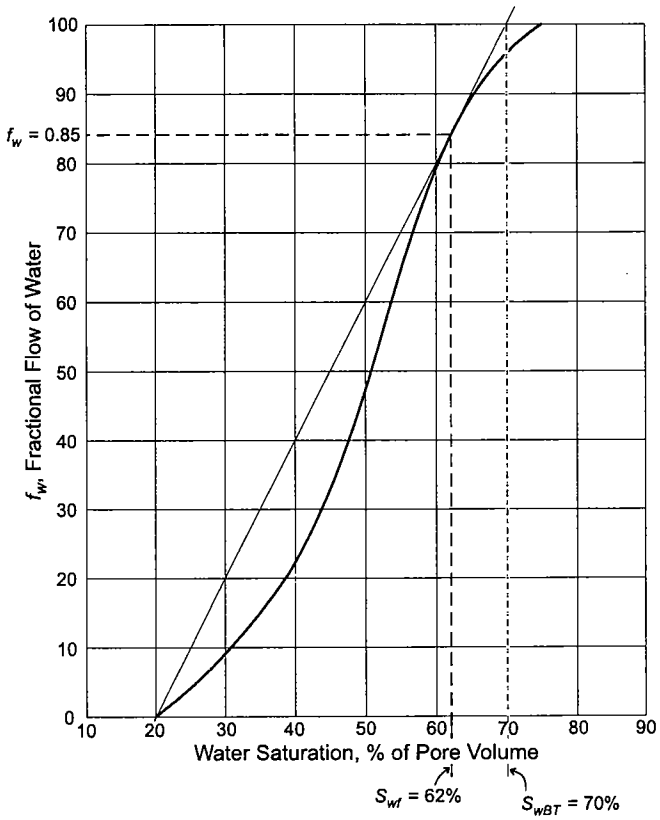

Figure 114. Extrapolation of the tangent to the fractional-flow curve to a value of $f_{w1.0}$. Extrapolation of this point to the water saturation (dotted line) yields the average salt-water saturation behind the flood front at breakthrough (S_{wBT}).

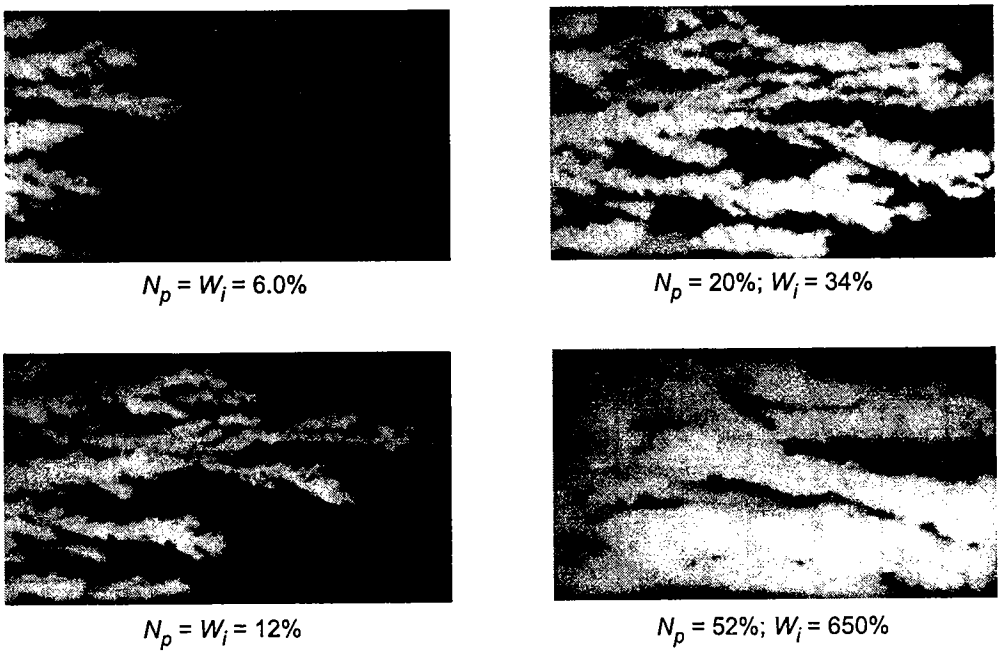

Figure 115. Displacement of one fluid by another, immiscible fluid. Notice the viscous fingering. (van Meurs, ©1957; reprinted by permission of Society of Petroleum Engineers.)

Areal Sweep Efficiency

7

CHAPTER 7

Areal Sweep Efficiency

INTRODUCTION

The concept of the frontal-advance theory discussed in the last chapter was devised with a linear plane between the injector and the producer. It also assumed that 100% of the pore volume was contacted by injected water. The cross-sectional area used in the frontal-advance equation, as illustrated, would not be appropriate in reservoirs unless the reservoirs were elongate and the injection occurred across the cross-sectional area of the reservoir. However, for most reservoirs, the linear-flow concept is not practical because most reservoirs have multiple injectors and multiple producers. These wells are often in patterns such that injection from one well could affect producers in other patterns. The injected water would spread radially from the injector, assuming the permeability to be homogeneous. In this scenario, the water that reaches a producer would travel along the shortest path from the injector. This path of injected water is referred to as a *stream line.* Figure 116 illustrates four injectors in a reservoir at various stages of injection. Well A is just under injection and shows the radial nature of the injection. Stream line 1 from well B has reached producing well E. Notice that the stream lines labeled 2 and 3 have not reached the producer yet, because their curved path requires them to travel farther. This implies that at breakthrough (stream line 1), not all the potential pore volume that will ultimately be affected has been swept.

This is an important point, because previously, when talking about breakthrough in a water-wet reservoir, reference was made that nearly all the oil would be produced. That point needs to be clarified here and expanded to mean that most of the oil from that stream line would be produced; however, other stream lines were yet to reach the wellbore. Figure 117 illustrates how multiple stream lines can reach a wellbore. This reservoir is in central Oklahoma. The reservoir had a gas cap, and three injectors were positioned in it to fill the void with water. Well 5 is an injector in the oil column. Wells 1 and 3 were influenced by the well 5 injector initially.

Figure 118 shows the production curves for wells 1–4. These curves are composed of two parts, oil production (solid line) and water production (dotted line). Well 3 has three points labeled *A*, *B*, and *C*. These points represent oil-production increases when a stream line is presumed to have entered the wellbore. Production at point *A* jumped from a background of 500–600 barrels of oil per month (BOPM) to over 2,000 BOPM near the end of 1990. This was the oil bank from the first stream line that reached the wellbore. In the middle of 1990, oil production fell dramatically, and water production increased to over 1,000 BWPD. This represents the water bank from the same stream line. A water breakthrough of this magnitude might imply that very little future oil production would be obtained from this well. In fact, the operator chose to shut in the well in 1992 to help maintain reservoir pressure. In mid-1992, the operator happened to put the well back on line and was

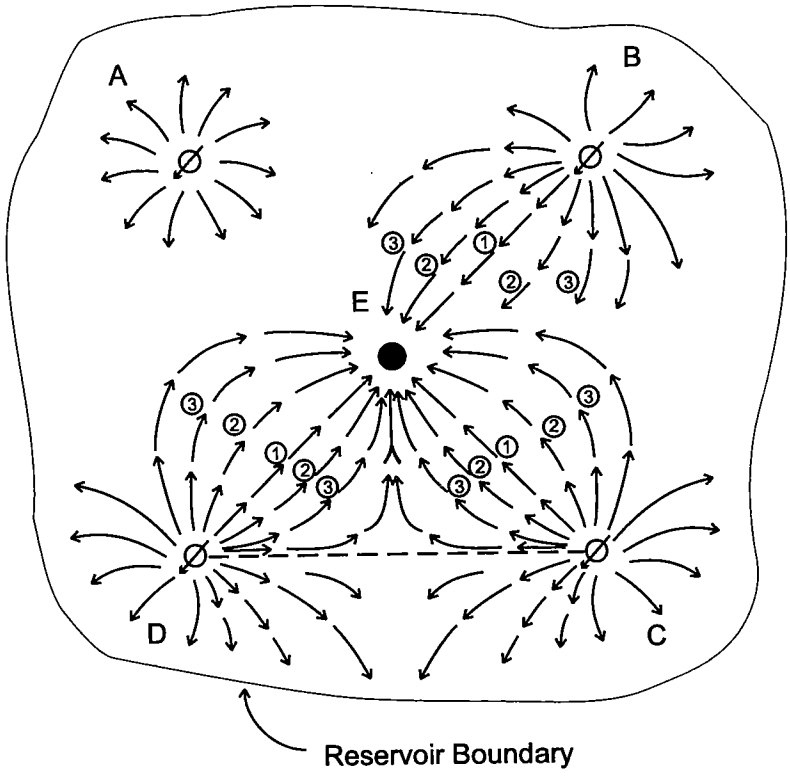

Figure 116. Illustration of four injectors under various stages of injection, and the direction of the stream lines from those injectors. Well E is a producer.

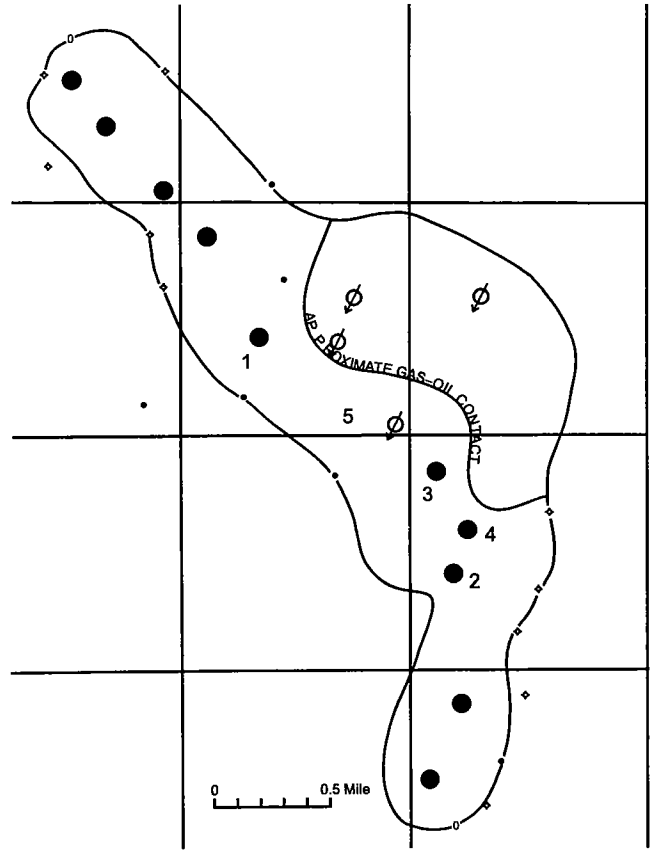

Figure 117. Map of a reservoir in central Oklahoma. Wells 1–4 are producers, and well 5 is an injector in the oil column.

surprised at an increase in the oil cut. Point *B* represents an increase in production under the assumption that it is coming from another stream line. Again, the water bank for this stream line hit, and water production increased dramatically in 1994. The well was shut in again and reopened in mid-1994 when oil production started to increase a third time from a possible third stream line. Well 4 indicates three separate oil-production increases similar to those of well 3. Well 2 illustrates two possible fronts entering the wellbore; the time interval from 1994 to 1995 was a period when oil production had dropped to a very low level, and the well was shut in. Well 1 perhaps is more typical of a normal response, with an oil bank reaching the wellbore at point *A*. Water-free production from the oil bank occurred for over a year, and then oil production dropped sharply (point *B*) as the water bank reached the wellbore. Notice how oil production gradually dropped over the last 5 years and how water production gradually increased.

Figure 116 also illustrates how some of the stream lines radiating from wells C and D will never reach the producer, because some of the stream lines intersect and interfere with each other. Once this interference occurs, the stream lines are either directed toward the producer or away from it. Figure 119 illustrates those stream lines that will affect the producer. The dashed line enclosing the injectors defines the pattern boundary. *Areal sweep efficiency* can be defined as the percentage of an area or a pattern contacted by water at a

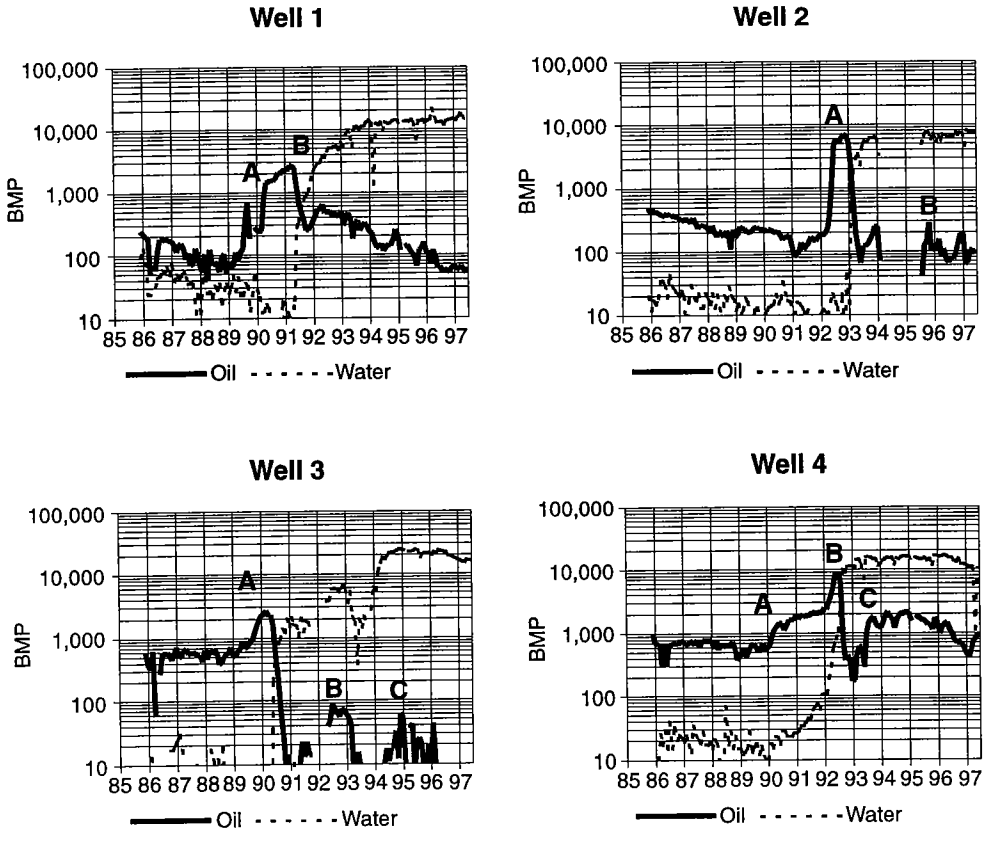

Figure 118. Production curves from wells of Figure 117, illustrating production increases when the oil banks of various stream lines reached the wellbore. *BPM* = barrels per month.

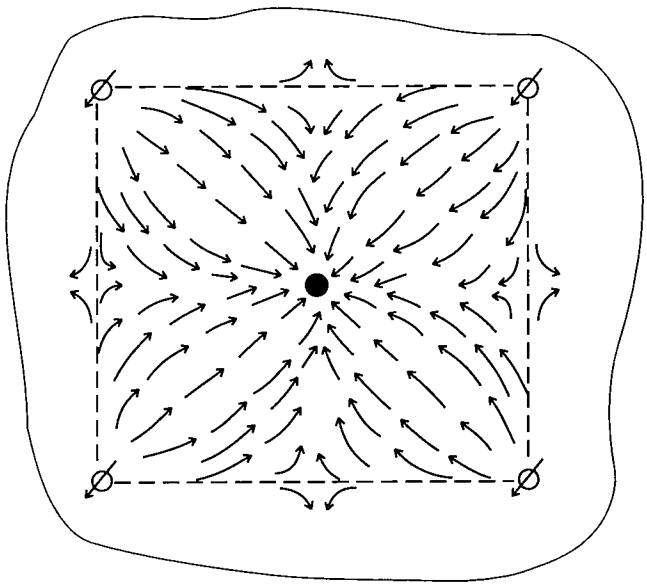

Figure 119. Illustration of those stream lines that will reach the center producer. Dashed line represents the pattern boundary.

given time. For example, if one-half of a pattern has been contacted by injected water when a stream line reaches the producer, as in stream line 1 of well A of Figure 116, the sweep efficiency is the fraction 0.50 at the time of breakthrough. Figure 120 illustrates this concept graphically. E_a from equation 5.1 (Fig. 55) is simply the total swept area divided by the total area influenced. Smith and Cobb (1987) describe four factors that affect areal sweep efficiencies: mobility ratio, geometry of the pattern, reservoir heterogeneities, and water-injection rate. In this chapter we will look at mobility ratio and flood patterns and their integration in order to predict areal sweep efficiency.

MOBILITY RATIO

The *mobility ratio* between fluids is perhaps one of the most important characteristics of a waterflood. Equation 7.1 (Fig. 121) defines mobility ratio as the mobility of the displacing fluid (water) divided by the mobility of the displaced fluid (oil). The mobility of a fluid is controlled by the effective permeability with respect to the viscosity of the fluid. As the viscosity increases, the mobility decreases. Equation 7.2 (Fig. 121B) is an algebraic term defining the mobility ratio. In this equation, M is equal to the mobility of water, which is the effective permeability of water divided by the viscosity of water divided by the mobility of oil, which is the effective permeability of oil divided by the viscosity of the oil. Reducing the equation results in the relationship on the right, which defines the mobility ratio as the relative permeability of water times the viscosity of oil divided by the relative permeability of oil times the viscosity of water.

In 1955, Craig and others suggested that the relative permeability of the water should be at the average water saturation at breakthrough, which was the S_{wBT} value defined in the last chapter. The relative permeability of the oil should be that of the oil-bank saturation ahead of the front. Figure 122 illustrates this relationship. All the terms in this expression have been defined previously. The mobility ratio remains constant until breakthrough, and then it increases as the average water saturation of the

A $N_p = N \times E_d \times E_a \times E_v$ (eq. 5.1)

B $E_a =$ 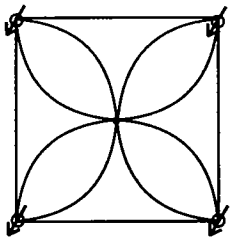 $=$ 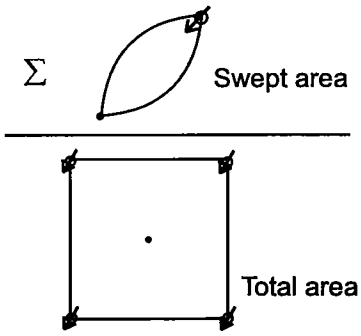

Where: Swept area is dependent on the economic effectiveness of the pattern

Figure 120. (A) General equation (Fig. 55) for estimating oil displaced by waterflooding. (B) Graphical definition of areal sweep efficiency.

A $$M = \text{Mobility ratio} = \frac{\text{Mobility of displacing phase (water)}}{\text{Mobility of displaced phase (oil)}} \quad \text{(eq 7.1)}$$

B $$M = \frac{k_w/\mu_w}{k_o/\mu_o} = \frac{k_w/\mu_o}{k_o/\mu_w} = \frac{k_{rw}/\mu_w}{k_{ro}/\mu_w} \quad \text{(eq 7.2)}$$

WHERE:

k_{rw} = Relative permeability for the average salt-water saturation behind the water bank $\bar{s}_w$

k_{ro} = Relative permeability in the oil bank

Figure 121 *(left)*. (A) Definition of *mobility ratio*. (B) Equation for mobility ratio in terms of relative permeabilities and viscosities of oil and water.

$$M = \frac{\mu_o}{\mu_w} \frac{(k_{rw})\,\bar{S}_{w\,BT}}{(k_{ro})\,S_{wi}} \qquad \text{(eq 7.3)}$$

WHERE:

$(k_{rw})\,\bar{S}_{w\,BT}$ = Relative permeability of the average salt-water saturation behind the front at breakthrough

$(k_{ro})\,S_{wi}$ = Relative permeability of the oil in the oil bank

μ_o = Viscosity of the oil

μ_w = Viscosity of the water

Figure 122. Equation for defining the mobility ratio, using the relative permeability to water at the average salt-water saturation in the reservoir at breakthrough, and the relative permeability to oil for the oil saturation ahead of the front.

flooded reservoir increases. A mobility ratio equal to 1 indicates that the mobilities of water and oil are identical. A mobility of less than 1 indicates that oil flows better than water, which implies that water is a good displacing fluid to move oil. A mobility ratio of greater than 1 indicates that oil is not as mobile as water and that water would not be as effective in displacing oil.

Two rules of thumb from Smith and Cobb (1987) could be appropriate here. First, mobility ratios in the range of 0.50 to 5.0 can be considered acceptable for a waterflood project. Second, a quick, rudimentary method of evaluating the mobility ratio of a potential waterflood project is to use 0.30 times the viscosity of oil. This value roughly approximates the mobility ratio. It will be shown in following sections that knowledge of the pattern and the mobility ratio is all that is needed to estimate areal sweep efficiencies.

ESTABLISHING AREAL SWEEP EFFICIENCY

Since 1933, various authors, using the principles of displacement of oil touched on in the last chapter, have studied areal sweep efficiency for various producer–injector patterns. As will be seen, the pattern chosen for a waterflood candidate has tremendous impact on the potential outcome of the project. Obviously, some patterns are more effective than others, and care should be taken when selecting a pattern. Another consideration for the selection of a pattern should be the high cost of drilling infill wells. At the time a waterflood project begins, a field is generally already developed. A knowledge of various flood patterns and their effectiveness with respect to one another is an important advantage when considering the economics of a waterflood candidate.

Several definitions should be expanded on. The minimum pattern possible is composed of one injector and one producer. In this pattern neither the injector nor the producer shares injection or production from other wells if these are the only two active wells. In terms of net wells, this situation would be considered one net producer and one net injector. If a pattern were repeated, some of the producers and injectors would share or influence production of other patterns. The result of this might be that only a portion of an injector would contribute to its pattern, and likewise only a portion of a pattern's production might come from the pattern itself (i.e., some production might come as a result of injection from other patterns). In this example, a net well, whether a producer or an injector, is the sum of those portions of either injectors or producers that contribute to a particular pattern. The pattern spacing is simply the well spacing times the number of net wells for the pattern.

Some patterns become more or less effective by the distance between wells and the distance between rows of wells. These patterns are defined by a ratio called the *d/a* ratio, in which *d* is the distance between adjacent rows and *a* is the distance between adjacent wells in a row.

A third relationship is whether a pattern is termed *normal* or *inverted.* A normal pattern consists of one net producing well to a pattern with various numbers of net injectors. An inverted pattern consists of one net injector to a varying number of net producing wells.

A considerable number of authors have extensively researched areal sweep efficiencies for the primary types of patterns used in waterflood projects. The results of these studies are published and should be use-

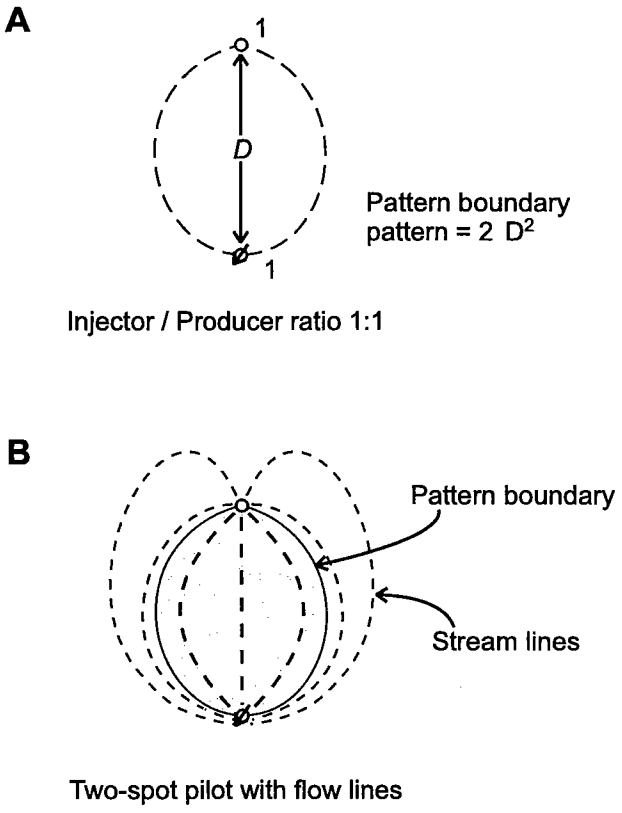

Figure 123. (A) Two-spot pattern. (B) Stream lines for a two-spot pattern. Shaded area represents the floodable area. Stream lines outside the floodable area contributing to production may increase the efficiency of the pattern.

ful in estimating the areal sweep efficiency (the E_a variable in eq. 5.1 of Fig. 55). Estimating E_a is simply a matter of determining the mobility ratio for the oil and establishing an injector–producer pattern for the reservoir and comparing this information to sweep efficiency previously determined for these criteria. Craig (1971) compiled an excellent resource of information for determining sweep efficiency. The remaining figures in this chapter highlight some of the primary patterns used in waterflooding and give basic graphs or tables that provide preliminary data for estimating areal sweep efficiency for each of these patterns.

TABLE 5. – Areal-Sweep Efficiency Studies–Isolated Two-Spot[a]

Date	Author(s)	Method	Mobility ratio	Areal-sweep efficiency at breakthrough (%)
1933	Wyckoff, Botset, and Muskat	Potentiometric model	1.0	52.5
1954	Ramey and Nabor	Blotter-type electrolytic model	1.0 ∞	53.8 27.7

Note: Base area = $2D^2$, where D is the distance between wells.

[a]Modified from Craig (©1971). Reprinted by permission of Society of Petroleum Engineers.

TABLE 6. – Areal-Sweep Efficiency Studies–Isolated Three-Spot[a]

Date	Author(s)	Method	Mobility ratio	Areal-sweep efficiency at breakthrough (%)
1933	Wyckoff, Botset, and Muskat	Electrolytic	1.0	78.5
1954	Ramey and Nabor	Blotter-type electrolytic model	∞	66.5

Note: Base area = $2D^2$, where D is the distance between injection and production wells.

[a]Modified from Craig (©1971). Reprinted by permission of Society of Petroleum Engineers.

Two-Spot Pattern

The two-spot pattern is the simplest of patterns. It consists of one injector and one producer. The pattern area used to establish the sweep efficiency is illustrated in Figure 123A. The pattern area is equal to 2 times the diameter squared and has an injector/producer ratio of 1:1. Because of the lack of wells, the pattern would be highly susceptible to directional permeability, fracturing, or compartmentalization within a reservoir. Figure 123B illustrates how the stream lines from outside the pattern area might influence the performance of this pattern. Care should be taken, especially for a pilot flood, to determine if the pattern is benefiting from production outside the pattern area that would ordinarily be produced by other patterns in the waterflood. If this occurs, the results of the pilot flood may be overly optimistic. Table 5 highlights studies for this pattern and areal sweep efficiencies at breakthrough for an oil whose mobility ratio is 1.0.

Three-Spot Pattern

The three-spot pattern adds an additional well to the two-spot pattern, either an injector or a producer. The area of the pattern is identical, being 2 times the distance (D) between the outer wells squared, as illustrated in Figure 124. In the example shown, the injector/producer ratio would be 1:2. Table 6 gives the results for sweep efficiencies determined from this pattern. The efficiencies are more than 50% greater than those for a two-spot pattern and even greater for mobility ratios higher than 1.0.

Four-Spot Pattern

The four-spot pattern is an even more efficient pattern, owing to the increase of wells. If the field is a multiwell field, the establishment of patterns would act to

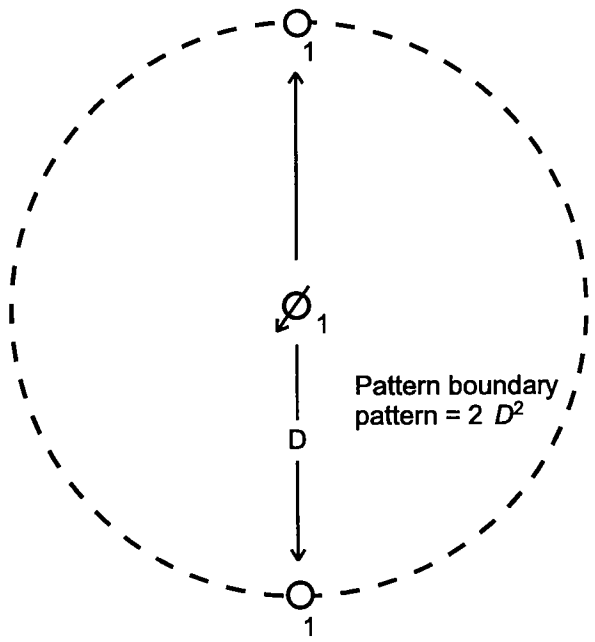

Figure 124. Three-spot pattern. Dashed line indicates pattern boundary.

confine injection to the patterns because of the interference from the injectors of other patterns. Figure 125A illustrates a regular four-spot pattern. In this example, the producer is surrounded by three injectors whose net injection into the pattern is shown. One-sixth of the injection for each injector is affecting the pattern. Therefore, the injector/producer ratio is a sum of the net injector, or three-sixths to one producer. Figure 125B illustrates the skewed four-spot pattern. Figure 126 illustrates the sweep efficiencies for the skewed four-spot pattern. Breakthrough should occur at a sweep efficiency of over 50%, depending on the value of the mobility ratio. The various values for displacement volume (V_d) are determined by the fraction of the cumulative injected fluid divided by the pattern pore volume times the displacement efficiency as determined in the last chapter. A V_d of 1.0 would indicate that 2.0 pattern pore volumes of fluid has been injected into a pattern whose displacement efficiency is 0.50. Table 7 gives references and criteria for establishing the sweep efficiencies of Figure 126.

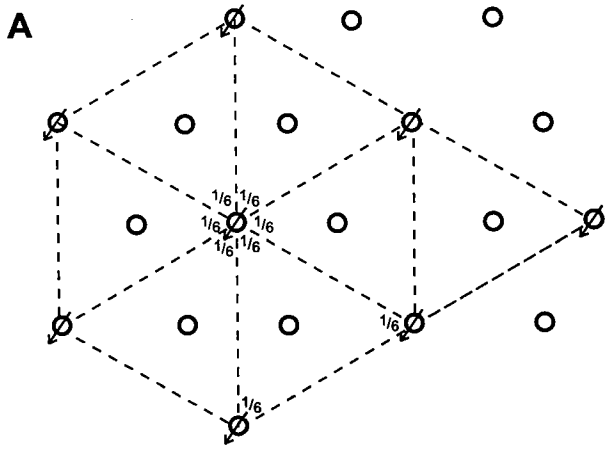

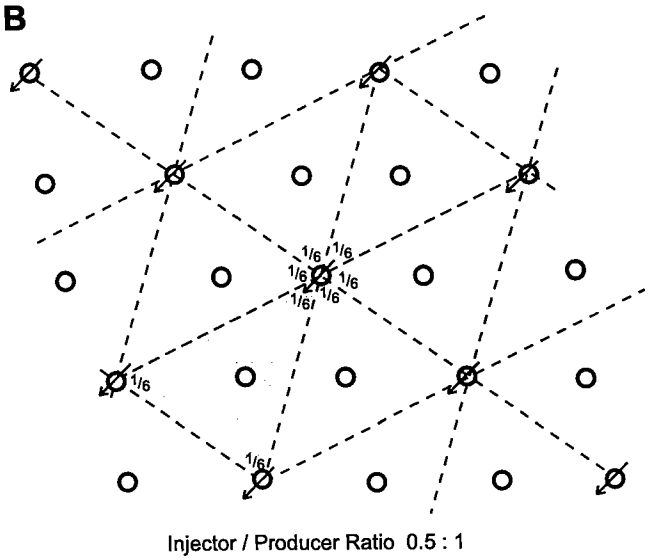

Figure 125. (A) Regular four-spot pattern. (B) Skewed four-spot pattern. Shaded area represents patterns.

TABLE 7. – Areal-Sweep Efficiency Studies– Developed Skewed Four-Spot[a]

Date	Author(s)	Method	Mobility ratio
1968	Caudle, Hickman, and Silberberg	X-ray shadowgraph using miscible fluids	0.1–10.0

[a]Modified from Craig (©1971). Reprinted by permission of Society of Petroleum Engineers.

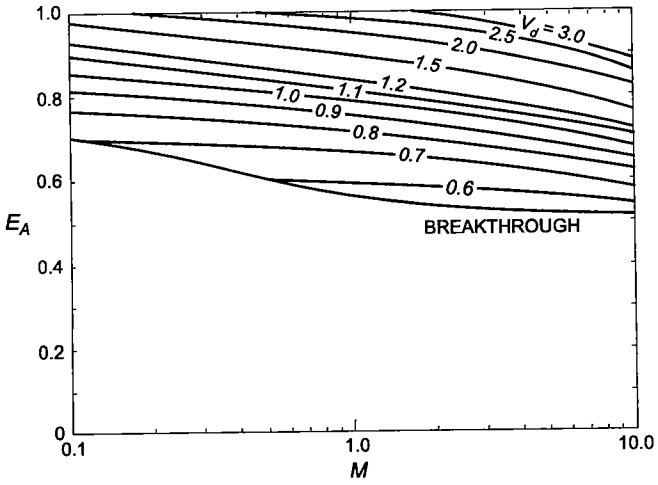

Figure 126. Areal sweep efficiencies for a skewed four-spot pattern, with various values of V_d (displaceable volume). (From Caudle and others, ©1968; reprinted by permission of Society of Petroleum Engineers.)

Direct Line-Drive Pattern

Direct line-drive patterns are probably the closest to approximating injection across a plane, as used in the concepts describing displacement efficiency in the previous chapter. Figure 127 illustrates the line-drive pattern and the *a* variable, which is the distance between adjacent wells in a row, and the *d* variable, which is the distance between adjacent rows of producers and injectors. The injector/producer ratio is 1:1. Figure 128 illustrates the plot for mobility ratio versus areal sweep efficiency for a direct line drive with a *d*/*a* ratio of 1.0. Table 8 lists data and references for studies of line-drive and staggered line-drive patterns with various *d*/*a* ratios and mobility ratios.

Staggered Line-Drive Pattern

Figure 129 illustrates the staggered line-drive pattern and is divided into an upper and lower part. The upper part (pattern 1) has a *d*/*a* ratio that is not equal to 0.5. The lower part (pattern 2) has a *d*/*a* ratio equal

TABLE 8. – Areal-Sweep Studies–Line-Drive Patterns[a]

Date	Author(s)	Method	Staggered or direct line drive	*d/a*	Mobility ratio
1933	Wyckoff, Botset, and Muskat	Electrolytic model	Direct	1.0	1.0
1934	Muskat and Wyckoff	Electrolytic model	Direct Staggered	0.5–4.0 0.5–4.0	1.0
1952	Aronofsky	Numerical and potentiometric model	Direct	1.5	0.1, 1.0, 10
1952	Slobod and Caudle	X-ray shadowgraph using miscible fluids	Direct	1.5	0.1–10
1954	Dyes, Caudle, and Erickson	X-ray shadowgraph using miscible fluids	Direct Staggered	1.0 1.0	0.1–17
1955	Cheek and Menzie	Fluid mapper	Direct	2.0	0.04–11.0
1956	Prats	Numerical approach	Staggered	1.0–6.0	1.0
1956	Burton and Crawford	Gelatin model	Direct	1.0	0.5–3.0

[a]Modified from Craig (©1971). Reprinted by permission of Society of Petroleum Engineers.

to 0.5. This is a highly symmetrical pattern and is the same as the five-spot pattern described directly following. The staggered line drive is formed by shifting either the rows of injectors or producers to an alternate cater-cornered position rather than having injectors and producers in an opposite position, as in the line-drive pattern. Cobb points out that the advantage of this pattern is to significantly increase the breakthrough efficiency over the line-drive pattern, especially for low *d/a* ratios. Figure 130 illustrates sweep efficiencies for a staggered line drive with a *d/a* ratio of 1.0. Figure 131 is another graph displaying sweep efficiencies as a function of the *d/a* ratios, with a mobility ratio of 1.0. Craig (1971) suggests that Prats' (1956) curve is perhaps the one to use with the most confidence. The injector/producer ratio for this pattern is 1:1.

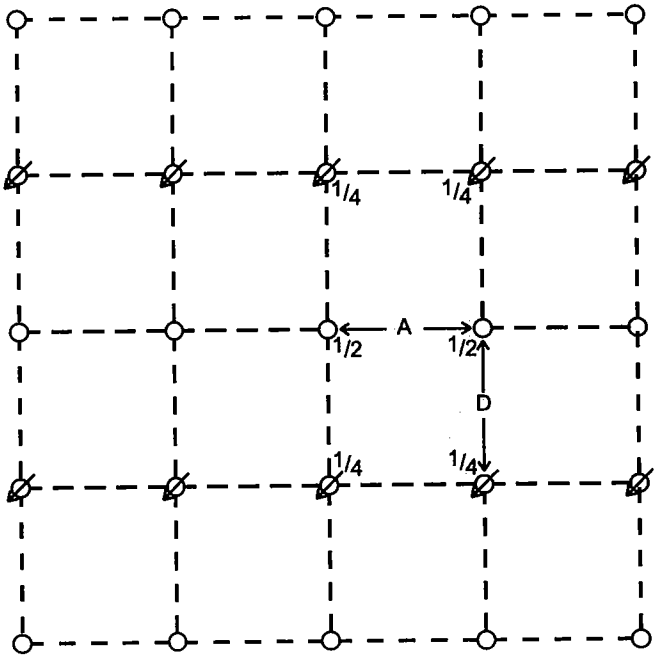

Figure 127. Direct line-drive pattern. Shaded area represents pattern.

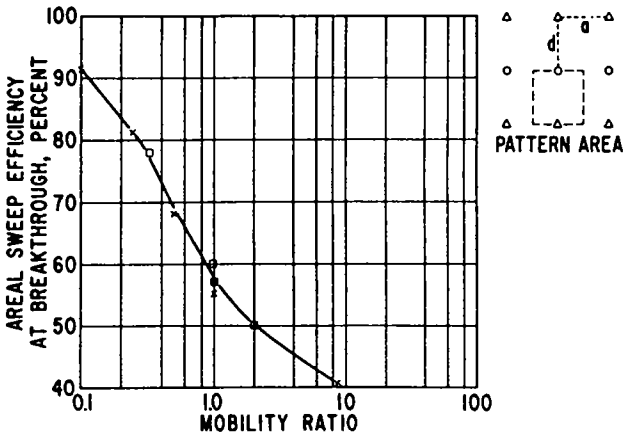

Figure 128. Areal sweep efficiency at breakthrough for a developed line-drive pattern and a *d/a* ratio of 1.0. (Craig, ©1971; reprinted by permission of Society of Petroleum Engineers.)

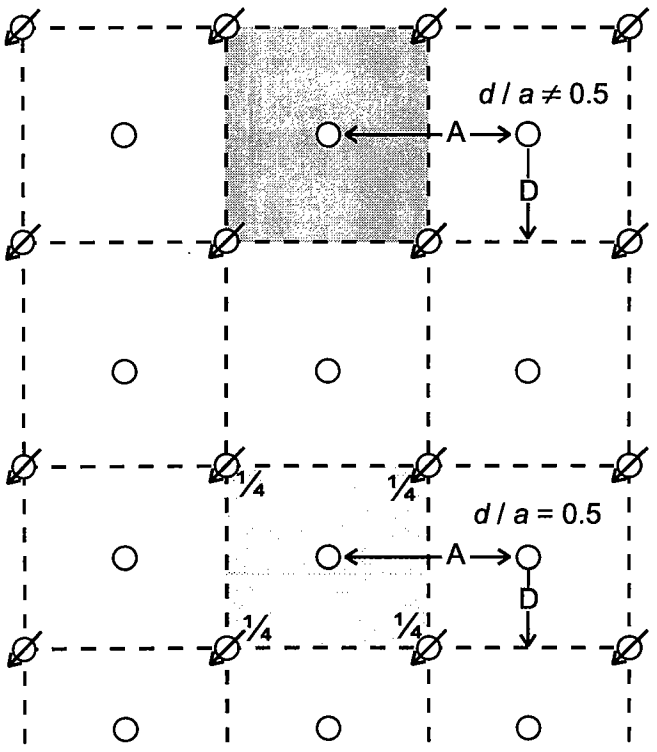

Figure 129. Staggered line-drive pattern. Shaded area represents patterns. Pattern 1 refers to a *d/a* ratio of 0.50, and pattern 2 refers to a *d/a* ratio of 0.50 and is the same as a five-spot pattern.

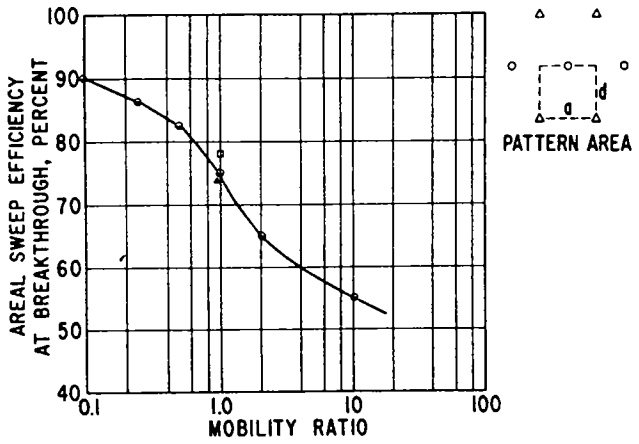

Figure 130. Areal sweep efficiency, at breakthrough, for a staggered line-drive pattern with a *d/a* ratio of 1.0. (Craig, ©1971; reprinted by permission of Society of Petroleum Engineers.)

Five-Spot Pattern

As mentioned previously, the five-spot pattern is a special line-drive pattern in which the *d/a* ratio is equal to 0.50. The pattern of wells is geometrical enough so that if the pattern needs to be adjusted because of premature water breakthrough, fracturing, etc., it can easily be modified. Figure 132A illustrates the normal five-spot pattern, and Figure 132B illustrates the inverted five-spot pattern. Notice that the normal pattern is one producer per portions of injectors, and the inverted pattern is one injector per portions of producers. Figure 133 represents the results of various investigators in analyzing the sweep efficiency of a developed five-spot pattern. The term *developed* means that the pattern is one of several adjacent patterns. The investigators all seem to agree as to the sweep efficiency where the mobility ratio is 1.0 or less, but vary when the mobility ratio exceeds 1.0. Craig (1971) suggests that the solid curve probably most closely approximates waterflood performance. Figure 134 also gives areal sweep efficiencies at breakthrough for a single, isolated injection well (inverted five-spot pattern) and a single, isolated producing well (normal five-spot pattern). The term *isolated* implies that the pattern could be that of a pilot waterflood with no adjacent pattern. Tables 9 and 10 give data and information for developed and isolated five-spot patterns, respectively.

The next two pattern types represent higher injector/producer ratios. These patterns might be considered in situations where high injection rates may be necessary in low-permeability reservoirs, for example. The inverted pattern could be used in cases of high permeability. The patterns are of two types, one in which the wells are directly across from each other, and one in which the wells are staggered.

Seven-Spot Pattern

Figure 135A illustrates the normal seven-spot pattern. The injector/producer ratio for the pattern is 2:1. Figure 135B illustrates the inverted seven-spot pattern with an injector/producer ratio of 1:2. Notice that the geometry of the pattern is similar to that of the four-spot pattern. Figure 136 represents sweep efficiencies for a normal seven-spot pattern at breakthrough. Two sets of data are presented. Craig (1971) recommends using the data represented by the solid line because of the reliability of the method of testing. Figure 137 shows data for the inverted seven-spot pattern. Craig

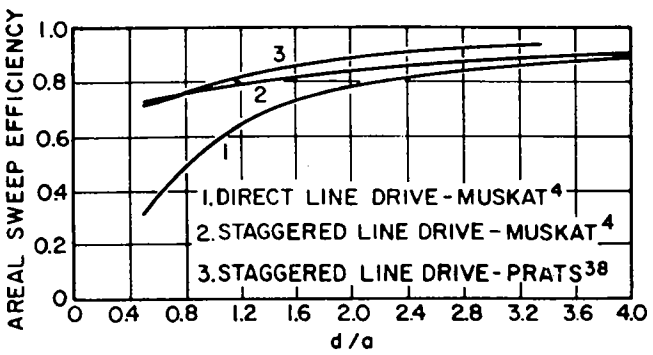

Figure 131. Areal sweep efficiencies for a direct line-drive pattern (1) and a staggered line-drive pattern (2, 3) with varying *d/a* ratios. Mobility ratio = 1.0. (Craig, ©1971; reprinted by permission of Society of Petroleum Engineers.)

(1971) also recommends the solid curve, which was generated from a study by Guckert (1961). Table 11 lists data, references, and sweep efficiencies for the normal seven-spot pattern, and Table 12 lists the same information for the inverted seven-spot pattern.

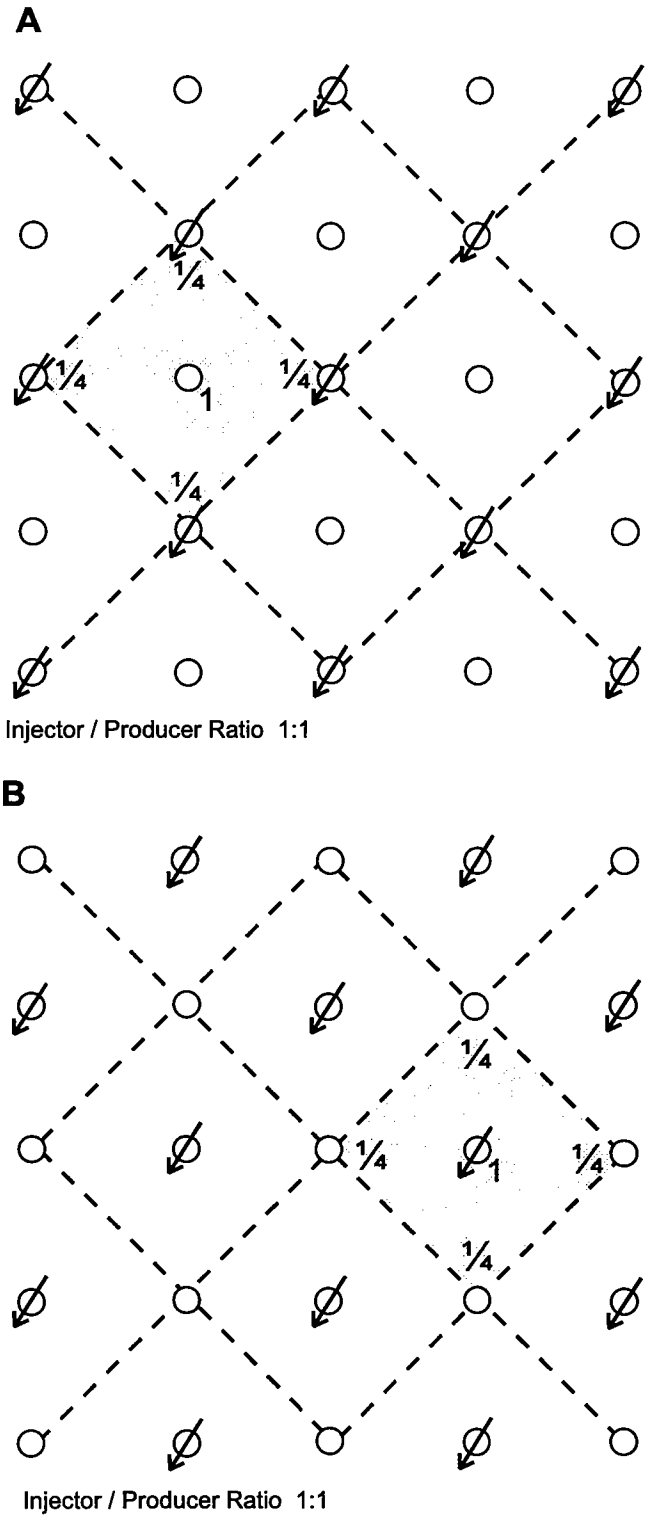

Figure 132. (A) Normal five-spot pattern. (B) Inverted five-spot pattern. Shaded area represents patterns.

Nine-Spot Pattern

Figure 138A illustrates a normal nine-spot pattern. The injector/producer ratio for this pattern is 3:1. The pattern has the flexibility of change, owing to the large number of wells. This pattern could easily convert to a line-drive pattern or a normal or inverted five-spot pattern, depending on response characteristics. Figure 138B illustrates the inverted pattern with an injector/producer ratio of 1:3. Figures 139–141 represent three different areal sweep efficiencies at water/oil producing-rate ratios of 0.50, 1.0, and 5.0, respectively. The variable V_d is used similarly as defined in the skewed four-spot pattern of Figure 126. Tables 13 and 14 give references and data for a normal nine-spot and an inverted nine-spot pattern.

It should be mentioned at this point that the patterns described, with their associated areal sweep-efficiency data, were determined from experiment models

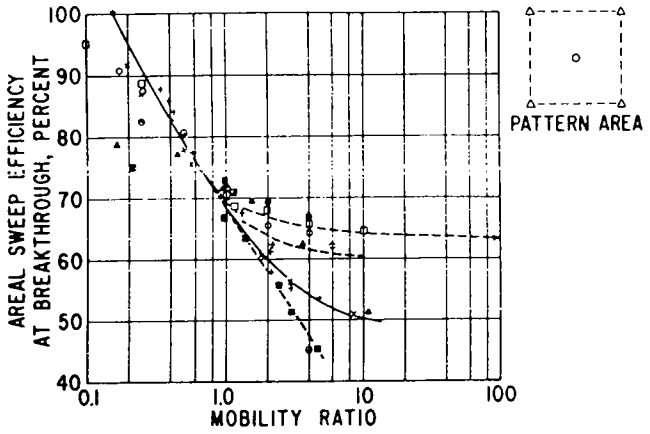

Figure 133. Areal sweep efficiencies at breakthrough for a developed five-spot pattern. (Craig, ©1971; reprinted by permission of Society of Petroleum Engineers.)

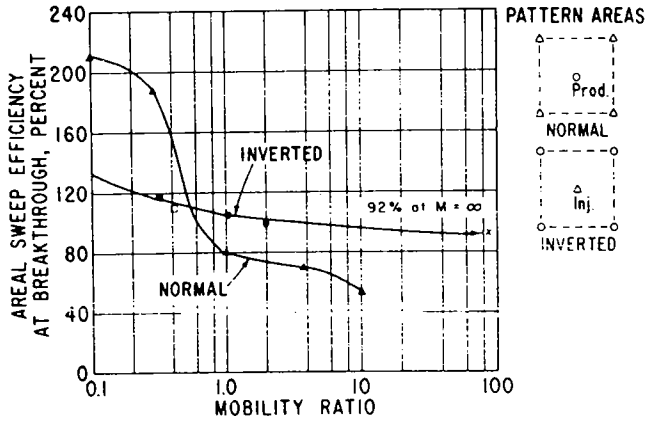

Figure 134. Areal sweep efficiencies for isolated normal and inverted five-spot patterns. (Craig, ©1971; reprinted by permission of Society of Petroleum Engineers.)

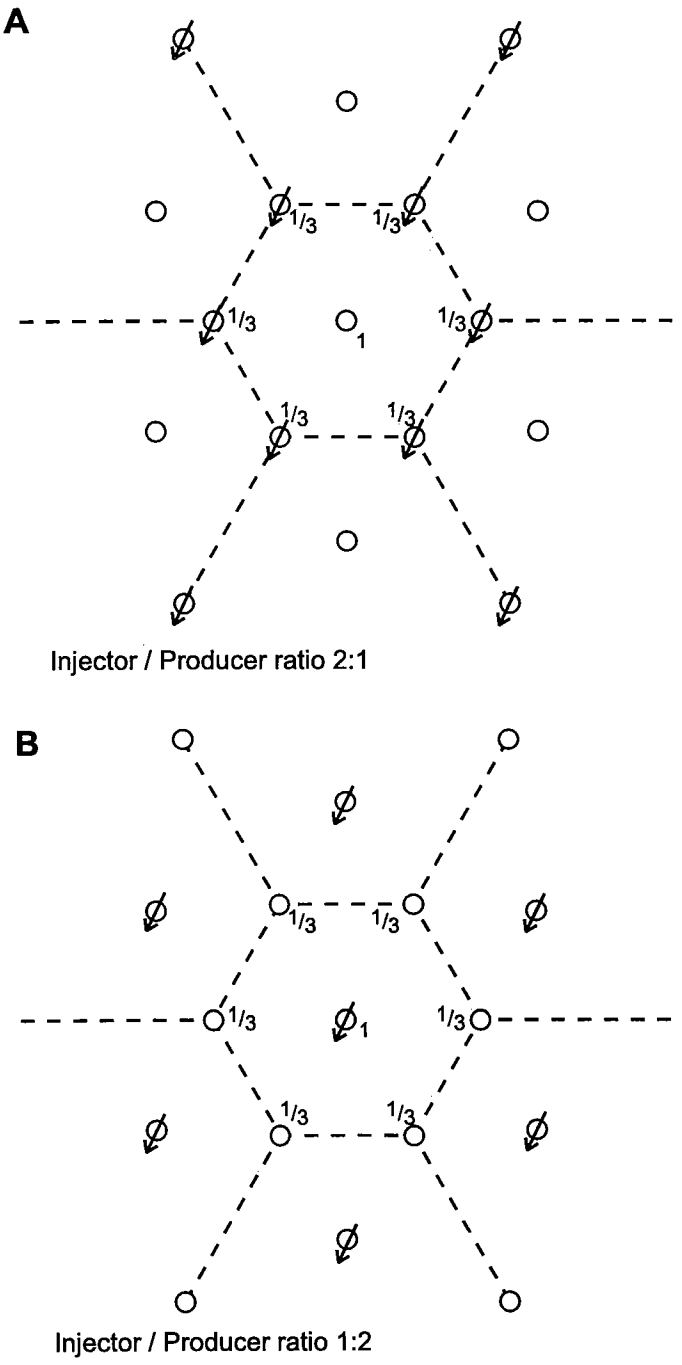

Figure 135. (A) Normal seven-spot pattern. (B) Inverted seven-spot pattern. Shaded area represents patterns.

TABLE 9. – Areal-Sweep Efficiency Studies– Developed Five-Spot[a]

Date	Author(s)	Method	Mobility ratio
1933	Wyckoff, Botset and Muskat	Electrolytic model	1.0
1934	Muskat and Wyckoff	Electrolytic model	1.0
1951	Fay and Prats	Numerical	4.0
1952	Slobod and Caudle	X-ray shadowgraph using miscible fluids	0.1–10.0
1953	Hurst	Numerical	1.0
1954	Dyes, Caudle, and Erickson	X-ray shadowgraph using miscible fluids	0.06–10
1955	Craig, Geffen, and Morse	X-ray shadowgraph using miscible fluids	0.16–5.0
1955	Cheek and Menzie	Fluid mapper	0.04–10.0
1956	Aronofsky and Ramey	Potentiometric model	0.1–10.0
1958	Nobles and Janzen	Resistance network	0.1–6.0
1960	Habermann	Fluid-flow model using dyed fluids	0.037–130
1961	Bradley, Heller, and Odeh	Potentiometric model using conductive cloth	0.25–4

[a]Modified from Craig (©1971). Reprinted by permission of Society of Petroleum Engineers.

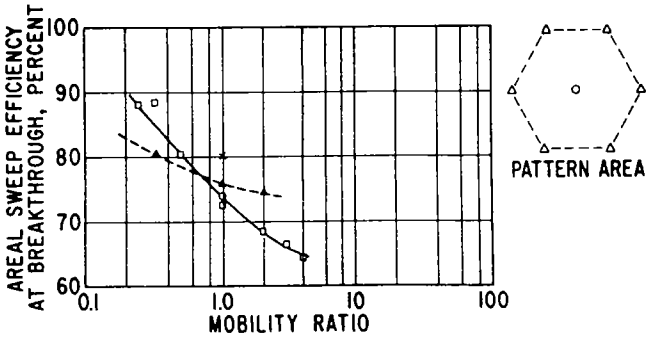

Figure 136. Areal sweep efficiencies for a developed normal seven-spot pattern. (Craig, ©1971; reprinted by permission of Society of Petroleum Engineers.)

with no gas saturation. The effects of gas saturation or of areal sweep efficiencies after breakthrough will not be dealt with further in this publication. The only intent is to provide a cursory means for determining E_a for preliminary review of a waterflood prospect. However, Craig (1971) states that the injected water advances radially and continues until either (1) the leading edge of the oil bank contacts an oil bank formed about an adjacent injector, or (2) the oil bank encounters a producing well. At this point the flood front begins to cusp toward the nearest producer. Craig (1971) also states: "If at this time the flood front should also be radial in the initially liquid-saturated reservoir, the areal sweep at water breakthrough with initial gas present would be the same as that with no gas. The performance at and after breakthrough would be the same."

TABLE 10. – Areal-Sweep Efficiency Studies– Normal and Inverted Five-Spot Pilot[a]

Date	Author(s)	Method	Type	Mobility ratio	Areal-sweep efficiency at breakthrough (%)
1958	Paulsell	Fluid mapper	Inverted	0.319	117.0
				1.0	105.0
				2.01	99.0
1959	Moss, White, and McNiel	Potentiometric	Inverted	∞	92.0
1960	Caudle and Loncaric	X-ray shadowgraph	Normal	0.1–10.0	*
1962	Neilson and Flock	Rock flow model	Inverted	0.423	110.0

Note: Base area = D^2, where D is the distance between adjacent producing wells.

[a]Modified from Craig (©1971). Reprinted by permission of Society of Petroleum Engineers.

*Depends on ratio of injection rate to producing rate.

TABLE 11. – Areal-Sweep Efficiency Studies– Developed Normal Seven-Spot Pattern[a]

Date	Author(s)	Method	Mobility ratio	Areal-sweep efficiency at breakthrough (%)
1933	Wyckoff, Botset, and Muskat	Electrolytic model	1.0	82.0
1934	Muskat and Wyckoff	Electrolytic model	1.0	74.0
1956	Burton and Crawford	Gelatin model	0.33	80.5
			0.85	77.0
			2.0	74.5
1961	Guckert	X-ray shadowgraph using miscible fluids	0.25	88.1–88.2
			0.33	88.4–88.6
			0.5	80.3–80.5
			1.0	72.8–73.6
			2.0	68.1–69.5
			3.0	66.0–67.3
			4.0	64.0–64.6

[a]Modified from Craig (©1971). Reprinted by permission of Society of Petroleum Engineers.

TABLE 12. – Areal-Sweep Efficiency Studies– Developed Inverted (Single Injection Well) Seven-Spot Pattern[a]

Date	Author(s)	Method	Mobility ratio	Areal-sweep efficiency at breakthrough (%)
1933	Wyckoff, Botset, and Muskat	Electrolytic model	1.0	82.2
1956	Burton and Crawford	Gelatin model	0.5	77.0
			1.3	76.0
			2.5	75.0
1961	Guckert	X-ray shadowgraph using miscible fluids	0.25	87.7–89.0
			0.33	84.0–84.7
			0.50	79.0–80.5
			1.0	72.8–73.7
			2.0	68.8–69.0
			3.0	66.3–67.2
			4.0	63.0–63.6

[a]Modified from Craig (©1971). Reprinted by permission of Society of Petroleum Engineers.

The produced oil, however, would be less by an amount equal to the volume of the gas saturation.

Another point to consider is the effects of fractures and directional permeabilities. These features can have disastrous effects on a waterflood project if the injector and producer are parallel to the direction of high permeability or fractures. Such a situation should be called to the attention of the engineering department when setting up final plans for an injector–producer pattern.

TABLE 13. – Areal-Sweep Efficiency Studies– Developed Normal Nine-Spot Pattern[a]

Date	Author	Method	Mobility ratio
1939	Krutter	Electrolytic model	1.0
1961	Guckert	X-ray shadowgraph using miscible fluids	1.0 and 2.0

[a]Modified from Craig (©1971). Reprinted by permission of Society of Petroleum Engineers.

TABLE 14. – Areal-Sweep Efficiency Studies– Inverted (Single Injection Well) Nine-Spot Pattern[a]

Date	Author(s)	Method	Mobility ratio
1964	Kimbler, Caudle, and Cooper	X-ray shadowgraph using miscible fluids	0.1–10.0
1964	Watson, Silberberg, and Caudle	Fluid-flow model using dyed miscible fluids	0.1–10.0

[a]Modified from Craig (©1971). Reprinted by permission of Society of Petroleum Engineers.

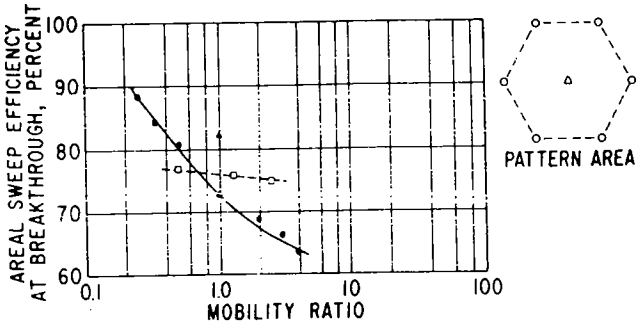

Figure 137. Areal sweep efficiencies for a developed inverted seven-spot pattern. (Craig, ©1971; reprinted by permission of Society of Petroleum Engineers.)

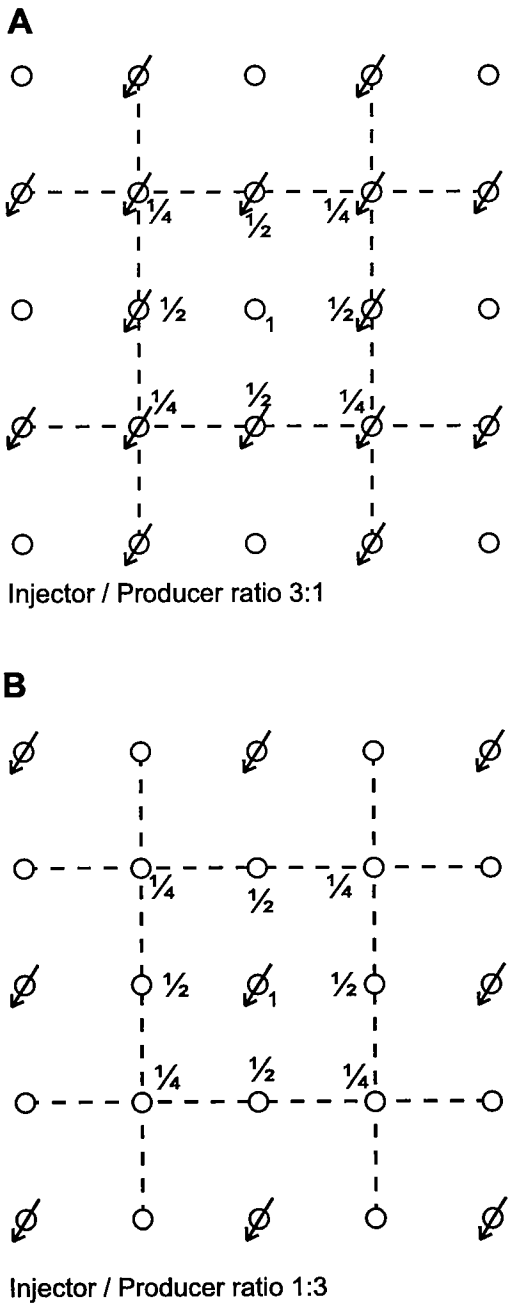

Figure 138. (A) Normal nine-spot pattern. (B) Inverted nine-spot pattern. Shaded area represents patterns.

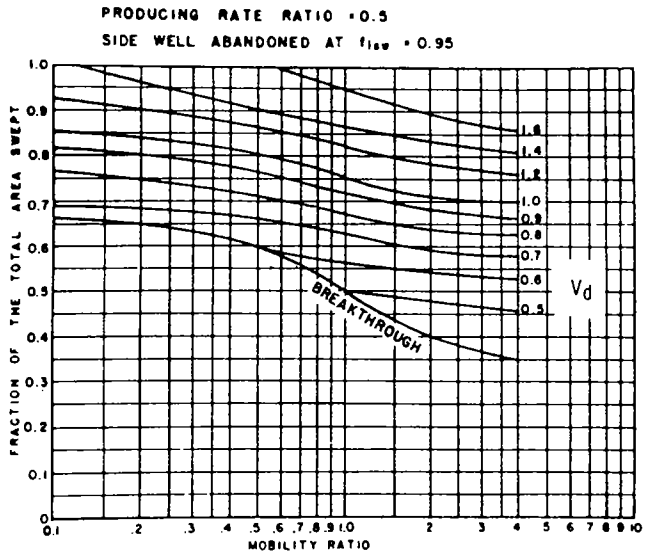

Figure 139. Areal sweep efficiencies for a normal nine-spot pattern at various V_d volumes. Producing-rate ratio = 0.50. (Kimber and others, ©1971; reprinted by permission of Society of Petroleum Engineers.)

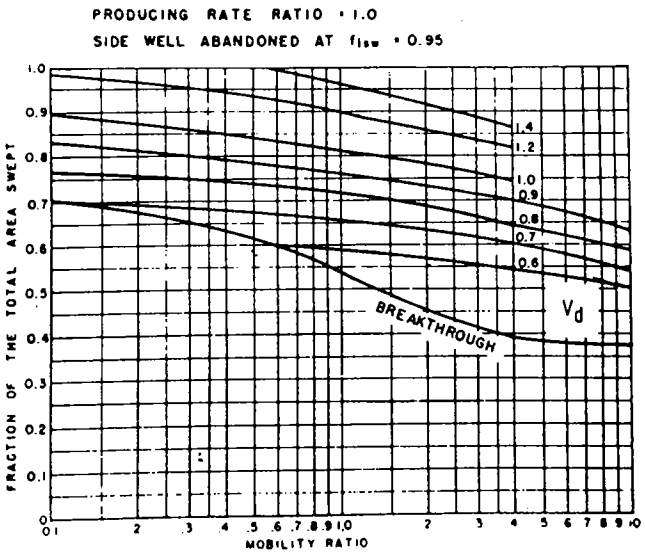

Figure 140. Areal sweep efficiencies for a normal nine-spot pattern at various V_d volumes. Producing-rate ratio = 1.0. (Kimber and others, ©1971; reprinted by permission of Society of Petroleum Engineers.)

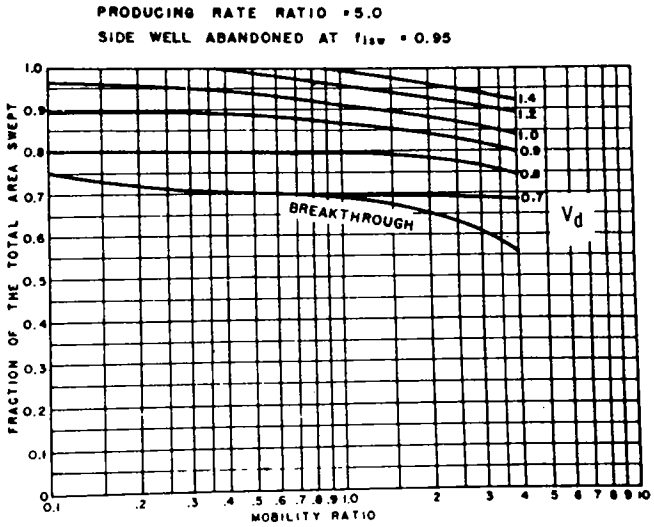

Figure 141. Areal sweep efficiencies for a nine-spot pattern at various corner-well producing cuts. Producing-rate ratio = 5.0. (Kimber and others, ©1971; reprinted by permission of Society of Petroleum Engineers.)

Vertical Sweep Efficiency

8

CHAPTER 8

Vertical Sweep Efficiency

INTRODUCTION

The discussion in Chapter 6 of displacement efficiency assumed that areal and vertical sweep efficiencies were not a factor and that the reservoir acts in a completely homogeneous manner in both areal and vertical directions. This discussion also treated the plane from injector to producer as a single layer. In the "real" world, this is not the situation. Reservoirs are commonly composed of layers of strata whose rock properties vary widely. Layers with higher permeabilities will get swept faster than those with lower permeabilities. The question is, how do we quantify the various permeable layers into a number that can be used in equation 5.1 of Figure 55 to represent the effect of vertical reservoir heterogeneity on the amount of oil displaced by waterflooding?

Craig (1971) defines *vertical sweep efficiency* as the cross-sectional area contacted by the injected fluid divided by the cross-sectional area enclosed in all layers behind the injected fluid front. This chapter gives a brief overview of the facets involved with permeability variations. A method will be offered to quantify vertical sweep efficiency (E_v) for use in a preliminary reserve evaluation of a potential waterflood prospect.

PERMEABILITY VARIATION

Sediments deposited in various depositional environments have characteristics unique to those environments. Energies involved with sediment transport, facies distribution, cementation, compaction, structural effects, and diagenesis affect porosity and permeability in both the areal and vertical directions. To compound the problem, deposition of multilayers of uniquely diverse sediments within a reservoir can cause the injected water to behave in a myriad of ways, each representative of the characteristics of that particular layer and each layer acting almost as an individual reservoir. A single layered, homogeneous porous system is not often found in reservoirs today. Reservoir heterogeneity probably has as much or more effect on a waterflood performance as any other parameter. A main problem with permeability variation is the difficulty in predicting its presence. Geologists' greatest contribution to the success of a waterflood project is their understanding of depositional environments and the recognition of potential porosity and permeability fluctuations. Such variations can also be on a reservoir-scale basis, such as faulting and fracturing, which were discussed briefly in the first waterflood workshop (Rottmann and others, 1998, p. 123–142). Recognition of permeability variations is difficult, but facies recognition from electric logs, cores, and samples, plus drillstem testing and production results, is also a necessary tool for interpretation. Smith and Cobb (1987) suggest that areal permeability variations are probably less severe than vertical permeability variations, except for fracturing and high-permeability trends.

Vertical permeability variations are commonly a result of stratification. Typically, stratified layers of distinctly different ranges of permeabilities offer greater velocity throughput than those of lower permeabilities. Breakthrough can occur from layers of high permeability while significant quantities of oil may still be approaching the wellbore from the less permeable layers. If the engineer is made aware of this possibility through a detailed geological evaluation, steps can be taken to alter or modify this outcome during planning and installation of the waterflood unit. Therefore, geological interpretation is critical in this respect.

A challenge for geologists and engineers is in estimating a permeability value for a similar-sized reservoir that would act as the defining permeability of a homogeneous reservoir and yet be representative of the heterogeneous reservoir as well. Figure 142A represents a common mathematical approach to finding weighted-average permeabilities for a reservoir. Each value of K_nH_n represents the weighted average for each

A

Weighted average

$$k_{AVG} = \frac{k_1 H_1 + k_2 H_2 + \ldots + k_n H_n}{H_1 + H_2 + \ldots + H_n} \qquad \text{(eq 8.1)}$$

WHERE:

k = Permeabilities fo the individual layers
H = Thicknesses of the individual layers

B

Geometric mean

$$k_{AVG} = (k_1 \times k_2 \times k_3 \times \ldots \times k_n)^{1/n} \qquad \text{(eq 8.2)}$$

Figure 142. (A) Weighted-average method for determining average permeability. (B) Geometric-mean method for determining average permeability.

layer. Smith and Cobb (1987) suggest that this result may be optimistic and does not recommend its use.

A second method suggested in Smith and Cobb (1987, p. 5–27) is to obtain the geometric mean for the permeabilities, as shown in equation 8.2 of Figure 142B. This technique was obtained from model studies using simulated flow patterns in media of varying permeabilities. Each permeable interval should be of equal thickness so that the outcome is equally weighted.

DYKSTRA-PARSONS COEFFICIENT

In 1944, Law (reported by Smith and Cobb, p. 5–27) demonstrated that rock permeabilities have a log-normal distribution. This implies that plotting the number of permeability samples against the log permeability will yield the familiar bell-shaped curve. In 1950, Dykstra and Parsons contributed a paper of monumental proportions that used a statistical approach for analyzing Law's log-normal permeability distribution and coined the term *coefficient of permeability variation.* Equation 8.3 of Figure 143 represents the definition for this coefficient, where $\bar{k}$ is the mean permeability, or 50.0%, and $k\sigma$ is the permeability at 84.1% of the cumulative sample. Figure 143B illustrates the statistical equivalent of equation 8.3. This coefficient is now called the *Dykstra-Parsons coefficient.* To determine the coefficient, the following steps are taken:

1. Permeabilities are divided into equal-thickness layers.
2. Permeabilities are arranged in decreasing order.
3. Calculate for each sample the percentage of the sample that has a permeability greater than, and express this number as percentage greater than.
4. Plot the data on log probability paper with the percentage-greater-than values on the x-axis, and the permeabilities on the y-axis.

A

$$V = \frac{\bar{k} - k_\sigma}{\bar{k}} \qquad \text{(eq 8.3)}$$

WHERE:

$\bar{k}$ = Mean permeability = Permeability value with 50% probability

k_σ = Permeability at 84.1% of the cumulative sample

B

$$V = \frac{k_{50} - k_{84.1}}{k_{50}} \qquad \text{(eq 8.4)}$$

WHERE:

V = Coefficient of permeability variation

k_{50} = Is the permeability at the 50%-greater-than point

$k_{84.1}$ = Is the permeability at the 84.1%-greater-than point

Figure 143. (A) Equation for coefficient of permeability variation (Dykstra-Parsons coefficient). (B) Statistical equivalent to equation 8.3.

TABLE 15. – Determination of Dykstra-Parsons Coefficient

Layers	Permeability ordering	Percentage greater than
1	51.0	0.00
2	49.0	4.76
3	46.0	9.52
4	36.0	14.29
5	20.0	19.05
6	18.0	28.57
7	17.9	38.10
8	10.0	42.86
9	9.1	47.62
10	6.9	52.38
11	5.6	61.90
12	0.9	66.67
13	0.5	76.19
14	0.2	85.71
15	0.1	90.48

5. Derive a best-fit curve for the plot of values.
6. Determine the permeability at the 50%-greater-than percentage and at the 84.1%-greater-than percentage and place into equation 8.4.

The values that result from equation 8.4 will vary from 0.0 to 1.0, with 0.0 representing a completely homogeneous reservoir and 1.0 representing a completely heterogeneous reservoir. Smith and Cobb (1987) point out that limestone reservoirs usually range from 0.90 to 0.95 and that sandstone reservoirs usually range from 0.60 to 0.95.

As an example for determining the Dykstra-Parsons coefficient, Table 15 represents a set of permeability data from a core of a reservoir in central Oklahoma that was divided into equal 1-ft layers and listed in decreasing order of permeability. The third column represents the percentage-greater-than values for the example. Figure 144 is a log probability plot of the percentage-greater-than values plotted versus the permeabilities from Table 15. The straight line is the best-fit curve for the points. The permeability at the 50%-greater-than point is 8 md, and the permeability at the 84.1%-greater-than point is 2.2 md. Substituting these values into equation 8.4 yields a value of 0.72, which is the coefficient of permeability variation. The next section will describe how this coefficient can be used to determine vertical sweep efficiencies.

ESTABLISHING VERTICAL SWEEP EFFICIENCY

The use of the Dykstra-Parsons coefficient is quite simple. Dykstra and Parsons correlated their value of permeability variations with various waterflood performances and derived the charts of Figures 145–148. To illustrate how these charts are to be used, we will examine Figure 145, which is a chart whose parameters include the Dykstra-Parsons coefficient on the y-axis, and the mobility ratio as a set of predetermined curves

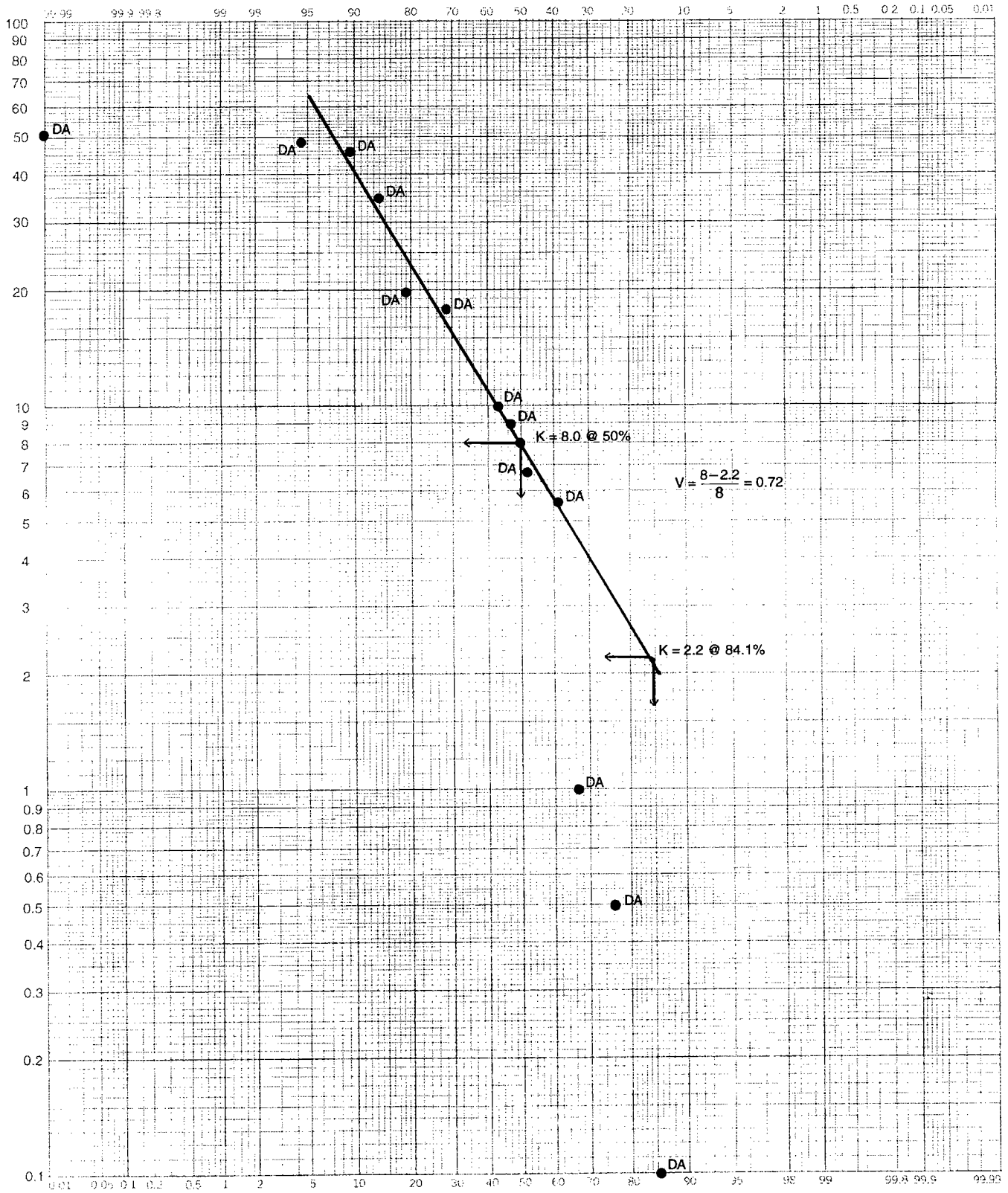

Figure 144. Plot of percentage-greater-than data from Table 15 on log probability paper. Value of permeability at 50% is 8.0 md, and value of permeability at 84.1% is 2.2 md. Substituting these permeabilities into equation 8.4 (Fig. 143B) yields a Dykstra-Parsons coefficient of 0.72.

for a producing water/oil ratio (WOR) of 1. The x-axis plots the vertical-sweep-efficiency value (E_v) when the values of the Dykstra-Parsons coefficient and the mobility ratio are plotted. To illustrate an example of determining E_v, begin by plotting the mobility ratio for a reservoir, which has a value equal to 2, and the Dykstra-Parsons coefficient of 0.72, which was derived from the example of Table 15 and Figure 144 to Figure 145. The E_v value is approximately equal to 0.27. This is the value used for E_v in equation 5.1 of Figure 55 for a producing

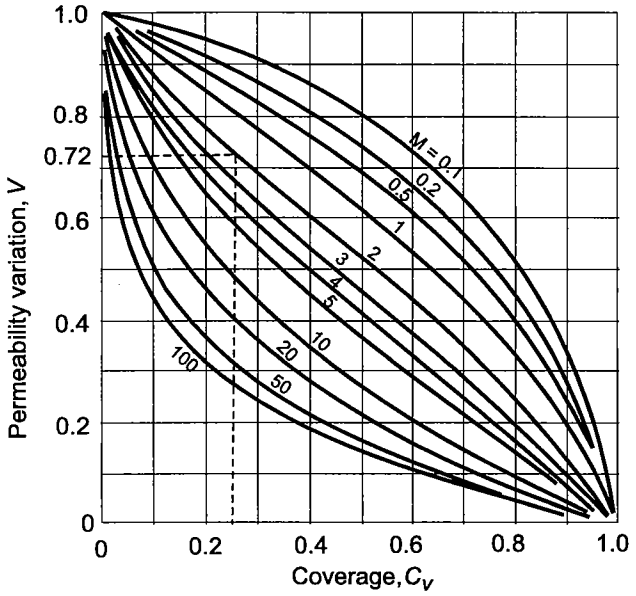

Figure 145. Vertical sweep efficiency for various mobility ratios at a WOR equal to 1.0. (Dykstra and Parsons, ©1950; reprinted courtesy of the American Petroleum Institute.)

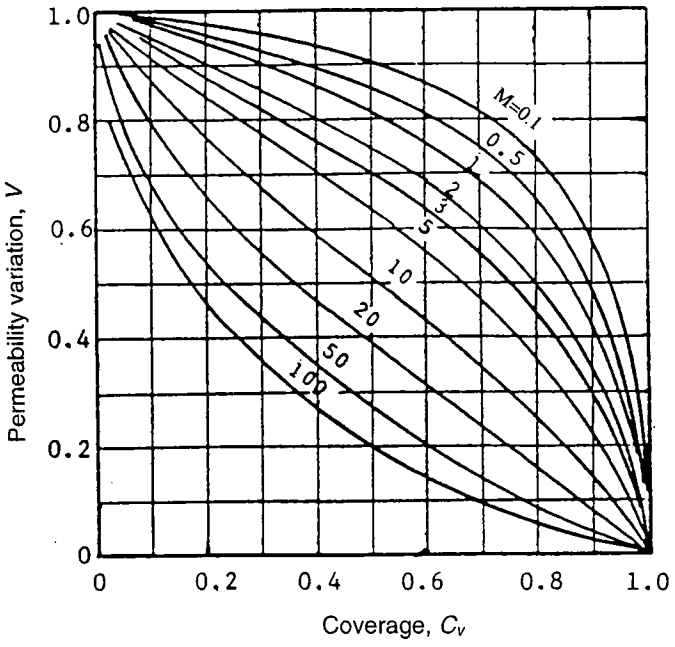

Figure 146. Vertical sweep efficiency for various mobility ratios at a WOR equal to 5.0. (From Smith and Cobb, 1987.)

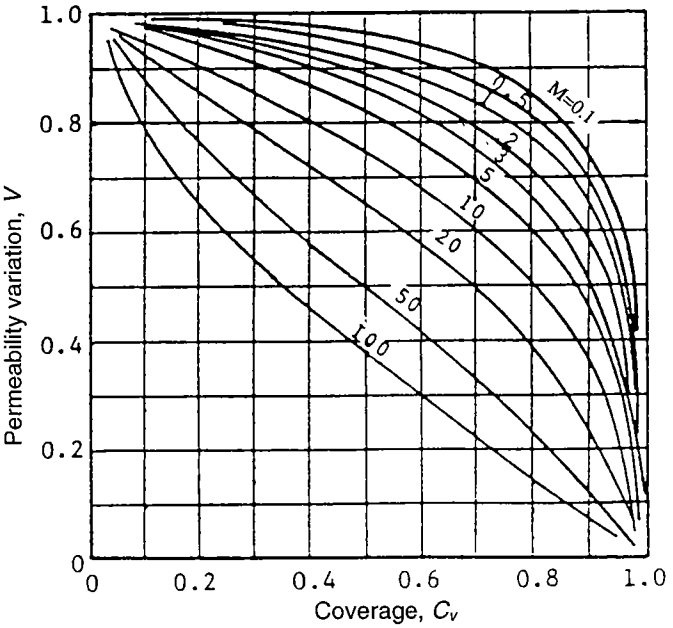

Figure 147. Vertical sweep efficiency for various mobility ratios at a WOR equal to 25. (Dykstra and Parsons, ©1950; reprinted courtesy of the American Petroleum Institute.)

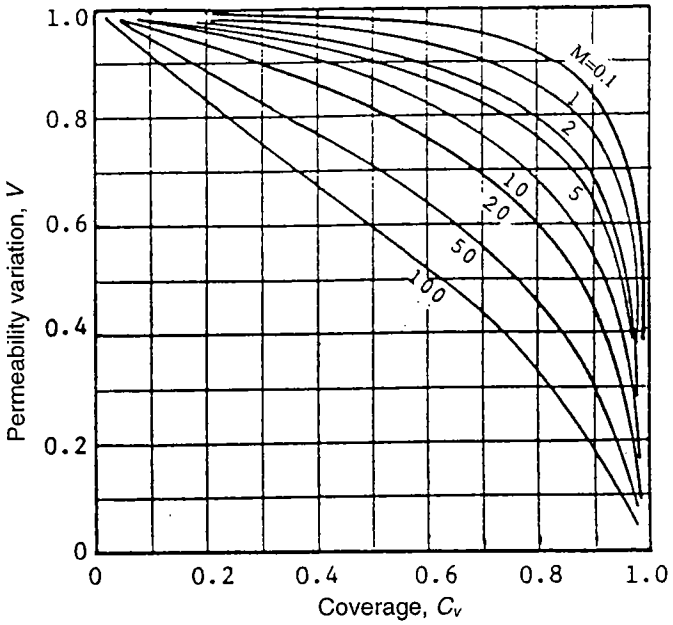

Figure 148. Vertical sweep efficiency for various mobility ratios at a WOR equal to 100. (From Smith and Cobb, 1987.)

WOR of 1. Figures 146–148 are similar charts for determining E_v for WORs of 5, 25, and 100, respectively. WORs of 100:1 are probably close to the economic limit of a waterflood project.

Because the value of E_v is established from Figures 145–148, it is a simple matter to use these values for E_v in equation 5.1 (Fig. 55). Various other techniques for determination and evaluation of reservoir heterogeneity are examined in more detail from the papers used as references for this chapter.

Selected References

SELECTED REFERENCES

American Petroleum Institute, 1960, History of petroleum engineering: Dallas, 1241 p.

Amyx, J. W.; Bass, D.; and Whiting, R. L., 1960, Petroleum reservoir engineering: physical properties: McGraw-Hill, New York.

Anderson, W. G., 1987, Wettability literature survey, part 6: the effects of wettability on waterflooding: Journal of Petroleum Technology, v. 51, p. 1605–1622.

Andrews, R. A., 1997, Fluvial-dominated deltaic (FDD) oil reservoirs in Oklahoma: the Red Fork play: Oklahoma Geological Survey Special Publication 97-1, 101 p.

Aronofsky, J. S., 1934, Mobility ratio—its influence on flood patterns during water encroachment: Transactions of AIME (American Institute of Mining and Metallurgical Engineers), v. 107, p. 62–76.

Aronofsky, J. S.; and Ramey, J. J., Jr., 1956, Mobility ratio—its influence on injection and production histories in five-spot water flood: Transactions of AIME (American Institute of Mining and Metallurgical Engineers), v. 207, p. 205–210.

Aydin, A., 1978, Small faults formed as deformation bands in sandstone: Pure Applied Geophysics, v. 116, p. 913–930.

Beard, D. C.; and Weyl, P. K., 1973, Influence of texture on porosity and permeability of unconsolidated sands: American Association of Petroleum Geologists Bulletin, v. 57, p. 349–369.

Borden, Guy, Jr.; and Rzasa, M. J., 1950, Correlation of bottom hole sample data: Transactions of AIME (American Institute of Mining and Metallurgical Engineers), v. 189, p. 345–348.

Botset, H. G., 1946, The electrolytic model and its application to the study of recovery problems: Transactions of AIME (American Institute of Mining and Metallurgical Engineers), v. 165, p. 15–25.

Bradley, H. B.; Heller, J. P.; and Odeh, A. S., 1961, A potentiometric study of the effects of mobility ratio on reservoir flow patterns: Society of Petroleum Engineers Journal, v. 1, p. 125–129.

Bruce, W. A.; and Welge, H. J., 1947, The restored-state method for determination of oil in place and connate water: American Petroleum Institute, Drilling and Production Practice, p. 166–173.

Buckley, S. E.; and Leverett, M. C., 1942, Mechanism of fluid displacements in sands: Transactions of AIME (American Institute of Mining and Metallurgical Engineers), v. 146, p. 107–116.

Burton, M. B., Jr.; and Crawford, P. B., 1956, Application of the gelatin model for studying mobility ratio effects: Transactions of AIME (American Institute of Mining and Metallurgical Engineers), v. 207, p. 333–337.

Carll, J. F., 1880, The geology of the oil regions of Warren, Venango, Clarion, and Butler Counties, Pennsylvania: Second Geological Survey of Pennsylvania, v. 3, 1875–79, 482 p.

Caudle, B. H.; and Loncaric, I. G., 1960, Oil recovery in five-spot pilot floods: Transactions of AIME (American Institute of Mining and Metallurgical Engineers), v. 219, p. 132–136.

Caudle, B. H.; and Witte, M. D., 1959, Production potential changes during sweep-out in a five-spot system: Transactions of AIME (American Institute of Mining and Metallurgical Engineers), v. 216, p. 446–448.

Caudle, B. H.; Erickson, R. A.; and Slobod, R. L., 1955, The encroachment of injected fluids beyond the normal well pattern: Transactions of AIME (American Institute of Mining and Metallurgical Engineers), v. 204, p. 79–85.

Caudle, B. H.; Hickman, B. M.; and Silberberg, I. H., 1968, Performance of the skewed four-spot injection pattern: Journal of Petroleum Technology, v. 20, p. 1315–1319.

Cheek, R. E.; and Menzie, D. E., 1955, Fluid mapper model studies of mobility ratio: Transactions of AIME (American Institute of Mining and Metallurgical Engineers), v. 204, p. 278–281.

Clark, N. J., 1969, Elements of petroleum reservoirs [revised edition]: Society of Petroleum Engineers of American Institute of Mining and Metallurgical Engineers, Henry L. Doherty Series, 250 p.

Core Laboratories, Inc., 1980, Fundamentals of core analysis: Training manual prepared and used by Core Laboratories, Inc., Houston.

Cotman, N. T.; Still, G. R.; and Crawford, P. B., 1962, Laboratory comparison of oil recovery in five-spot and nine-spot waterflood patterns: Producers Monthly, v. 26, p. 10–13.

Craft, B. C.; and Hawkins, M. F., 1959, Applied petroleum reservoir engineering: Prentice-Hall, Chemical Engineering Series, 437 p.

Craig, F. F., 1971, The reservoir engineering aspects of waterflooding: Society of Petroleum Engineers of AIME (American Institute of Mining and Metallurgical Engineers) Monograph, Henry L. Doherty Series, v. 3, 134 p.

Craig, F. F., Jr.; Geffen, T. M.; and Morse, R. A., 1955, Oil recovery performance of pattern gas or water injection operations from model tests: Transactions of AIME (American Institute of Mining and Metallurgical Engineers), v. 204, p. 715.

Crawford, P. B., 1960, Laboratory factors affecting water flood pattern performance and selection: Journal of Petroleum Technology, v. 12, p. 11–15.

Crawford, P. B.; and Collins, R. E., 1954, Estimated effect of vertical fractures on secondary recovery: Transactions of AIME (American Institute of Mining and Metallurgical Engineers), v. 201, p. 192–196.

_____1954, Analysis of flooding horizontally fractured thin reservoirs: World Oil, v. 139, (Aug.) p. 139, (Sept.) p. 173, (Oct.) p. 214, (Nov.) p. 212, (Dec.) p. 197.

Crawford, P. B.; Pinson, J. M.; Simmons, J.; and Landrum, B. L., 1956, Sweep efficiencies of vertically fractured five-spot patterns: Petroleum Engineer , v. 28, p. B95–B102.

Deppe, J. C., 1961, Injection rates—the effect of mobility ratio, areal sweep, and pattern: Society of Petroleum Engineers Journal, v. 1 , p. 81–91.

Dougherty, E. L.; and Sheldon, J. W., 1964, The use of fluid–fluid interfaces to predict the behavior of oil recovery processes: Society of Petroleum Engineers Journal, v. 4, p. 171–182.

Dusseault, M. B.; and Van Domselaar, H. R., 1984, Unconsolidated sand sampling in Canadian and Venezuelan oil sands: Proceedings of UNITAR Second International Oil Conference on the Future of Heavy Crudes and Tar Sands, Caracas, Venezuela, p. 336–348.

Dyes, A. B., 1952, Discussion of mobility ratio, its influence on flood patterns during water encroachment: Transactions of AIME (American Institute of Mining and Metallurgical Engineers), v. 195, p. 22–23.

Dyes, A. B.; Caudle, B. H.; and Erickson, R. A., 1954, Oil production after breakthrough—as influenced by mobility ratio: Transactions of AIME (American Institute of Mining and Metallurgical Engineers), v. 201, p. 81–86.

Dyes, A. B.; Kemp, C. E.; and Caudle, B. H., 1959, Effect of fractures on sweep-out pattern: Transactions of AIME (American Institute of Mining and Metallurgical Engineers), v. 216, p. 73–77.

Dykstra, H.; and Parsons, H. L., 1950, The prediction of oil recovery by waterflooding, *in* Secondary recovery of oil in the United States [2nd edition]: American Petroleum Institute, New York, p. 160–174.

Fay, C. H.; and Prats, M., 1951, The application of numerical methods to cycling and flooding problems: Proceedings of Third World Petroleum Congress, v. 2, p. 555–563.

Ferrell, H.; Irby, T. L.; Pruitt, G. T.; and Crawford, P. B., 1960, Model studies for injection–production well conversion during a line drive water flood: Transactions of AIME (American Institute of Mining and Metallurgical Engineers), v. 219, p. 94–98.

Fettke, C. R., 1938, Bradford oil field, Pennsylvania and New York: Pennsylvania Geological Survey, 4th Series, M-21, 454 p.

Frick, T. C.; and Taylor, R. W. (eds.), 1962, Reservoir engineering, *v. 2 of* Petroleum production handbook: Society of Petroleum Engineers of AIME (American Institute of Mining and Metallurgical Engineers).

George, C. J.; and Stiles, L. H., 1978, Improved techniques for evaluating carbonate waterfloods in West Texas: Journal of Petroleum Technology, v. 30, p. 1547–1554.

Guckert, L. G., 1961, Areal sweepout performance of seven and nine-spot flood patterns: Pennsylvania State University unpublished M.S. thesis.

Habermann, B., 1960, The efficiency of miscible displacement as a function of mobility ratio: Transactions of AIME (American Institute of Mining and Metallurgical Engineers), v. 219, p. 264–272.

Hall, H. N., 1953, Compressibility of reservoir rocks: Transactions of AIME (American Institute of Mining and Metallurgical Engineers), v. 198, p. 309–311.

Harper, T. R.; and Moftah, I., 1985, Skin effect and completion options in the Ras Budran reservoir: Society of Petroleum Engineers of AIME (American Institute of Mining and Metallurgical Engineers), Middle East Oil Technical Conference and Exhibition, Bahrain, March 11–14, SPE 13708, p. 211–219.

Hartsock, J. H.; and Slobod, R. L., 1961, The effect of mobility ratio and vertical fractures on the sweep efficiency of a five-spot: Producers Monthly, v. 25, p. 2–7.

Hele-Shaw, H. S., 1897, Experiments on the nature of the surface resistance in pipes and on ships: Transactions of Institution of Naval Architects, v. 39, p. 145.

Henley, D. H., 1953, Method for studying waterflooding using analog, digital, and rock models: Paper presented at 24th Technical Conference on Petroleum, Pennsylvania State University.

Hunter, Z. Z., 1956, Progress report, North Burbank Unit water flood—Jan. 1, 1956: Drilling and Production Practices, American Petroleum Institute, p. 262.

_____1956, 8½ million extra barrels in 6 years: Oil and Gas Journal, v. 54 (Aug. 27), p. 92.

Hurst, W., 1953, Determination of performance curves in five-spot waterflood: Petroleum Engineering, v. 25, p. B40–B46.

Hutchinson, C. A., Jr., 1959, Reservoir inhomogeneity assessment and control: Petroleum Engineer, v. 31, p. B19–B26.

Jackson, J. A. (ed.), 1997, Glossary of geology [4th edition]: American Geological Institute, 769 p.

Jamison, W. R.; and Stearns, D. W., 1982, Tectonic deformation of Wingate Sandstone, Colorado National Monument: American Association of Petroleum Geologists Bulletin, v. 66, p. 2584–2608.

Jennings, H. Y., 1966, Waterflood behavior of high viscosity crude in preserved soft and unconsolidated cores: Journal of Petroleum Technology, v. 18, p. 116–120.

Keelan, D. K., 1972, A critical review of core analysis techniques: Journal of Canadian Petroleum Technology, v. 11, p. 42–55.

Kimbler, O. K.; Caudle, B. H.; and Cooper, H. E., Jr., 1964, Areal sweepout behavior in a nine-spot injection pattern: Journal of Petroleum Technology, v. 16, p. 199–202.

Koeller, R. C.; and Craig. F. F., Jr., 1956, *Discussion of* Mobility ratio—its influence on injection and production histories in five-spot water flood: Transactions of AIME (American Institute of Mining and Metallurgical Engineers), v. 207, p. 291–292.

Krutter, H., 1939, Nine-spot flooding program: Oil and Gas Journal, v. 38 (Aug. 17), p. 50.

Kulander, B. R.; Dean, S. L.; and Ward, B. J., Jr., 1990, Fractured core analysis: interpretation, logging, and use of natural and induced fractures in core: American Association of Petroleum Geologists, Methods in Exploration Series, no. 8, 88 p.

Landrum, B. L.; and Crawford, P. B., 1957, Estimated effect of horizontal fractures in thick reservoirs on pattern conductivity: Transactions of AIME (American Institute of Mining and Metallurgical Engineers), v. 210, p. 399–401.

_____1960, Effect of directional permeability on sweep efficiency and production capacity: Transactions of AIME (American Institute of Mining and Metallurgical Engineers), v. 219, p. 407–411.

Law, J., 1944, Statistical approach to the interstitial heterogeneity of sand reservoirs: Transactions of AIME (American Institute of Mining and Metallurgical Engineers), v. 155, p. 202–222.

Lee, B. D., 1948, Potentiometric model studies of fluid flow in petroleum reservoirs: Transactions of AIME (American Institute of Mining and Metallurgical Engineers), v. 174, p. 41–66.

Lorenz, J. C.; and Finley, S. J., 1988, Significance of drilling-

and coring-induced fractures in Mesaverde core, northwestern Colorado: Sandia National Laboratories, Albuquerque, New Mexico, SAND87-1111, UC Category 92, 34 p.

Matthews, C. S.; and Fischer, J. J., 1956, Effect of dip on five-spot sweep pattern: Transactions of AIME (American Institute of Mining and Metallurgical Engineers), v. 207, p. 111–117.

Moore, A. D., 1949, Fields from fluid flow mappers: Journal of Applied Physics, v. 20, p. 790.

_____1950, The further development of fluid mappers: Transactions of AIME (American Institute of Mining and Metallurgical Engineers), v. 69, pt. 2, p. 1615–1624.

_____1952, Mapping technique applied to fluid mapper patterns: Transactions of AIME (American Institute of Mining and Metallurgical Engineers), v. 71, pt. 1, p. 1–4.

Mortada, M.; and Nabor, G. W., 1961, An approximate method for determining areal sweep efficiency and flow capacity in formations with anisotropic permeability: Society of Petroleum Engineers Journal, v. 1, p. 277–286.

Moss, J. T.; White, P. D.; and McNiel, J. S., Jr., 1959, In-situ combustion process—results of a five-well field experiment: Transactions of AIME (American Institute of Mining and Metallurgical Engineers), v. 216, p. 55–64.

Muskat, M., 1946, Flow of homogeneous fluids through porous systems: J. W. Edwards, Inc., Ann Arbor, Michigan.

_____1948, The theory of nine-spot flooding networks: Producers Monthly, v. 13, p. 14.

_____1950, Physical principles of oil production: McGraw-Hill, New York, 922 p.

Muskat, M.; and Wyckoff, R. D., 1934, A theoretical analysis of waterflooding networks: Transactions of AIME (American Institute of Mining and Metallurgical Engineers), v. 107, p. 62–76.

Naar, J.; Wygal, R. J.; and Henderson, J. H., 1962, Imbibition relative permeability in unconsolidated porous media: Society of Petroleum Engineers Journal, v. 2, p. 13–23.

Neilson, I. D. R.; and Flock, D. L., 1962, The effect of a free gas saturation on the sweep efficiency of an isolated five-spot: Bulletin of Canadian Institute of Mining and Metallurgy, v. 55, p. 124–129.

Nelson, R. A., 1985, Geologic analysis of naturally fractured reservoirs: Gulf Publishing, Houston, Petroleum Geology Engineering, v. 1, 320 p.

Nobles, M. A.; and Janzen, H. B., 1958, Application of a resistance network for studying mobility ratio effects: Transactions of AIME (American Institute of Mining and Metallurgical Engineers), v. 213, p. 356–358.

Owens, W. W.; and Archer, D. L., 1971, The effect of rock wettability on oil-water relative permeability relationships: Journal of Petroleum Technology, v. 23, p. 873–878.

Paulsell, B. L., 1958, Areal sweep performance of five-spot pilot floods: Pennsylvania State University unpublished M.S. thesis.

Pinson, J.; Simmons, J.; Landrum, B. J.; and Crawford, P. B., 1963, Effect of large elliptical fractures on sweep efficiencies in water flooding or fluid injection programs: Producers Monthly, v. 27, p. 20–22.

Pittman, E. D., 1981, Effect of fault-related granulation on porosity and permeability of quartz sandstones, Simpson Group (Ordovician), Oklahoma: American Association of Petroleum Geologists Bulletin, v. 65, p. 2381–2387.

Prats, M., 1956, The breakthrough sweep efficiency of a staggered line drive: Transactions of AIME (American Institute of Mining and Metallurgical Engineers), v. 207, p. 361–362.

Prats, M.; Strickler, W. R.; and Matthews, C. S., 1955, Single-fluid five-spot floods in dipping reservoirs: Transactions of AIME (American Institute of Mining and Metallurgical Engineers), v. 201, p. 160–167.

Prats, M.; Matthews, C. S.; Jewett, R. L.; and Baker, J. D., 1959, Prediction of injection rate and production history for multifluid five-spot floods: Transactions of AIME (American Institute of Mining and Metallurgical Engineers), v. 216, p. 98–105.

Prats, M.; Hazebroek, P.; and Allen, E. E., 1962, Effect of off-pattern wells on the behavior of a five-spot flood: Transactions of AIME (American Institute of Mining and Metallurgical Engineers), v. 225, p. 173–178.

Ramey, H. J., Jr.; and Nabor, G. W., 1954, A blotter-type electrolytic model determination of areal sweeps in oil recovery by in-situ combustion: Transactions of AIME (American Institute of Mining and Metallurgical Engineers), v. 201, p. 119–123.

Rapoport, L. A.; Carpenter, C. W., Jr.; and Leas, W. J., 1958, Laboratory studies of five-spot waterflood performance: Transactions of AIME (American Institute of Mining and Metallurgical Engineers), v. 213, p. 113–120.

Raza, S. H.; Treiber, L. E.; and Archer, D. L., 1968, Wettability of reservoir rocks and its evaluation: Producers Monthly, v. 32, p. 2–7.

Rottmann, Kurt; Crutchfield, D. R.; Tew, George; Wilson, Dan; Sutherland, Mark; and Nizami, Saleem, 1998, Geological considerations of waterflooding: a workshop: Oklahoma Geological Survey Special Publication 98-3, 171 p.

Salathiel, R. A., 1973, Oil recovery by surface film drainage in mixed-wettability rocks: Journal of Petroleum Technology, v. 25, p. 1216–1224.

Sandrea, R. J.; and Farouq Ali, S. M., 1967, The effects of isolated permeability interferences on the sweep efficiency and conductivity of a five-spot network: Society of Petroleum Engineers Journal, v. 7, p. 20–30.

Schilthuis, R. J., 1936, Active oil and reservoir energy: Transactions of AIME (American Institute of Mining and Metallurgical Engineers), v. 118, p. 33.

Sheriff, R. E., 1984, Encyclopedic dictionary of exploration geophysics [2nd edition]: Society of Exploration Geophysicists, Tulsa, Oklahoma, 323 p.

Slider, H. C., 1983, Worldwide practical petroleum reservoir engineering methods: Pennwell Books, Tulsa, Oklahoma, 826 p.

Slobod, R. L.; and Caudle, B. H., 1952, X-ray shadowgraph studies of areal sweepout efficiencies: Transactions of AIME (American Institute of Mining and Metallurgical Engineers), v. 195, p. 265–270.

Slobod, R. L.; and Crawford, D. A., 1962, Evaluation of reliability of fluid flow models for areal sweepout studies: Producers Monthly, v. 26, v. 27, p. 18–22.

Smith, J. T.; and Cobb, W. M., 1987, Waterflooding: Willima Cobb & Associates, Inc., Dallas, unpublished short course notes.

Standing, M. B., 1977, Volumetric and phase behavior of oil field hydrocarbon system, *pt. 2 of* Preliminary reservoir data: Society of Petroleum Engineers of AIME (American Institute of Mining and Metallurgical Engineers), 130 p.

Stiles, L. H., 1976, Optimizing waterflood recovery in a mature waterflood, the Fullerton Clearfork Unit: Society of Petroleum Engineers of AIME (American Institute of Mining and Metallurgical Engineers), 51st Annual Fall Technical Conference and Exhibition, New Orleans, October 3–6, SPE 6198, 12 p.

Still, G. R.; and Crawford, P. B., 1963, Laboratory evaluation of oil recovery by cross-flooding: Producers Monthly, v. 27, p. 12–19.

Terwilliger, P. L.; Wilsey, L. E.; Hall, H. N.; Bridges, P. M.; and Morse, R. A., 1951, An experimental and theoretical investigation of gravity drainage performance: Transactions of AIME (American Institute of Mining and Metallurgical Engineers), v. 192, p. 285–296.

Underhill, J. R.; and Woodcock, N. H., 1987, Faulting mechanisms in high-porosity sandstones; New Red Sandstone, Arran, Scotland, *in* Jones, M. E.; and Preston, R. M. F. (eds.), Deformation of sediments and sedimentary rocks: Geological Society [London] Special Publication 29, p. 91–105.

van der Knaap, W., 1958, Non-linear elastic behavior of porous media: Presentation at meeting of Society of Petroleum Engineers of AIME (American Institute of Mining and Metallurgical Engineers), Houston.

van Meurs, P., 1957, The use of transparent three-dimensional models for studying the mechanism of flow processes in oil reservoirs: Transactions of AIME (American Institute of Mining and Metallurgical Engineers), v. 210, p. 295–301.

Van Wagoner, J. C.; Mitchum, R. M.; Campion, K. M.; and Rahmanian, V. D., 1990, Siliciclastic sequence stratigraphy in well logs, cores, and outcrops: concepts for high-resolution correlation of time and facies: American Association of Petroleum Geologists, Methods in Exploration Series, no. 7, 55 p.

Wagner, O. R.; and Leach, R. O., 1959, Improving oil displacement efficiency by wettability adjustment: Transactions of AIME (American Institute of Mining and Metallurgical Engineers), v. 216, p. 65–72.

Watson, R. E.; Silberberg, I. H.; and Caudle, B. H., 1964, Model studies of inverted nine-spot injection pattern: Journal of Petroleum Technology, v. 16, p. 801–804.

Welge, H. J., 1952, A simplified method for computing oil recovery by gas or water drive: Transactions of AIME (American Institute of Mining and Metallurgical Engineers), v. 195, p. 91–98.

Wyckoff, R. D.; Botset, H. G.; and Muskat, M., 1933, The mechanics of porous flow applied to waterflooding problems: Transactions of AIME (American Institute of Mining and Metallurgical Engineers), v. 103, p. 219–242.

APPENDIX 1

Abbreviations and Symbols Used in This Volume

A	floodable area
a	distance between adjacent wells in a row
API	American Petroleum Institute
BBL	barrel(s)
B_g	gas formation volume factor
B_{gi}	initial gas formation volume factor
BO	barrels of oil
B_o	oil formation volume factor
B_{oB}	oil at bubble-point pressure
B_{oi}	initial oil formation volume factor
BOPD	barrels of oil per day
BOPM	barrels of oil per month
BW	barrels of water
CAL	caliper
CDP	conductivity-derived porosity
C_o	oil compressibility
COND	conductivity
cp	centipoise (a standard unit of viscosity)
C_w	water compressibility
d	distance between adjacent rows of producing and injection wells
DEN	density
DEN POR	density porosity
DEN ϕ	density porosity
E_a	areal sweep efficiency
E_d	displacement efficiency
E_v	vertical sweep efficiency
F	Fahrenheit
FVF	formation volume factor
f_w	fractional flow of water
G	original gas in reservoir
G_F	volume of free gas
GOR	gas/oil ratio
G_p	produced gas
G_{pc}	gas production from gas cap
G_{ps}	solution-gas production
GR	gamma ray
H	average height of floodable area
k	absolute permeability
L	length that a given water saturation travels
M	mobility of water
MMBO	million barrels of oil
N	original oil in place
NEU POR	neutron porosity
N_p	cumulative oil production
OIP	oil in place
OOIP	original oil in place
OWC	oil–water contact
P_{BP}	bubble-point pressure
P_i	initial pressure
psi	pounds per square inch
psia	pounds per square inch, absolute
PVT	pressure, volume, temperature
RES	resistivity
R_p	cumulative produced gas/oil ratio
R_s	current gas/oil ratio
R_{si}	original gas/oil ratio
SCF	standard cubic feet (of gas)
S_{df}	water saturation at flood front
S_{di}	initial saturation of displacing fluid
S_g	gas saturation
S_o	oil saturation

S_{or}	mobile-oil saturation
SP	spontaneous potential
STB	stock-tank barrels
S_w	water saturation
S_{wbt}	water saturation at breakthrough
S_{wc}	formation-water saturation
V_d	displaceable volume
V_g	volume of gas
V_o	volume of oil
V_{oi}	initial volume of oil
V_p	pore volume
W	average width of floodable area
W_e	water entry
W_i	cumulative injected water
WOR	water/oil ratio
W_p	produced water
Z	gas deviation factor
Δp	change in pressure
ΔV	change in pore volume
ϕ	porosity

APPENDIX 2
Glossary of Terms
(as used in this volume)

Definitions modified from Anderson (1987), Craft and Hawkins (1959), Craig (1971), Frick and Taylor (1962), Jackson (1997), Sheriff (1984), Slider (1983), and Smith and Cobb (1987).

absolute permeability—The ability of a rock to conduct a fluid; e.g., gas, at 100% saturation with that fluid.

acre-foot—The volume of liquid or solid required to cover 1 acre to a depth of 1 foot, or 43,560 cubic feet. It is commonly used in measuring volumes of water, reservoir storage space, or reservoir rock.

API gravity—A standard adopted by the American Petroleum Institute for expressing the specific weight of oils. API gravity = (141.5/specific gravity at 60°F) – 131.5. This arbitrary scale simplifies the construction of hydrometers because it enables the stems to be calibrated linearly. The lower the specific gravity, the higher the API gravity.

area—As used in this publication, a two-dimensional surface, usually measured from an isopach map.

areal sweep efficiency—That fraction of a waterflood pattern that has been contacted by water at a given time during a flood.

bubble point—A state of fluids characterized by the coexistence of a liquid phase with an infinitesimal quantity of gas phase in equilibrium.

bubble-point pressure—The liquid pressure in a system at its bubble point.

bulk volume—A distinct mass of a rock or reservoir exclusive of porosity.

capillary pressure—The difference in pressure across the interface between two immiscible fluid phases jointly occupying the interstices of a rock. It is due to the tension of the interfacial surface, and its value depends on the curvature of that surface.

centipoise (cp)—A unit of viscosity equal to 10^{-3}kg/s.m. The viscosity of water at 20°C is 1.005 cp.

compressibility—The change of volume and density under hydrostatic pressure.

compressibility factor—A multiplying factor introduced into the Ideal Gas Law to account for the departure of true gases from ideal behavior. Syn.: *gas-deviation factor; supercompressibility factor.*

darcy—A standard unit of permeability, equivalent to the passage of 1 cubic centimeter of fluid of 1 centipoise viscosity flowing in 1 second under a pressure differential of 1 atmosphere through a porous medium having an area of cross section of 1 square centimeter and a length of 1 centimeter.

Darcy's law—The velocity of a homogeneous fluid in a porous medium, proportional to the pressure gradient and inversely proportional to the fluid viscosity.

displacement efficiency—The volume of "wet" hydrocarbons swept out of individual pores or small groups of pores, divided by the volume of hydrocarbons in the same pores at the start of cycling.

drag zone—The zone behind the displacing front of a waterflood.

drainage process—A decrease in the wetting-fluid saturation of a porous medium.

Dykstra-Parsons coefficient—A statistical approach for predicting the effects of variable permeability on waterflood performance. The method assumes that the reservoir is composed of a number of layers with varying permeabilities and no cross-flow.

effective permeability—The ability of a rock to conduct one fluid, e.g., gas, in the presence of other fluids, e.g., oil or water.

effective-permeability ratio—The effective permeability of one fluid (usually water) divided by the effective permeability of a second fluid (usually oil) in a two-phase system.

effective porosity—The percentage of the total volume of a given mass of soil or rock that consists of interconnecting voids.

floodable area—That portion of a reservoir under waterflood operation that is or will be contacted by the displacing fluid.

formation volume factor—The factor applied to convert a barrel of gas-free oil in a stock tank at the surface into an equivalent amount of oil in the reservoir. It generally ranges between 1.14 and 1.60. See also: *shrinkage factor.*

fractional flow—During production, that percentage of a fluid's contribution to the total fluid production.

fractional-flow equation—A method used to derive the fractional flow of a fluid (usually water) for any given saturation of the fluid in the reservoir.

fracture—(a) A crack, joint, fault, or other break in rocks. (b) Deformation owing to a momentary loss of cohesion or of resistance to differential stress and a release of stored elastic energy.

frontal-advance theory—The theory of the way in which water displaces oil from a reservoir of complex permeability and porosity.

gas cap—Free gas occurring above oil in a reservoir, and present whenever more gas is available than will dissolve in the associated oil under existing pressure and temperature.

gas-cap drive—Energy within an oil pool, supplied by expansion of an overlying volume of compressed free gas as well as by expansion of gas dissolved in the oil.

gas deviation factor—See: *compressibility factor.*

gas/oil ratio—(a) The quantity of gas produced with the oil from an oil well, usually expressed as the number of cubic feet of gas per barrel of oil. Abbr.: GOR. (b) *reservoir gas/oil ratio.*

height—The vertical distance above a datum, usually the Earth's surface. May refer to vertical thickness, usually of strata.

hydrocarbon pore volume—The volume of a rock or reservoir that contains hydrocarbons.

hydrostatic pressure—The pressure exerted by the water at any given point in a body of water at rest.

Ideal Gas Law—As used in this publication, the pressure–volume–temperature (PVT) relationship of an ideal gas at a given state, equal to the PVT relationship of the gas at a different state.

imbibition—The tendency of granular rock or any porous medium to absorb a fluid, usually water, under the force of capillary attraction, and in the absence of any pressure.

imbibition process—An increase in the saturation of the wetting fluid in a porous medium.

immiscible—Said of two or more phases that, at mutual equilibrium, cannot dissolve completely in one another.

impermeable—Said of a rock, sediment, or soil that is incapable of transmitting fluids under pressure.

initial production—The volume or quantity of gas or oil initially produced by a well in a certain interval of time, usually 24 hours.

injector—A well used to introduce fluids into a reservoir, either for disposal or as a displacing fluid or agent.

irreducible (residual) oil saturation—That portion of an oil saturation that remains in a reservoir regardless of the amount of displacing fluid with which it comes in contact and which passes through the reservoir.

irreducible (residual) water saturation—That portion of a water saturation that remains in a reservoir regardless of the amount of displacing fluid with which it comes in contact and which passes through the reservoir.

isopach—A line drawn on a map through points of equal true thickness of a designated stratigraphic unit or group of stratigraphic units.

material-balance method—A method of calculating oil in place by the accounting or balancing of fluids and their properties that remain in the reservoir, with the fluids and properties that have been produced.

millidarcy (md)—The customary unit of measurement of fluid permeability, equivalent to 0.001 darcy.

mixed wettability—Pertains to a reservoir that is not homogeneous in its wettability. Commonly, the larger pores may be oil-wet, and the smaller pores water-wet.

mobile-oil saturation—That portion of the total oil saturation that is mobile in response to a displacing agent or other factor such as gravity.

mobile-water saturation—That portion of the total water saturation that is mobile in response to a displacing agent or other factor such as gravity.

mobility—The ratio of the permeability to the viscosity of a fluid.

mobility ratio—The ratio of the mobility of the displacing fluid to that of the displaced fluid.

natural water drive—Energy within an oil or gas pool, resulting from hydrostatic or hydrodynamic pressure transmitted from the surrounding aquifer.

oil bank—The mass of increased oil saturation moving in a reservoir in front of, and displaced by, an injected fluid.

oil compressibility—The change in volume of oil with a change in reservoir pressure.

oil saturation—That portion of the total fluid saturation of a rock or reservoir that consists of oil.

oil–water contact—The boundary surface between an accumulation of oil and the underlying "bottom water." Syn.: *oil–water interface.*

oil-wet reservoir—A reservoir whose preferential wetting agent is oil in the presence of other immiscible fluids.

permeability—The capacity of a porous rock, sediment, or soil for transmitting a fluid; it is a measure of the relative ease of fluid flow under unequal pressure. The customary unit of measure is the *millidarcy.* Cf: *absolute permeability; effective permeability; relative permeability.* Adj.: *permeable.*

pore volume—That portion of bulk volume that consists of voids.

porosity—The ratio of the aggregate volume of interstices in a rock or soil to its total volume. It is usually stated as a percentage. Cf: *effective porosity.* Syn.: *total porosity.*

pressure sink—An area of low reservoir pressure generally created by a producing well.

relative permeability—The ratio between the *effective permeability* to a given fluid at a partial saturation and the permeability at 100% saturation (the *absolute permeability*). It ranges from zero at a low saturation to 1.0 at a saturation of 100%.

relative-permeability ratio—The relative permeability of one fluid (usually water) divided by the relative permeability of a second fluid (usually oil) in a two-phase system.

residual oil—Oil that is left in the reservoir rock after the pool has been depleted.

residual-oil saturation—See: *irreducible oil saturation.*

residual-water saturation—See: *irreducible water saturation.*

rock compressibility—The change in volume of rock in response to external pressure.

salt-water saturation—That portion of the total fluid saturation of a porous medium that consists of salt water.

saturated reservoir—The inability of an oil reservoir to dissolve additional gas in response to increased pressure.

shrinkage factor—The factor that is applied to convert a barrel of oil in the reservoir into an equivalent amount of gas-free oil in a stock tank at the surface. It generally ranges between 0.68 and 0.88. See also: *formation volume factor.*

solids volume—The amount of remaining reservoir volume after the pore volume is subtracted from the bulk volume.

solution-gas drive—Energy within an oil accumulation supplied by expansion of gas dissolved in the oil.

stream line—A theoretical path of fluid, usually from an injector to a producing well and always perpendicular to isopotential lines.

supercompressibility factor—See: *compressibility factor.*

swept area—That portion of a reservoir that has been contacted by an injected displacing fluid.

unitization—Consolidation of the management of an entire oil or gas pool, regardless of property lines and lease boundaries, in the interest of efficient operation and maximum recovery.

vertical sweep efficiency—The cross-sectional area contacted by the injected fluid divided by the cross-sectional area enclosed in all layers behind the injected-fluid front.

viscosity—The property of a substance to offer internal resistance to flow; its internal friction.

volumetric method—A method for calculating oil in place, using the volumetric properties of a reservoir.

water bank—The mass of increased water saturation moving in a reservoir behind the displaced front.

water breakthrough—The increase of water production in a producing well as a result of the injected fluid having reached the wellbore.

water compressibility—The change in volume of water in response to external pressure.

water drive—Energy within an oil or gas pool that results from hydrostatic or hydrodynamic pressure transmitted from the surrounding aquifer. Cf: *solution-gas drive; gas-cap drive.*

waterflooding—A secondary-recovery operation in which water is injected into a petroleum reservoir to force additional oil out of the reservoir rock and into producing wells.

water leg—A water-saturated zone that extends below an oil- or gas-saturated zone.

water-wet reservoir—A reservoir whose preferential wetting agent is water in the presence of other immiscible fluids.

wettability—The tendency of one fluid to spread on or adhere to a solid surface in the presence of other immiscible fluids.